Managing the Uncertainty Associated with Hydrogen Gas Hazards and Operability Issues in Nuclear Chemical Plants

FAYAZ AHMED

https://orcid.org/0000-0002-6805-3796

A thesis submitted in partial fulfilment of the requirements of London South Bank University for the Degree of Doctor of Philosophy

This research programme was carried out in collaboration with Sellafield Ltd.

April 2021

LIST OF PUBLICATIONS BY THE CANDIDATE

Based on the output of the research, the following papers have been published by the candidate:

Ahmed, F. (2017b) Bayesian Belief Networks - A robust approach to quantified risk and uncertainty analysis, *Institution of Chemical Engineers*, *The Chemical Engineer,* 911, pp. 28-32.

Ahmed, F. (2019a) Managing hydrogen gas hazards, *Nuclear Future, The Professional Journal of the Nuclear Institute*, 15(2), pp.46-50.

Ahmed, F. (2019b) Application of Bayesian Belief Networks to assess hydrogen gas retention hazards and equipment reliability in nuclear chemical plants, *Proceedings* of *the Institution of Chemical Engineers Hazards 29 Conference, Symposium Series No.166*, Birmingham, 22-24 May 2019.

ABSTRACT

The complex and diverse nature of reprocessing and decommissioning operations in existing nuclear chemical plants within the UK results in a variety of challenges. The challenges relate to the quantified risk from hydrogen explosions and how best to manage the associated uncertainties.

Several knowledge gaps in terms of the Quantified Risk Assessment (QRA) of hydrogen hazards have been identified in this research work. These include radiolytic hydrogen explosions in sealed process pipes, the failure of ventilation systems used to dilute radiolytic hydrogen in process vessels, the decision uncertainty in installing additional hydrogen purge systems and the uncertainty associated with hold-up of hydrogen in radioactive sludges. The effect of a subsequent sudden release of the held-up hydrogen gas into a vessel ullage space presents a further knowledge gap. Nuclear decommissioning and reprocessing operations also result in operational risk knowledge gaps including the mixing behaviour of radioactive sludges, the performance of robotics for nuclear waste characterisation and control of nuclear fission products associated with solid wastes.

Bayesian Belief Networks (BBNs) and Monte Carlo Simulation (MC) techniques have been deployed in this research work to address the identified knowledge gaps. These techniques provide a powerful means of uncertainty analysis of complex systems involving multiple interdependent variables such as those affecting nuclear decommissioning and reprocessing.

Through the application of BBN and MC Simulation methodologies to a series of nuclear chemical plant case studies, new knowledge in decommissioning and reprocessing operations has been generated. This new knowledge relates to establishing a realistic quantified risk from hydrogen explosions and nuclear plant operability issues. New knowledge in terms of the key sensitivities affecting the quantified risk of hydrogen explosions and operability in nuclear environments as well as the optimum improvements necessary to mitigate such risks has also been gained.

ACKNOWLEDGEMENTS

I would like to thank my lead supervisor at LSBU, Dr Paul Holborn, for his continued support and direction throughout the research programme. Also, I would like to thank my second LSBU supervisor Dr James Ingram for his support.

I would like to express an acknowledgement with thanks to my sponsoring company Sellafield Ltd. (SL) for providing me with the opportunity to undertake this research. I would like to thank my departmental managers Mr Mike Stevens and Mr Anthony Tilstone of SL for fulfilling my research aspiration and providing the funding for the research. Also, I would like to thank my company based supervisors, Dr Martin Fairclough and Mr Phil Vesey of the SL Hydrogen Working Party for their guidance and support.

Most importantly this thesis is dedicated in the loving memory of my mother and father, who were a continued source of inspiration and encouragement.

DECLARATION

I, Fayaz Ahmed declare that the research and the results presented within this thesis are my own, having been generated by myself as a result of my original work. The work has not been previously submitted for another degree or award at any academic institution.

ABBREVIATIONS

Abbreviation	Description
ALARP	As Low As Reasonably Practicable
AIT	Autoignition Temperature
API	Application Programming Interface
BBN	Bayesian Belief Network
BoS	Basis of Safety
BS	British Standard
CBA	Cost Benefit Analysis
CCF	Common Cause Failure
CISWG	Characterisation, Inventory, Sludge Wastes Group
COM	Component Object Model
CPT	Conditional Probability Table
DAG	Directed Acyclic Graphs
DN	Decision Network
DF	Disproportionate Factor
DSEAR	Dangerous Substances and Explosive Atmospheres Regulations
EPS	Engineered Protection System
ETA	Event Tree Analysis
EFR	Explosions and Fire Research
FTA	Fault Tree Analysis
HAZAN	Hazard Analysis
HAZOP	Hazard and Operability
HEP	Human Error Probability
HIAD	Hydrogen Incidents and Accidents Database
HMSO	Her Majesty's Stationary Office
HRA	Human Reliability Analysis
HSE	Health and Safety Executive
HSL	Health and Safety Laboratory
HTG	Hydrogen Technical Guide
HWP	Hydrogen Working Party
IAEA	International Atomic Energy Authority
IChemE	Institution of Chemical Engineers
ID	Identification
IEC	International Electrotechnical Commission

Abbreviation	Description
IEEE	Institute of Electrical and Electronics Engineers
IEF	Initiating Event Frequency
IM	Importance Measure
ISO	International Organisation for Standardisation
ILW	Intermediate Level Wastes
LFL	Lower Flammability Limit
LLW	Low Level Waste
MCDA	Multi Criteria Decision Aid
LNG	Liquefied Natural Gas
LOCA	Loss of Cooling Accident
LOPA	Layer of Protection Analysis
LSBU	London South Bank University
MBGW	Miscellaneous Beta Gamma Wastes
MPE	Most Probable Explanation
MTBF	Mean Time Between Failure
MC	Monte Carlo
MIE	Minimum Ignition Energies
MS	Mitigating System
NDA	Nuclear Decommissioning Authority
NPRD	Nonelectronic Parts Reliability Data
ONR	Office for Nuclear Regulation
OPM	Operational Preventative Measure
PDF	Probability Density Function
Pfd	Probability of failure on demand
PRA	Probabilistic Risk Assessment
QRA	Quantitative Risk Assessment
SAP	Safety Assessment Principle
SL	Sellafield Ltd
SME	Subject Matter Expert
SVG	Scalable Vector Graphics
UK	United Kingdom
UFL	Upper Flammability Limit
WPC	Waste Processing Cell
WTT	Waste Treatment Table

NOMENCLATURE

Symbol	Description
AW	Active water mass fraction
α	Alpha radiation, unit Becquerel
β/γ	Beta-Gamma radiation, unit Becquerel
DPG	Dry powder grout mass
DS	Density of sludge, Kg/m^3
DSM	Dry sludge mass, Kg
$E_{(\alpha)}$	Rate of absorption of alpha radionuclide decay energy by the medium, MeV/s
$E_{(\beta/\gamma)}$	Rate of absorption of beta-gamma radionuclide decay energy by the medium, MeV/s
$G(H_2)_{(\alpha)}$	Number of hydrogen molecules evolved per 100eV of alpha decay energy absorbed by the medium
$G(H_2)_{(\beta/\gamma)}$	Number of hydrogen molecules evolved per 100eV of beta-gamma decay energy absorbed by the medium
IW	Inactive water mass (Kg)
k	This is a dimensional constant, $1.44x10^{-15}$ used for calculating the radiolytic hydrogen generation rate, when the rate of absorption of decay energy is expressed in units MeV/s
M_j	Mass of PuO_2 compound
mSv	Millisievert. This is a unit of radiological dose.
nC	Nanocoulomb. This is a unit of electrostatic charge.
P	Failure probability of repairable items
P(A)	Prior probability of occurrence of hypothesis A
P(A|B)	Conditional probability for the likelihood of observing hypothesis A given that B is true
P(B)	Probability of occurrence of event B
P(B|A)	Conditional probability for the likelihood of observing hypothesis A given that B is true
P(B)	Probability of occurrence of event B
P(B|A)	Probability of event B occurring given that A is true
P(t)	Failure probability over time t
Q_H	Hydrogen generation rate, L/hr
SM	Safe critical mass (Kg)
SD	Dry sludge to dry mass ratio
t	Time, years
T_R	Equipment repair time (years)
T_s	Proof test interval (years)
V_{AW}	Volume fraction of active water

Symbol	Description
W_{AW}	Weight fraction of active water
ρ_{AW}	Density of active water, kg/m^3
ρ_S	Density of sludge, kg/m^3
W_S	Weight fraction of sludge
V_S	Volume fraction of sludge
Vskip	Volume of skip waste content
v/v	Volume fraction
VW	Active water volume fraction
w/w	Weight fraction
W_i	Mass of water
λ	Failure rate of a repairable plant item (y^{-1})
λ_S	Unrevealed failure rate (yr^{-1})

TABLE OF CONTENTS

LIST OF FIGURES

LIST OF TABLES

CHAPTER 1 : INTRODUCTION

1.1 Background

In this age of diminishing fossil fuels, the UK energy market is becoming increasingly dependent on nuclear power. The success of the nuclear power option partly relies on the safe performance of existing nuclear chemical plants, which are approaching the end of their operational life. Accordingly, the UK government strategy, led by the Nuclear Decommissioning Authority (NDA), is to enable an accelerated hazard reduction through decommissioning of the existing aged nuclear facilities [*NDA, 2016*]. However, accelerated risk reduction requires a good understanding of the key hazards and how the associated uncertainties can be managed effectively.

Some facilities within existing nuclear chemical plants awaiting decommissioning were used for underwater storage of metallic magnesium waste, referred to as 'Magnox', generated from historic de-canning of nuclear fuel rods. As part of the NDA's hazard reduction programme, the waste is required to be removed from these existing facilities, containerised, and stored safely in small vessels until a suitable geological waste repository becomes available. Reprocessing operations within nuclear chemical plants also result in heat generating radioactive liquors that are required to be cooled before further treatment.

Often safe storage of the retrieved waste from existing facilities is achieved through immobilisation by mixing with cement grout formulations. Characterisation, size reduction of the waste, and selection of appropriate waste mixing parameters are necessary to ensure acceptable product quality whilst maintaining the desired throughput.

The waste characterisation and size reduction operations need to be performed remotely using robotics. The use of robotics is necessary primarily to protect the workforce from the radioactivity associated with the waste that would require a high degree of containment and isolation. Some decommissioning operations require the radioactivity content of the solid waste to be controlled to prevent a nuclear fission chain reaction, commonly referred to as a 'criticality' [*Putley and Prescott, 2007*].

The diverse nature of nuclear reprocessing and decommissioning operations discussed above results in a variety of uncertainties. Perhaps one of the greatest uncertainties is the risk from hydrogen gas released either during the corrosion of Magnox waste as a result of underwater storage or due to radiolysis of radioactive liquors. Long-term corrosion of Magnox waste also leads to the formation of magnesium hydroxide sludge. One of the most significant challenges comes from the hold-up of hydrogen in sludge

waste forms and a sudden discontinuous release of the gas. Potentially up to 40 litres of hydrogen could be released discontinuously into a typical $3m^3$ storage vessel with an ullage space volume of 200 litres.

The properties of hydrogen are unique in that its flammable concentration band is wide and the energy required for ignition is very low such that the likelihood of ignition of this gas is higher in comparison with other combustible gases [*Gummer and Hawksworth, 2008*]. *Zalosh et al, 1978* carried out a statistical review of hydrogen incidents in the United States energy sector over a 16 year period. As illustrated in Figure 1-1, they showed that the ignition sources for a significant proportion, i.e., up to 28%, of the hydrogen incidents were unknown.

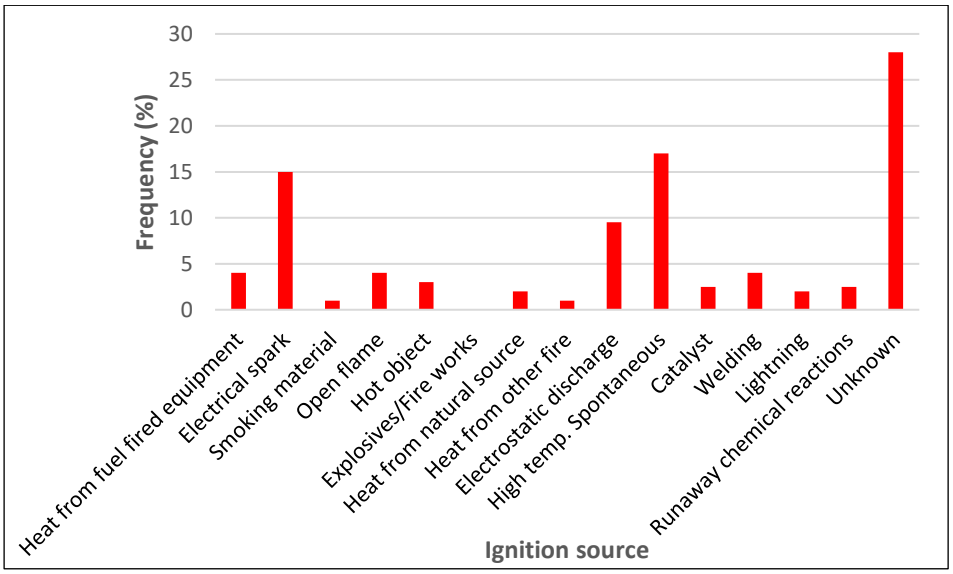

Figure 1-1: Distribution of hydrogen incidents by ignition source [*Zalosh et al, 1978*]

The severity of the hazard from hydrogen is dependent on the type of hydrogen incident, which varies from pressure ruptures and burst tanks to large scale explosions. The European Hydrogen Incidents and Accidents Database (HIAD) reported by *Galassi et al, 2010,* shows that from the various types of hydrogen incidents over the period 1985 to 2006, 48% of the events resulted in an explosion (Figure 1-2). The relatively high proportion of the events resulting in a fire or an explosion shows that a hydrogen incident is likely to cause a significant hazard in terms of potential consequences.

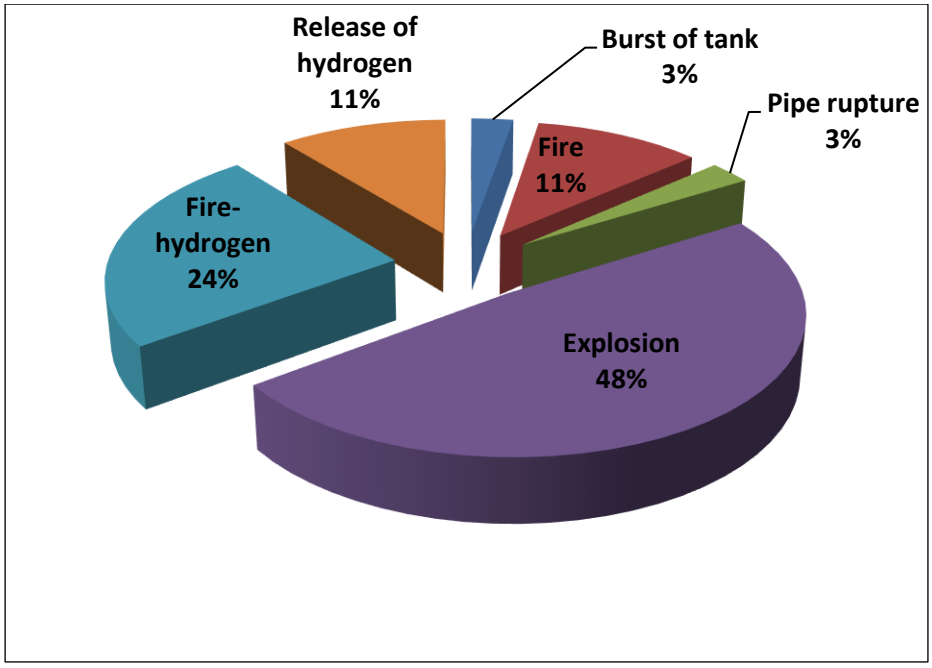

Figure 1-2: Distribution of consequence type from hydrogen generation [*Galassi, et al, 2010*]

The consequences of hydrogen explosions in chemical process plants can be significant, ranging from mortality or serious workforce injury to loss of plant assets. The types of consequences from a sample of 213 hydrogen incidents before 2007 in France and other European countries [*French Republic, Ministry of ecology, energy, sustainable development, and country planning, 2009*] are illustrated in Figure 1-3. This study showed that from the various types of consequences, damage to internal plant assets was by far the most frequent.

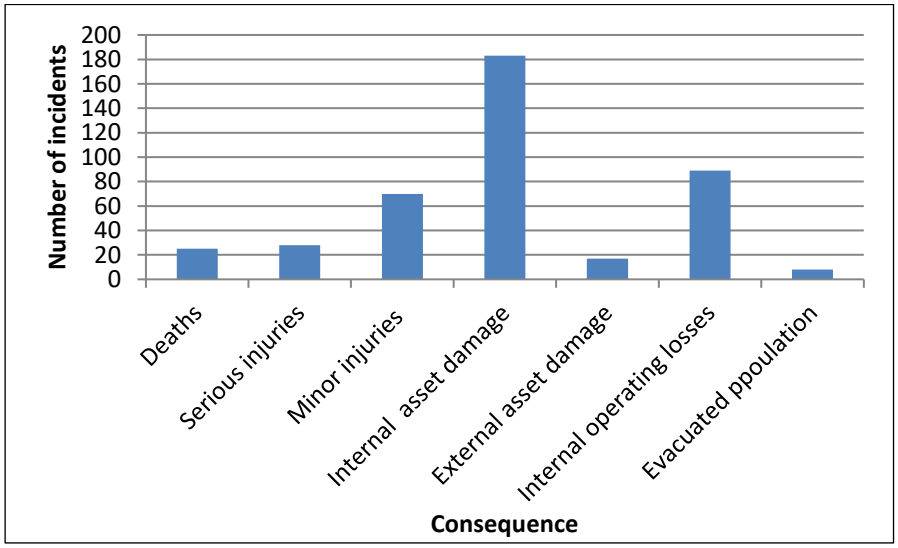

Figure 1-3: Histogram of number of hydrogen incidents vs consequence [*French Republic, Ministry of ecology, energy, sustainable development, and country planning, 2009*]

Intuitively, hydrogen explosions causing plant damage within nuclear installations can result in the added consequence of a radiological release. The well documented severe nuclear accidents such as Chernobyl, Three Mile Island, and Fukushima Daichaii [*Gharari et al, 2018*] demonstrate the radiological detriment associated with hydrogen explosions which must be avoided (Figure 1-4).

Figure 1-4: Hydrogen explosions at the Fukushima Daichaii nuclear power plant [***Opensourceinvestigations.com***]

The worldwide major incidents have led to the development of a robust regulatory framework within the UK's nuclear waste reprocessing and decommissioning industry. The Office for Nuclear Regulation (ONR) Safety Assessment Principles (SAPs) [*ONR, 2020*] require demonstration of robust design and safety systems against initiating events that could lead to radiological consequences. This is referred to as a 'fault-tolerant' design by *ONR, 2020*. Given that a fault leading to a hydrogen explosion in a nuclear environment could lead to a radiological risk, the design against such a hazard would also require demonstration of fault tolerance in order to satisfy the ONR SAPs.

In addition to the ONR expectations, the Health and Safety at Work Act, 1974 places a legal requirement for the Duty Holder of a nuclear facility to reduce the risk to its employees and the members of the public so far as reasonably practicable, or 'As Low As Reasonably Practicable' (ALARP) [*HSE, 1992*]. The Health and Safety Executive (HSE) decision-making process, referred to as 'Reducing Risks, Protecting People', sets the regulatory framework for ensuring the risk is ALARP [*HSE, 2001*]. However, the demonstration of ALARP often requires supporting evidence that the quantified risk is sufficiently low.

There are many dependent variables associated with the hydrogen generation and explosion mechanisms in nuclear chemical plants. The complexities associated with

the quantified risk from hydrogen mean that new approaches, in addition to current standard practice, for managing the uncertainties need to be found for certain nuclear decommissioning and processing situations.

One key factor in the risk of hydrogen explosions is the likelihood of ignition. In many traditional nuclear safety assessments, the probability of ignition has been conservatively assumed to be unity. However, this assumption may be somewhat pessimistic such that the final calculated risk can be misleadingly high. This subsequently leads to a complex design of high integrity safety systems against hydrogen accumulation, as well as extensive design substantiation [*HSE, 2014*]. Whilst such design substantiation is appropriate for greenfield hydrogen safety cases, this has a detrimental impact on nuclear decommissioning operations as the resultant increased timescales for design implementation can hinder decommissioning. Such detriments are contrary to the strategy set by the government [*NDA, 2016*] and the Office for Nuclear Regulation (ONR) for the acceleration of nuclear decommissioning [*ONR, 2017*]. Effectively this suggests that the risk from decommissioning operations needs to be balanced against the risk from the delay.

Significant research has already been undertaken by the Explosions and Fire Research (EFR) group at London South Bank University (LSBU) to explore the viability of technologies for the management of the hydrogen hazard in nuclear chemical plants. Based on this underpinning research work, using a combination of empirically derived relationships and best practice, a Hydrogen Technical Guide (HTG) and associated road map has been developed by *Ingram et al, 2001* and *Jones et al, 2006a*. This guidance was produced to enable assessment of hydrogen releases, the potential consequences and to identify appropriate risk mitigation and prevention techniques.

The HTG was developed in support of the Sellafield Ltd (SL) Hydrogen Working Party (HWP), the body advising hydrogen safety issues encountered across the Sellafield sites, and it has been used comprehensively in a wide range of nuclear safety cases. However, the complexities associated with specific processing and decommissioning environments present some knowledge gaps and uncertainties on the hydrogen assessment methodologies given in the guide.

Much of the research work carried out at LSBU has concentrated on ignition of hydrogen and consolidating factors that affect the likelihood of ignition. A plethora of research data are available on factors affecting ignition and the behaviour of various risk prevention and mitigation techniques. However, the application of these data to accurately assess the quantified risk, i.e., the likelihood, of hydrogen explosions and

hence to aid appropriate decision making in nuclear safety cases is an area of uncertainty which needs to be further explored.

Standard industry practice for a Quantified Risk Assessment (QRA) of an accident scenario is to initially conduct Hazard and Operability (HAZOP) studies to identify credible faults at a facility [*Bedford and Cooke, 2001, Vose, 2008*]. This is followed by a Hazard Analysis (HAZAN) of the identified faults. Fault Tree Analysis (FTA) and Event Tree Analysis (ETA) are often undertaken in support of the HAZANs to assess the quantified risk. A major drawback in both techniques is that they have a limited ability to model risk scenarios where there are many dependencies and complex interactions between parameters affecting the fault hypothesis. The complex interactions associated with hydrogen ignition hazards in nuclear chemical plants is an example which falls in this category.

Monte Carlo (MC) simulation [*Vose, 2008*] and Bayesian Belief Networks (BBN) [*Bolstad, 2007, Jensen and Nielsen, 2007*] are alternative techniques which can provide a means for overcoming the limitations of FTA and ETA discussed above, allowing uncertainty and interactions between different factors to be considered in a risk assessment. In particular, the BBN approach can provide a powerful way of structuring probabilistic information and dependencies between key factors, managing uncertainty, and quantifying the likelihood of different outcomes occurring [*Hanea et al 2009, Pasman et al, 2012*]. As such the application to hydrogen safety issues has been identified as a research priority [*Kotchourko et al, 2013*].

During the research on hydrogen issues in nuclear chemical plants, discussions were also held with the SL sludge wastes, criticality and equipment reliability groups to identify any uncertainties in these areas. Based on the discussions with these groups, as detailed in the meeting minutes by *Ahmed, 2015, Ahmed, 2017c* and *Ahmed, 2018b*, it is considered that the BBN technique could also be applied to resolve plant operability uncertainties. The specific operability issues are associated with waste mixing and use of robotics for nuclear waste characterisation and size reduction. It is considered that the uncertainty associated with criticality reactions in containers of solid wastes could also be assessed using BBNs.

1.2 Aim

The main objective of the proposed research is to explore the application of the emerging BBN and MC QRA techniques to analyse the uncertainty associated with hydrogen hazards and identify fit for purpose means of managing the uncertainty. The research investigates the application of BBN and MC analysis to issues covered in the

SL Hydrogen Technical Guide, e.g., to provide an improved means of incorporating expert judgement into the decision-making process.

Whilst the research focusses on the uncertainties associated with hydrogen hazards, it also examines the application of the BBN technique to resolve plant operability issues. This includes grout mixing of sludge wastes, characterisation of solid wastes using robotics and the likelihood of a criticality. A further aim is to examine how BBN's and MC simulations may be used to supplement the Event and Fault Tree Analysis used in the current SL safety analysis.

The above aims have been achieved through the following activities:

i) Performance of a literature review of the SL Hydrogen Technical Guide (HTG), previous research in the field of hydrogen safety, risk assessment and uncertainty management with particular emphasis on BBN and MC simulation techniques.

ii) Gaining familiarity and practice with software simulation packages (e.g., Netica and RiskAmp) to determine an appropriate research methodology.

iii) Development of a suitable approach for modelling the uncertainty associated with hydrogen hazards and other nuclear plant operability issues using Bayesian Belief Networks and Monte Carlo simulations. The approach included engaging SL Subject Matter Experts, e.g., incorporating the HWP advice into the analysis.

iv) Application of the BBN approach developed in (iii) to a selection of hydrogen safety and plant operability case studies. This included identification of areas where the greatest uncertainties lie in terms of hydrogen safety and other operability issues in nuclear chemical plants. The best practicable means of managing the uncertainty were also identified, e.g., through the derivation of conditions for achieving the least hazardous state and the mitigating measures needed to reduce the risk.

v) Validation and comparison of the case study results through testing each model with a range of values for the input parameters and demonstrating consistency with expected trends. A comparison with the relevant existing experimental and modelling work was also undertaken to demonstrate the reliability of the results. To identify the method that gave the best results, sensitivity analyses were carried out and the BBN and MC results were compared with the FTA and ETA techniques.

vi) Using the evidence from (iv) and (v) to recommend the most appropriate strategies for managing the hydrogen hazards and operability issues. The

evidence was also used to recommend appropriate methods for the risk assessment of hydrogen hazards and plant operability issues at SL.

1.3 Thesis Structure

To demonstrate how each research objective has been met, the thesis is structured as follows:

Chapter 2 provides a literature review of the hydrogen release mechanisms in nuclear decommissioning and reprocessing environments. The current standard practice, procedures, and guidance being used at these facilities for quantified risk assessments are reviewed, focusing on hydrogen safety. A literature review of industrial applications of modern QRA methodologies, i.e., FTA, ETA, BBN, and MC, primarily in the field of hydrogen safety, is also undertaken.

Chapter 3 determines the methodology to be used in the research project to analyse and manage the uncertainty from hydrogen safety and operability issues in nuclear chemical plants. Research into the selection of appropriate software systems for undertaking the uncertainty analysis is also discussed.

The meetings held with the SL hydrogen safety, sludges, and reliability engineering specialists aimed to identify suitable case studies in nuclear chemical plant areas that present the greatest uncertainties and how they could be resolved. Chapters 4 to 10 provide details of the main research involving the application of the BBN and MC methods as a means of uncertainty analysis, to seven plant case studies representing specific nuclear decommissioning and reprocessing operations.

Chapter 4 details Case Study 1 on the BBN analysis of radiolytic hydrogen generation in sealed process pipes. In this case study expert opinion is applied to reduce the uncertainty on the likelihood of hydrogen deflagration or detonations in sealed pipes.

Chapter 5 details Case Study 2 on the application of BBNs to investigate the uncertainty associated with the mixing of radioactive sludges in the waste treatment and encapsulation process. Through the application of BBNs, the case study determines whether the grouted sludge can be removed from the mixing vessel without reducing plant throughput. The output of the research based on this case study has also been published by the candidate in the Institution of Chemical Engineers (IChemE) Chemical Engineer magazine [*Ahmed, 2017b*]. This is summarised in Appendix H, Table H-1.

Chapter 6 details Case Study 3 on the application of the MC simulation and BBN techniques to investigate the likelihood of a ventilation extract system failure to dilute hydrogen gas in the ullage space of a process vessel. This case study demonstrates

how MC simulations could be mapped on to FTAs as an improved means of determining the uncertainty associated with failures of the hydrogen dilution systems. A comparison of the results is also made with a BBN analysis of the same model. The output of the research based on this case study, in terms of the methodology for the assessment of the hydrogen dilution system reliability, has been published by the candidate in the Proceedings of the IChemE Hazards 29 Conference [*Ahmed, 2019b*]. This paper is summarised in Appendix H, Table H-3.

Chapter 7 details Case Study 4 which explores the uncertainty associated with hydrogen hold-up in sludge waste forms and a sudden discontinuous release of the gas into the ullage space of a transportable vessel. Through the application of BBNs, the potential for exceeding the Low Flammable Limit (LFL) of the hydrogen in air mixture in the vessel ullage space is investigated. The output of the research based on this case study has also been published by the candidate in the Nuclear Future, Journal of the Nuclear Institute [*Ahmed, 2019a*]. Appendix H, Table H-2 provides a summary of this paper.

Chapter 8 investigates the application of BBNs to determine the likelihood of a criticality in containers of material mixed with PuO_2. This fifth case study explores the use of probability distributions of the mass of PuO_2 and water as an improved means of analysing the uncertainty associated with the risk of a criticality. Through the application of Bayesian inference the best means of reducing the risk of a criticality to negligible levels is investigated.

Chapter 9 examines the application of the Bayesian Decision Network methodology for installing a compressed air supply to mitigate the risk of hydrogen explosions in ancillary process vessels. This sixth case study also compares the performance of the standard FTA technique with BBNs and demonstrates the benefits of the latter in terms of assessing equipment reliability.

Chapter 10 details the seventh case study which explores the use of Bayesian networks to assess the reliability of robots for waste characterisation and size reduction in radiation environments.

Chapter 11 provides a discussion and conclusions of the research detailed in Chapters 2 to 10. Based on a critical analysis of the key findings, recommendations are also made.

CHAPTER 2 : LITERATURE REVIEW

2.1 Introduction to Chapter 2

This chapter provides a literature review, with the prime objective of identification of areas of uncertainty and knowledge gaps in the field of hydrogen safety and operability issues in nuclear chemical plants. A critical review of worldwide literature is given in terms of the key factors affecting the risk of hydrogen explosions. This is followed by a review of standard practices, procedures and guidance being applied for the assessment of the risk of hydrogen explosions. Any knowledge gaps from the existing worldwide research, practices and procedures in the field of hydrogen safety are then identified.

A review of alternative modern techniques which could be applied as an enhanced means of assessing the risk and uncertainty associated with hydrogen explosions and plant operability issues is also carried out. To investigate the benefits of the alternative techniques, a literature review of industrial applications of such methodologies, primarily in the context of hydrogen safety, is also undertaken.

The literature review also includes research in the form of advice sought from the SL Subject Matter Experts (SMEs) in hydrogen safety, as well as other operability issues, to identify knowledge gaps in terms of risks and uncertainties in nuclear chemical plants. The overall aim is to identify plant case studies which require resolution of such knowledge gaps and uncertainties.

2.2 Review of research in the field of hydrogen safety

2.2.1 Sources of hydrogen gas in nuclear chemical plants

Hydrogen gas generation is common in many nuclear chemical plants, therefore as discussed by *Ingram et al, 2001*, hydrogen safety has become a key priority for such facilities. In particular, the need for consistency in the hydrogen safety cases for various nuclear chemical plants was identified in 1995. Accordingly, a Hydrogen Working Party (HWP) group was organised within Sellafield Ltd (SL) with the main purpose of setting a benchmark to ensure consistency between the various safety cases.

As with any gas explosion scenario, the key variable that dictates the risk of a hydrogen explosion in a vessel, pipe or an enclosure is the rate of accumulation of the gas, which is affected by the source. Hence, the HWP initially focussed on the identification of the various sources of hydrogen and the types of nuclear chemical plants where the gas is generated. In support of the HWP, as reported by *Ingram et al, 2001* a Hydrogen Technical Guide (HTG) was developed by the LSBU Explosions and Fires Research (EFR) group. The main purpose of the HTG was to enable assessment of hydrogen release mechanisms including the generation rate, potential consequences and to

suggest appropriate risk mitigation and prevention techniques. Key aspects of the HTG are that it provides:

- Details of the hydrogen hazards which could potentially arise in nuclear chemical plants.
- Guidance on design principles for new and existing plants, e.g., use of active or passive safety systems and control of hydrogen concentration in vessels and enclosures.
- Guidance on the decision-making process for designers and assessors, using a road map approach.

As part of this research project, case histories of nuclear chemical plants in which hydrogen generation was a problem or where a problem was initially perceived to exist, were reviewed. This review was achieved through discussions with the HWP to identify any areas of uncertainty. Additionally, the HTG was reviewed to identify uncertainties, e.g., factors affecting the derivation of the hydrogen generation rate, ignition sources and the associated probability in nuclear decommissioning and reprocessing environments.

Based on the discussions with the HWP and a review of the HTG, Appendix A1 lists the hydrogen generation mechanisms and the associated hydrogen safety issues for the various nuclear chemical plants. The main hydrogen generation mechanisms can be summarised as follows:

- Corrosion of metallic magnesium fuel cladding (Magnox) waste retrieved from storage facilities to form magnesium hydroxide sludge and hydrogen gas within transportable storage vessels, referred to as the ‘skips’.
- The slow release of hydrogen due to radiolysis of aqueous liquors within the storage skips.
- Transient discontinuous release of stored hydrogen gas from sludge waste forms in storage skips.
- Generation of hydrogen due to radiolysis in process plant vessels used for reprocessing of radioactive liquors.
- Generation of radiolytic hydrogen in sealed process pipes containing radioactive liquors.

The following sections provide a detailed review of each of the main sources of hydrogen generation mechanisms identified above, i.e., radiolysis, chemical corrosion and release of stored gas from sludge wastes such as magnesium hydroxide.

2.2.2 Hydrogen generation due to radiolysis

Radiolysis is by far the most common source of hydrogen in process vessels and pipes containing radioactive liquors. The precise mechanism for hydrogen generation through radiolysis is that the decay energy from the alpha (α) and beta-gamma (β/γ) radioactivity in aqueous liquors results in the dissociation of the water molecules. This leads to the formation of hydrogen gas and the hydroxyl radical. *Le Caer, 2011* provides a detailed description of the mechanism of water radiolysis to form hydrogen. This occurs over three distinct phases, i.e., Physical, Physico-chemical and Chemical phases, as summarised below:

The Physical stage involves the absorption of the radiation energy to form ionised water molecules (H_2O^+) and excited electrons (e^-), as well as the excitation of the water molecules in accordance with the following reactions:

$$H_2O \rightarrow \text{Ionising radiation} \rightarrow H_2O^+ + e^- \quad (2\text{-}1)$$

$$H_2O \rightarrow \text{Excitation} \rightarrow H_2O^* \quad (2\text{-}2)$$

In the Physico-chemical phase the ionised water and water molecules react to form the $HO^{\bullet}$ radical and the hydronium ion (H_3O^+). Dissociative relaxation of the H_2O^* species and solvation of electrons to form e^-_{aq}, also occur as follows:

$$H_2O^+ + H_2O \rightarrow H_3O^+ + HO^{\bullet} \quad (2\text{-}3)$$

$$H_2O^* \rightarrow \text{Dissociative relaxation} \rightarrow HO^{\bullet} + H^{\bullet} \quad (2\text{-}4)$$

$$e^- \rightarrow \text{Electron solvation} \rightarrow e^-_{aq} \quad (2\text{-}5)$$

In the Chemical Stage, the solvated electrons and the radicals react to form hydrogen and the hydroxide anion (OH^-) as represented by the following reactions:

$$e^-_{aq} + H^{\bullet} + H_2O \rightarrow H_2 + OH^- \quad (2\text{-}6)$$

$$H^{\bullet} + H^{\bullet} \rightarrow H_2 \quad (2\text{-}7)$$

$$e^-_{aq} + e^-_{aq} + 2H_2O \rightarrow H_2 + 2OH^- \quad (2\text{-}8)$$

Ingram et al, 2001 consider that the prime source of radioactivity within the sealed process pipework, such as cooling coils, is the radioactive process liquor within the bulk liquor storage tanks. If a radiolysis reaction occurs in the pipework, the resultant hydrogen gas would mix with oxygen either from the air in the pipework or from radiolysis. This could potentially result in a flammable gas mixture forming within the pipe ullage space.

The actual rate of radiolytic hydrogen generation is directly proportional to:

- The amount of radioactivity available for decay.
- The rate of absorption of the energy by the water.
- The 'G value' which is the number of molecules of hydrogen produced per 100eV of energy absorbed.
- The magnitude of the G value, which is affected by the vessel or pipe contents being irradiated by the α or β/γ radiation.

On the above basis the rate of radiolytic hydrogen generation, $Q_{H,}$ can be expressed by equation 2-9:

$$Q_H = kG(H_2)_{(\alpha)}E_{(\alpha)} + kG(H_2)_{(\beta\,\gamma)}E_{(\beta\,\gamma)} \quad (2\text{-}9)$$

Where:

- $G(H_2)_{(\alpha)}$ and $G(H_2)_{(\beta/\gamma)}$ are the G values for alpha and beta-gamma radiation, respectively.
- $E_{(\alpha)}$ and $E_{(\beta/\gamma)}$ are the rates of absorption of alpha and beta-gamma decay energy (MeV/s), which are the product of the amount of radioactivity by the alpha and beta-gamma decay energies, respectively.
- k is a constant with a value of 1.44×10^{-15}.

The Hydrogen Technical Guide (HTG) considers that the G value for aqueous solutions will differ from nitrate solutions. In nuclear reprocessing operations, the nitrate solutions are produced when the metallic cladding waste from the spent reactor fuel rods is dissolved in nitric acid to remove the residual radionuclide material. The resulting nitrate solutions are required to be stored in vessels prior to treatment and disposal. For aqueous liquors, the alpha and beta-gamma radiation G values are reported as 1.6 and 0.45 molecules H_2 /100eV, respectively, by *Bibler et al, 2007*. They have also reported a worst case decay energy of alpha radionuclides as 5.5MeV. For beta-gamma radionuclides a decay energy of up to 0.662 MeV is also known [*IAEA, 2003*] . For nitrate solutions arising from nuclear reprocessing operations, much lower G values are reported by the HTG.

Whilst equation 2-9 represents the most common methodology for the assessment of radiolytic hydrogen generation rate and given that this is directly proportional to the G value, the HWP advice is that this parameter must be treated with caution. For instance, if there is any uncertainty on the type of radiation present in a vessel or pipe, i.e., alpha,

beta, gamma or all three, then potentially this could lead to inaccuracies in the G value and hence the rate of hydrogen generation.

A further complexity associated with radiolysis is that the chemical composition of the pipe or vessel medium, e.g., the presence of ferrites, can prevent the radiolytic decomposition of water. For instance, *Le Caer, 2011* provides a detailed review of radiolysis of water in nuclear reactors and considers that the hydrogen and hydroxyl radicals produced from the reaction can lead to the conversion of the product species back to water. Essentially the radiolytic decomposition of water is dependent on its purity. Hence, the possibility of chemical contaminants in the pipe or vessel medium, such as ferrites, is a factor which should be taken into consideration when assessing the likelihood of radiolytic hydrogen generation.

2.2.3 Hydrogen generation due to corrosion of stored metallic magnesium

Historic nuclear reprocessing operations required long-term storage of Magnox waste, submersed in water, within large storage facilities. Such storage operations have resulted in corrosion of the waste to form magnesium hydroxide sludge and generation of hydrogen gas as a secondary product. As part of the Nuclear Decommissioning Authority's (NDA) strategy for disposal of bulk Magnox waste retrieved from the storage facilities, there is a requirement for interim safe storage of the material immersed in water in small transportable skips over many years. This will result in corrosion of the waste and generation of hydrogen gas within the skip ullage space. Continuous corrosion of Magnox waste over time will also result in the formation of magnesium hydroxide sludge.

Averill et al, 2018, have undertaken a close examination of the reaction of uncorroded Magnox with water leading to the production of hydrogen gas in skips. The main factors that contribute to the corrosion reaction, and hence the rate of hydrogen generation, were identified as:

- Amount of uncorroded Magnox available for the reaction.
- The pH of the waste material.
- Waste temperature.
- Mechanical damage to the protective film on the Magnox.

One of the main uncertainties identified by *Averill et al, 2018* was the amount of Magnox available for the reaction. It was considered that this is a key factor which is dependent on the surface area of the uncorroded Magnox for a given amount of the waste. Potential damage to the protective layer on the Magnox that forms when the waste pH is higher than 11, will also lead to an increased surface area available for the corrosion reaction.

It was also considered that a waste temperature range of 55 to 65^{o}C has a significant effect on the corrosion rate. A mean hydrogen generation rate of 0.2 L/hr was predicted which was based on the following values for the key variables:

- Mean weight to surface area ratio of 2.8.
- Mean mass of uncorroded Magnox of 4.6kg.
- Mean waste temperature of 22.5 ^{o}C.
- 85% chance of no mechanical damage to the Magnox protective coating.

2.2.4 Sudden release of stored hydrogen

Some of the hydrogen gas can potentially be held within the sludge material in skips, leading to swelling or expansion of the waste. This type of gas behaviour has been studied by *van Kessel and van Kesteren, 2002*, who reported that the gas generated in sludge beds being released to the surface is dependent on the sludge shear strength. For materials, such as Magnox sludge with low shear strengths, the evolved gas bubbles will most likely lead to the gas being trapped within the waste and hence expansion. Ultimately a proportion of the held-up gas within the sludge matrix could be released discontinuously to the skip liquor surface. Some of the evolved hydrogen will continually flow to the surface of the skip liquor and be released via the filtered vents such that an equilibrium hydrogen concentration is reached in the skip ullage space. However, the volume of hydrogen released discontinuously could potentially be significant, leading to a concentration of hydrogen in the ullage space close to or above the Lower Flammable Limit.

2.2.5 Hydrogen flammability

Knowing the precise concentration range at which hydrogen in air mixtures are flammable is key to determining the likelihood of hydrogen explosions in a given environment. For instance, some hydrogen generating environments can be rich in oxygen while in other cases the oxygen level is low. The hydrogen flammability will differ in either of these cases.

The unique properties of hydrogen, i.e., a wide flammability range, high burning rate in comparison with hydrocarbons, and a large amount of energy released following an explosion are well acknowledged for instance by *Coward et al, 1952* and *Gummer et al 2008*. Further research on the flammability of hydrogen and hydrocarbons has also been carried out by *Cashdollar et al, 2000* in support of the Pittsburgh Research Laboratory in the US. In reference to this existing literature, the flammability range of hydrogen in air mixtures at atmospheric pressure is known to be 4 - 75% v/v. This wide range would

suggest that the likelihood of hydrogen explosions is significant. Therefore, implementing adequate controls against the hazard would become challenging.

A further challenge faced within nuclear chemical plants is the uncertainty associated with the flammability of hydrogen in depleted oxygen environments such as sealed pipes. For instance, the oxygen level in isolated cooling coils within tanks containing radioactive liquors is likely to be depleted due to the gradual consumption of the gas by corrosion of ferritic contaminants within the pipework. Such depleted oxygen environments will result in a flammability range that is different from normal hydrogen in air mixtures.

For depleted oxygen atmospheres, *Holborn et al, 2013* have undertaken a detailed review of the Upper Flammability Limit (UFL) of hydrogen. For hydrogen rich mixtures where the oxygen depletion is achieved using 65%v/v of added nitrogen, *Holborn et al, 2013* show that the UFL is as low as 10%v/v. For environments without any oxygen depletion, the UFL is 75%v/v. In terms of the LFL for depleted oxygen atmospheres, *Holborn et al, 2013* suggest that the prediction of this limit is significantly more complex due to instabilities of the flame front which typically occur at the low hydrogen concentration ranges.

For isolated and sealed cooling coils in nuclear chemical plants, the potential for detonation of hydrogen in air mixtures also needs to be considered. Based on the work of *Grossel,2002, Kuo, 2005 and Nettleton, 1987; Dahoe, 2011* summarises that for mixtures of hydrogen in pure oxygen within confined spaces, the lower and upper limits of hydrogen concentration required for a detonation are 15%v/v and 90%v/v respectively. This suggests that for atmospheres rich in oxygen within confined areas, the hydrogen concentration range required for a detonation is very wide. Hence in these conditions the likelihood of a detonation is significantly increased. The confined lower and upper detonation limits for hydrogen in air mixtures are reported as 18.3%v/v and 58.9%v/v [*Lewis and von Elbe,1961*]. Whilst no specific detonation limits are specified in literature for depleted oxygen atmospheres, by inference it is considered plausible that the lower detonation limit would be above 18.3% v/v and the upper limit being below 58.9%v/v.

The work of *Coward et al, 1952*, concerning the wide flammability range of hydrogen, has led to an investigation of the main causes and effects of hydrogen explosions in the hydrogen processing industry, by *Mirza et al, 2018*. Their research revealed that the main root causes are technical and process plant design errors and operator error is the second most common cause. Almost 90% of the hydrogen explosion events in the processing industry resulted in harmful consequences to the operators and damage to

plant assets. A key recommendation against operator error is to provide adequate training and monitoring of maintenance workers.

2.2.6 Sources of hydrogen ignition

Ignition sources of hydrogen and the associated ignition probability under different nuclear reprocessing and decommissioning environments is a further area of uncertainty which affects the scope of this research project. The HTG outlined by *Ingram, et al, 2001* presents the current standard methodology for the assessment of ignition probability of flammable hydrogen in air mixtures. A step-by-step road map approach is presented to provide an assessment method for safety cases where a quantification of the ignition probability is required. However, the guidance places an important caveat that a quantification of the ignition probability should only be undertaken in cases where no deterministic options are available and where special probabilistic risk arguments are needed.

In addition to the caveat discussed above concerning the ignition road map technique outlined by *Ingram et al, 2001*, it is noted that the method is restricted to a particular set of initiating events and ignition source conditions which may not always be relevant to some fault scenarios. The lack of flexibility in the road map means that alternative solutions for assessing the probabilistic risk from ignition need to be found. Bayesian Belief Networks and Monte Carlo Simulation, which are the context of this research project, could provide a much more sophisticated means of assessing the quantified risk from hydrogen.

Ignition of explosive gaseous mixtures is characterised by two parameters, which are the Minimum Ignition Energy (MIE) and the Autoignition Temperature (AIT). For hydrogen, the International Organisation for Standardisation (ISO) gives the MIE and AIT values of 0.017mJ and 585^{o}C respectively [*ISO/TR15916, 2015*]. Any ignition source that leads to operation above these limits will cause an ignition. In *BS EN 1127-1,2019* the main ignition sources for gaseous explosive atmospheres are identified as:

- Mechanically generated impact, friction and grinding.
- Static electricity
- Hot surfaces, flames and hot gases, leading to operation above the AIT.
- Electrical equipment and components
- Adiabatic compression and shock, due to sudden compression of gases and pressure relief leading to a high gas temperature.

Figure 2-1 illustrates the possible causes of each of these ignition sources in nuclear plants and the protective measures suggested by *BS EN 1127-1,2019.*

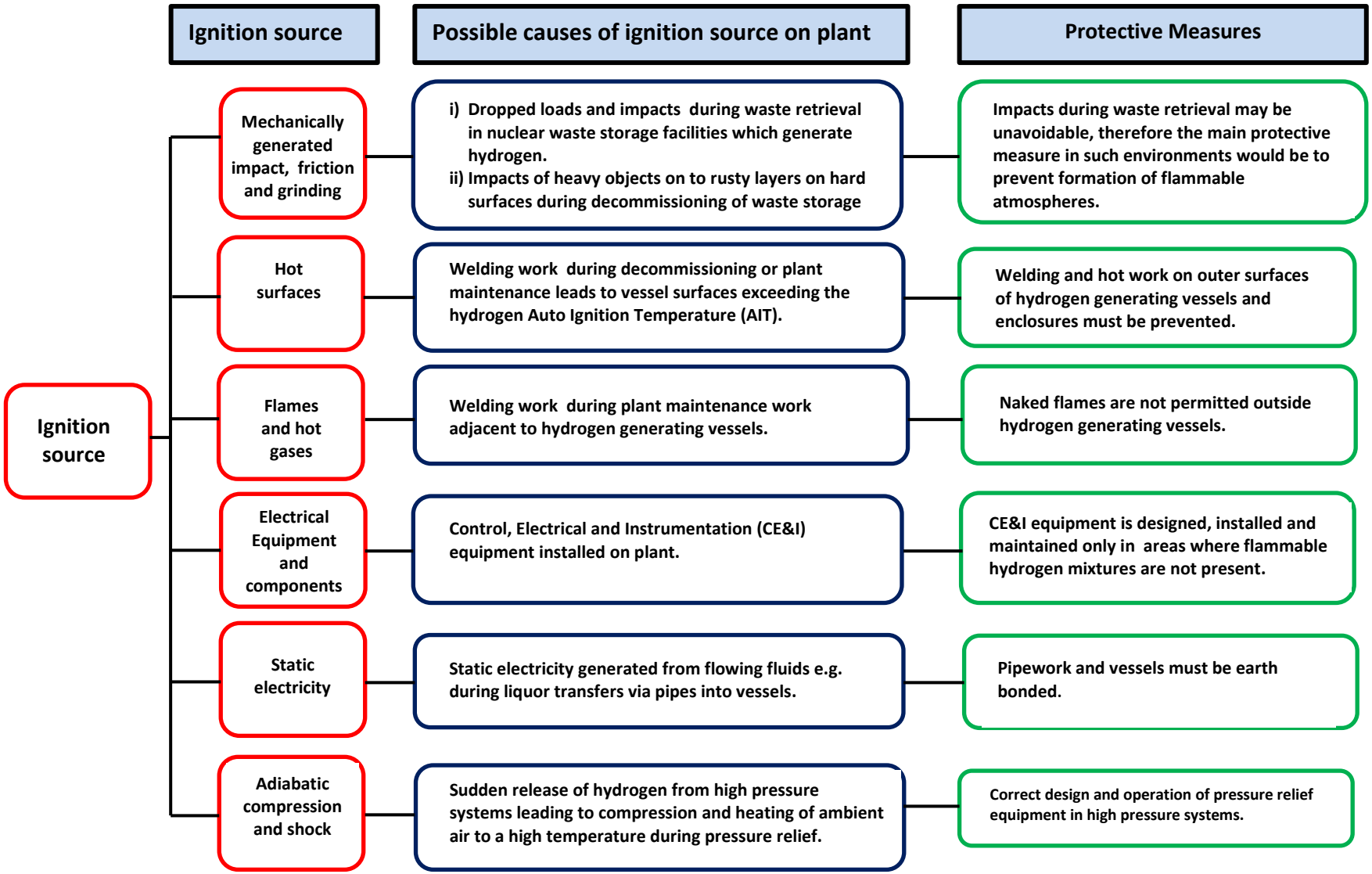

Figure 2-1: Ignition sources of hydrogen and associated protective measures in nuclear environments [*BS EN 1127-1,2019*]

The following sub-sections provide a review of the mechanisms and data for the main ignition sources relevant to nuclear decommissioning, which are mechanical impacts and static electricity.

2.2.6.1 Mechanically generated impact, friction and grinding

In previous experimental work by *Jones et al, 2006b*, it was shown that the most significant ignition sources of hydrogen with respect to energy and the likelihood of occurrence in nuclear decommissioning environments, are mechanical impacts on to metallic surfaces. *Rogers et al, 2006* show that friction also has the potential to cause localised hot spots, thus resulting in a credible ignition source. They have demonstrated that impacts, friction or grinding between metallic surfaces such as iron and steel can lead to the generation of burning particles and high localised temperatures. This can lead to an ignition of the flammable gaseous atmosphere. *Averill et al, 2015* state that the potential for an ignition is even higher if the impacting surfaces involve oxidising substances such as rust i.e., iron oxide, and magnesium particles. Iron oxide and magnesium can react together exothermically to produce large amounts of heat and temperatures exceeding 2000K.

Hydrogen ignition probability data based on mechanical impacts have also been determined previously. *Averill et al, 2014* have undertaken experimental work involving impacts of large mass projectiles on to a steel anvil plate covered with rust and magnesium particles in flammable mixtures of hydrogen in air. The impact energy was controlled by varying the projectile velocity. From a total of 11 tests involving a projectile mass of 14kg and an impact kinetic energy of 83J, only 1 ignition event was observed, giving an ignition probability of 0.09. However, for the same projectile mass but at a higher impact kinetic energy of 330J, all 11 tests resulted in an ignition, equating to an ignition probability of 1. With a higher projectile mass of 50kg but a lower impact energy of 140J, 10 tests from a total of 11 resulted in an ignition, equivalent to a probability of 0.91. The general trend from these results is that the likelihood of ignition rises with increasing impact energy and projectile mass.

2.2.6.2 Static electricity

Solid insulating materials such as plastics have the tendency to gain electrostatic charge. An electrostatic discharge can occur when two surfaces separate, potentially leading to an incendive spark. This charge transfer effect is analogous to a human hand contacting a plastic electrical switch that leads to a minor shock. Since plastics are used widely in industry, an electrostatic discharge from such materials is one of the most common ignition sources for flammable gas mixtures.

Various researchers including *Gummer et al, 2008*, *Ellis, 2008* and *Ackroyd, 2009* have investigated the effect of electrostatic discharges in flammable atmospheres. *Gibson and Harper, 1988* carried out experimental work to determine the ability of electrostatic discharges from non-conductors, such as polyethylene sheets, to cause an ignition of flammable gas atmospheres. They established that in order to ignite a flammable gas atmosphere with a Minimum Ignition Energy (MIE) of 0.04mJ, a discharge range of 8-20 nanocoulombs (nC) is needed. They also determined the effect of electrostatic discharges on the ignition probability for flammable atmospheres, with an MIE of 0.04mJ, and showed that it is directly proportional to the area of the charged surface.

The results of the experimental work by *Gibson and Harper,1988* are given in Figure 2-2 which shows that polyethylene sheets with a charged area of up to 10cm^2 resulted in an ignition probability of approximately 0.2. The lowest ignition probability of 0.001 was determined for a charge area of 4cm^2. This would suggest that the best means of minimising the risk of electrostatic discharges from non-conductors in flammable gas atmospheres would be to restrict the surface charge area to 4cm^2. The MIE of 0.04mJ used in these experiments is close to the value of 0.02mJ for hydrogen. Therefore, it is considered that these ignition probability results are representative of hydrogen gas flammable atmospheres.

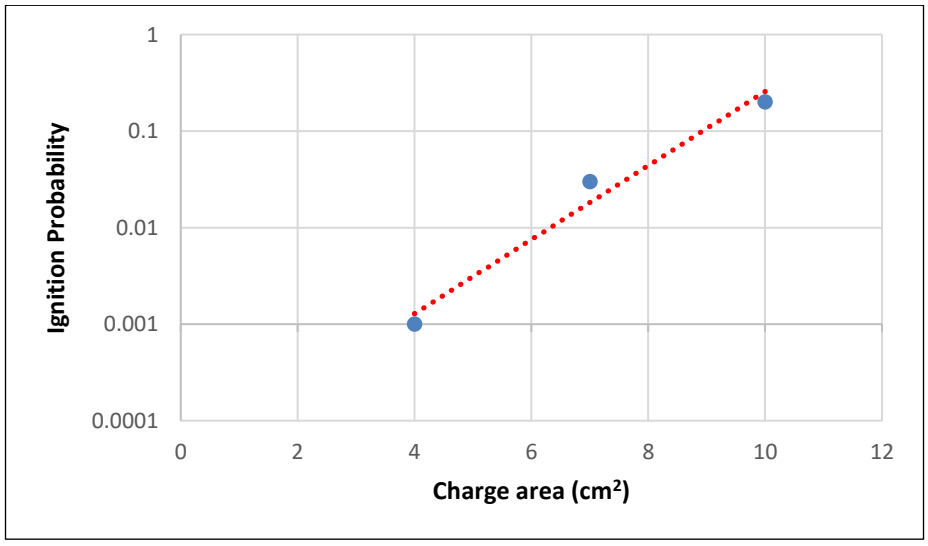

Figure 2-2: Ignition probability data for electrostatic discharges from polyethylene sheets [*Gibson and Harper,1988*]

Hydrogen is also known to ignite due to self-heating because of the exothermic combustion of the gas in the presence of an oxidant and a subsequent rapid rise in temperature beyond the AIT. Such a phenomenon is referred to as spontaneous ignition. *Gummer et al, 2008* have undertaken a literature review of the possible mechanisms that could contribute to spontaneous ignition. They concluded that a leakage of hydrogen gas

at high pressure and ambient temperature, and a subsequent electrostatic discharge, is likely to be the main source of spontaneous ignition.

2.2.7 Safety hierarchy for the management of the hydrogen ignition hazard

Based on the guidance by *Ingram et al, 2001*, the safety hierarchy principles for hydrogen hazards in nuclear chemical plants are illustrated in Figure 2-3.

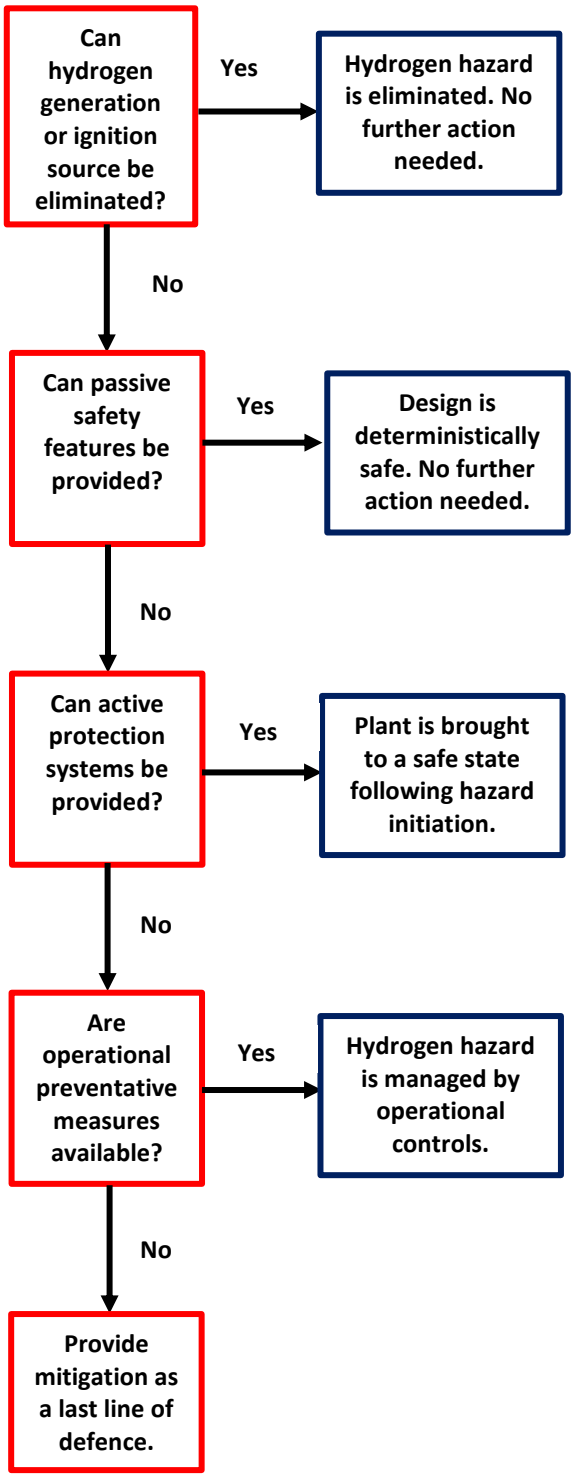

Figure 2-3: Hierarchy of plant controls against hydrogen ignition hazards

The hierarchy in Figure 2-3, which is based on the ONR Safety Assessment Principles (SAPs) [*ONR, 2020*], requires that the hydrogen explosion hazard should eliminated by design as a priority. Hazard elimination by design could be achieved e.g., by removal of the ignition sources. If this elimination is not possible then the system should be designed with passive features such that it can withstand hydrogen explosions, thus preventing any consequences. If passive features cannot be provided, then active safety measures, e.g., dilution or inerting systems, should be considered thus preventing the onset of the hydrogen explosion event.

If active safety systems cannot be provided then the next step in the hierarchy is to control the hazard through Operational Preventative Measures (OPMs) such as plant checks to ensure the system is operating in a safe configuration. If OPMs also cannot be provided, then mitigating measures such as building evacuation systems should be considered and minimise the consequences. However, this is the least preferred control measure in the hierarchy as it does not prevent the explosion hazard.

Typically, for the management of the slow hydrogen release mechanisms such as radiolysis, *Ingram et al, 2001* suggest the use of hydrogen dilution methods such as forced ventilation extract systems. In the case of skips of stored radioactive wastes, generating radiolytic hydrogen, passive features such as vent outlets in the vessels would also provide an effective means of eliminating the hazard.

Puttick, 2008 has explored the application of Basis of Safety (BoS) principles to identify the most appropriate means of minimising the risk from explosive atmospheres. He also considers the effectiveness of control of ignition sources as a Preventative BoS measure. He discusses that although avoidance of an ignition source is a good means of preventing a fire or explosion, this is dependent on a detailed knowledge of the plant and process.

2.3 Modern QRA techniques for nuclear safety cases

Quantitative risk analysis (QRA) provides a methodical structure for identification of hazards on a plant and means of preventing or mitigating fault scenarios [*Bedford et al, 2001, Vose, 2008*]. The uncertainties associated with dependencies between factors affecting the likelihood of a hazard scenario can potentially lead to errors and misjudgement of the true risk. Ultimately an inaccurately quantified risk can lead to an incorrect decision. This section explores the importance of accurate risk analysis in nuclear safety cases, from a regulatory perspective, and the tools used for risk quantification.

2.3.1 Radiological accident risk criteria and ALARP

The harm potential due to a release of radioactivity following a loss of containment from nuclear chemical plants can be significant. Some of the well-known major nuclear incidents linked with hydrogen explosions, such as Chernobyl and Fukushima as detailed by *Gharari et al, 2018*, have led to the development of numerical risk targets for the nuclear industry [*HSE, 2006*]. Although the numerical risk criteria are not legal limits, there is a legislative requirement to reduce the risk as far as reasonably practicable irrespective of whether the accident frequency is above the limits. However, the numerical criteria can help in determining whether the risk is As Low As Reasonably Practicable (ALARP). For example, a risk which exceeds the target may be a strong indicator that it is not ALARP. Compliance with the ALARP principle can be best illustrated by the 'Risk Carrot' in Figure 2-4.

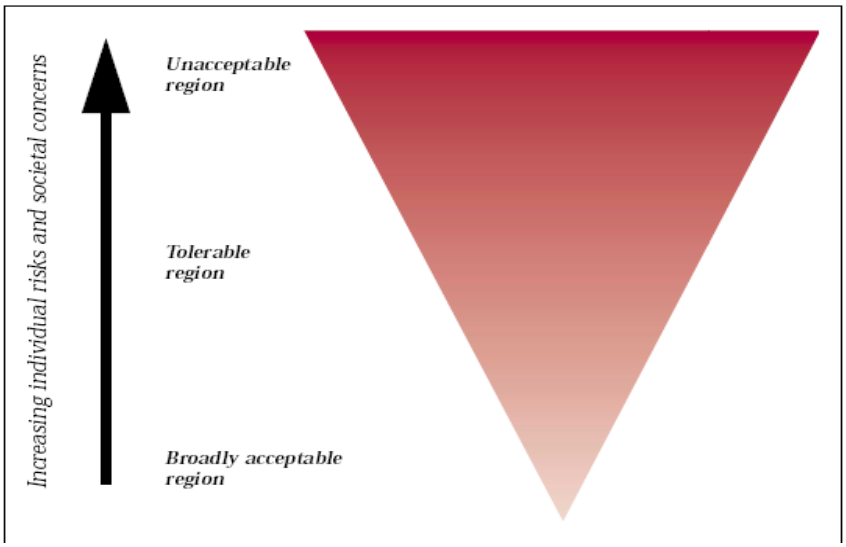

Figure 2-4: The 'Risk Carrot' illustrating the ALARP regions

The ONR identifies levels of accident risk tolerability [*HSE, 2006*]. If the frequency of an accident, that leads to significant on-site workforce consequences, exceeds 1E-3/year then the risk is unacceptable. The risk is also considered unacceptable if the frequency of an accident, that leads to significant off-site public consequences, exceeds 1E-4/year. Accordingly, improvements must be made to reduce the risk. A plant facility which fails to satisfy the tolerable risk requirements has the potential to be shut down by the regulator. Therefore, an accurate assessment of the risk plays a vital role in meeting regulatory expectations.

As discussed by *Jones-Lee and Aven, 2011,* the ALARP principle is also often used as a decision-making tool to implement improvements to reduce the risk as far as reasonably practicable, i.e., in the Broadly Acceptable region. The authors highlight that

some regulators require that the cost of an improvement should be lower than the benefits. For the nuclear industry, the ONR require that the cost of the improvement should not outweigh the benefit [*HSE, 2020*]. In this case the term benefit equates to the total cost of an accident, e.g., costs due to damage to plant assets, that could be saved if an improvement is made such that the accident is prevented. To justify a plant improvement, *HSE,2020* stipulates that the monetary value of the benefit must be greater than the total cost of the improvement.

2.3.2 Standard practice for QRA in nuclear safety cases

The standard practice for QRAs in nuclear safety cases is to initially conduct a hazard identification exercise through Hazard and Operability (HAZOP) studies where credible faults, often termed as 'Initiating Events', are identified [*Bedford and Cooke, 2001, Mannan, 2004*]. If the Initiating Event cannot be eliminated, it requires a formal risk assessment involving an analysis of the magnitude of the consequences and the frequency of occurrence of the fault, i.e., the Top Event. Hence the calculated fault frequency is compared with the target frequencies specified within the accident risk criteria. The higher the consequence, the lower is the required target frequency of occurrence of the fault [*HSE, 2006*]. Figure 2-5 illustrates these basic components of the Quantified Risk Assessment process.

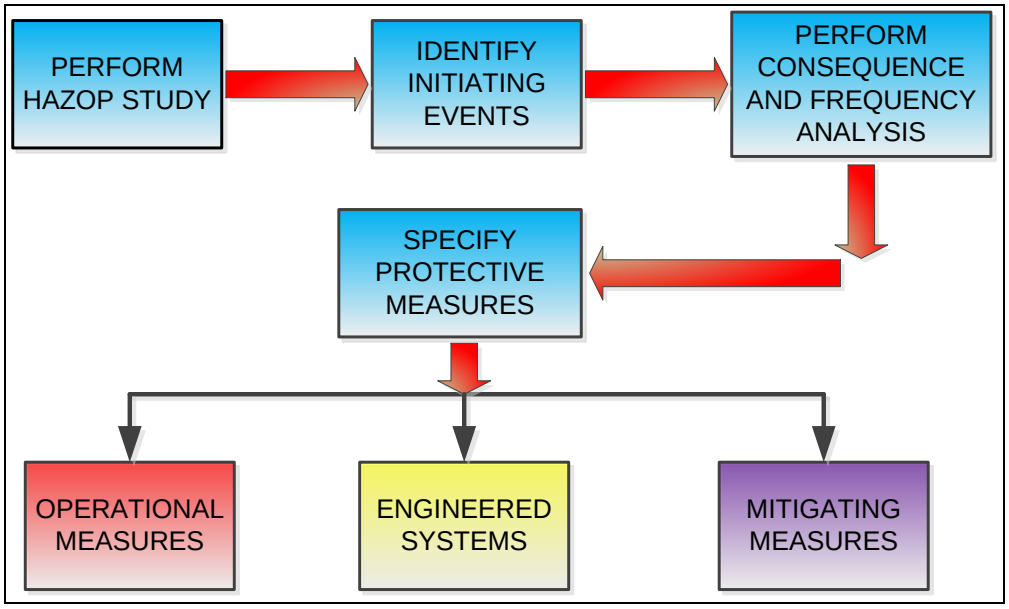

Figure 2-5: Quantified risk assessment process in nuclear safety cases

Several analytical methods of fault frequency analysis are available. Fault Tree Analysis (FTA) and Event Tree Analysis (ETA) are currently the two most common techniques used in nuclear safety cases. To understand the uses and limitations of these

techniques, a literature review and the theories associated with the two methodologies are given in the following sections.

2.3.3 Fault Tree Analysis

Fault Tree Analysis (FTA) involves the construction of a logical description of the failure paths which lead to the specified event. Software programs such as Logan [*Logan, 2018*] are commonly used in the nuclear industry to facilitate the FTA process. The key features of an FTA are:

- It provides a graphical analysis of the conditions leading to the occurrence of a defined outcome, i.e., the Top Event.
- The graphical structure enables visibility of the key failure modes.
- Boolean logic, i.e., 'AND' or an 'OR' gate, is applied to the individual causes of events to enable quantification of the outcome.
- The final output is a frequency or a probability of the Top Event.

Baig et al, 2013 provide full details of the method for construction of fault trees together with an illustrating example on an estimation of system reliability. They provide a detailed explanation on the functionalities of the OR and AND logic gates and the rules for their application when quantifying frequencies or probabilities of the events. An important aspect of the FTAs is that they are based on the derivation of 'minimal cut-sets' using Boolean algebra. A cut-set is a term used to describe a combination of base events in a fault tree which cause the Top Event to occur. The fundamental laws of Boolean algebra and the minimum cut-set theory is detailed by *Stamatelatos et al, 2002*. A further important feature of the FTA technique is that it is often used to determine the reliability and unavailability of a plant component or a system of components. The unavailability of a plant component, i.e., a failure to carry out its normal duty, can occur due to any of the following reasons:

- The plant item is in a state of failure which is unrevealed to the operators.
- The plant item is being repaired following a revealed failure.
- Testing or inspection of the plant item is being undertaken.

The unavailability of standby plant equipment, which is in a failed state and unrevealed to operators, can be determined knowing the component failure rate and the time intervals for proof testing, using a series of well documented expressions [*Stamatelatos and Vesley, 2002*, *Lees, 1992 and Ridley,2000*]. For example, the probability of unavailability (P) of a component, with a failure rate of λ_s, which is regularly proof tested at a time interval of T_s, is given by equation 2-10 [*Ridley, 2000*]:

$$P = 1 - \left(\frac{1 - e^{-\lambda_s T_s}}{\lambda_s T_s}\right) \quad (2\text{-}10)$$

In reliability theory, for plant items which are continuously operating, e.g., vent extract fans, power supply and vent damper, their failure would be immediately revealed and repairs would be undertaken accordingly. For such revealed failures of repairable plant items, even if there is a lack of experimental or manufacturer's data on individual component failure probabilities, they can be predicted knowing the mean failure rate, λ, and the repair time, t. *Lees, 1992,* suggests the use of equation 2-11 for the estimation for this revealed failure probability.

$$P(t) = 1 - e^{-\lambda t} \quad (2\text{-}11)$$

Equations 2-10 and 2-11 are programmed into the FTA software, LOGAN [*Logan, 2018*], for calculation of the unrevealed and revealed failure probabilities.

Often plant component failure data are presented in the form of Mean Time Between Failures (MTBF) [*Siemens, 2011*], such that for a continuous failure rate f, the MTBF would equate to 1/f. On this basis equation 2-11 would be expressed in the form given by equation 2-12.

$$P(t) = 1 - e^{-\frac{t}{MTBF}} \quad (2\text{-}12)$$

The equipment unavailability probabilities define the robustness of an Engineered Protection System (EPS) against the Initiating Event. Effectively a very low unavailability of the EPS, typically less than 1E-4, indicates the system is highly reliable, which would subsequently lead to a low Top Event frequency when combined with the Initiating Event frequency. Figure 2-6 illustrates the structure of a fault tree, showing the relationship between the Initiating Event, the EPS and the Top Event frequency, which is represented by the title 'Unmitigated Fault Sequence'.

2.3.4 Event Tree Analysis

After Fault Tree Analysis, the second most common method of QRA is Event tree analysis (ETA). Similar to FTA, it enables the estimation of fault frequencies or probabilities of the outcomes from an Initiating Event. It is a cause and effect type of an analysis, whereby a cause, i.e., the Initiating Event, is defined and all of its effects i.e., frequency and the probability of the different outcomes are determined [*BS EN 62502, 2011*]. The basic process for construction of an Event Tree Analysis for quantified risk assessments is well documented by *Vilchez et al, 2011*, *Hong et al 2011, and BS EN 62502, 2011*.

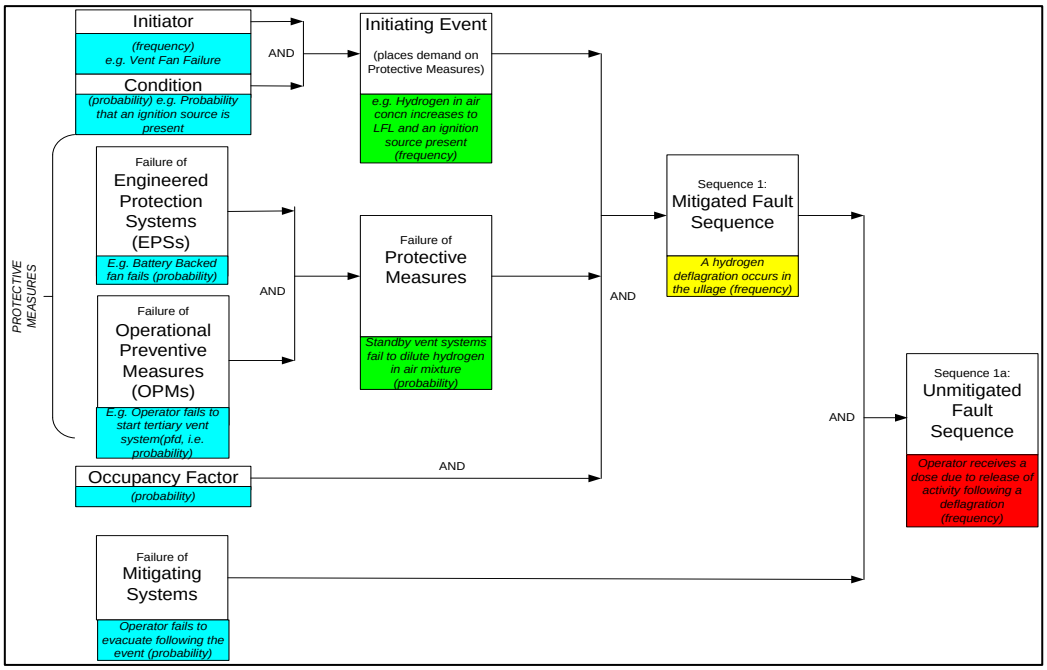

Figure 2-6: Generic Structure of a Fault Tree

Essentially the ETA method is similar to FTA in that it involves the specification of the Initiating Event Frequency and the probabilities of failure on demand (Pfd) of Engineered Protection Systems (EPSs), Operational Preventative Measures (OPMs) and Mitigating Systems. Boolean algebra is programmed within the ETA software, such as LOGAN, which can evaluate the Top Event frequency. A numerical example of a simple Event Tree Analysis is given in Figure 2-7.

Initiating Event Frequency (/y)	Engineered Protection System Functional?	Operational Preventative Measure Functional?	Mitigation System Functional?	Outcome Code	Description of Outcome	Frequency (/y)
F=0.2	Pfd=0.02	Pfd=0.3	Pfd=0.1			
	Yes			a	No consequence	0.196
	No	Yes		b	No consequence	0.0028
		No	Yes	c	Worker Dose >2mSv	0.00108
			No	d	Worker Dose >20mSv	0.00012

Figure 2-7: Example of a Simple Event Tree

The numerical estimation of fault probabilities and frequencies in Event Trees is relatively simple however, the basic rules of Boolean algebra are still applied here. For example, Figure 2-7 shows that for outcome ‘b’, the Initiating Event occurs at a frequency of 0.2/yr and the EPS has to fail with a probability of failure of 0.02. For outcome ‘b’ the failure path assumes that the OPM is functional, but it has a Pfd of 0.3, should it fail. In this situation, the ETA program automatically calculates the success probability of the OPM as 1-0.3 because the rule is that the probabilities of failure and success for a node must

add to 1 [*BS EN 62502, 2011*]. Applying the rules of Boolean algebra, the ETA program calculates the frequency of outcome 'b' by multiplying the Initiating Event Frequency with the Pfd of the EPS and the probability of success of the OPM, i.e., 0.2 x 0.02 x (1-0.3) = 0.0028/yr.

ETAs are often used for analysing the effect of multiple Mitigating Systems, such as hardwired alarms, which enable a fault to be revealed and allow corrective action to be taken. Figure 2-8 illustrates how several different outcomes may arise following a demand placed on two separate Mitigating Systems.

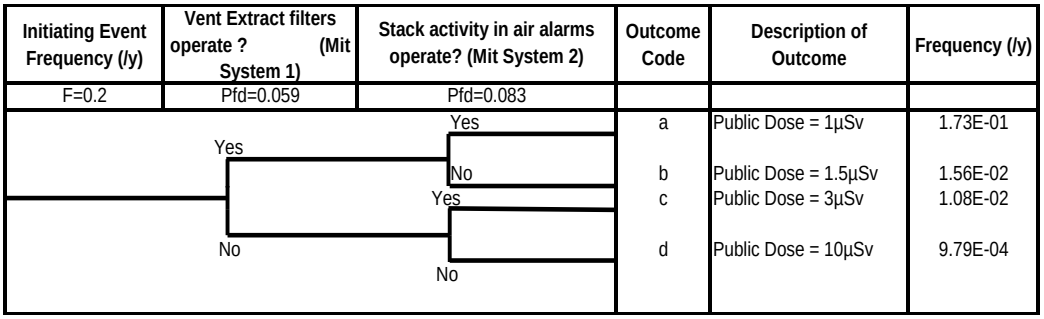

Figure 2-8: Event Tree Modelling Multiple Mitigating Systems

2.4 Alternative QRA techniques

2.4.1 Bayesian Belief Network (BBN) Analysis

BBNs provide a graphical means for modelling the relationship between the causes and effects of a particular event based on the statistical hypothesis, Bayes' theorem [*Bolstad, 2007*]. Bayes' theorem is based on the concept of 'conditional probability'. The term conditional probability can be defined as the probability of a hypothesis given the occurrence of another event. So, in terms of hydrogen safety, the hypothesis could be 'the likelihood of a hydrogen explosion in a vessel'. The use of conditional probability allows this uncertainty to be resolved by allowing for some evidence that affects the likelihood of the hypothesis. In this case, the hypothesis would be phrased as 'the likelihood of a hydrogen explosion given that hydrogen is present in the ullage space of the vessel'.

In accordance with *Bolstad, 2009,* the conditional probability of a hypothesis A given that an event B has occurred can be expressed as:

$$p(A \mid B) = p(A \text{ and } B)/p(B) \quad (2\text{-}13)$$

$$p(A \mid B) = p(A \cap B)/(p(B) \quad (2\text{-}14)$$

The term p(A∩B) in equation 2-14 is the probability of both events A and B occurring. This may also be expressed as the probability of A as a product of the probability of B given that hypothesis A occurs:

$$p(A \cap B) = p(A)x\, p(B|A) \tag{2-15}$$

Similarly, p(A∩B) can also be expressed as the probability that event B occurs times the occurrence of hypothesis A given that event B has occurred:

$$p(A \cap B) = p(A)x\, p(B|A) = p(B)x\, p(A|B) \tag{2-16}$$

Therefore, solving for p(A|B) gives the following relationship (equation 2-17) which leads to the Bayes theorem (equation 2-18).

$$p(A \cap B) = p(A)x\, p(B|A) = p(B)x\, p(A|B) \tag{2-17}$$

$$p(A|B) = \frac{p(A)x\, p(B|A)}{p(B)} \tag{2-18}$$

Where:

- p(A) and p(B) are the probabilities of observing events A and B which are independent of one another.
- p(A) is referred to as the 'Prior' probability of the hypothesis before taking into consideration the evidence.
- p(A | B) is termed the 'Posterior', which is a conditional probability representing the likelihood of observing hypothesis A given that B is true.
- p(B | A) is the probability that event B occurs given that A is true.

Effectively, equation 2-18 provides the relationship between the likelihood of hypothesis p(A) before any evidence is available and the likelihood of hypothesis A when evidence B has been allowed for, i.e., p(A|B).

Consider a plant consisting of 1000 sealed pipes in which one explosion incident has been previously observed such that the Prior probability p(A) = 1/1000 or 0.1%. It is assumed that upon sampling of the pipes, hydrogen was detected in 5% of the cases, so p(B) = 0.05. If it is also assumed that the probability that hydrogen would have been detected given that an explosion event occurred is unity, i.e., p(B|A) = 1, then applying Bayes theorem shows that if hydrogen is detected in a given pipe, the probability of an explosion rises from 0.1% to 2% i.e., p(A | B) = (1 x 0.001)/0.05 = 2%.

The above example applies Bayes theorem to a relatively simple uncertainty analysis with only two events. However, when there are many events and interdependencies, the

Bayesian algorithm for estimation of the likelihood of the hypothesis would become extremely complex and almost impossible to calculate manually. Hence software applications such as Netica [*Norsys,2010*] have been developed based on Bayes theorem which enable modelling of a hypothesis of any given number of variables in the form of a graph network, commonly referred to as the Bayesian Belief Network (BBN).

2.4.2 Concept of Bayesian Belief Network Analysis

To demonstrate the complexity relating to the derivation of the algorithms and hence quantification of the BBNs for multivariable systems, the theory associated with this graphical analysis method is first explored. BBNs provide the ability to evaluate the conditional dependencies between a given set of random variables by calculating the joint probability distribution. The cause and effect relationship between the variables, or nodes, is presented in the form of directed links, where A $\rightarrow$ B indicates that the node A is a cause or 'Parent' to node B ('Child'). In accordance with *Chengyan et al, 2019,* the joint probability of a set of random variables A1, A2 ……A_n for a graphical network structure can be approximated by the following relationship.

$$p\ (A1, A2\ \ldots\ldots A_n) = \prod_{i=1}^{n} p(Ai \mid parents\ (Ai)) \tag{2-19}$$

Where n is the total number of random variables and Ai is any given random variable.

Equation 2-19 suggests that the joint probability is a product of the probability of each of the random variables conditional to the probability of the associated parents. This in turn requires prediction of the parent node conditional probabilities, e.g., through expert judgment or experiments. If a node has no parents associated with it, then its probability is equivalent to the Prior value.

2.4.3 BBN analysis of a hypothesis with three variables

Consider a Bayesian network consisting of three random variables A1 to A3, where nodes A1 and A2 are parents to node A3 (Figure 2-9).

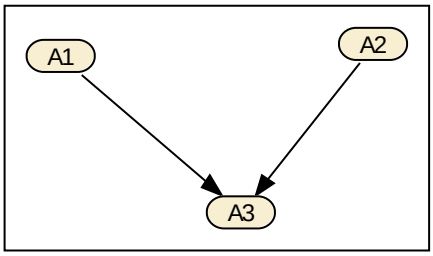

Figure 2-9: Bayesian Belief Network with three random variables

Based on the principles of equation 2-19, the joint probability for the hypothesis in Figure 2-6 would be expressed as:

$$p(A1, A2, A3) = p(A3 \,|\mathrm{A2}, \mathrm{A1})p(A2)p(A1) \tag{2-20}$$

In this case the probability of Node A3 is conditional to the occurrence of the two parent nodes A1 and A2, which would be equivalent to the first term in equation 2-20. If each of the random variables has two possible discrete states, i.e., true or false, denoted by the letters T and F respectively, then the first term in equation 2-20 would equate to:

$$p(A3 = T \,|\mathrm{A2}, \mathrm{A1}) = \sum_{\mathrm{A1A2} \in \{T,F\}} p(A3 = T, A2, A1) \tag{2-21}$$

Effectively equation 2-21 can be translated as the total probability if A3 is fixed to the true state but events A1 and A2 are either true or false. Here A3 is dependent on two variables, each with two states such that there are 2^2, i.e., four possible combinations of events as shown in the Conditional Probability Table 2-1.

Node A1	Node A2	Node A3
True	True	True
True	False	True
False	True	True
False	False	True

Table 2-1: CPT matrix for A3=T | A2,A1

Hence based on the CPT in Table 2-1 and equation 2-21 the probability A3=T | A2,A1 would be calculated using equation 2-22 as follows:

$$\begin{aligned} &p(A3 = T \mid \mathrm{A2}, \mathrm{A1}) \\ &= p(A3 = T, A1 = T, A2 = T) + p(A3 = T, A2 = F, A1 = T) \\ &+ p(A3 = T, A2 = T, A1 = F) + p(A3 = T, A2 = F, A1 = F) \end{aligned} \tag{2-22}$$

Consider a hypothetical case where the true state probabilities of the variables A1 and A2 are known to be 0.3 and 0.4, respectively. Since the total probability of each node must add to 1, this would lead to the probabilities of A1 and A2 being false as 0.7 and 0.6, respectively. It is also assumed that the following CPT values (Table 2-2) for each of the combinations given in equation 2-22 are known through expert judgment or experimental evidence.

A1	A2	p (A3 = True)	p (A3 = False)
True	True	0.8	0.2
True	False	0.3	0.7
False	True	0.9	0.1
False	False	0.99	0.01

Table 2-2: CPT values for A3 | A2,A1

Using equation 2-22, and the CPT values in Table 2-2, the probability of A3 being true, given A2 and A1, can be calculated as:

$$p(A3 = T \mid \mathrm{A2}, \mathrm{A1}) \\ = (0.8 \times 0.3 \times 0.4) + (0.3 \times 0.6 \times 0.3) \\ + (0.9 \times 0.4 \times 0.7) + (0.99 \times 0.6 \times 0.7) = 0.818$$

This manually calculated value for p(A3=T|A2,A1) based on equation 2-22 can be verified by replicating the Bayesian network in Netica using the CPT values in Table 2-2. The BBN results are shown in Figure 2-10. All numerical values given in Figure 2-10 are percent probabilities and the result for the true state in Node A3 represents the function p(A3=T| A2,A1). It can be seen from the true state of Node A3 in Figure 2-10 that the software yields the same result of 0.818 as the hand calculation using equation 2-22 and Table 2-2. This shows that the software based results are consistent with the theoretical model predicted by equation 2-22.

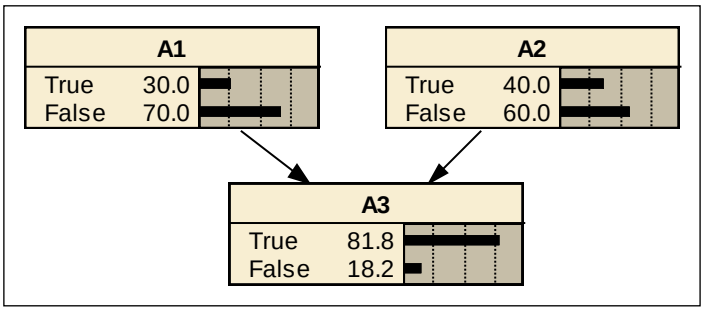

Figure 2-10: Quantified BBN for p (A3 | A2,A1) using Netica software

The computation by hand using equation 2-22 for this BBN with three variables is still relatively simple, however this is time consuming and there is the potential for error when the probabilities for each combination of events are manually transposed into the equation. The BBN software prevents such errors and performs the same calculation without any time being incurred for a network of any size and complexity. Furthermore, this particular model is based on two parents and binary states, i.e., true or false, such that the CPT matrix for Node A3 has only four possible combinations.

If for instance each of the two parent nodes has three possible states such as Low, Medium and High, then the number of combinations in the CPT matrix for Node A3 would

increase to 3^2, i.e., 9, as shown in Table 2-3. Thus, the number of computations in equation 2-22 will increase, from the previous four, to nine. The Bayesian network software can handle any number of states for a given variable.

A1	A2	A3
Low	Low	True
Low	Medium	True
Low	High	True
Medium	Low	True
Medium	Medium	True
Medium	High	True
High	Low	True
High	Medium	True
High	High	True

Table 2-3: Possible combinations of events in a CPT for node A3 with two parents and three states

2.4.4 Reverse inference

With prior beliefs the Bayesian network provides the probability of an effect given a cause, for example the probability of a hydrogen explosion given the presence of an ignition source. However, by allowing for some evidence, the model can also be used to undertake an inverse analysis, or 'reverse inference' to predict the probability of a cause given that an effect has occurred. The probability of hydrogen being detected given that a hydrogen explosion occurs would be a typical example of such reverse inference. This requires the conditional probabilities of all combinations of events to be summed over the probabilities of all the 'nuisance variables'. In statistics, a nuisance variable is one which is not directly relevant to the question being posed for the evidence-based updating, but still needs to be accounted for in the analysis.

If for example in Figure 2-10 there is a need to determine the probability of A2 given that event A3 has occurred, i.e., p(A2=T|A3=T), the nuisance variable is A1. Hence the following equations would be used to predict the probability.

$$p(A2 = T|A3 = T) = \frac{p(A3 = T, A2 = T)}{p(A3 = T)} \quad (2\text{-}23)$$

$$= \frac{\sum_{\mathrm{A1}\in\{T,F\}} p(A3=T, A1, A2=T)}{\sum_{\mathrm{A1,A2}\in\{T,F\}} p(A3=T, A1, A2)} \quad (2\text{-}24)$$

The numerator in equation 2-24 is the sum of the probabilities of all combinations of events where the nuisance variable A1 is either in a true or false state given that the variables A3 and A2 are true. The denominator is determined by summing the probabilities of all possible combinations where A3 is fixed to the true state and A1 and A2 are either in the true or false state. Effectively the denominator is the probability A3=T|A2,A1, so its numerical value is the same as that determined previously by equation 2-22 and Table 2-2, i.e.,0.818.

Hence:

$$p(A2=T|A3=T) = \frac{p\,(A3=T, A1=T, A2=T) + p(A3=T, A1=F, A2=T)}{p(A3=T, A1=T, A2=T) + p(A3=T, A2=F, A1=T) + p(A3=T, A2=T, A1=F) + p(A3=T, A2=F, A1=F)} \quad (2\text{-}25)$$

Using equation 2-25 and the CPT for node A3 (Table 2-3) as well as the prior probabilities of nodes A1 and A2 given in Figure 2-10, the value of p(A2=T|A3=T) can be calculated as follows:

$$\frac{(0.8 \times 0.3 \times 0.4) + (0.9 \times 0.4 \times 0.7)}{(0.8 \times 0.3 \times 0.4) + (0.3 \times 0.6 \times 0.3) + (0.9 \times 0.4 \times 0.7) + (0.99 \times 0.6 \times 0.7)} = 0.426$$

The same result is obtained in Netica which yields the true state probability of 0.426 for node A2 when the node A3 true state is instantiated to 100% (Figure 2-11). This again proves consistency of the software-based results with the hand calculation. This instantiation of Node A3 in Netica was achieved through a simple click of the true state to a 100%. Accordingly, significant time and effort was saved by avoiding the application of equation 2-25 manually to perform the manipulation of numerical conditional probability values.

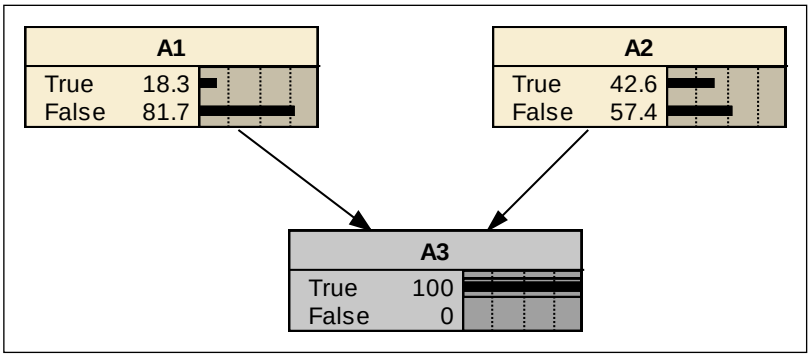

Figure 2-11: Updated Bayesian Network for p(A2=T|A3=T) using Netica software

2.4.5 Increase in BBN complexity with four variables

The complexity in the reverse inference calculation rises with increasing number of variables. Consider a Bayesian network with four nodes (Figure 2-12) each comprising two possible states, i.e., true or false. In this case Node A3 is a parent to Node A4 and A1 and A2 are the input parent nodes.

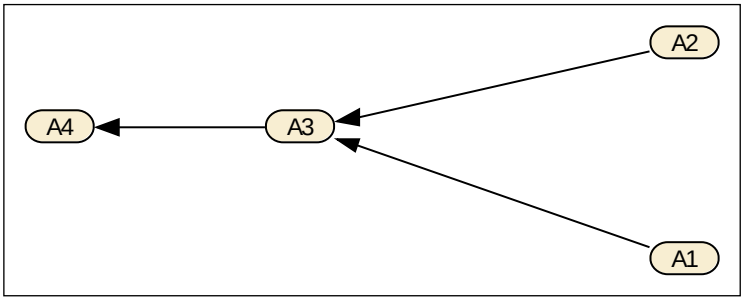

Figure 2-12: Typical Bayesian Belief Network with four random variables

If for instance there is a requirement to determine the probability of A3 being true given that A4 is true then in accordance with the concept for reverse inference, A1 and A2 are the nuisance variables. Therefore, the following equations apply for derivation of p(A3=T| A4=T).

$$p(A3 = T|A4 = T) = \frac{p(A4 = T, A3 = T)}{p(A4 = T)} \quad (2\text{-}26)$$

$$= \frac{\sum_{\mathrm{A1,A25}\in\{T,F\}} p(A4 = T, A3 = T, A2, A1)}{\sum_{\mathrm{A1,A2,A3}\in\{T,F\}} p(A4 = T, A1, A2, A3)} \quad (2\text{-}27)$$

Where T and F denote the true and false states, respectively.

The prior probabilities for nodes A1 and A2 are assumed to be 0.8 for p(A1=T), 0.2 for p(A1=F), 0.1 for p(A2 =T) and 0.9 for p(A2=F). Since nodes A4 and A3 are dependent on the parent nodes, both the numerator and denominator of equation 2-27 require the CPTs for these nodes to be taken into consideration. It is assumed that the following CPTs (Table 2-4 and Table 2-5) apply to nodes A3 and A4, respectively.

A1	A2	A3=True	A3=False
True	True	0.4	0.6
True	False	0.3	0.7
False	True	0.3	0.7
False	False	0.9	0.1

Table 2-4: CPT for Node A3

A3	A4=True	A4=False
True	0.8	0.2
False	0.3	0.7

Table 2-5: CPT for Node A4

The numerator in equation 2-27 indicates that nodes A4 and A3 are fixed to be true whilst A1 and A2 can be either in a true or false state. Hence four combination of events need to be considered when evaluating the numerator probability, as shown in equation 2-28.

$$\sum_{\mathrm{A1,A25}\in\{T,F\}} \mathrm{p}(A4=T,A3=T,A2,A1) = TTTT + TTTF + TTFT + TTFF \tag{2-28}$$

Each of the terms on the right side of equation 2-28 are abbreviated forms of the following expressions, with numerical values for each combination based on the CPTs given in Table 2-4 and Table 2-5:

$$TTTT = p(A4=T,A1=T,A2=T,A3=T)$$

$$= p(A4=T|\mathrm{A3}=\mathrm{T})\,p(\mathrm{A3}=\mathrm{T}|\mathrm{A2}=\mathrm{T},\mathrm{A1}=\mathrm{T})p(\mathrm{A2}=\mathrm{T})\,p(\mathrm{A1}=\mathrm{T}) \tag{2-29}$$

$$= 0.8 \times 0.4 \times 0.1 \times 0.8 = 0.0256$$

$$TTTF = p(A4=T,A3=T,A2=T,A1=F)$$

$$= p(A4=T|\mathrm{A3}=\mathrm{T})p(\mathrm{A3}=\mathrm{T}|\mathrm{A2}=\mathrm{T},\mathrm{A1}=\mathrm{F})p(\mathrm{A2}=\mathrm{T})p(A1=F) \tag{2-30}$$

$$= 0.8 \times 0.3 \times 0.1 \times 0.2 = 0.0048$$

$$TTFT = p(A4=T,A3=T,A2=F,A1=T)$$

$$= p(A4=T|\mathrm{A3}=\mathrm{T})p(\mathrm{A3}=\mathrm{T}|\mathrm{A2}=\mathrm{F},\mathrm{A1}=\mathrm{T})p(\mathrm{A2}=\mathrm{F})p(A1=T) \tag{2-31}$$

$$= 0.8 \times 0.3 \times 0.9 \times 0.8 = 0.1728$$

$$TTFF = p(A4=T,A3=T,A2=F,A1=F)$$

$$= p(A4=T|\mathrm{A3}=\mathrm{T})p(\mathrm{A3}=\mathrm{T}|\mathrm{A2}=\mathrm{F},\mathrm{A1}=\mathrm{F})p(\mathrm{A2}=\mathrm{F})p(A1=F) \tag{2-32}$$

$$= 0.8 \times 0.9 \times 0.9 \times 0.2 = 0.1296$$

Since the denominator in equation 2-27 comprises three variables, A1, A2 and A3, with two states for each variable, there are altogether 2^3, i.e., eight combinations of events which must be accounted for as follows:

$$\sum_{\mathrm{A1,A2,A3}\in\{T,F\}} p(A4=T,A1,A2,A3)$$
$$= TTTT + TFTT + TTFT + TFFT + TTTF + TFTF + TTFF + TFFF \quad (2\text{-}33)$$

The combination terms TTTT, TTTF TTFT and TTFF in equation 2-33 are the same as those calculated above for the numerator. The other four additional terms and the associated numerical values are derived below.

$$TFTT = p(A4=T,A3=F,A2=T,A1=T)$$
$$= p(A4=T|\mathrm{A3=F})p(\mathrm{A3=F|A2=T,A1=T})p(\mathrm{A2=T})p(A1=T) \quad (2\text{-}34)$$
$$= 0.3\times 0.6\times 0.1\times 0.8 = 0.0144$$

$$TFFF = p(A4=T,A3=F,A2=F,A1=F)$$
$$= p(A4=T|\mathrm{A3=F})p(\mathrm{A3=F|A2=F,A1=F})p(\mathrm{A2=F})p(A1=F) \quad (2\text{-}35)$$
$$= 0.3\times 0.1\times 0.9\times 0.2 = 0.0054$$

$$TFTF = P(A4=T,A3=F,A2=T,A1=F)$$
$$= p(A4=T|\mathrm{A3=F})p(\mathrm{A3=F|A2=T,A1=F})p(\mathrm{A2=T})p(A1=F) \quad (2\text{-}36)$$
$$= 0.3\times 0.7\times 0.1\times 0.2 = 0.0042$$

$$TFFT = p(A4=T,A3=F,A2=F,A1=T)$$
$$= p(A4=T|A3=F)p(A3=F|A2=F,A1=T)p(A2=F)p(A1=T) \quad (2\text{-}37)$$
$$= 0.3\times 0.7\times 0.9\times 0.8 = 0.1512$$

Substituting equations 2-28 and 2-33 into equation 2-27 gives:

$$p(A3=T|A4=T)$$
$$= \frac{TTTT + TTTF + TTFT + TTFF}{TTTT + TFTT + TTFT + TFFT + TTTF + TFTF + TTFF + TFFF} \quad (2\text{-}38)$$

Substituting the quantified values for each of the true and false state combination terms into equation 2-38, the probability p(A3=True|A4=True) can be calculated as follows:

$$p(A3=T|A4=T)$$
$$= \frac{0.0256 + 0.0048 + 0.1728 + 0.1296}{0.0256 + 0.0144 + 0.1728 + 0.1512 + 0.0048 + 0.0042 + 0.1296 + 0.0054}$$
$$= 0.655$$

The quantified result for p(A3=True|A4=True) can be compared with the same reverse inference model replicated in Netica (Figure 2-13). This shows that when Node A4 is instantiated to a 100% true state the resulting probability of Node A3 being true is 65.5% i.e., 0.655 which is exactly the same as the hand calculation performed above. Hence the software results are consistent with the hand calculation based on first principles.

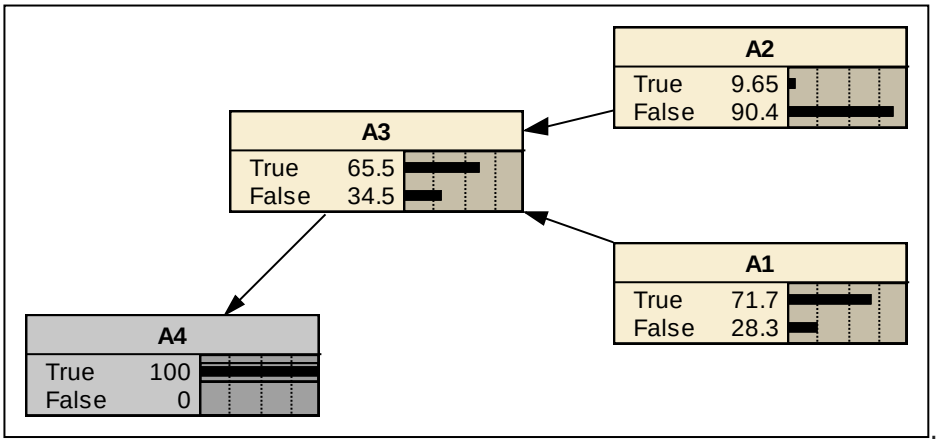

Figure 2-13: Updated Bayesian Network in Netica for p(A3=True | P4=True)

The hand calculation of (A3=True|P4=True) detailed above demonstrates the substantial rise in complexity and the number of computations required for the reverse inference with increasing number of variables. The calculation shows that even with three parent nodes and two states, the resulting eight different combinations in the CPT matrix lead to a significant increase in the computation for the reverse inference. Any further increases in the number of parent nodes would lead to difficulties in undertaking reverse inference manually. This demonstrates the usefulness of the Bayesian Network software when modelling multiples variables and interdependencies.

2.4.6 Monte Carlo Simulation

In a Monte Carlo simulation, the parameter of interest varies in accordance with an assumed probability distribution, which is randomly sampled repeatedly, typically hundreds of thousands of times, to approximate the distribution i.e., as a Probability Density Function (PDF). By determining the PDF for each parameter in a given fault scenario, the distribution can then be input to a Fault Tree Analysis (FTA). This results in a Top Event frequency or probability as a density function [*Bilgic et, al, 1994*]. Knowing the distribution of the parameter of interest, or the Top Event, essential statistical data about the fault scenario in the form of mean, standard deviation or variation can be determined. This can provide a better understanding about the credibility or likelihood of occurrence of the fault or the variables affecting the fault. An illustration of the application

of Monte Carlo Simulation to FTA is given in Figure 2-14, which is based on the concept by *Lees, 1992*.

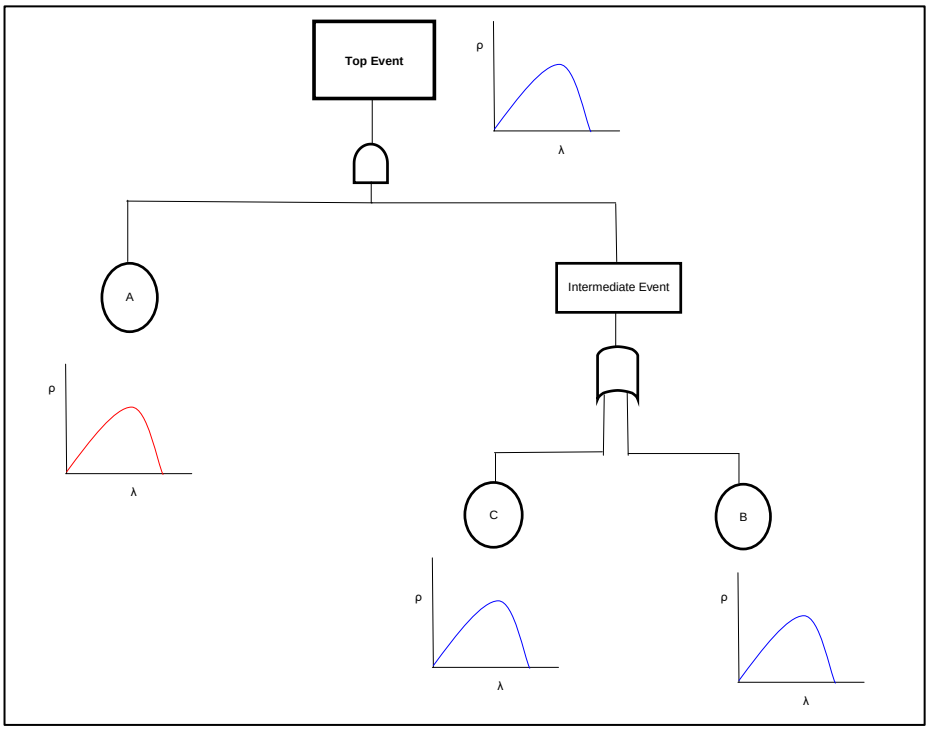

Figure 2-14: Mapping of Monte Carlo Simulation on to Fault Tree Analysis [*Lees, 1992*]

Monte Carlo Simulation has been widely applied for uncertainty analysis in the nuclear industry. For example, an uncertainty analysis for the most likely accident scenario in a nuclear research reactor was conducted by *Bilgic et, al, 1994*. They concluded that the use point values of conditional probabilities do not give a sound argument on the failure probability. In comparison the use of a Monte Carlo Simulation to generate probability distributions provides a better accuracy.

Similar to the Monte Carlo Analysis conducted by *Bilgic et, al, 1994*, characterising the conditional probabilities for events such as hydrogen generation in nuclear chemical plant applications would be considered beneficial. Software packages such as RiskAmp by *Structured Data LLC, 2007* are available to facilitate this analysis. The RiskAmp tool is particularly useful due to the large number of functionalities it provides such as modeling probability distributions of parameters. The benefits of RiskAmp are reviewed further in Chapter 3, Section 3.5.

2.5 Industrial application of Bayesian Network and Monte Carlo simulation methods

2.5.1 Application of Bayesian Networks in the nuclear decommissioning sector

The application of Bayesian Belief Networks to determine the likelihood of hydrogen

ignition during nuclear decommissioning operations has been explored by *Averill et al, 2018.* They performed a BBN analysis for hydrogen accumulation when storing stacks of containers ('boxes') of grouted Magnox waste. As hydrogen continues to evolve due to corrosion of the waste during long-term storage, there is the potential for the gas to accumulate within the gap between the stacked boxes. Important aspects of the Bayesian networks are explained including the use of expert opinion when determining the prior distributions.

It is observed that *Averill et al, 2018* focussed on corrosion of the Magnox metal as the main source of hydrogen generation in nuclear decommissioning environments. However, since the corrosion of Magnox waste also results in the formation of magnesium hydroxide sludge, it is considered that some of the hydrogen generated will be held up by the sludge. The application of Bayesian networks to quantify the uncertainties associated with hydrogen hold-up in sludge material, waste expansion and transient release of the gas, is an area which has not been previously considered. This area presents a knowledge gap that requires further research.

2.5.2 Application of BBNs and MC techniques to other industries

Several researchers, including *Hanea et al, 2009, Pasman and Rogers, 2012, Khakzad et al, 2011 and Khan et al, 2015,* have previously undertaken a comparison of the performance of the Bayesian technique with the standard, Layer of Protection Analysis (LOPA), FTA and ETA methods. LOPA is a quantitative technique that takes into consideration faults that could potentially lead to high consequences and frequencies. Depending on the magnitude of the consequences, it aims to demonstrate the number of independent layers of protection needed to adequately reduce the risk.

Hanea et al, 2009 applied the Bayesian methodology to analyse the uncertainty associated with factors affecting evacuation of personnel from buildings in the event of a major fire. It is shown that fire evacuation of personnel involves many dependencies and techniques such as ETA and FTA are unable to handle dependability between many interacting variables. Both ETA and FTA are binary systems, characterised by two states through the AND and OR logic gates, thus resulting in an inability to perform an uncertainty analysis. BBNs on the other hand can analyse multistate variables of any given distribution. The use of conditional probabilities in BBNs enables the analysis of an event which is conditional to the occurrence of other events.

Hanea et al, 2009 also state that the BBNs not only allow an estimate of the average risk, but they also provide probabilistic information about extreme fire scenarios. Such

information can be usefully applied at the design stage of a building to ensure adequate control measures are in place and minimise the risk from extreme fires.

Yun et al, 2009 discuss the benefits of combining the standard Layer of Protection Analysis (LOPA) with Bayesian Analysis for Liquefied Natural Gas (LNG) installations. Due to the lack of equipment failure rate data in this industry, they demonstrate how BBNs can be used to update the Prior failure rate information obtained from other industries. By combining the Prior probabilities, based on previous information from other industries and the likelihood based on LNG plant specific data, Bayes theorem can calculate a more accurate value of the failure probability relevant to LNG plants.

Pasman, 2011 and Pasman and Rogers, 2012 have considered the risks associated with hydrogen as an energy carrier and hydrogen supply transportation. They demonstrate that Bayesian Networks are ideal for hydrogen risk assessments because this technique provides a structured approach for analysing the complexities associated with the behaviour of the gas. The complexities relate to the broad flammability range of hydrogen i.e., 4 to 74% in air and the low ignition source energy, such that the uncertainty range in terms of the likelihood of ignition is also wide. Effectively this means that the possible number of initiating events that could lead to a hydrogen explosion is large. To manage against the various initiating events multiple safety systems would be needed. The interdependencies between the multiple safety systems would lead to complexities in terms of establishing a safe and reliable operating system. BBNs can use probability distributions, taking into consideration the uncertainty ranges instead of point source values of the input data. Furthermore, BBNs can track the sensitivity of the key variables thus removing any inaccuracies.

Pasman and Rodgers, 2013 applied the LOPA and Bayesian techniques to a Loss of Cooling Accident (LOCA) in a nuclear reactor which leads to a runaway reaction. Although the LOPA method can overcome the uncertainties associated with the reactor component failure rate data, when applied in conjunction with the Bayesian technique an enhanced sensitivity analysis was achieved. This combined Bayesian-LOPA method showed that if the initiating event frequency of the LOCA is increased then then there is a benefit in making at least one improvement.

The potential for deterioration of safety culture in process plants due to commercial pressures such as throughput, plant efficiency and cost reduction is discussed by *Pasman et al, 2013*. Accordingly, they emphasise the need for holistic safety which must take account of risks from management system failures in addition to technical safety

issues, e.g., equipment failures. The paper recommends that tools such as Bayesian Networks are ideal for hazard analysis and selection of optimal options to improve safety.

Haugom et al, 2011 have also explored the application of BBNs in the quantification of risks associated with the use of hydrogen gas as an energy carrier. It is argued that in comparison with FTA and ETA techniques, BBNs provide greater clarity and they are more adaptable when modelling technological uncertainties. This is essential particularly for hydrogen risk assessments where the accident and incident history data are limited. However, it is also highlighted that when the input probability data are limited, consultation from experts must be sought to validate such data.

Miki et al, 2013 demonstrated the benefits of the BBN uncertainty analysis capability to determine the rate coefficient of the reaction $H + O_2 \rightarrow OH + O$. The BBN analysis was able to show that the uncertainty in the rate coefficient is highly dependent on temperature.

A detailed review of the performance of BBN technique in comparison with FTA has also been undertaken by *Khakzad et al, 2011 and Khan et al 2015*. By applying the BBN technique to worked examples on safety analysis of gas processing facilities, they demonstrated that the updating feature of the BBN technique enables a dynamic safety analysis which is crucial in this industry. Whilst BBNs are similar to FTA in a number of ways, they are far more superior in terms of their ability to handle functional uncertainty and dependability between any given number of variables and states. Furthermore, BBNs provide the ability to carry out evidence based inference which enables prediction of the probability of a causal event given the occurrence of the top event. This is a unique feature of BBNs which is lacking in FTA.

The benefits of the Bayesian networks were also demonstrated by the statisticians Stone and Co [*arXiv, 2014*] in the search for the disappeared Air France flight 447. They applied the Bayesian technique to combine evidence gathered from the previous failed searches for the flight wreckage and expert judgement to update the probability distribution for the location of the wreckage. This use of previous search data and updating the probability distribution of the flight location enabled successful location of the flight wreckage. The article emphasises that the Bayesian tool alone cannot solve the problem. The analyst and experts in the relative field have an important role in terms of prediction of the probability distributions and using the evidence appropriately to determine the Posterior probabilities.

The importance of an uncertainty analysis of the key data for a QRA is also well recognised by the oil refining industry. *Yang et al, 2010* used the Bayesian technique to

update the failure rate of equipment, originally taken from databases, with the data obtained from plants. They claim that equipment reliability and failure rate data in databases tends to be too broad and not representative of the problem in question. They also state that the BBN technique can overcome this problem by updating the Prior distributions with plant data.

Yang et al, 2010 also applied Monte Carlo (MC) simulations to perform an uncertainty analysis on the probability distribution of the Top Event, which could lead to a significant hazard such as fire and explosions due to overfilling of vessels with flammable liquids. They state that the BBN and MC techniques help to reduce the uncertainties by analysing the probability values of the basic events and the top event over ranges and distributions, thus improving the risk quantification.

Operation of process plants is often dependent on human intervention, however minimisation of operator error to reduce the risk from potential hazards such as hydrogen explosions presents a significant challenge. *Mkrtchyan et al, 2016* have applied Bayesian Belief Networks to a Human Reliability Analysis (HRA).They emphasised that QRAs often need to handle uncertainty associated with the data for the analysis. While BBNs can combine limited available data and expert judgment to obtain the most accurate results, often no conditional probability data are available for the analysis. They investigated the application of the following methods, which can be used to build the Conditional Probability data for BBNs in HRA:

- Functional interpolation [*Podofillini and Dang, 2013*].
- The Elicitation BBN [*Wisse et al, 2008*].
- The Cain Calculator [*Cain, 2001*].
- Fenton method [*Fenton et al, 2007*].
- Rǿed method [*Rǿed et al, 2014*].

Each of the above methods was investigated by comparing the following factors relevant to HRAs:

- Method requirements with increasing size and complexity of the BBN.
- Influence of strong factors and interactions.
- Uncertainty on the BBN relationships.

As discussed in Chapter 1, potential injuries to the workforce from hydrogen explosion hazards can be significant. *Moura et al, 2016* discuss that on-site accidents not only have a negative impact on the workers, but they can also be detrimental to the employers due to extended leave. Hence if the rate of accidents is reduced, the company profit will rise.

If the accident rate data are analysed with a good accuracy, then appropriate company safety improvement plans can be identified to reduce the risk. The authors demonstrated the benefits of the Bayesian technique to analyse the rates of workplace accidents and recovery. Using Bayesian inference the Population Variability Distribution of the parameters associated with the rates of accident and recovery was determined. *Fenton and Neil, 2001,* demonstrate the application of BBNs in conjunction with other techniques. They show how the Multi Criteria Decision Aid (MCDA) technique could be used to analyse decision uncertainties involving multiple attributes such as safety, cost and environmental factors.

2.5.3 Validation and verification of BBN and MC techniques

The key benefits of the BBN and MC simulation techniques are discussed in Sections 2.4. However, the Validation and Verification (V&V) of the models generated from these software-based techniques is important, particularly in the case of hydrogen explosions in nuclear plants where the risk could potentially be significant. An inaccurate model could result in the quantified risk being underestimated leading to inadequate protection against the hydrogen explosion hazard. Conversely, an overly conservative model could lead to an increased complexity in the design and implementation of protection systems against the hazard, which also needs to be avoided. Therefore, to prevent such negative impacts it is important that the BBN and MC simulation models are given a proportional level of scrutiny through a fit for purpose validation and verification.

Various researchers have undertaken reviews of the V&V methods in engineering applications. *Pitchforth and Mengersen, 2013* demonstrate how BBNs based on expert elicitation could be validated. *Kleemann et al, 2017* show the application of quantitative and qualitative methods to validate a BBN analysis of the effect of changing weather systems on agricultural land in Africa. In terms of BBNs for engineering applications, *Sargent, 2011* provides a generic review of the procedure for computer software-based model validation and accreditation. This is equally relevant to BBN and MC simulation models for nuclear plant applications. Essentially, *Sargent 2011* suggests four different approaches to software model validation and verification, which include:

i) Validation by the model development team itself through tests such as sensitivity analysis, evaluation of the results and comparison with expected trends as the model develops.

ii) Involvement of the end users of the software model, such as design engineers and plant operators to take lead in the model development as they understand the system and operations relevant to the problem entity.

iii) Verification and validation by an independent body outside the model development team and the end users. This process can be conducted by the independents either continuously as the model develops or after the initial development. However, the latter approach can incur significant time and costs.

iv) Application of a scoring technique based on a set of chosen success criteria for a valid model.

Sargent, 2011 considers that the V&V is a cyclic procedure which is linked to the overall modelling process. In other words, the scope of the V&V must take into consideration the initial development of the Conceptual Model. This is defined as a logical representation of the hypothesis being modelled, including the key variables and their associated interactions. The main phases of this cyclic process are represented in Figure 2-15 [*Sargent, 2011*].

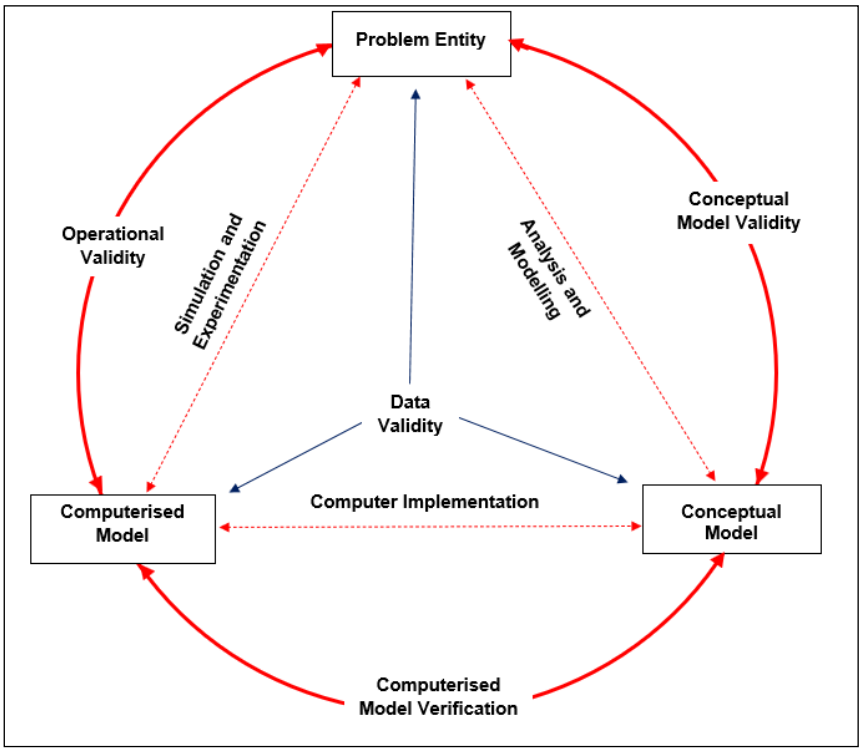

Figure 2-15: Software based model development, verification and validation cycle [*Sargent, 2011*]

Effectively, any inconsistencies revealed during the V&V process would mean that the Conceptual Model should be checked and revisited. The first stage of the modelling process is to define the Problem Entity for the hypothesis being modelled. For instance, this could be the likelihood of a hydrogen explosion, given the presence of certain conditions. This is followed by the development of the Conceptual Model. The Software Model is developed through a replication of the Conceptual Model and tested quantitatively using various sets of data. The input data source for the Software Model can be experimental, expert opinion or obtained from the literature.

The development of the Conceptual and Software models is proceeded by Validation and Verification. The Conceptual Model Validation aims to ensure that all key assumptions and the principles, e.g., equations and variables affecting hydrogen generation rates, are correct. This validation is likely to require input from the end users as well as reference to literature. The Software Model Verification step aims to demonstrate that the Conceptual Model as well as the quantified input data have been applied appropriately. This verification also entails a comparison of the model output results with expected trends.

For BBN models, the inference or 'updating' capability of the software such as Netica [*Norsys, 2010*] is a useful tool for evaluation of the model behaviour with changes to the input data. The output from the updated model can then be compared with expected trends, which forms a key part of the verification process. Another feature built within the BBN software is reverse inference which enables determination of the input conditions needed for a given outcome. This is particularly useful for testing the model with extreme conditions such as the conditions required for a high probability of a hydrogen explosion.

The Operational Validation step in Figure 2-15 represents the process for demonstrating that the model output is reasonably accurate across the whole range of the input data. The main Operational Validation techniques suggested by *Sargent, 2011* include:

- Validation of the modelling data through a comparison with literature and historical trends from the operational plants.
- Consultation with Subject Matter Experts (SMEs) and the model end users to gain confidence that the Conceptual Model and the output results are plausible.
- Conducting computer experiments during the simulation and experimentation stage, e.g., by testing the model output results with extreme conditions.
- Performance of a sensitivity analysis to changes in input variable magnitude, ensuring that the parameters with the highest sensitivity are reasonably accurate.
- Application of graphics to illustrate the change in model output results with a variation in input data and demonstrating that the model behaves as expected.
- Ensuring that the parameter data are consistent with plant operation, e.g., radiolytic hydrogen generation rates being significantly low in comparison with the Magnox corrosion mechanism.

A review of the literature suggests that the generic V&V process given by *Sargent 2011*, has not been previously applied to BBN models for nuclear engineering applications. However, the method has been utilised in the aviation industry. For instance, *Schietekat et al, 2016* applied each of the processes given in Figure 2-15 to the V&V of a BBN model for aircraft vulnerability due to launches of air missiles. Initially the Problem Entity was

identified, by engaging the clients to understand their needs and the environment in which the model was used. In this case the client specification and user environment were identified as, ‘generate a model for research and training purposes that determines how the factors associated with air missile launches affect aircraft vulnerability’.

Having defined the Problem Entity, *Schietekat et al, 2016* developed the Conceptual Model through the of identification of the key variables, causes and effects with respect to aircraft vulnerability due to air missiles. The key variables were identified as the miss distance, which is the closest distance that the missile will pass the aircraft, the aspect angle between the missile and the aircraft, the aircraft altitude, and the likelihood that an air missile is launched. A graphical cause and effect structure was developed and agreed with the client. This agreement with the client end user formed the first step in the validation of the Conceptual Model. The Conceptual Model was subsequently replicated to form a Computerised Model of the BBN using the Hugin software [*Hugin, 2016*].

The Computerised Model developed by *Schietekat et al, 2016* consisted of a BBN with two Child nodes i.e., ‘launch’ and ‘miss distance’ which required generation of Conditional Probability Tables (CPTs) and appropriate validation of the data. The CPT for the ‘launch’ node was initially created in a spreadsheet using expert elicitation based on the user knowledge. As part of the Conceptual Model validation, the CPT was checked by the domain experts. It was however recognised that there is an uncertainty associated with data from the experts due to unrealistic confidence and bias, therefore the review of such data was given an increased scrutiny. The CPT for the BBN ‘miss distance’ node was generated based on data from the previous aircraft computer simulations for operator training.

The Computerised Model of the BBN with the CPT data in Hugin was subsequently verified by *Schietekat et al, 2016,* using the diagnostic and predictive inferencing techniques. Effectively the inferencing capabilities of the BBN enabled validation through a ‘what-if’ type analysis. At this stage of the V&V process the model was also validated to show that it provides a suitable representation of reality. This required the output from the BBN inferencing tests to be reviewed by the client and the domain experts in terms of their opinion on the plausibility of the results and the closeness to reality. Any inconsistencies in the inference results led to the Computerised and Conceptual Models being rechecked. For instance, by instantiating the nodes for aspect angle, range and altitude to mid-range values, a relatively high probability of >60% for a missile being launched was predicted by the BBN. The domain experts were able to verify the plausibility of this result through experience and knowledge from historic events.

2.6 Identification of knowledge gaps in nuclear chemical plants

Based on the literature review in the preceding sections, this section identifies distinct knowledge gaps relating to the QRA approach, hydrogen safety and operability issues associated with nuclear chemical plants. For cross-referencing purposes, an identification number is assigned to each knowledge gap.

2.6.1 Knowledge gap relating to the QRA approach

The literature review of the QRA techniques as detailed in Section 2.5 shows that the FTA and ETA methodologies present a deficiency in terms of modelling dependability between variables. Furthermore, only two states can be modelled in FTAs and ETAs i.e., a failure or no failure. However, some risk assessments would require consideration of many interacting parameters. The BBN technique provides the ability to assess dependability between variables with any given number of states. Also, the effect of change in one variable on the other parameters within the BBN is immediately observable.

Literature review of the Monte Carlo Simulation method in Section 2.5 shows that it has the advantage of modelling the likelihood of the primary events in the form of a Probability Density Function (PDF) in a Fault Tree. Figure 2-14 provides an illustration of this concept. Standard FTAs often use single bounding case values, instead of a PDF, which can lead to overly pessimistic end results. The output from the MC analysis is the probability distribution curve which provides a more accurate and better understanding of the credibility of the fault hypothesis and the key sensitivities in terms of the mean, standard deviation and variance.

Despite the good supporting literature on the performance of the BBN and MC methods, through discussion meetings with the SL SMEs, it was revealed that that the FTA and ETA techniques continue to be applied in nuclear safety cases and engineering analysis. For instance, during the discussions with the Criticality and Equipment Reliability groups, it was understood that FTA is the formal methodology applied to criticality and reliability assessments [*Ahmed, 2017c, Ahmed, 2018b*]. Discussions with the CISWG revealed that the safety case for the likelihood of a discontinuous release of hydrogen from sludge wastes is based on the ETA method [*Ahmed, 2017a*].

It is considered that the MC and BBN techniques could provide significant benefits in terms of the uncertainty analysis. The lack of use of such methods within nuclear chemical plants presents a knowledge gap in terms of the uncertainty associated with the variables affecting hydrogen safety and operability issues (**Knowledge Gap KG1**).

2.6.2 Knowledge gaps associated with hydrogen safety cases

A series of meetings were held with the SL Hydrogen Working Party (HWP) and the Characterisation, Inventory, Sludge Waste (CISWG) groups to identify the main nuclear chemical plant processes where hydrogen generation is currently a significant issue. Based on the minutes of these meetings provided by *Ahmed, 2016, Ahmed, 2017c, Ahmed, 2018a and Ahmed, 2019c*, and a review of the Hydrogen Technical Guide (HTG) by *Ingram et al, 2001*, the key hydrogen issues in nuclear chemical plants are:

- Corrosion of metallic magnesium fuel cladding (Magnox) waste under water, within transportable storage skips, to form magnesium hydroxide sludge and a continuous release of hydrogen, referred to as 'chronic' hydrogen.
- Slow release of hydrogen due to radiolysis of aqueous radioactive liquors within the stored skips.
- Radiolysis of radioactive liquors within process vessels and sealed process pipes.
- Hydrogen hold-up in sludge waste forms and a sudden discontinuous release of the gas into the ullage space of the storage skip.

The safety cases for the hydrogen generation processes listed above are reliant on accurate assessments of the likelihood of flammable hydrogen in air mixtures developing in the ullage spaces of vessels and enclosures. It is recognised that deterministic features such as passive vents have been introduced into the design of the transportable storage skips. These passive features enable continuous venting of the chronic hydrogen. However, there is still the need to analyse the uncertainty associated with chronic hydrogen generation rates and the impact of hydrogen hold-up and discontinuous gas release scenarios on the risk of hydrogen explosions. This is necessary in order to demonstrate that the deterministic features and other risk reduction measures are adequate.

The HTG outlined by *Ingram et al, 2001* has provided extremely useful knowledge about the factors which must be taken into consideration in the quantification of the likelihood of hydrogen explosions. However, it is restricted to certain types of faults and combination of events. This could potentially lead to making assumptions about given fault scenarios which are not a true representation of the fault being assessed. For instance, when assessing the probability of ignition from free falling objects, the guidance requires the assessor to confirm if rust is present on the impacted surface and if the total kinetic energy of the object before the impact is >40J. If rust is present but the kinetic is

not >40J, then the guidance suggests a single value of <0.1 for the ignition probability. The ignition probability could be sensitive to a range of values for the kinetic energy and the quantity of rust present. Hence the use of single values for the variables may not give an accurate assessment of the risk of hydrogen explosions.

For nuclear decommissioning safety cases such as interim storage of waste where an incorrect judgement about the likelihood of hydrogen explosions would have significant repercussions, an accurate quantification of the risk is vital. Bayesian Networks and Monte Carlo simulations could be used to undertake an uncertainty analysis for such safety cases thus improving risk quantification. The current safety cases for interim storage of waste within skips are based on the standard FTA and ETA approach without undertaking an uncertainty analysis. Clearly this is a knowledge gap which could be addressed through the BBN analysis. Furthermore, the uncertainty associated with the discontinuous release of hydrogen is a knowledge gap that needs to be addressed (**Knowledge Gap KG2**).

A further issue identified in Section 2.2 is the uncertainty associated with the sources of hydrogen and the potential impact on the estimation of the hydrogen generation rates (**Knowledge Gap KG3**). The uncertainty about the sources of hydrogen means that some of the hydrogen management strategies given in the Ignition Roadmap [*Ingram et al, 2001*], such as the use of intrinsically safe or inert mixtures as feed cannot be used. The effect of the uncertainties associated with the sources of hydrogen, such as radiolysis, could be resolved by BBNs, for example by using the technique to determine the sensitivity to factors such as the ‘G values’. This would give a more representative estimate of the hydrogen generation rates.

It is known that the presence of radioactive liquors in sealed process pipework in a high radiation environment can lead to the generation of radiolytic hydrogen gas. If the hydrogen gas is not vented it could result in a detonation depending on the pipe geometry. It is considered that the uncertainty of hydrogen detonations in sealed pipes is a knowledge gap. This uncertainty could be managed more effectively by undertaking a Bayesian analysis of the variables which have an impact on the consequences of hydrogen accumulation in sealed process pipes (**Knowledge Gap KG4**).

The HTG [*Ingram et al, 2001*] suggests that the slow release of hydrogen through radiolysis could be managed using highly reliable ventilation extract systems. However, there is a knowledge gap associated with the reliability of the ventilation systems and the performance of such systems against time limitations. For instance, the time taken to reach the LFL and the 8% hydrogen concentration limit for ‘plant resilience’, in

comparison with the time taken to repair the vent system following a failure, is a knowledge gap that needs to be addressed (**Knowledge Gap KG5**).

Resilience is a phrase used in nuclear safety cases to describe the robustness of process plants in terms of the design and response against extreme scenarios such as hydrogen explosions. The initiative for demonstration of plant resilience was introduced in nuclear safety cases following the Fukushima Daichaii power plant incident in 2011. *Hollnagel and Yushi, 2013* provide a detailed review of the catastrophic events that led to the disaster in Fukushima Daichaii and argue that this occurred due to a lack of resilience. Given that many existing nuclear chemical plants are aged facilities, in modern SL safety cases the 8% hydrogen concentration is used as a limit beyond which there is an increased likelihood of damage to structures following a hydrogen explosion. Hence to demonstrate plant resilience, reliable systems would be needed to prevent reaching the 8% hydrogen concentration. It is considered that **Knowledge Gap KG5** could be addressed through an uncertainty analysis using BBNs and MC simulations e.g., by determining a probability of failure of the main plant components. This way the system reliability could be determined and any areas for improvement identified.

To demonstrate that the risk of hydrogen explosions is ALARP, fit for purpose decisions are necessary on whether it is acceptable to install mitigating measures. Current practice for decision making in nuclear chemical plants is either qualitative or to apply the HSE Cost Benefit Analysis (CBA) technique [*HSE, 2020*]. Whilst the use of CBA as a means of ALARP justification is also well recognised [*French et al, 2005*], the technique does not directly link the decision utilities with the risk variables such as those affecting hydrogen explosions. Consequently, an analysis of the sensitivity to changes in the risk factors on the decision outcome is not possible using the current approach (**Knowledge Gap KG6**). As detailed in Chapter 3 Netica software by *Norsys, 2010* provides the Decision Network tool that links the decision nodes with the risk variables. This tool could be used to provide an enhanced means of assessing the decision uncertainties.

2.6.3 Knowledge gaps associated with plant operability issues

Managing the uncertainty associated with hydrogen hazards in nuclear chemical plants is the focus in this research project. However, during the investigation of knowledge gaps associated hydrogen hazards, discussions with various groups within SL were held including the CISWG, Criticality and the Reliability Engineering teams. During these discussions, uncertainties on plant operability, throughput and non-hydrogen related safety issues were also identified.

Discussions with the CISWG led to the identification of a knowledge gap concerning the uncertainty associated with effective mixing of radioactive sludge wastes in nuclear chemical plants. The uncertainty is associated with sludge mixing parameters which affect sludge behaviour and the ability to remove the product effectively from the mixing vessel whilst maintaining acceptable product quality. Although some trial work on the mixing vessel behaviour has been previously conducted, there is a need to analyse the effect of changing mixing parameters without undertaking additional time-consuming experiments. This is a knowledge gap which could be addressed through a BBN uncertainty analysis (**Knowledge Gap KG7**).

As an example of how **Knowledge Gap KG7** could be addressed, the parameters affecting the likelihood of the grouted mix being removed, the product quality and the uncertainty ranges associated with all the variables would need to be modelled in a BBN. Using the Bayesian updating feature, the likelihood of the sludge being removed and achieving a good product quality could be determined by fixing each variable with a given value. By repeating the analysis an optimum set of operational parameter values required for a successful mixing campaign could be determined.

Safe storage of radioactive waste material in skips requires the use of robotics for characterization and size reduction of the waste. Journal articles published by *Tsitsimpelis et al, 2019, Bloss, 2010, Bogue, 2011, Fuji et al, 1976, Cateret et al, 1997 and Fischetti, 1985,* discuss the effectiveness of robotics in nuclear applications. However, a high reliability of the robotic systems is desired in order to minimise the risk of a breakdown and hence preventing radiological impact due to recovery operations. There is an uncertainty associated with the key parameters e.g., common mode failures, which could be investigated in order to improve the overall robot reliability (**Knowledge Gap KG8**). It is considered that the BBN updating capability could be used to undertake reliability and sensitivity analyses of the robot system.

Processed nuclear fuel rods result in the generation of solid metallic waste including PuO_2 powder consisting of the fissile radionuclide Pu-239. If the metallic waste also contains water moisture and subsequently stored in containers there is the potential for a fission chain reaction, referred to as a ‘criticality’, leading to a release of gamma radiation [*Knief,2008*]. Water behaves as a ‘moderator’ for the criticality chain reaction by reducing the speed of the neutrons involved in the fission and increasing the chances of the reaction. However, there is an uncertainty on the distribution of the fissile Pu-239 mass and water volume needed for a criticality. Hence this results in a knowledge gap on the likelihood of a criticality within the storage containers (**Knowledge Gap KG9**). It is considered that a BBN analysis could be undertaken to quantify the probability of a

criticality and to identify the best practicable means of reducing the likelihood of the event.

2.7 Identification of nuclear chemical plant case studies

Based on the knowledge gaps KG1 to KG9 identified in Section 2.6, Table 2-6 identifies the case studies for investigation, as part of this research project. Chapters 4 to 10 provide the details of the research undertaken for each of the seven case studies.

Case Study	Description	Knowledge Gap ID
1	Bayesian Belief Network analysis of radiolytic hydrogen in sealed process pipes	KG3, KG4
2	Bayesian Belief Network analysis of uncertainty associated with mixing of radioactive sludges in the waste treatment and encapsulation process	KG7
3	Monte Carlo simulation of a forced ventilation system failure to dilute radiolytic hydrogen in the ullage space of a vessel and comparison with Bayesian network analysis	KG1, KG5
4	Bayesian belief uncertainty analysis of hydrogen generation in transportable vessels containing intermediate level wastes	KG1, KG2
5	Bayesian Belief Network analysis of the likelihood of a criticality in containers of material mixed with PuO_2	KG9
6	Bayesian Decision network analysis for installing a compressed air supply to mitigate the risk of hydrogen explosions in ancillary process vessels	KG6
7	Application of Bayesian networks to assess reliability of robots for processing operations in radiation environments	KG1,KG8

Table 2-6: List of research case studies linked to knowledge gaps

CHAPTER 3 : METHODOLOGY

3.1 Introduction to Chapter 3

This chapter investigates the methodology to be used in the research project to analyse and manage the uncertainty associated with hydrogen safety and operability issues in nuclear chemical plants. Based on the literature review in Chapter 2, two specific Quantified Risk Assessment (QRA) techniques have been identified namely, Bayesian Belief Networks (BBN) and Monte Carlo (MC) simulations. Both these techniques provide the ability to undertake an uncertainty analysis, using computer software. As part of the methodology, a description of the design of the project is given, followed by the procedures used for the BBN analysis and MC simulations. A discussion on the choice of the selected software in comparison with other commercially available systems is also given.

3.2 Description of design of the research project

This research project involves the application of modern QRA techniques to analyse the risk and uncertainty associated with hydrogen safety and operability issues in nuclear chemical plants. Although both the BBN and MC techniques will be applied in this project it is emphasised that in line with the main objectives of this research project, as identified in Chapter 1, the focus is on the application of the BBN technique.

The main stages of the project are:

1) Identification of suitable plant case studies. This stage involved engaging the Subject Matter Experts (SMEs) from the SL Hydrogen Working Party (HWP), Characterisation, Inventory, Sludge Wastes Group (CISWG), Reliability Engineering and Criticality Assessment. The discussions with these groups aimed to identify the key areas of uncertainty concerning hydrogen safety and plant operability.
2) Identification of key variables for the uncertainty analysis of each of the case studies. Here the interactions between the variables were also identified through discussion meetings with the SL SMEs.
3) Development of the Concept BBNs and MC simulations for the identified case studies using the information gathered in stages 1 and 2 and agreeing with the SL SMEs.
4) Prediction and agreement with the SL SMEs the source data for input to the BBN and MC analysis. The Conditional Probability Tables (CPTs) for the discrete nodes in the BBN analysis were also agreed with the SL SMEs.

5) Comparison of performance of the BBN and MC techniques with the Fault and Event tree analysis approach currently used within the safety cases for nuclear plants to evaluate hydrogen safety and plant operability issues.

The above process for undertaking the BBN and MC analyses and the learning gained from experience, e.g., the problems encountered and how they were resolved, were also used to suggest recommendations for improvements.

3.3 Methodology used for construction of Bayesian Belief Networks

The Bayes theorem concept and an illustrative example on the application of the Bayesian Belief Networks to hydrogen explosion hazards is detailed in Chapter 2 on Literature Review. This section discusses the generic BBN analysis process.

A BBN identifies believed relations between a group of variables relevant to the problem. A typical problem modelled in a BBN in terms of hydrogen safety would be the risk of a hydrogen explosion occurring in the ullage space of a vessel or an enclosure. The process for construction of a BBN for this problem would be:

- The BBN assessor initially predicts the variables affecting hydrogen generation and ignition.
- Causal relations between the variables are then predicted; this involves engaging the opinions from the SL SMEs.
- The causal relations are represented in a directed acyclic graph which consists of a group of random variables or nodes.
- If there is a causal dependability between two nodes in the graph, the corresponding two nodes are connected by an arc.
- An arc from a node A to a node B indicates that the random variable A (often termed as the ‘Parent Node’) causes the random variable B (‘Child Node’).
- One node is used for each variable, which may be either ‘discrete’ or ‘continuous’.
- A discrete variable consists of a set of possible states, for example the answer to a question i.e., ‘yes’ or ‘no’ or an assumption which is true or false.
- A continuous variable consists of a range of values which may be defined as a probability distribution, e.g., Normal Distribution.
- Conditional probabilities for the identified relations are derived using experimental data, mathematical model equations and the SL SME opinion.

- Conditional Probability Tables (CPTs) are finally compiled. A CPT for a Child Node identifies the probabilities of the node accepting each of its values which are conditional on the values of the Parent node.

Figure 3-1 summarises the BBN analysis process in the form of sequence of main steps. Based on the output from this research project, this BBN analysis process was also discussed by the candidate in the Nuclear Future journal publication [*Ahmed, 2019a*].

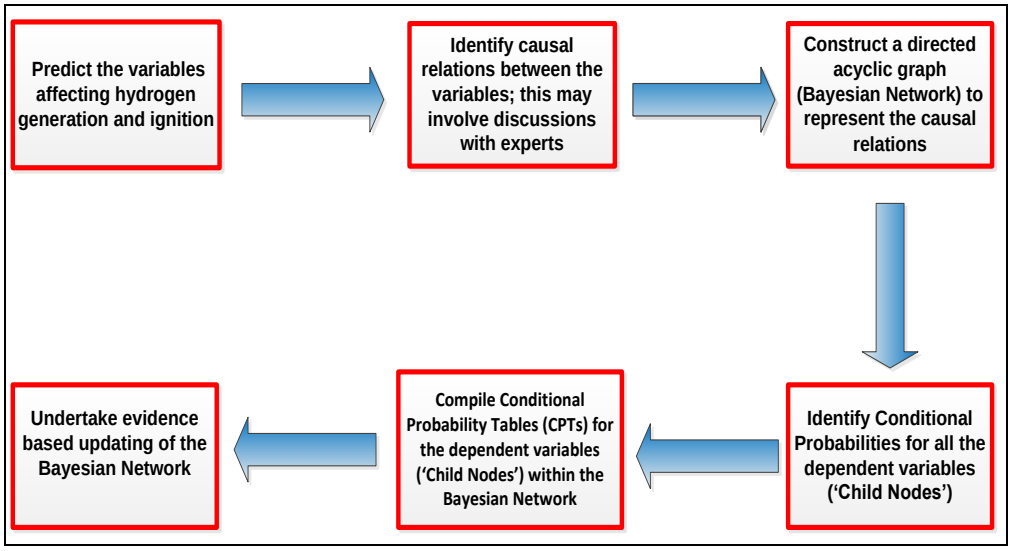

Figure 3-1: Overall Process of Bayesian Analysis [*Ahmed, 2019a*]

3.4 Selection of Software Systems for BBN Analysis

As discussed previously, the Bayesian algorithm for large systems with multiple variables and interactions would be difficult to compute manually. Therefore, commercial software systems for BBN analysis have been developed by external organisations. The most widely used software systems include:

- Netica [*Norsys Software Corporation, 2010*]
- Hugin [*Hugin Expert A/S, 2018*]
- Bayes Server [*Bayes Server, 32 Bit ,2018*]

From the list above, this section details the research into the most widely used software and selects the system appropriate for this research project.

3.4.1 Netica

Netica, by *Norsys 2010*, is commonly used in the fields of medical diagnosis, finance and engineering. The software has an Application Programming Interface (API) which is compatible with the modern programming languages including C, C++ and Java. Using the Component Object Model (COM) interface Netica can also be programmed

to enable usage of other languages such as Visual Basic. The distinct software functionalities associated with Netica are discussed below.

3.4.1.1 Ability to Evaluate Discrete and Continuous Nodes

Netica provides the choice for modelling both Discrete and Continuous variables. Furthermore, in Netica deterministic and probabilistic equations as a function of the parent nodes can be entered to enable the CPT of the Child Node to be determined. For example, say there is a requirement to calculate the probability distribution of total hydrogen generation rate, denoted by a Discrete Node C. This is the sum of the chronic hydrogen generation rate (Discrete Node A) and the radiolytic hydrogen generation rate (Discrete Node B). Knowing the probability distributions of Node A and Node B, as given in Figure 3-2, Netica then calculates the distribution of Node C using equation 3-1:

$$C(A, B) = A+B \qquad (3\text{-}1)$$

Figure 3-2 shows that with the mean values of 1.6L/hr and 0.164L/hr for Nodes A and B respectively, the calculated mean value for Node C is 1.76L/hr.

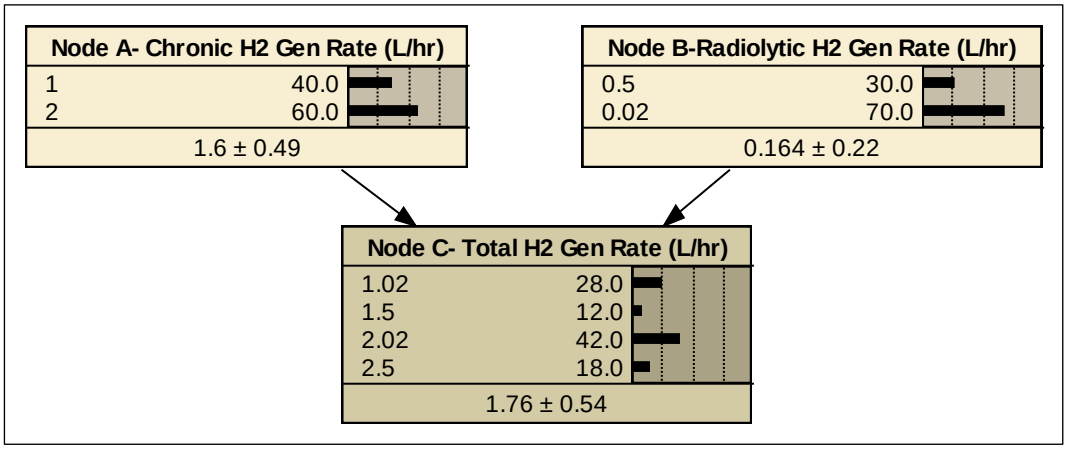

Figure 3-2: BBN using equation 3-1 to calculate Node C probability distribution

An important rule that must be taken into consideration, when applying equations to discrete and continuous nodes is that the child node, which links to any given number of discrete parent nodes, should also be modelled as a discrete node. Otherwise, the calculated result for the child node can be inconsistent and not representative of the true model.

3.4.1.2 Utilisation of Equations to Evaluate Large CPT Matrices

A significant benefit in the ability to use equations in Netica is that this enables the calculation of the conditional probabilities and compilation of the CPT of the parent nodes by converting the equation to a table. This is particularly advantageous when

handling multiple parent nodes for any given child node, resulting in a large CPT matrix. The size of the CPT matrix for a Child node is proportional to the number of its individual states and the number of Parent nodes states. In the case of the Bayesian Network in Figure 3-2, Netica calculates the CPT for Node C based on equation 3-1 as shown in Figure 3-3.

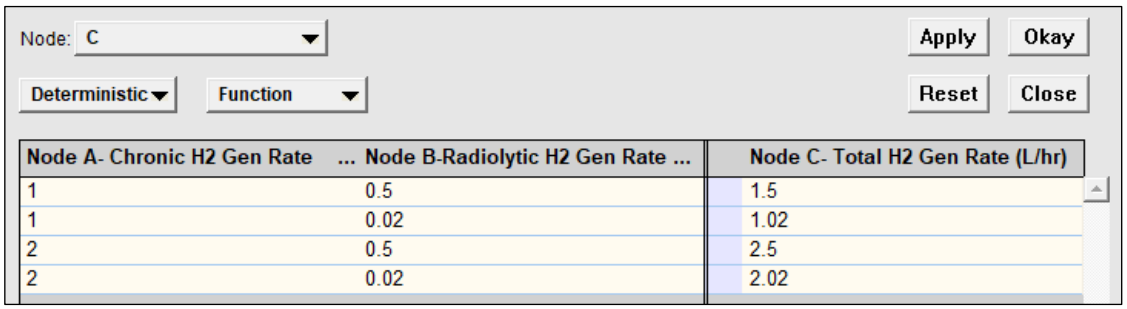

Node A- Chronic H2 Gen Rate	... Node B-Radiolytic H2 Gen Rate ...	Node C- Total H2 Gen Rate (L/hr)
1	0.5	1.5
1	0.02	1.02
2	0.5	2.5
2	0.02	2.02

Figure 3-3: Netica output for Node C CPT, total hydrogen generation rate

As well as giving the capability of entering specific equations derived by the user, such as equation 3-1, the Netica software provides a library of standard equations and mathematical functions. For example, if it is hypothesised that a certain parameter follows a Normal Distribution, the function NormalDist (x, μ, σ) can be selected from the library, where x is the parameter value, μ is the population mean and σ is the standard deviation. Other mathematical equations listed in the library, relevant to this research project, include the Boolean functions. For example, to model a Boolean 'OR' node, represented by a Child node X which is affected by either of the parent nodes Y_1 , Y_2 or Y_3, the following OR functionality can be selected from the library (equation 3-2):

$$p\,(X \mid Y_1,\, Y_2,\, Y_3) = \; or(\, Y_1,\, Y_2,\, Y_3) \tag{3-2}$$

Similarly, to model the Boolean 'AND' logic between nodes Y_1,Y_2 and Y_3, the Netica library enables selection of the following functionality (equation 3-3).

$$p\,(X \mid Y_1,\, Y_2,\, Y_3) = \; and(\, Y_1,\, Y_2,\, Y_3) \tag{3-3}$$

3.4.1.3 Ability to Discretise Continuous Nodes

A Continuous Node based on an equation also requires an input of the range in terms of the maximum and minimum values of the variable, for the purpose of 'discretisation'. The term discretisation is defined as the conversion of a continuous variable into discrete intervals to enable the BBN model to assign a probability density to each interval. This is necessary before the equation can be converted to a CPT table. The conversion process in Netica involves the identification of a random location in every discretised cell for the equation calculation. The BBN user is then requested to input the number of random samples to take from each cell, e.g., 100 or 1000. Whilst

discretisation does result in some error, this is reduced with increasing number of samples per cell. The Network results may also be sensitive to the choice of discretisation. Therefore, the sensitivity to the discretisation should be tested. An example of discretisation of continuous variables is given in Figure 3-4. Using the minimum and maximum values of 0 and 2.31E6 respectively for a Continuous variable which models the alpha activity concentration in a skip, the range is discretised into 10 equal intervals as shown in Figure 3-4.

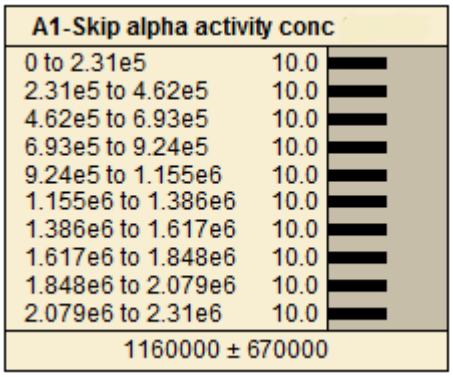

Figure 3-4: Example showing discretisation of a Continuous variable in Netica

For each of the discretised intervals, Netica calculates the probability distribution using the equation p (A1 |) = UniformDist(A1,0,2.31E6). Based on 10,000 samples per cell, a mean activity concentration value of 1.16E6 is calculated in Figure 3-4.

3.4.1.4 Belief Updating and Probabilistic Inference Using Netica

An important aspect of Bayesian Belief Networks is that they can use probabilistic inference to incorporate new evidence of any given variable and predict new probabilities of the other dependant nodes. This form of belief updating is particularly advantageous when undertaking a sensitivity analysis to identify variables which have the greatest impact on the likelihood of a given hypothesis. Netica is able to perform probabilistic inference and belief updating using the 'Findings' function which can be demonstrated using hydrogen ignition as the hypothesis. The hypothesis assumes that an ignition of hydrogen gas mixture occurs due to the following causes and the associated Prior probabilities. These events are based on the ignition probability values derived from the HTG and the associated Ignition Road Map for mechanical surfaces contaminated with reactive materials:

- A prior probability of 15% is assumed for a flammable hydrogen in air mixture.
- A prior probability of 10% is assumed for a mechanical impact following a vertical drop of an object with a mass of 2kg from a height>2m (4m maximum).

- The impact energy for a mass of 2kg dropped from a height of up to 2m is 2kg x 10m/s^2 x 2m i.e., 40J and similarly 80J for a drop height of 4m.
- A 50% probability is assumed for reactive substances present on the target.
- For an impact from a drop height of <2m, with an energy of less than 40J on to a hard surface with or without the reactive substances, the HTG suggests an ignition probability of < 0.1. Hence an ignition probability value of 8% is used.
- For an impact from a drop height of up to 4m, with an energy of >70J on to a hard surface with reactive substances, the HTG suggests that the ignition probability is very high. A high ignition probability of 60% is therefore used.
- For an impact from a drop height of up to 4m, with an energy of >70J on to a hard surface with no reactive substances, the HTG suggest that the ignition probability is low. A value of 10% is used.

Based on the key assumptions listed above, the following CPT data for each combination of events are derived (Table 3-1).

Reactive Substance	Vertical Drop Height	Hydrogen Concentration	% Probability of Ignition	% Probability of No Ignition
Present	Above 2m	Above LFL	60	40
Present	Above 2m	Below LFL	0	100
Present	Below 2m	Above LFL	8	92
Present	Below 2m	Below LFL	0	100
Not Present	Above 2m	Above LFL	10	90
Not Present	Above 2m	Below LFL	0	100
Not Present	Below 2m	Above LFL	8	92
Not Present	Below 2m	Below LFL	0	100

Table 3-1: Matrix of CPT for all Possible Events Modelled in BBN (Figure 3-5)

The BBN for the hypothesis discussed above is shown in Figure 3-5. The probabilities 1.6% and 98.4% calculated in the BBN represent the likelihood of an ignition when taking into consideration all possible events listed in Table 3-1.

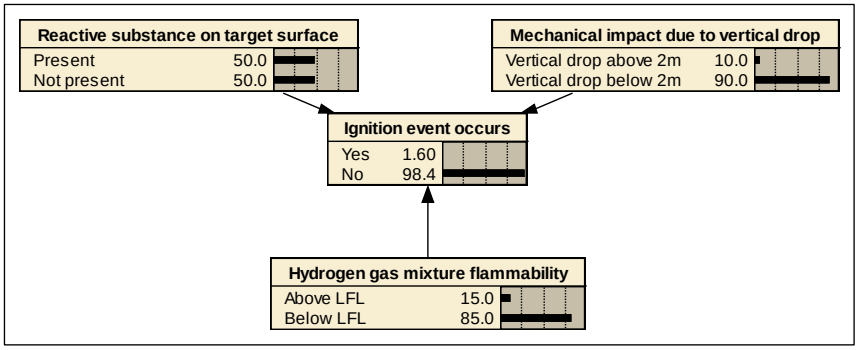

Figure 3-5: Effect of impacts, H_2 concentration and reactive substances on ignition probability

If new evidence indicates that a vertical drop from a height >2m can occur i.e., the probability of a vertical drop is increased from 10% to 100% (Posterior), then Figure 3-6 shows that the probability of ignition increases to 5.3%. There is only a slight increase in the ignition probability in Figure 3-6 because the probabilities of the other two nodes are still the same as the original prior values.

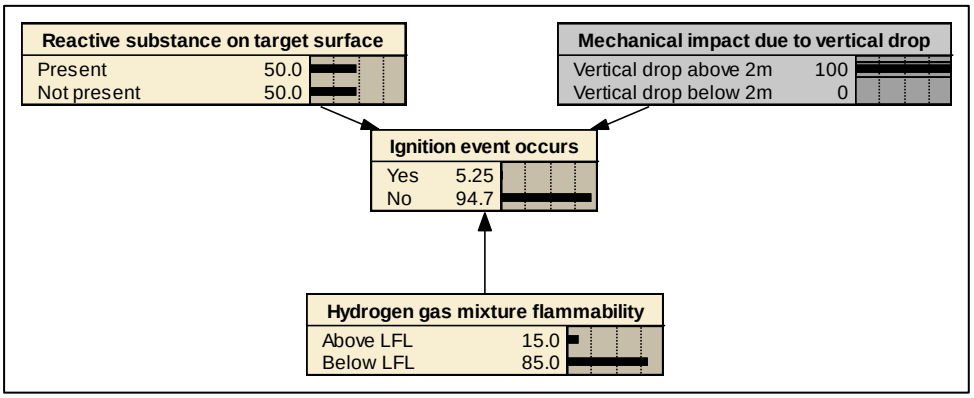

Figure 3-6: Effect of increase in mechanical impact probability on ignition probability

If new evidence shows that a flammable mixture can arise, then the instantiation of the Hydrogen Flammable Mixture node results in an increase in ignition probability to 10.7%, as shown in Figure 3-7.

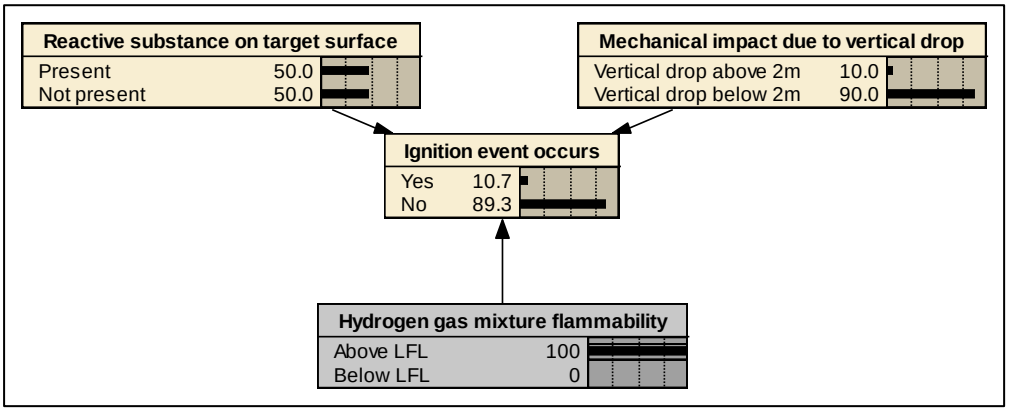

Figure 3-7: Effect of Increase in flammable mixture probability on ignition probability

If both the vertical drop and the flammable mixture events arise coincidently then, as expected, Figure 3-8 shows that the ignition probability increases even further to 35%.

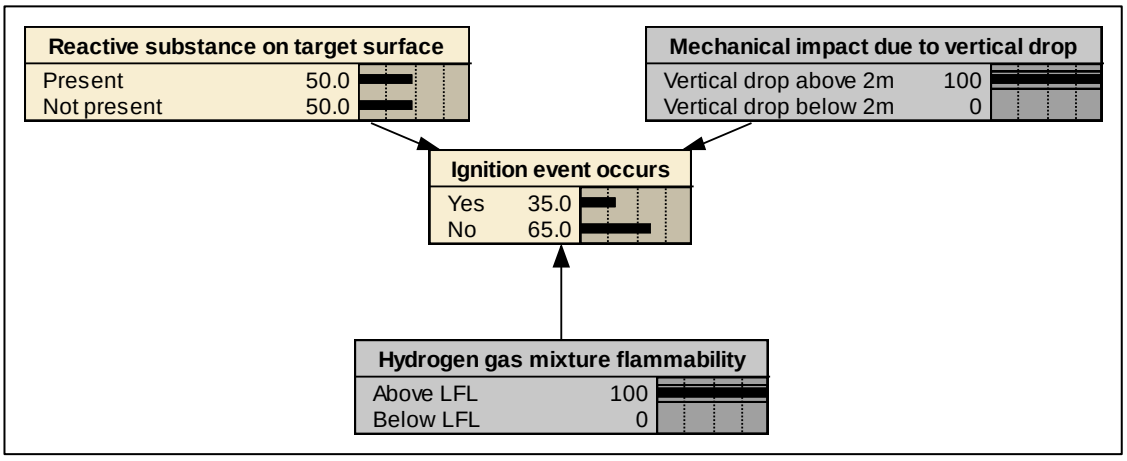

Figure 3-8: BBN for effect of increase in flammable mixture and mechanical impact probabilities on ignition probability

The illustrations given in Figure 3-5 to Figure 3-8 demonstrate the significant benefits of the BBN approach. For example, it provides a visibility of the interactions between all the nodes. Also, the changes to the probabilities values of various nodes following input of new evidence are easily observable. The ability of BBNs to model multiple dependencies also means that more than two states can be analysed, whereas the FTA and ETA are binary systems limited to two states, e.g., true or false states via AND and OR gate application.

From the analysis given above it can be observed that the BBN technique is dependent on a knowledge of the conditional probabilities of the dependent variables. Possible ways of determining the conditional probabilities would be to conduct a survey of plant performance to obtain realistic estimates of the failure rates of plant components. Expert opinion from plant operators could also be gained in terms of likelihood of failure modes. Furthermore, manufacturer's data could be used to determine the failure probabilities.

3.4.1.5 Application of Utility Nodes to Construct Decision Networks

The Decision Net functionality of Netica can assist with problems involving important decision making by incorporating controllable variables, i.e., the decision nodes and the variables which require optimisation, i.e., the utility nodes [*Shachter and Peat,1992*]. The utility node is based on the concept of the level of satisfaction or value, for example a monetary value. A utility with the highest monetary value would represent the best choice by the decision maker and conversely the lowest utility value indicates the worst decision. Important methodology rules for the construction of Decision Nets

are that the utility is always a continuous node, but it has no dependent variables, i.e., Child nodes. Netica provides the ability of modelling more than one utility by summing the values.

A demonstration of a decision net is given in Figure 3-9 which considers a decision on whether to install a hydrogen monitoring system to monitor the hydrogen gas concentration in the ullage space of a vessel. Without the hydrogen monitors, the likelihood of a hydrogen explosion is known to be 5% probability. Hence the monitors would reveal a high hydrogen concentration in the ullage space, allow remedial action to be taken and prevent a consequence. The likelihood of a hydrogen explosion is represented by the beige Nature Node and the decision to install the hydrogen monitors, to detect hydrogen concentration in the ullage space, is shown as the blue Decision Node. The Decision Node affects the relative monetary value for each decision. This is modelled in the 'Utility Node', shown as a pink hexagon.

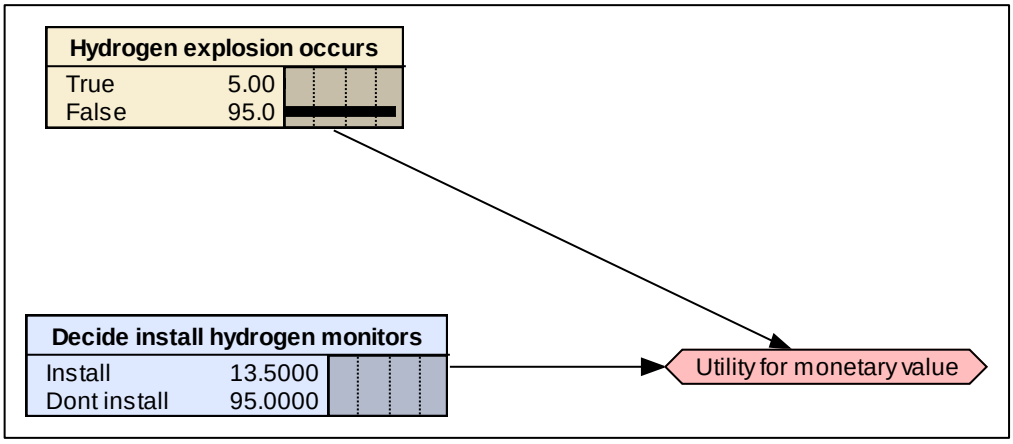

Figure 3-9: Simple Decision Net for installation of hydrogen monitors

In this demonstration the decision maker would be most satisfied if the likelihood of a flammable concentration is false, and he does not install the hydrogen monitors as there is no detriment in terms of consequence or cost. A monetary utility of 100 is assigned for this decision. The next most preferred decision would be if the flammable concentration likelihood is true, and he installs the hydrogen monitors. Although the hydrogen monitors will prevent a flammable concentration, a lower utility of 80 is assigned as the cost of installation has incurred.

A decision to install the hydrogen monitors when the likelihood of a flammable concentration is false, would be dissatisfying as expenditure has incurred without any justification. A low utility of 10 is therefore assigned for this decision. However, the most unsatisfactory decision would be if the likelihood of a hydrogen explosion is true, but a choice has been made for not installing the monitors. For this decision, the lowest utility

of zero is assigned. On this basis the decision matrix for the network in Figure 3-9 is given in Table 3-2.

Utility for monetary value	Decision, Install hydrogen monitors	Hydrogen explosion occurs
80	Install	TRUE
10	Install	FALSE
0	Do not install	TRUE
100	Do not install	FALSE

Table 3-2: Monetary values for hydrogen monitors Decision Net

Using the monetary values for each decision listed in Table 3-2, the Decision Net in Figure 3-9 shows that the utility value for the decision for not installing the hydrogen monitors is higher, i.e., 95.0 in comparison with the decision to install the monitors which is 13.5. Hence by taking into consideration the dependencies between the Nature Nodes, Decision Nodes and the Utility Nodes an optimal decision can be reached during a decision making process.

Similar to Belief Networks, Decision Networks (DNs) can also be updated with new evidence and hence enable prediction of the impact on a decision. Suppose new evidence suggests that the likelihood of a hydrogen explosion is equivalent to a probability of 80%, instead of the previous 5% value. Using the Netica Findings function with this new piece of evidence, the updated DN in Figure 3-10 shows that the utility for the decision to install the monitors is now higher, i.e., 66.0 than the utility of 20.00 for not installing the monitors. Thus, provided that the utility values can be justified, the DN updating function provides a powerful and constructive way of identifying key sensitivities that affect the end decision.

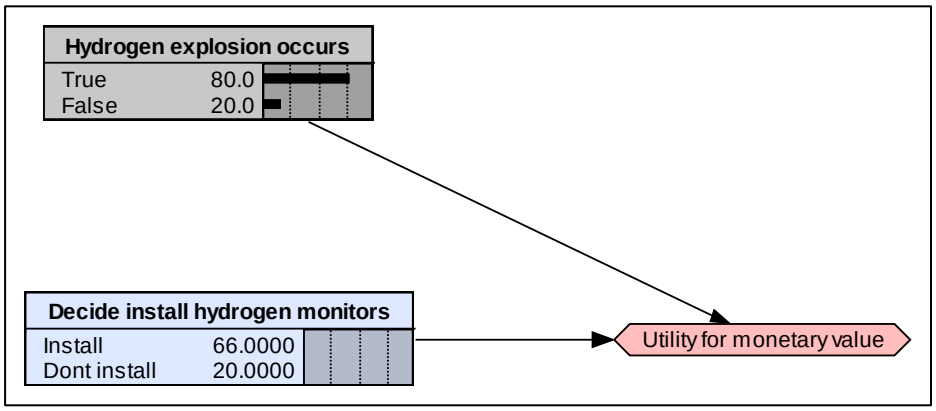

Figure 3-10: Updated Decision Net for 80% Probability of a hydrogen explosion

It is considered that the important decision making processes involved during development of the hydrogen hazard management strategies for nuclear safety cases

would benefit from the application of Decision Nets using Netica. Currently a road map approach has been identified in the Hydrogen Technical Guide [*Ingram et al, 2001*] which is limited to a particular set of Initiating Events and ignition source conditions, which may not always be relevant to some fault scenarios. The lack of flexibility in the Road Map approach could be overcome by applying the Netica Decision Net tool. A typical plant case study to which Decision Nets could be applied would be the optimisation of the hydrogen hazard management strategies for nuclear reprocessing plants where radiolytic hydrogen generation presents a significant challenge.

3.4.1.6 Other distinct features of Netica

In addition to the technical features discussed above, Netica output in terms of presentation is also exceptional. High quality presentations in the form of Scalable Vector Graphics (SVG) can be generated which are often necessary when presenting the Bayesian network in small print such as technical papers for journals.

Netica is able to create node sets, i.e., grouping of nodes in terms of commonality, which can be colour coded for ease of reviewing large complex networks. The output of each node can be presented in different formats such as histograms and scale meters. The quantified information can also be hidden to display only the network structure. It is also possible to cut and paste individuals nodes or node sets from the Netica *.neta file into a different network without resulting in a loss of the probabilistic logic or data from the original model.

Often the CPTs are large matrices that require presentation in Microsoft documents. The Netica 'Report → CPT Tables' function is programmed to link the CPTs directly with Excel spreadsheets to enable pasting of large matrices into a spreadsheet and subsequently into other Microsoft documents such as Word and PowerPoint. The finalised network diagram, or individual nodes including the BBN results as presented on the Netica home screen, can simply be selected and pasted directly into a Microsoft document as a picture file. This is achievable without the need to create a separate Bitmap file.

The discretisation of continuous nodes in Netica is easily achievable using shortcuts. For example, if the range of a continuous variable is such that it begins with 0, ends in 15 and there are 10 equal intervals, the shortcut [0,15]/10 could be entered. This automated discretisation saves significant effort when handling complex networks and reduces the possibility of errors if the intervals are entered manually.

When dealing with complex Networks, Netica can also significantly save effort by providing the capability of repeating a change to multiple nodes simultaneously e.g.,

when changing discretisation limits, increasing the number of states in discrete nodes and updating the network using the 'Enter → Findings' function. If there is a need to edit the name of a variable in the Network, Netica automatically modifies any equation associated with the changed variable, thus reducing the effort in finding errors.

3.4.2 HUGIN

HUGIN was one of the first software systems developed in Denmark for modelling Directed Acyclic Graphs (DAG), i.e., Bayesian networks. The probabilistic inference algorithm supported by HUGIN is the junction tree. Similar to Netica, the HUGIN software is compatible with Java, C and Visual Basic. The program files supported by HUGIN are 'OOBN' HKB and NET. Since Netica supports NET files, it is possible for HUGIN files to be read by Netica. The HUGIN software is most commonly used in the crime prevention sector including fraud detection and money laundering. Similar to Netica, as the software also provides the Decision Network capability, it is also widely popular in the commercial environment in terms of business decision solutions.

3.4.2.1 Trials with Hugin Lite software

To test the functionalities of the Hugin software a simple Bayesian Network was constructed which modelled the hypothesis of the likelihood of a hydrogen explosion occurring in a vessel. The model was based on a hypothetical ignition source probability of 5% and a probability of 20% for the presence of a flammable hydrogen concentration. The output of the BBN from Hugin is shown in Figure 3-11.

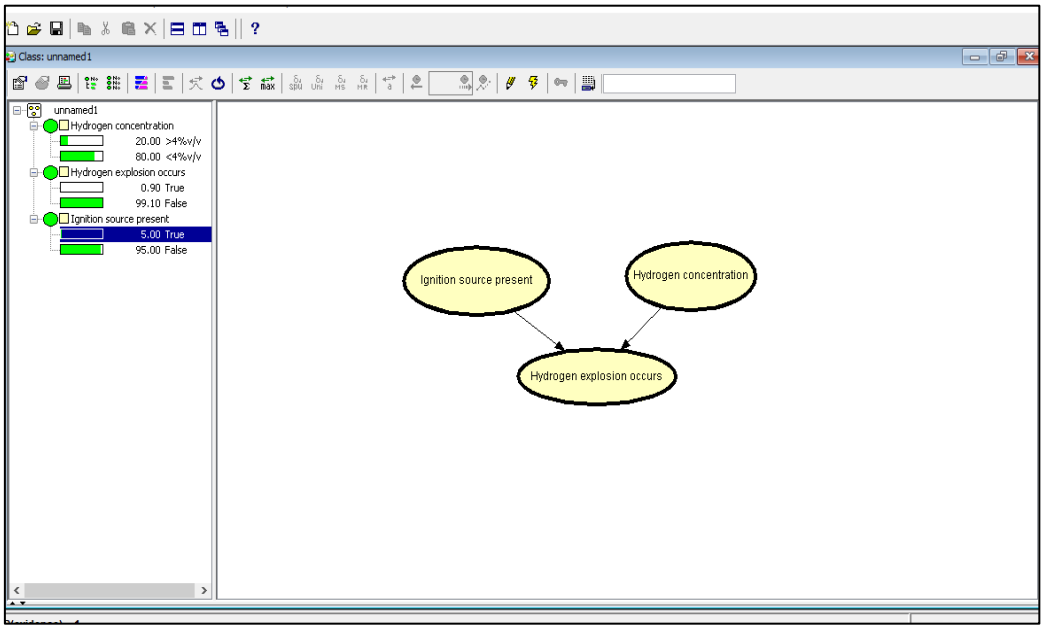

Figure 3-11: Simple Bayesian Network for a hydrogen explosion scenario using HUGIN Lite software

It was observed that the Hugin software has very similar functionalities to Netica in terms of constructing the network by selecting the nature nodes and the links. Compiling the CPT data for discrete and continuous nodes is also very similar to the process applied in Netica. Also, as with Netica, the Hugin model can be updated by entering specific findings or by instantiating a particular node to 100% probability. The results of the updated model in Hugin with a 100% ignition probability, represented by the red bar, are shown in Figure 3-12.

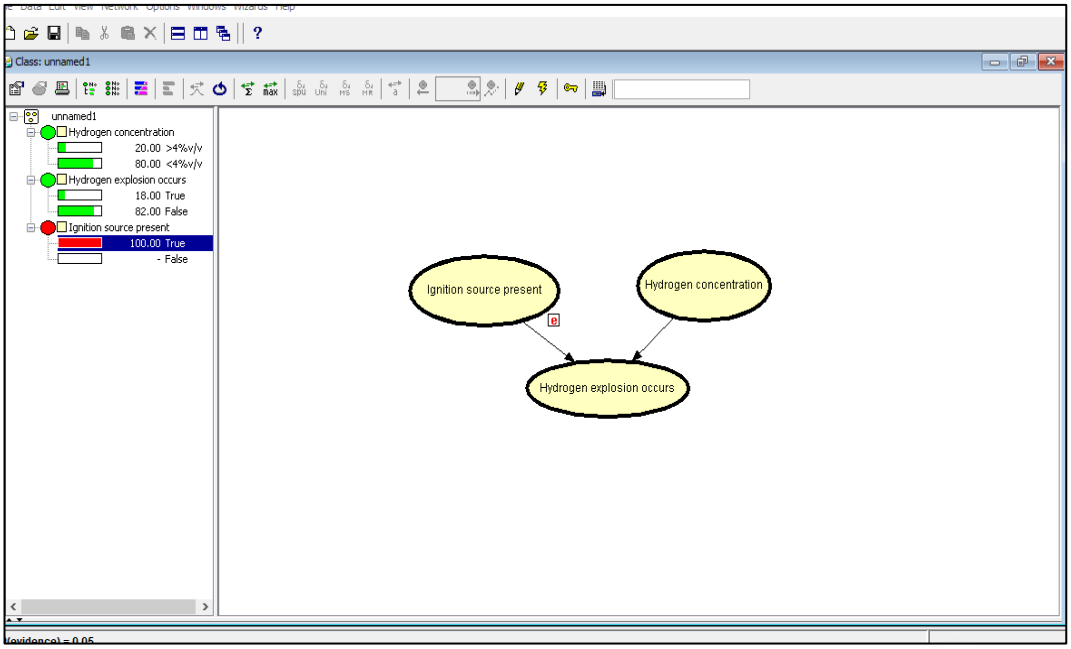

Figure 3-12: Updated Hugin Lite BBN for hydrogen explosion scenario

3.4.2.2 Comparison of HUGIN with Netica

In comparison with Netica, although it is possible in Hugin to use equations to automatically calculate the CPT data, the main drawback of Hugin is that this functionality is not readily implementable using this software. Use of equations for discrete or continuous nodes in Hugin requires a separate Expression Builder and input of discretisation data manually which can lead to errors. Netica on the other hand is superior in this respect as user defined equations can be easily inserted within the node description dialogue box by simply selecting the 'Equation' functionality. Discretisation within Netica is also a simple process that allows use of shortcuts to automatically designate equal intervals between the minimum and maximum value of a given variable.

A further observation made in the trial of the Hugin software was that it does not provide the link with Excel spreadsheet for reporting CPT data. This is an important functionality that is featured in Netica, where automatic transfer of large CPT matrices from the

Netica files into Excel and subsequently into other Microsoft documents was proven extremely useful. A further shortfall of Hugin is its inability to allow cut and paste part of or the whole network into Microsoft Word. This is a useful feature of Netica that was shown to be useful for easy presentation of the BBN results within this thesis. On the basis of the similarities and shortfalls of Hugin discussed above, it is concluded that Netica is far more superior due to its additional functionalities which are important to the scope of this research project.

3.4.3 Bayes Server, 32 Bit

Bayes Server is commercially popular in the artificial intelligence, aerospace and preventative maintenance industries. The most widely used application is the Bayes Server decision tool in the medical diagnosis sector. Similar to Netica and Hugin, the main functionalities of Bayes Server are Bayesian Belief Networks and Decision Networks.

3.4.3.1 Trial with Bayes Server, 32 Bit

Similar to the trial hypothesis used for testing Hugin, a trial was undertaken to test the functionalities of the Bayes Server 32 Bit software. The test used a simple hydrogen explosion scenario using discrete nodes to model ignition source and hydrogen concentration as parent nodes to the likelihood of a hydrogen explosion in a vessel ullage. The output from Bayes Server is shown in Figure 3-13.

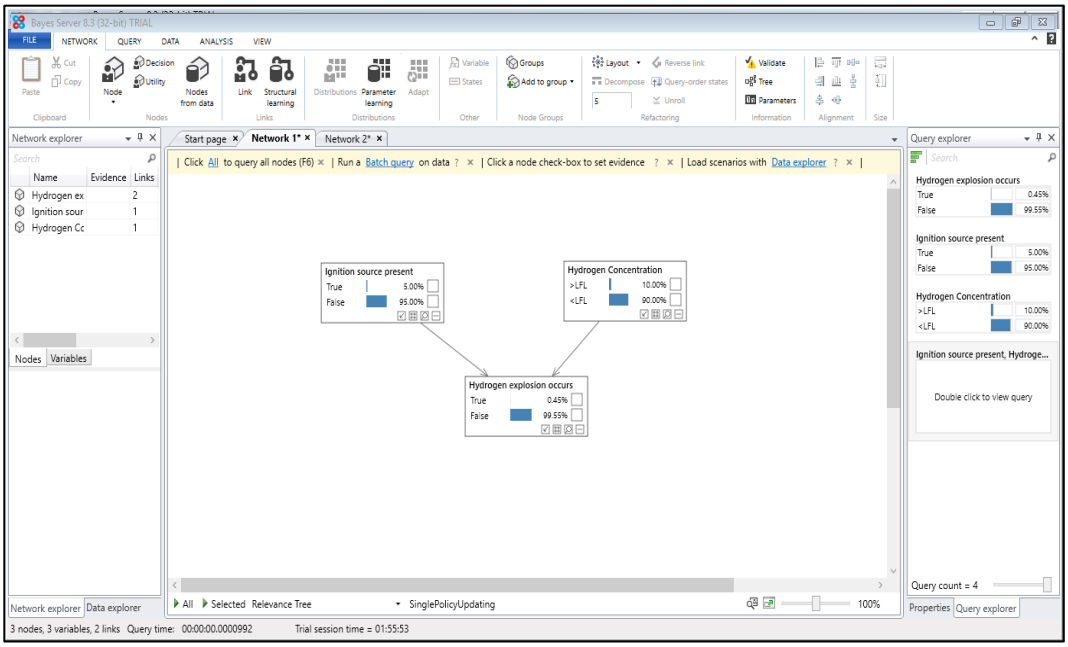

Figure 3-13: Simple BBN for a hydrogen explosion scenario using Bayes Server

3.4.3.2 Comparison with HUGIN and Netica

Whilst Bayes Server can model BBNs as well as Decision Networks, it was generally observed that that software is limited in comparison with Hugin and Netica. Firstly, for continuous nodes the Bayes Server is limited to modelling a Gaussian Distribution for a given mean and standard deviation. The functionality of using equations to automatically calculate the CPTs does not exist in Bayes Server. This is a significant lacking in terms of the application of the software to the scope of this research project where complex models involving the use of equations to predict the CPTs are a necessity. Secondly, as for Hugin, Bayes Server does not provide the functionality of linking large CPT matrices to Excel, hence making it impossible to present the detailed data in Microsoft Word. Given the shortfalls discussed above both for Hugin and Bayes Server, it is concluded that Netica is far more superior in terms functionality and practicality.

3.4.4 Validation of the Netica software

Discussions have been held with the company Norsys, via e-mail, with regards to evidence on the validation of the Netica software [*Norsys Software Corporation,2021*]. They provided confirmation that the software is validated based on the following prime reasons:

- Wide ranging regression tests have been undertaken on the Netica Bayesian inference algorithm and the functionalities of all features of the software are confirmed in terms of accuracy.
- During the testing of the Netica software, for Quality Assurance purposes, many random problems have been solved and the results compared well expected trends.
- During the initial development of the software, over 10 to 15 years ago, Norsys received very few alerts from the customers in terms of any suspicious behaviour of the software, which were resolved and no further alerts have been received.
- Well known customers of the software including the US defence and intelligence agencies have purchased the software and continue to place further orders, thus providing reassurance that the software has been successfully implemented.

Based on the above comparison and the evidence on validation, it is concluded that Netica should be adopted as the software for modelling BBNs for this research project.

3.5 Methodology used for Monte Carlo simulations

The standard FTA technique has the disadvantage that often single bounding case failure probability values are used for the primary events. This leads to overly pessimistic failure results for the Top Event. The Monte Carlo (MC) technique can remove such pessimisms by modelling failures of each of the primary events in fault trees as a probability density function. Figure 2-14 in Chapter 2 provides an illustration of the application of MC simulation to FTAs, which is based on the method detailed by *Lees, 1992*. The main steps involved in an MC simulation are:

- A number is drawn based on the probability density for the given parameter to be used in the fault tree calculations.
- Repeating this, typically 10 to 100 thousand times, allows a probability distribution to be obtained for the top event of the fault tree.

There are several software systems available for modelling Monte Carlo simulations including @ Risk by *Palisade, 2019*, Model Risk by *Vose software, 2020* and Risk Solver by *FrontlineSolvers, 2020*. For research purposes the software package RiskAmp, by *Structured Data LLC, 2007,* has been used to facilitate the MC analysis due to its following key features:

- RiskAmp has over 40 in-built distributions, including Triangular, Normal and PERT distributions.
- It has a library of up to 20 statistical functionalities.
- RiskAmp can provide a direct link with Excel spreadsheets, thus enabling easy transfer of simulation result reports to other Microsoft applications.
- The software features an in-built wizard for automatic generation of simulation result tables and histograms which can be readily transferred to Microsoft Word.

3.6 Validation and verification of the output from BBNs and MC Simulations

Based on Chapter 2, Section 2.5.3, a Validation and Verification (V&V) process was applied to demonstrate, with a good degree of confidence, the accuracy of the output from the BBN and MC simulation models. Similar to the V&V process for computerised models suggested by *Sargent, 2011* and *Schietekat et al, 2016*, the following steps were applied to the V&V of BBN and MC simulation models for the case studies in this research project.

3.6.1 Agreement of the model hypothesis

The problem entity or hypothesis being modelled in a BBN or MC simulations was validated in terms of the requirements of the end users such as plant operators, system

engineers or safety assessors. For instance, in Case Study 2, the end users of the BBN model were the plant operators who needed to know the likelihood of good quality sludge being removed from the mixing vessel for a given set of plant operating conditions. Hence the precise description of the hypothesis being modelled was agreed with the end users at the initial stages of the model development.

3.6.2 Validation of the Concept Model

The concept BBNs and MC simulation, which provide a logical representation of the problem entity and the interacting factors, were checked for plausibility and agreed with the end users and the SMEs. Essentially the end users and the SMEs were involved in the development of the cause-and-effect diagrams that represent the concept BBNs and MC simulation. Once an agreement on the logic used in the cause-and-effect diagrams was reached with the SMEs and the end users, the Concept Model was considered validated. The development of the Concept Model was an iterative process, linked with the final output from the model. For instance, if there was any inconsistency in the output results in comparison with the expected trends, the relevant concept diagram was revisited as part of the validation process.

3.6.3 Validation of BBN and MC simulation input data

The input data for the BBN and MC simulations were based on existing validated sources and plant trends. For example, the equipment reliability information used for the MC simulation in Case Study 3 and robot system failure in Case Study 7 was obtained from existing published data on equipment failure rates. The data used for the calculation of radiolytic hydrogen generation rates, i.e., the G-values and the alpha and beta-gamma radioactivity decay energies, were also obtained from published sources. Input data based on plant trends were also used as far as possible. For example, plant trends indicated that the hydrogen generation rate from corrosion of Magnox in nuclear waste storage facilities is at least two orders of magnitude higher, i.e., typically 2L/hr, in comparison with radiolysis of aqueous liquors. This plant trend formed an important basis of analysis in Case Study 4.

Previous experimental data were also used as far as possible. For example, the ignition probability of hydrogen, applied to Case Studies 1 and 6, was based on the experimentally predicted ignition probabilities reported in the Hydrogen Technical Guide for nuclear decommissioning and reprocessing environments.

3.6.4 Validation and verification of the output from BBN and MC simulation software

Similar to the process used by *Schietekat et al, 2016* the output from the BBNs was verified through the application of the Bayesian inference. The Netica updating feature was applied to test the model in terms of its behaviour under expected and extreme conditions. For example, as a simple test, it was expected that setting the ignition probability to zero should also return the probability of hydrogen explosion to zero. Reverse inference was also applied to test the likelihood of a cause given the occurrence of a consequence and to determine if the output result was in agreement with expected behaviour.

Where possible, a comparison of the BBN results with previous experiments was also carried out as part of the validation process. For example, previous experimental results, based on a specific set of plant operating conditions were available in support of the sludge mixing Case Study 2. Bayesian inference was used, replicating the input parent node states with the experimental values to determine if the BBN output was consistent with the experimental observations.

CHAPTER 4 : CASE STUDY 1- BAYESIAN BELIEF NETWORK ANALYSIS OF RADIOLYTIC HYDROGEN IN SEALED PROCESS PIPES

4.1 Introduction to Chapter 4

Many nuclear chemical plants, such as plant P4 discussed in Appendix A1, consist of storage vessels containing heat generating radioactive liquors which are required to be cooled using closed circuit cooling coils prior to further treatment (Figure 4-1). Such process pipework in aged facilities has the potential to corrode thus leading to migration of radioactivity from the tank liquor into the pipework. Failure of a cooling coil and subsequent leakage of radioactivity into the pipework is normally revealed by the water gamma monitor instruments connected to the coil outlet. Under these circumstances, the failed cooling coil pipework is required to be isolated from the tank.

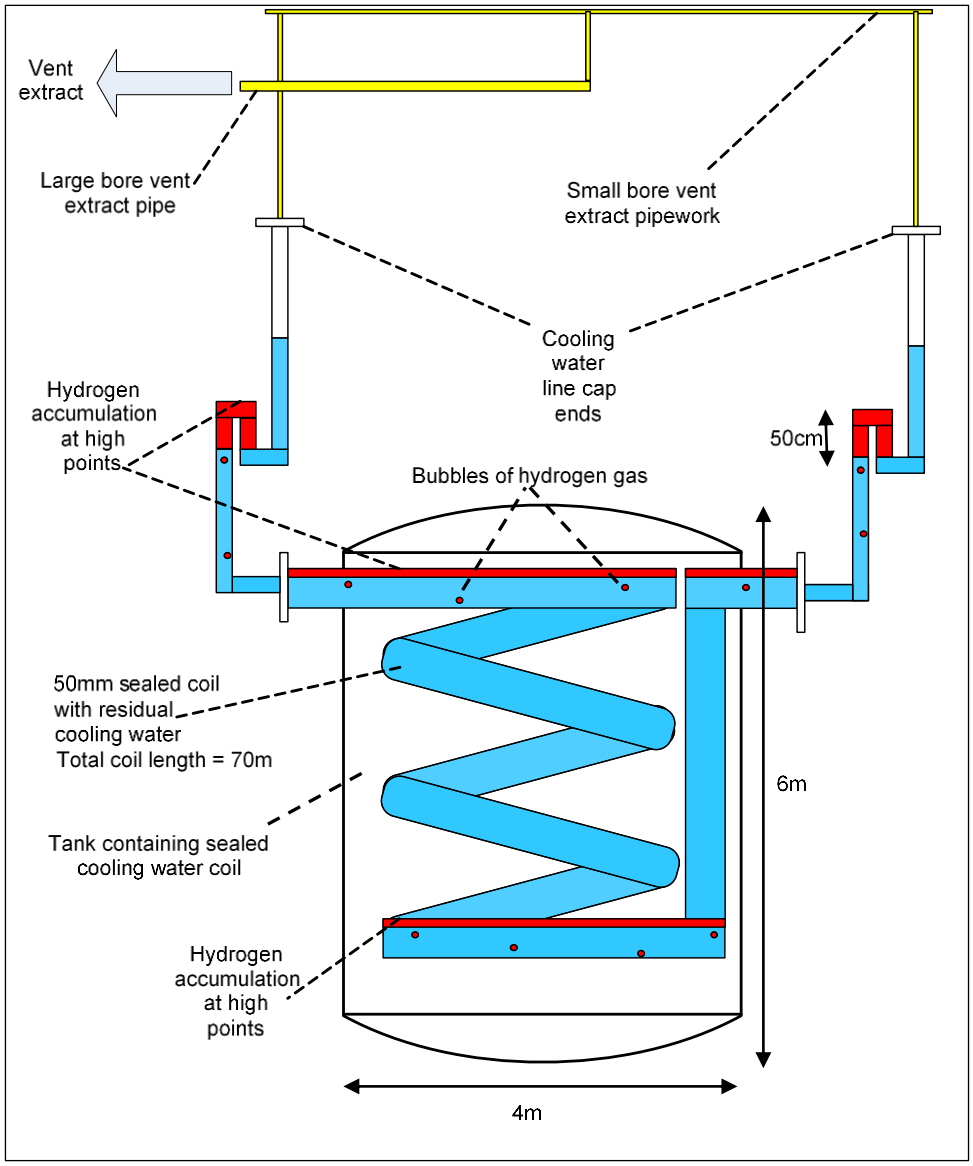

Figure 4-1: Process vessel with sealed cooling water pipework containing radiolytic hydrogen

Isolation of the cooling coils is achieved by capping and venting to prevent spread of radioactivity into other pipework outside the tank. With alpha, beta and gamma radiation associated with the aqueous radioactive liquors, water dissociates via the process of radiolysis to form the hydrogen and the hydroxyl radical. Therefore, any radioactivity leaking into the corroded pipework could potentially lead to the generation of hydrogen through radiolysis.

This case study investigates the application of the Bayesian Belief Network methodology to identify key sensitivities which would affect the likelihood of a radiolytic hydrogen deflagration or detonation in the isolated cooling coil pipes. The potential for significant radiological and physical consequences following a deflagration or a detonation is also investigated. Once this likelihood has been analysed the BBN model could be used to identify the correct option for managing the hazard.

4.2 Hydrogen hazard management strategies for sealed pipes

In pipes containing flammable mixtures of hydrogen in air and the presence of an ignition source, typically a combustion reaction in the form of a deflagration will initially occur. In a deflagration the rate of combustion is relatively low and the characteristic flame travels at subsonic velocities leading to relatively low overpressures of less than 1 bar. A sudden transition from a deflagration to a detonation (DDT) can also occur at supersonic flame velocities leading to explosion shock waves and significant overpressures, well above 1 bar. In a DDT involving gaseous mixtures such as hydrogen in air, the intersecting shock waves form a diamond shaped cell structure as illustrated in Figure 4-2 [*Dahoe, 2011*].

A key factor that characterises the detonability of a mixture of fuel and air is the detonation cell size, which is the dimension λ in Figure 4-2. The detonability is inversely proportional to the cell size. Prior to year 2000, initial experimental research on DDTs in systems containing various fuels (including hydrogen) and air mixtures showed that for a DDT to occur the physical size of the compartment, or the critical diameter (D) in the case of tubes, needs to exceed the cell size (λ) [*Lee, 1987*]. The critical diameter (D) is defined as the minimum diameter of a pipe needed for the shock wave to be released to the outside of the containment of the pipe leading to a detonation. On this basis, in order to minimise the risk of a DDT in smooth pipes, the concept of $D > \lambda$ was adopted in the Sellafield Ltd (SL) Hydrogen Technical Guide. In other words, to minimise the risk of a DDT the pipe diameter needed to be below the cell size, λ.

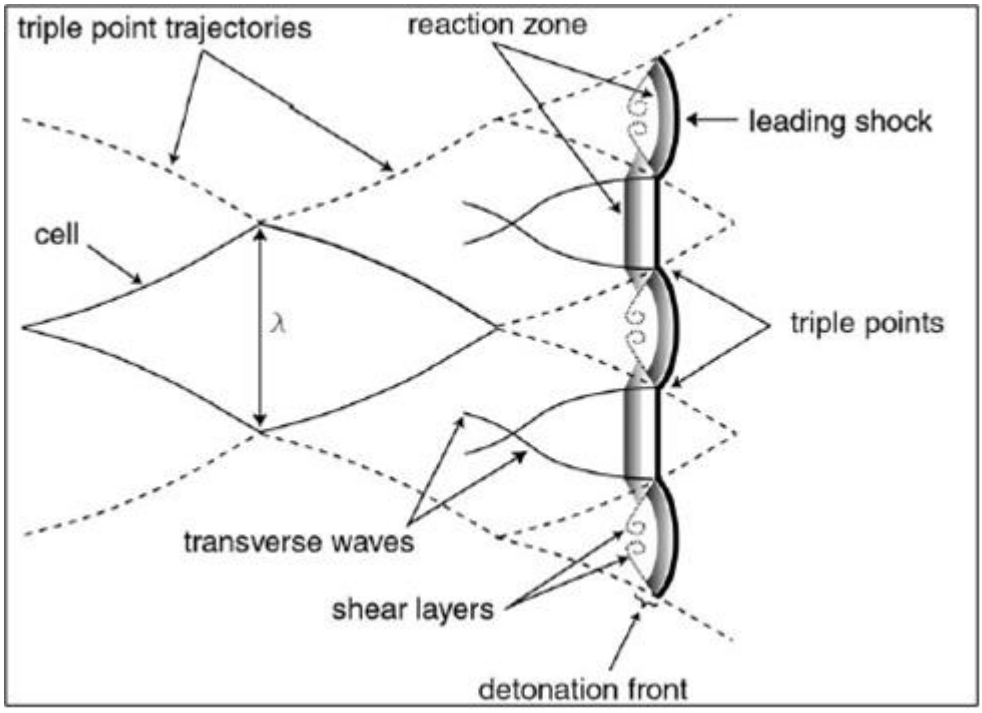

Figure 4-2: Formation of a cellular structure by a detonation wave [*Dahoe, 2011*]

Another main variable that affects the detonability is the hydrogen in air concentration. *Lee, 1987* shows that the detonability of a mixture of hydrogen in air is the highest at a cell size of approximately 15mm. This occurs at the stoichiometric hydrogen in air concentration of 29.5% volume and an initial pressure of 1 atmosphere. He also demonstrated that for a DDT phenomenon to occur, the critical diameter, D, would need to exceed the cell size, λ, i.e., $D>\lambda$. The dependency of the cell size on the initial pressure has also been investigated by *Stamps, and Tiezen,1991* who demonstrated similar cell sizes, i.e., typically 15mm for hydrogen in air mixtures at 1 atmosphere. They showed that at pressures higher than 1 atmosphere, there is a negligible decrease in the cell size.

Subsequent to the initial research by *Lee, 1987*, further advice on the DDT criteria was sought from Professor J. H. Lee, by the SL HWP in 2001. Professor Lee is the author of *Lee, 1987* who specialises in the field of combustion sciences at McGill University in Canada. He advised that since there is an uncertainty associated with the values of the experimentally derived cell sizes, the DDT criteria are only approximate and should not be used as scientific laws. However, based on the available experimental data on cell sizes and taking into consideration the mechanisms associated with DDTs, Professor Lee advised that, qualitatively, the criteria $D>\lambda$ is correct.

Further work on the DDT phenomenon was also undertaken *by Ciccarelli and Dorofeev, 2008* who suggested a more stringent criterion of $D>\lambda/\pi$. However, given the

uncertainty associated with the cell sizes and taking into consideration the cautionary advice from Professor Lee, the stringent criterion *by Ciccarelli and Dorofeev, 2008* is currently under review by SL. It could be argued that the use of overly conservative criteria, such as $D>\lambda/\pi$, for existing facilities which are approaching the end of the operational life may not be appropriate. Potentially this could lead to a misleadingly high risk. Hence taking into consideration the advice from Professor Lee, for existing process pipes where there is the potential for hydrogen accumulation, the design criterion of <15mm pipe diameter has been currently adopted by SL as a means of minimising the likelihood of a DDT. While pipe diameters less than 15 mm will reduce the risk of a DDT, given the uncertainty associated with the cell size, it is considered that a small residual risk may still exist.

To manage against the risk hydrogen detonations in isolated cooling coils, the hazard management strategy on plant is to install small bore ventilation extract pipes. However, breaking into existing cooling coils to install the ventilation pipework in a radioactive environment introduces other hazards e.g., an ignition source, dose uptake during the ventilation system installation work. In support of the ALARP decision making process on whether to install the small bore ventilation extract pipes, an uncertainty analysis is needed to determine the key sensitivities that affect the deflagration or a detonation within the sealed pipes and a subsequent radiological impact. The identified key sensitivities could then be used to make an informed decision on ways of managing the hazard.

4.3 Construction of the Bayesian Belief Network

The hypothesis described in Section 4.1 is modelled using the Bayesian Belief Network (BBN) software, Netica by *Norsys, 2010*. The main objective of the BBN is to identify key sensitivities which would affect the overall likelihood of a deflagration or a detonation in sealed pipes and hence the radiological impact.

In order to predict the variables which, affect the potential for radiolysis and the subsequent radiological consequences from hydrogen detonations or deflagrations, initially equation 2-9 for radiolytic hydrogen generation rate, given in Chapter 2, was used. This initial understanding was used to compile a first draft of a concept model for the BBN analysis. A meeting was with a group of SL specialists and Hydrogen Working Party (HWP) members in which the first draft was subsequently reviewed and further variables and dependencies were discussed and agreed. *Ahmed, 2016* provides details of the minutes of the meeting with the HWP members. The finalised concept model for the Bayesian network as agreed with the Hydrogen Working Party is presented in Figure 4-3.

Based on the concept model, a Bayesian network was constructed which consisted of a series of Discrete nature nodes numbered 1 to 22. Conditional Probability Tables (CPTs) for the Child nodes, were then derived based on the Prior beliefs by the HWP [*Ahmed, 2016*].

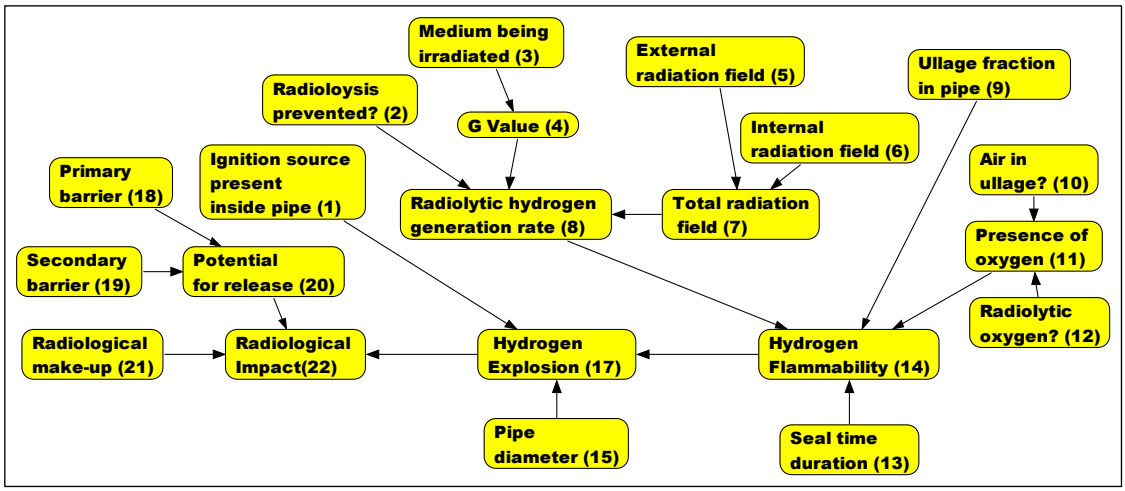

Figure 4-3: Bayesian Network concept model for consequences from hydrogen explosions in sealed pipes

The discussion on the derivation of the concept model in terms of the key variables, their dependencies and the derivation of the CPTs is given below.

The accumulation of hydrogen gas in the pipework is primarily dependent on the rate of generation, which is affected by:

- The G(H_2) value (Node 4), i.e., the number of molecules of hydrogen generated per 100eV of α or β/γ radioactivity, and the radiation field that the pipe is exposed to.
- The amount of radioactivity associated with liquor within the pipework (Node 6).
- The external radiation field, particularly if the surrounding tank liquor contains gamma radiation which can penetrate the pipework and hence affect the rate of absorption of energy by the pipe liquor (Node 5).
- The radioactivity, both internal and external to the pipework constitutes the total radiation field (Node 7).
- Chemical composition of the pipework, which can lead to the radiolysis being prevented (Node 2).

Each of the above discrete nodes in the BBN required an understanding of their states, i.e., High and Low values, which were agreed with the HWP members [*Ahmed, 2016*]. A high G value of 0.45 is known for gamma activity in aqueous solutions and a low

value of 0.003 is typically applicable to nitrate solutions. The nitrate solutions are generated during reprocessing operations which involve dissolving the decanned metallic waste from the spent fuel rods in nitric acid to separate the nuclear fission products from the metal.

Where a relatively small volume is immersed in a large volume e.g., cooling coils in tanks, the G values for alpha and beta activity are bound by the values for gamma activity. In vessels containing relatively small volumes of up to $1m^3$ of radioactive liquor, a typical hydrogen generation rate of 0.01L/hr is known. This value represents the low state for Node 8. In vessels containing large volumes of liquor, i.e., $>1m^3$, a hydrogen generation rate of 1L/hr is known. This represents the high state for Node 8. A low total radiation field represents the condition that leads to a low hydrogen generation rate of 0.01l/hr and a high radiation field leads to a hydrogen generation rate of 1/L/hr.

4.4 Derivation of CPT Data

The greatest uncertainty on prediction of radiolytic hydrogen generation rate lies around the G value which is dependent on the pipe contents being irradiated by the α or β/γ radiation. Therefore, the medium being irradiated (Node 3), i.e., nitrate or aqueous solutions, is modelled as the Parent node to the G Value. Based on a knowledge of the existing pipework inventories, the HWP members agreed that for Node 3, approximately 70% of the sealed pipes contain water and the remaining 30% contain nitrate solutions [*Ahmed, 2016*]. On this basis it was judged that there is approximately a 90% chance that the G value is high for pipework containing water. Accordingly, Table 4-1 summarises the CPT for the G value.

G Value		**Pipe Medium**
High	**Low**	
0.9	0.1	Water
0.1	0.9	Nitrate solution

Table 4-1: CPT for G value

Using the Prior probability distributions for nodes 2, 4 and 7 as discussed above, the CPT for radiolytic hydrogen generation rate, node 8, was derived. This is given in Appendix A2 Table A-1. The CPT in Appendix A2 Table A-1 is based on the logic that if radiolysis is not prevented, the total radiation field and the G value are both high, then there is a high chance, that the radiolytic hydrogen generation rate is also high. A probability of 0.95 was applied for the hydrogen generation rate being high.

The main variables which would affect the likelihood a hydrogen explosion in the sealed pipe are the hydrogen flammability of the pipe gaseous mixture (Node 14) and the

presence of an ignition source inside the pipe (Node 1). Hence as shown in Figure 4-3, Nodes 14 and 1 are the Parents to the likelihood of a hydrogen explosion (Node 17). The pipe diameter (Node 15) affects the likelihood of a deflagration and detonation predicted by Node 17. Therefore Node 15 is also a parent to Node 17.

The degree of hydrogen flammability is dependent on the Parent nodes radiolytic hydrogen generation rate (Node 8), the likelihood of presence of oxygen (Node 11) and the time span over which the pipe has been sealed (Node 13). The longer the seal time duration, the greater is the potential for a flammable mixture arising in a given pipe ullage fraction (Node 9). This is the ratio of volume of free space in the pipe to the volume occupied by the liquid. An ullage fraction greater than 0.5 is denoted high. A fraction less than 0.5 is considered low. Based on a knowledge of existing nuclear chemical plant vessels consisting of cooling coils, the HWP indicated that most of this pipework has remained sealed for over 10 years. Hence a probability of 90% that the pipes have been sealed for over 10 years was considered reasonable [*Ahmed, 2016*].

The flammability range of hydrogen in air mixtures at atmospheric pressure is known to be 4 - 75% v/v. However, due to the gradual consumption of the oxygen by corrosion of ferritic contaminants within the sealed pipes, this environment is likely to be oxygen depleted. Such oxygen depleted environments will result in a flammability range that is different to normal hydrogen in air mixtures. From a detailed review of hydrogen flammability in Chapter 2, Section 2.2.5, the following key points can be listed:

- For hydrogen rich mixtures with depleted oxygen, the Upper Flammability Limit (UFL) is as low as 10% v/v, however the LFL is uncertain.
- The confined lower and upper limits of detonation of hydrogen in oxygen rich atmospheres are 15%v/v and 90%v/v respectively.
- The confined lower and upper detonation limits for hydrogen in air mixtures, without oxygen depletion are reported as 18.3% v/v and 58.9%v/v, respectively.
- For oxygen depleted atmospheres, by inference it is considered plausible that the lower detonation limit would be above 18.3% v/v and the upper limit below 58.9% v/v.

Based on the data given above, for the sealed pipework it is considered that hydrogen concentrations of up to 18%v/v are more likely to lead to a deflagration. For the Bayesian analysis, a high hydrogen flammability denotes a concentration >=18%v/v. A low hydrogen flammability denotes a concentration of <18% v/v. Due to the uncertainty on the LFL for oxygen depleted environments as discussed above, a precise limit for

the mixture being non-flammable cannot be specified, as it could potentially be above the 4% v/v value for normal hydrogen in air mixtures.

For the node Hydrogen Flammability (Node 14), the derivation of the CPT, given in Appendix A2, Table A-2, was based on the following logic:

i) If the ullage atmosphere is hydrogen rich but oxygen deficient then the UFL would be lower than normal thus leading to a low flammability or non-flammable atmosphere. In this case it is considered that there is an equal chance that the atmosphere has a low flammability, or it is not flammable. However, the possibility of a high flammability is considered nil in this case.
ii) If the ullage atmosphere is not oxygen deficient then provided that the hydrogen generation rate is high, the ullage fraction is small and the seal time duration is long, there is a significant chance of a high hydrogen concentration and hence high flammability. On this basis a probability of 0.95 was applied for the hydrogen flammability being high.
iii) If the hydrogen generation rate is low but the ullage atmosphere is not oxygen depleted, then for a long seal time duration, there is still a high probability that the flammability is high.

The transformation from a deflagration to a detonation also depends on the pipe diameter (Node 15). The opinion of the HWP was that for most of the pipes, i.e., for approximately 80% of the population, the pipe is diameter is above 15 mm. This variable affects the probability of a deflagration and transformation to a detonation in Node 17, which is also dependent on the hydrogen flammability. As discussed in Section 4.2, when the pipe diameter less than the 15 mm cell size, it is considered unlikely that a detonation will occur in an atmosphere consisting of a stoichiometric mixture of hydrogen in air. Hence for pipe diameters 15 mm or less and a high flammability equivalent to the stoichiometric concentration, a relatively low probability of 0.1 for a DDT is considered reasonable. However, for pipe diameters larger than 15mm, a higher probability of 0.4 for a DDT is assigned.

Of course, the likelihood of a hydrogen explosion is also dependent on the ignition source probability. The prior belief by the HWP was that if the pipe condition is poor and corroded which is also exposed to a chemical or mechanical process then there is a 95% chance that an ignition source is present. On the other hand, if the pipe is fully welded which is not exposed to a chemical or mechanical process environment, then the ignition source probability would reduce to approximately 5% [*Ahmed, 2016*].

It is considered that most of the sealed pipes are fully welded, therefore the HWP members' view was that an ignition probability of 5% is a good approximate [*Ahmed, 2016*]. Appendix A2 Table A-3 gives the CPT for the hydrogen explosion node which takes into consideration the CPTs for hydrogen flammability (Appendix 2, Table A-2), the ignition source probability and pipe diameter. The basis of the CPT for the hydrogen explosion node, when taking into consideration the effect of all three of these variables is given below.

If an ignition source is present and hydrogen flammability is high, then a detonation is likely. The HWP members considered that a deflagration must occur before the transformation to a detonation can take place. On this basis their opinion was that the probability of a deflagration occurring is still higher than a detonation. Therefore, a probability ratio of 3:2 was considered plausible [*Ahmed, 2016*].

For a low hydrogen flammability, it was considered that a small probability of around 0.15 for a detonation would exist if the atmosphere is oxygen deficient such that the UFL is close to 18%v/v. This is based on the literature review given in Section 2.2.5 where it is discussed that for normal hydrogen in air atmospheres, the concentration range for a detonation in confined areas is 18-59% [*Lewis and von Elbe,1961*]. By inference, for atmospheres with a reduced oxygen concentration the lower hydrogen concentration limit for a detonation would be above 18%. As discussed previously, for situations where the hydrogen flammability is high and the pipe diameter is larger than 15mm, then the probability of a detonation is 0.4. However, since a deflagration has to occur before a detonation, the probability of deflagration is still higher than 0.4.

The radiological impact or consequence (Node 22) is dependent on:

- The radioactivity content of the pipework, i.e., High, Intermediate or Low in accordance with the International Atomic Energy Agency (IAEA) safety guide and classification of radioactive wastes (*IAEA, 2009*).
- The radiological composition across the whole population of sealed pipes, which is approximately 70% High, 20% Medium and 10% Low.
- The physical strength of the primary containment of the pipework and secondary containment provided by the concrete structure in which the vessel and the associated sealed pipework are present.
- The likelihood of failure of the primary and secondary containment layers following a deflagration or a detonation.

For good primary and secondary containment strength, at approximately a 60% and 70% chance respectively, the likelihood of a release following an explosion is low.

The total energy released from a detonation or a deflagration, characterised by the peak overpressure, will have an impact on the performance of the primary and secondary containment layers and hence the final radiological consequence. *Shepherd, 2009* has examined the potential overpressures resulting from DDTs for various flammable gas mixtures including hydrogen in air. For the hydrogen in air stoichiometric concentration of 29.5% and initial conditions of 25^{o}C and 1 atmosphere , it is shown that the detonation overpressure is 15.6 bar i.e.,1.6MPa. For deflagrations, a maximum credible overpressure of up to 12.6kPa, based on a hydrogen in air concentration of 12.5%, has been experimentally determined by *Schiavetti and Carcassi, 2017*.

Shepherd, 2009 also carried out experimental work on structural response of piping systems following detonations of flammable gaseous mixtures internal to the pipes. From the DDT experimental work using 6 m length by 2.54 cm thick stainless steel tubes, it was observed that the explosion overpressures were sufficiently substantial to cause rupture of the closed-end pipe. Based on this experimental evidence, it is considered that the likelihood of a failure of the primary containment of the sealed pipework being considered in this case study following a detonation is very high. This is particularly the case for the proportion of the sealed pipework which is weak due to age and deterioration over time.

The secondary containment layer outside the sealed pipework and vessel is a concrete structure with wall penetrations through which process instrumentation systems are routed. It is considered that if the detonation overpressure is significant enough to cause rupture of the stainless steel pipework, then this will also potentially lead to the penetrations in the secondary containment layer being detrimentally affected. Potentially this could lead to radioactive gases from the ruptured pipework being routed through the penetrations and into the operating areas. This interpretation is based on the research by *Gupta and Langer, 2019,* who considered that the release of combustion gases through the penetrations from pressurised cells is a credible scenario.

Using the evidence above in terms of the effect on the primary and secondary containment layers, the following basis was used to derive the CPT in Appendix A2, Table A-4 for the radiological impact Node 22:

i) If a detonation occurs and the pipework containment is weak such that the potential for a release from the pipework is also high, then it is very likely that the radiological impact would be significant. A probability of 0.9 was therefore applied for the radiological impact being high.

ii) If a deflagration occurs without leading to a detonation, then due to the lower overpressure, the damage to the pipework would be less severe than for case (i) above. Hence a lower probability of 0.8 for high radiological impact is applied.

4.5 BBN results based on prior probabilities

Based on the concept model in Figure 4-2 and the CPTs in Appendix A2, Table A-1 to Table A-4, a BBN was constructed using the Netica software, as shown in Figure 4-4.

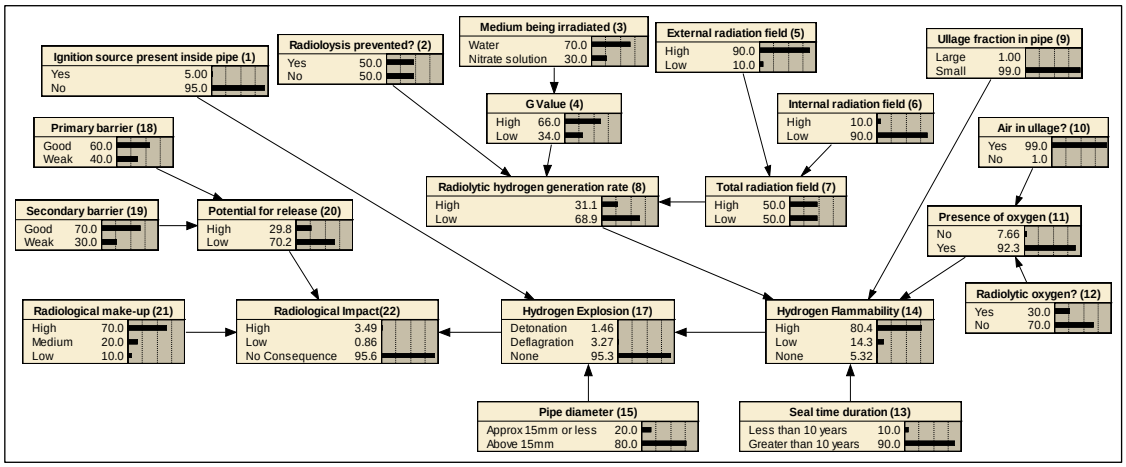

Figure 4-4: BBN for hydrogen explosions in sealed pipes

With the Prior Conditional Probabilities of the main variables, and assuming that the primary and secondary containment for the sealed pipe is good, but a probability that the radiological composition of the pipe is high, then the BBN analysis in Figure 4-4 suggests that there is approximately a 4.7% chance that an explosion i.e. detonation or a deflagration, will occur but less than a 96% chance that there is no radiological consequence. This result seems reasonable as the model is based on a low ignition probability of 5% but a high probability that the primary and secondary containment of the sealed pipe is good such that a significant release of gases from the pipework would be highly unlikely.

4.6 BBN tests for consistency

Having established the Bayesian network based on prior probabilities, it is necessary to demonstrate whether the model behaves in the expected way under a given set of conditions. These tests for consistency can be undertaken through instantiation of the key variables using the BBN updating feature. For instance, if the ignition source probability is set to zero, then a hydrogen explosion probability should also change to

zero. This belief was tested by instantiating the presence of an ignition source (Node 1) to a 100% 'No' state. With this change as shown in Figure 4-5, the resultant radiological consequence probability is zero, thus demonstrating expected behaviour.

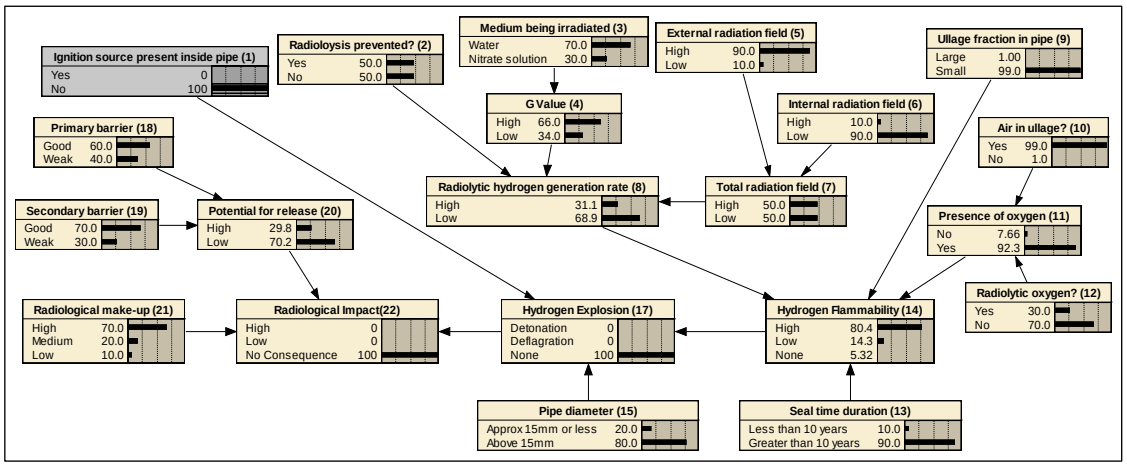

Figure 4-5: Updated BBN with ignition probability set to zero

If an observation which confirms the presence of an ignition source, i.e.,100% probability, is entered in the model then Figure 4-6 shows that the total probability of radiological consequences increases sharply to 87%.

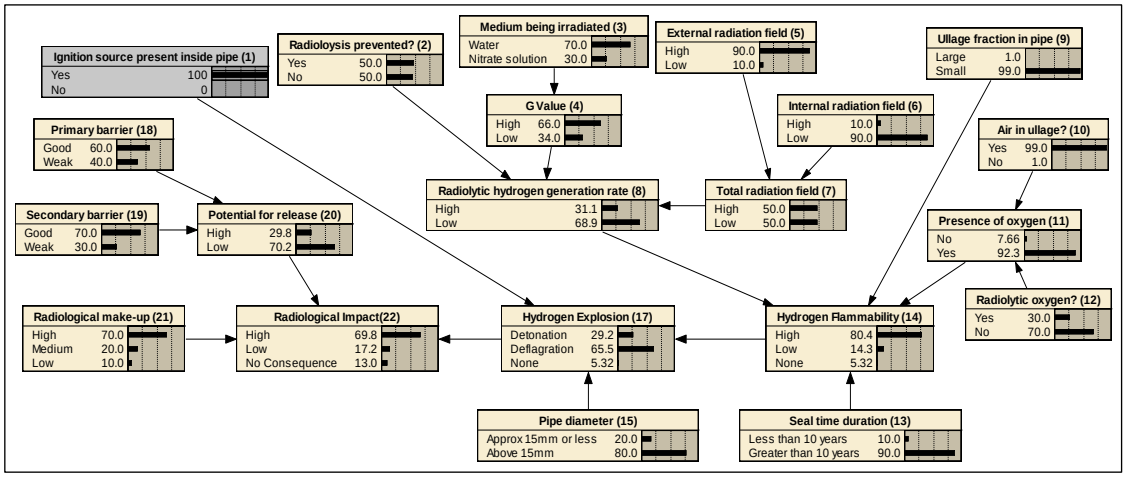

Figure 4-6: Updated BBN with ignition source probability set to 100%

If a flammable atmosphere is not present in the sealed pipe, then the radiological consequences and hydrogen explosion probabilities should change to zero. Figure 4-7 agrees with this expectation, i.e., when the hydrogen flammability node is instantiated to a 100% 'None' state, the radiological consequences and hydrogen explosion probabilities also update to the 100% 'None' state.

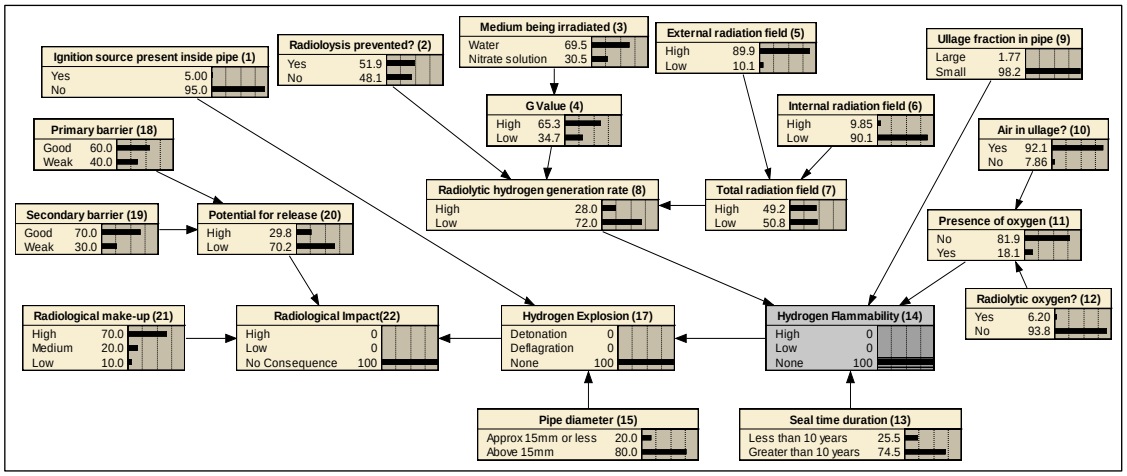

Figure 4-7: BBN to show the effects of no presence of flammable atmosphere

4.7 Sensitivity Analysis

Following on from the verification of the BBN, the updating feature of Netica can now be used to undertake a sensitivity analysis and determine how the model behaves with changes to data for specific variables. In this way the model could be used to determine the optimum conditions necessary for managing the hydrogen hazard.

4.7.1 Determination of the most effective means of managing the hydrogen hazard during normal operations

The ideal plant configuration for managing the hydrogen hazard in the sealed process pipework is clearly that which results in a low probability of a radiological impact. Whilst theoretically a 100% probability of a zero radiological impact would be achieved if the ignition probability is zero, realistically it is considered that this is not possible as a complete elimination of the sources of ignition would be difficult to justify. Hence a sensitivity analysis is undertaken to identify the scenarios that would result in the lowest credible probability of a radiological impact, recognising that this cannot be zero.

If the ignition source probability is reduced from 5% to 3%, then the updated BBN in Figure 4-8 shows that the likelihood of no radiological consequences increases from the prior value of 95.6% (Figure 4-4) to 97.4% probability. A further reduction in the ignition probability to 1% results in an increase in the likelihood of no consequences to 99% probability (Figure 4-9). As shown in Appendix A2, Figure A2-1, an additional small increase in the likelihood of no consequences to a probability of 99.3% is observed if the probability of presence of air in the ullage reduces from 99% to 50%. Appendix A2 Figure A2-2 shows that if the probability of presence of radiolytic oxygen in the pipe is also reduced from 30% to 10%, there is a small decrease in the likelihood of the ullage atmosphere being non-flammable.

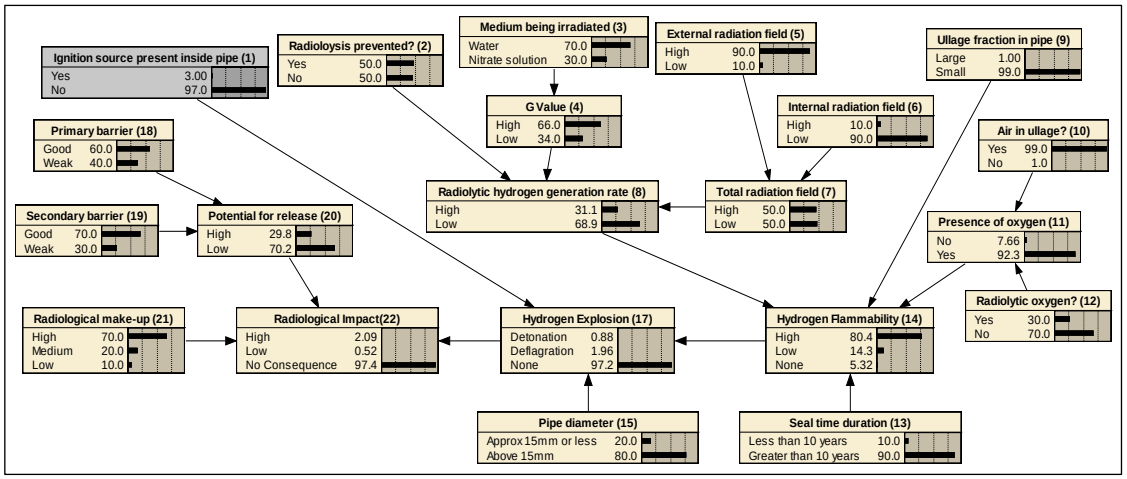

Figure 4-8: Updated BBN for ignition probability reduced to 3%

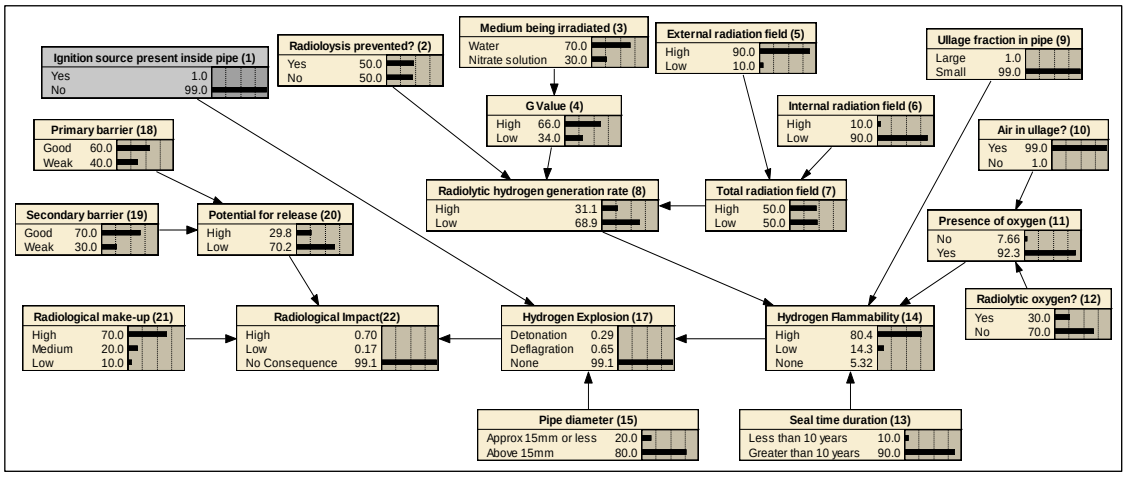

Figure 4-9: Updated BBN ignition probability reduced to 1%

Appendix 2, Figure A2-2 shows that the combined effect of the updated conditions in Figure 4-8, Figure 4-9 and Appendix 2 Figure A2-1 is an increased likelihood of no radiological consequences from 95.6% to 99.3%. Therefore, the likelihood of a consequence has reduced from the prior value of 4% to just under 1%. These inferencing results show that the ignition source probability presents the highest sensitivity to the likelihood of radiological consequences. To a lesser extent the hydrogen flammability, due to the presence of air or radiolytic oxygen, also has an effect.

4.7.2 Other means of managing the hydrogen hazard

Given that the physical consequences of a detonation are likely to be more severe in comparison with those from a deflagration, it is considered that control of factors that affect the detonation would also provide an effective means of managing the hazard. Figure 4-10 shows that if the probability of a detonation is instantiated to 100% in node

17, the likelihood of a high radiological impact increases from the Prior value of 3% (Figure 4-4) to 77%. The probability of no consequence in this case is just above 5%.

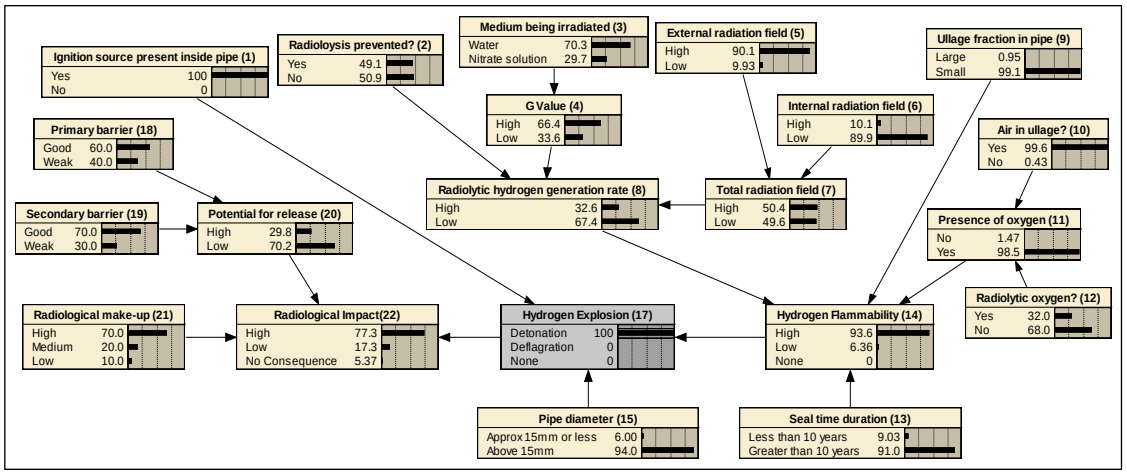

Figure 4-10: Updated BBN to determine the effects of a detonation

As a comparison, if Node 17 is instantiated to a 100% deflagration probability, then Figure 4-11 shows that the probability of no consequence is around 9%, i.e., almost twice the value of 5% based on a detonation. These results therefore indicate that if the likelihood of a detonation is eliminated, the chances of significant consequences could be reduced by a factor of two.

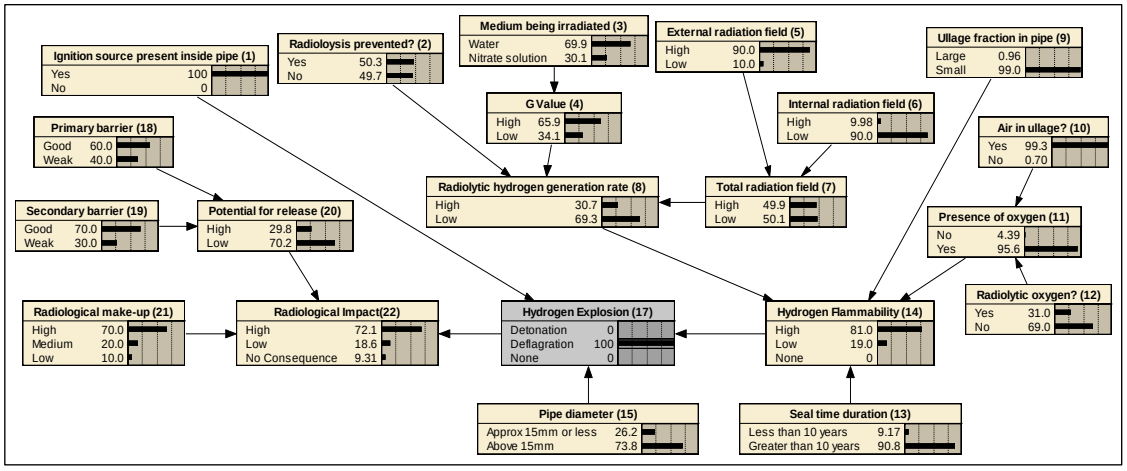

Figure 4-11: Updated BBN to determine the effects of a deflagration

4.7.3 Sensitivity to changes in the main parent node CPT data

The BBN prior model is based on the derivation of CPT data for the main parent nodes such as hydrogen flammability and hydrogen explosion which in turn affect the likelihood of radiological consequences. Given the uncertainty associated with such CPTs, it would be beneficial to determine the sensitivity of the model to potential changes in such data. Figure 4-12 examines the effect of a decrease in the Node 14 None state CPT values by 20% on the likelihood of no radiological consequences.

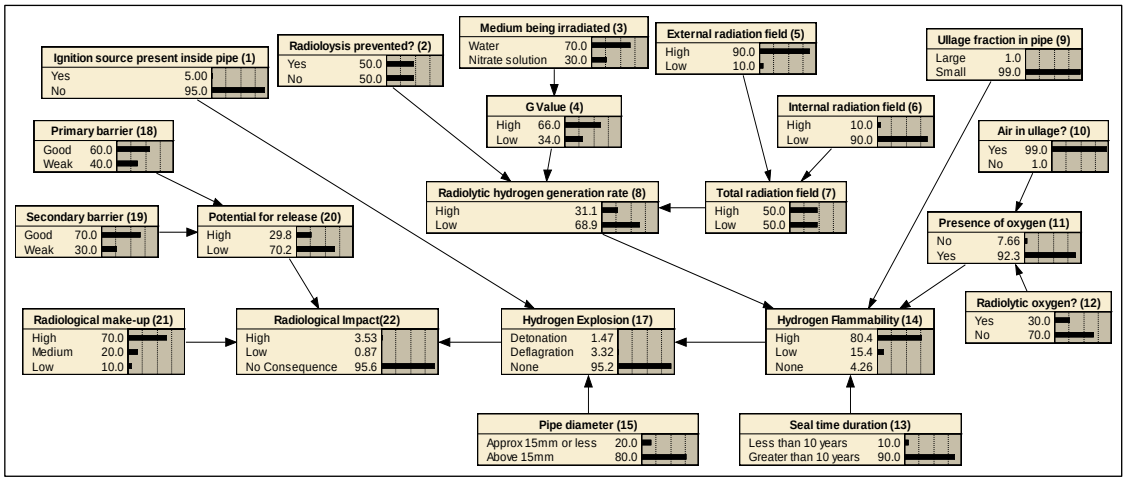

Figure 4-12: Sensitivity to decrease in Node 14 'None' state CPT values by 20%

In comparison with the model based on Prior values (Figure 4-4), a 20% reduction in the 'None' state CPT values of Node 14 results in a negligible decrease in the probability of no radiological consequences . Equally, a 20% rise in the 'None' state CPT values of Node 14 results in a negligible increase in the probability of no consequence (Figure 4-13).

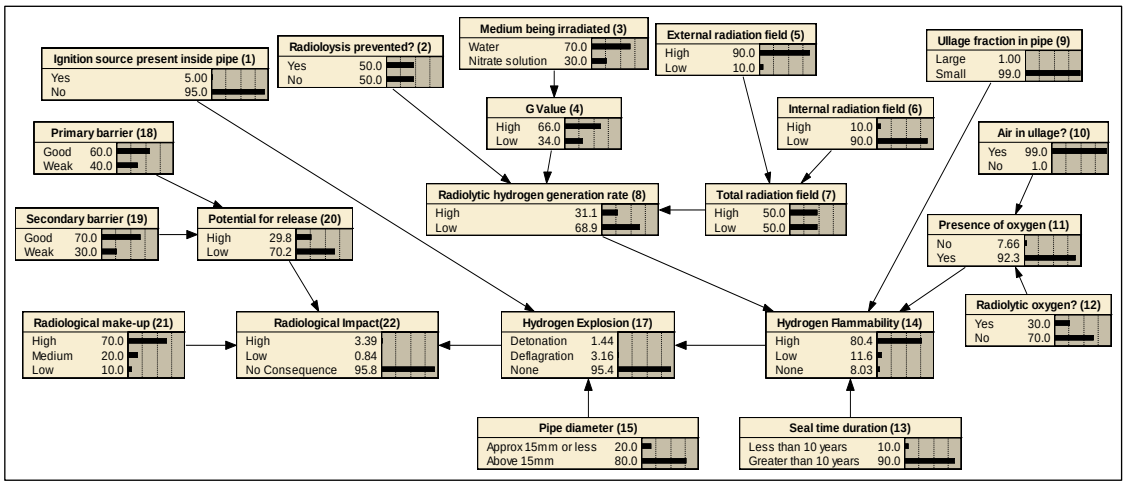

Figure 4-13: Sensitivity to increase in Node 14 'None' state CPT values by 20%

The sensitivity to a 20% increase in the 'None' state CPT values for the hydrogen explosion node was also tested as shown in Figure 4-14. In comparison with the model based on Prior values (Figure 4-4), there is a negligible increase in the probability of no radiological consequences.

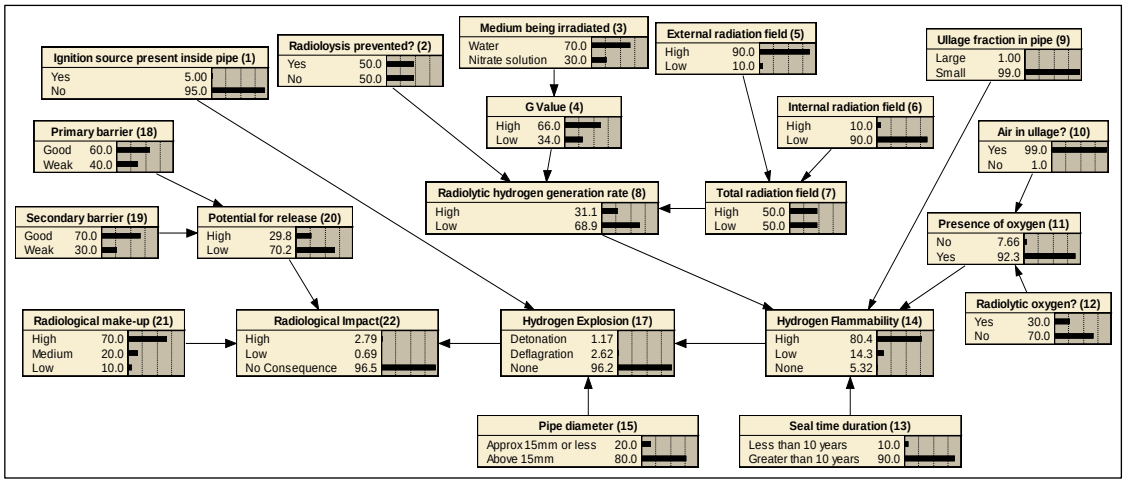

Figure 4-14: Sensitivity to increase in Node 17 'None' state CPT values by 20%

The hydrogen generation rate, modelled in Node 8, is also a key variable which affects the hydrogen flammability, hydrogen explosion and the radiological consequence probabilities. Therefore, the sensitivity to a 20% increase in the High state of Node 8 is also tested in Figure 4-15. Although this results in a slight increase in the probability of the high hydrogen flammability state from 80% (Figure 4-4) to 81%, there is a negligible effect on the total hydrogen explosion and radiological consequence probabilities.

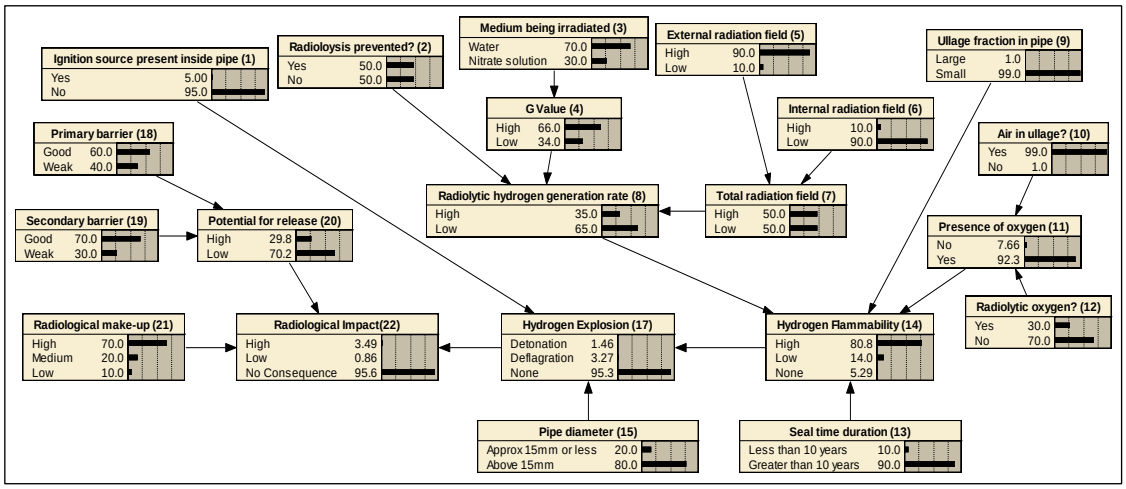

Figure 4-15: Sensitivity to increase in Node 8 'High' state CPT values by 20%

The general trend that can be observed from the sensitivity analysis is that up to a 20% increase and decrease in the CPT values for the main parent nodes has a negligible effect on the likelihood of radiological consequences. The total probability of a radiological impact always remains below the ignition probability value of 5%. This is plausible as the probability of a hydrogen explosion and subsequent consequences can never exceed the likelihood of an ignition.

4.8 Consideration of plant trends and further expert judgement

The BBN model in the preceding sections was based on initial prior beliefs and opinion of members of the SL Hydrogen Working Party. However, to validate the model and ensure that the results are reasonable, a comparison with plant trends as far as possible is considered beneficial. Therefore, further research into the likelihood of the key variables was undertaken through discussions with the SL Chemical Engineer Subject Matter Experts (SMEs) for sealed process pipework on plant. For parameters where direct plant trends were not available, further advice from the SMEs in the form of expert judgment was consolidated in the model as part of the validation process. *Ahmed, 2019c* provides minutes of the discussion with the SMEs. The following sub-sections provide details of this review process for each of the key variables and updating of the model accordingly.

4.8.1 Presence of ignition sources

The SME judgement was that since the pipes are welded and sealed, they are not exposed to any mechanical or chemical ignition sources. The condition within the pipes is benign such that static discharge is also considered unlikely. This judgment agrees with the fact that no ignition events in sealed pipes such as cooling coils have been observed on plant. However, given that hydrogen rich atmospheres would only require a small ignition energy, this event cannot be completely ruled out. Collectively in terms of the overall balance of risk, the low ignition probability of 5% in the BBN model is considered reasonable.

4.8.2 Seal time duration

The current model assumes that most of the pipes have been sealed for at least a period of 10 years. This assumption was reviewed with the SMEs who agreed that the pipework has typically remained sealed for 10 years.

4.8.3 Pipe medium and associated G values

Most of the cooling coils are used for the cooling of heat generating aqueous liquors. The radioactivity associated with these liquors external to the coils is predominantly gamma radiation. On this basis a high G value of 4.59litres/kWh, equivalent to 0.45 molecules of hydrogen per 100eV of energy absorbed, for the cooling water in the coils has been substantiated for such systems by the SMEs. For a minority of the cooling coils used for cooling nitrate solutions, where holes larger than 1 mm may have developed due to long-term corrosion, the SME view is that there is the possibility of ingress of this liquor into the pipes. Hence for this small minority of cooling coils a relatively low G value of less than 1 litre/kWh for nitrate solutions would apply. On this

basis it is considered that the ratio of 7:3 for water to nitrate solutions modelled in the BBN Node 3 is reasonable.

4.8.4 Pipework primary containment integrity

Apart from pinhole leakages in cooling water pipework, evidence shows that no abnormal radioactivity levels have been previously detected by the gamma monitors downstream of the cooling water pipework. This suggests that the pipework containment is in good condition. On this basis the probability of 60% used in the BBN Node 18 for pipework integrity being good, was considered reasonable.

4.8.5 Hydrogen flammability

Although no direct sampling data for hydrogen and oxygen concentrations were avalaible, the expert judgment of the SMEs was that the radiolysis reaction occurs over two phases. In the first phase hydrogen as well as radiolytic oxygen will be generated. However in sealed pipes such as cooling coils the dissolved oxygen will soon be depleted by other contimnants in the water such as ferritic materials which have a high affinity for the gas. In the second phase, the rate of depletion of the oxygen is greater than the rate of generation. Effectively the hydrogen will dominate the gas composition in the ullage such that the oxygen concentration will reduce to negligible levels. Over long periods, there is a high likelihood that the coil environment will change to a hydrogen rich atmosphere due to the lack of oxygen. As such, the likelihood of high flammable concentrations being reached will be small.

Whilst the potential for flammable concentrations cannot be completely ruled out, the SME judgement suggests that these events will occur over short transients. Given that the seal time duration is 10 years which is extensive, and taking into consideration oxygen depletion by ferritic contaminants, it was judged that the potential for radiolytic oxygen to be present in the pipes is relatively small. A probability of no more than 5% for presence of radiolytic oxygen was therefore considered reasonable. However the possibility of air leaks into the pipes due to pin holes developing over time could not be ruled out. A probability of 10% for the presence of oxygen due to air leaks was considered reasonable.

Based on the new evidence of the primary event probabilities discussed above, the BBN model was modified as shown in Figure 4-16.

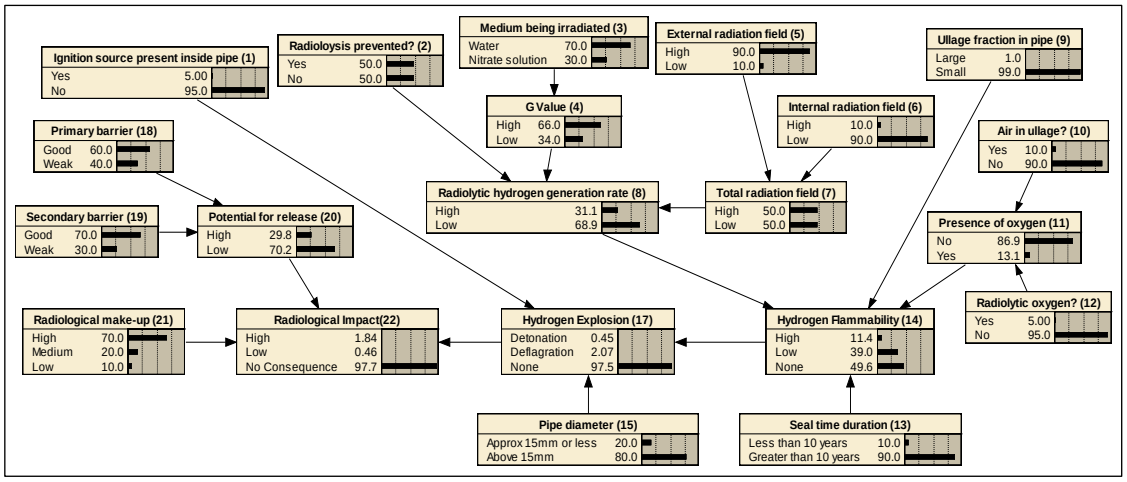

Figure 4-16: Modified BBN model in accordance with plant trends and expert judgment

It can be seen in Figure 4-16 that due to a reduction in the presence of air and radiolytic oxygen probabilities from 99% and 30% (Figure 4-4) to 10% and 5% repectively, the probability of high flammability has decreased from 80% to 11%. This has resulted in nearly a two fold reduction in the hydrogen explosion probability to less than 3%. This result reaffirms the insights from the original model that after ignition source probability, the presence of oxygen presents the next highest sensitivity to the occurrence of a hydrogen explosion.

4.9 Management of the risk from fault scenarios

The analysis given in the preceding sections is based on normal plant operations, which require the cooling coils to be isolated once any radioactivity in the pipework is detected. This isolation also prevents the atmosphere inside the cooling coils and the upstream pipework from being exposed to any strong external ignition sources. In these plant isolation conditions, relatively low ignition source probabilities of up to 0.05 were considered realistic. A fault condition however could arise leading to a failure of the pipework isolation valve, located in the operating areas of the building. Any uncontrolled repair work on the failed isolation valve could potentially lead to the hydrogen atmosphere in the pipework being exposed to strong mechanical ignition sources. Hence this fault scenario could lead to an increased risk.

As discussed in Chapter 2, Section 2.3.1, the risk targets for nuclear facilities [*HSE, 2006*] specify frequency limits of 1E-3/yr against faults leading to on-site radiological consequences. The ideal plant configuration for managing the hydrogen hazard in the sealed pipework is clearly that which does not exceed these targets. In order to make a direct comparison with these risk limits, the frequency of a hydrogen explosion and

subsequent radiological consequences following an accident scenario needs to be determined.

During the isolation valve repair work, the generation of a strong ignition source due to potential mechanical impacts is considered credible. The ignition roadmap that supports the SL Hydrogen Technical Guide, suggests an ignition source probability of approximately 0.1 if the impacted pipe surface is rusty. This condition is considered highly likely given the pipework age. The effect of an ignition source probability increased to 0.1 can be analysed by updating Node 1 of the BBN in Figure 4-4 based on prior probabilities. As shown in Figure 4-17, for a higher ignition probability of 0.1, the likelihood of a radiological impact increases to 8.7%.

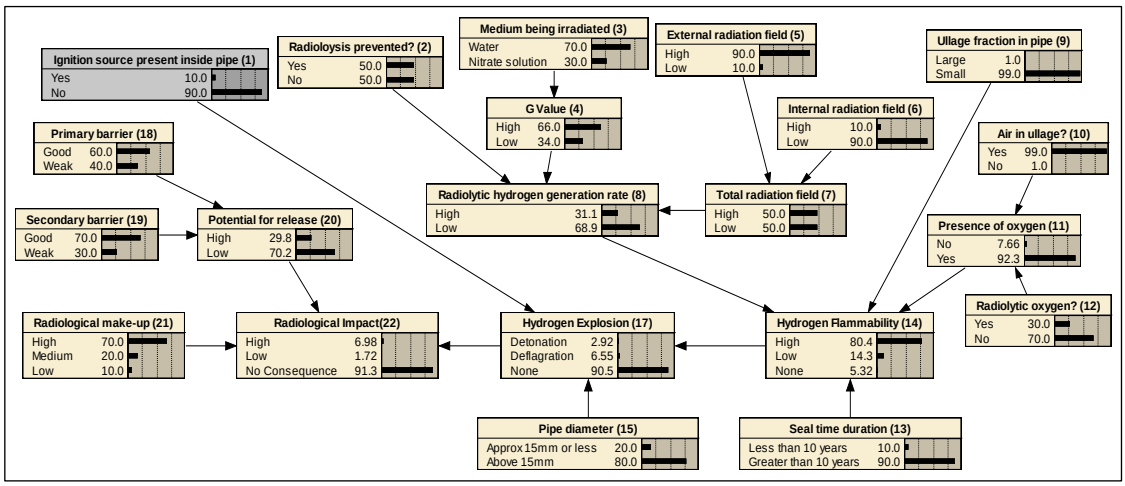

Figure 4-17: BBN for an increased ignition probability of 0.1

In nuclear safety cases, risk assessments for fault scenarios require a quantification of the Initiating Event Frequency (IEF). As shown in equation 4-1, the IEF combined with the probability of a hydrogen explosion leading to a radiological consequence and the probability of failure on demand (pfd) of protective measures against the fault would give a frequency of the Top Event (TE). Effectively, the frequency of the Top Event represents the quantified risk from the fault scenario.

$$TE\ frequency\ = IEF\ \times probability\ of\ a\ radiological\ impact \times pfd\ of\ protective\ measures \quad (4\text{-}1)$$

The Initiating Event for the fault being considered is a failure of the sealed pipework isolation valve. For hand-operated isolation valves, a failure rate of 15 per 10^6 hours i.e., 0.13/year is reported by *Lees,1992b* . This represents the IEF for the fault. The protective measures against the Initiating Event are plant procedures which must be followed by the valve maintenance team. These procedures would ensure a safe system of work, including the use of appropriate tools and environment for the valve replacement.

A human error probability of 0.1 for the maintenance workers failing to follow the safe procedure, is applied. Also, a probability of 0.1 is applied for a failure of the plant management team to provide a safe system of work. These probabilities are the suggested values in accordance with HSE guidance on human error assessments [*HSE, 2017*]. Both human errors would need to occur to result in a complete failure of the protective measures, giving an overall probability of failure of protective measures of 0.01. The probability of a radiological impact due to an increased ignition probability during the maintenance work is 8.7% (Figure 4-17). Based on these probabilities and the IEF of 0.13/year, the frequency of the Top Event, i.e., the frequency risk, can be calculated using equation 4-1, as follows:

$$Top\ Event\ frequency = 0.13 \times 0.087 \times 0.01 = 1.1 \times 10^{-4}/year$$

If the frequency of 1.1E-4/year is compared with the HSE onsite risk target of 1E-3/year, it is demonstrated that the risk from a fault leading to a failure of the sealed pipework isolation valve and a subsequent hydrogen explosion is below the criteria. However, to satisfy the ALARP principle, additional protection could be provided by permanently isolating and venting of the failed cooling coils, similar to the arrangement in Figure 4-1.

4.10 Conclusions for Chapter 4

This case study has investigated the application of the Bayesian Belief Network methodology to identify key sensitivities which would affect the likelihood of a hydrogen deflagration or detonation within existing sealed process pipework. Based on the Prior probability data, using expert opinion from the Hydrogen Working Party, the initial BBN model showed that the ignition source probability presents the greatest sensitivity to the likelihood of a deflagration or a detonation and subsequent consequences. This suggests that any modification work to the pipework must be carefully controlled to minimise ignition sources. For example, any pipe cutting or grinding operations could be undertaken in an inert atmosphere, thus reducing the ignition probability.

A further way of managing the hydrogen hazard would be to control factors which affect hydrogen flammability i.e., radiolytic hydrogen generation rate and presence of radiolytic oxygen or air. Expert judgement suggests that the oxygen concentration of the sealed pipework is negligible. On this basis the probability of a high flammability reduces significantly. An analysis of the risk from fault scenarios leading to a failure of the sealed pipework isolation valves and exposure of the pipework hydrogen atmosphere to external ignition sources shows that the risk is below the HSE risk limits. However, to demonstrate ALARP, further improvements such as capping and venting the pipework would provide an enhanced means of protection against the fault.

CHAPTER 5 : CASE STUDY 2- BAYESIAN BELIEF NETWORK ANALYSIS OF UNCERTAINTY ASSOCIATED WITH MIXING OF RADIOACTIVE SLUDGES IN THE WASTE TREATMENT AND ENCAPSULATION PROCESS

5.1 Introduction to Chapter 5

Plant P8 provides the process for treatment and encapsulation of Intermediate Level Wastes (ILWs) retrieved from storage facilities in plant P5. The main ILWs processed in plant P8 include magnesium hydroxide and uranium hydroxide sludge wastes which are the products of corrosion of the Magnox waste in plant P5. The waste encapsulation process in plant P8 involves mixing the sludge with cement grout formulations in a rotational mixing vessel as shown in Figure 5-1.

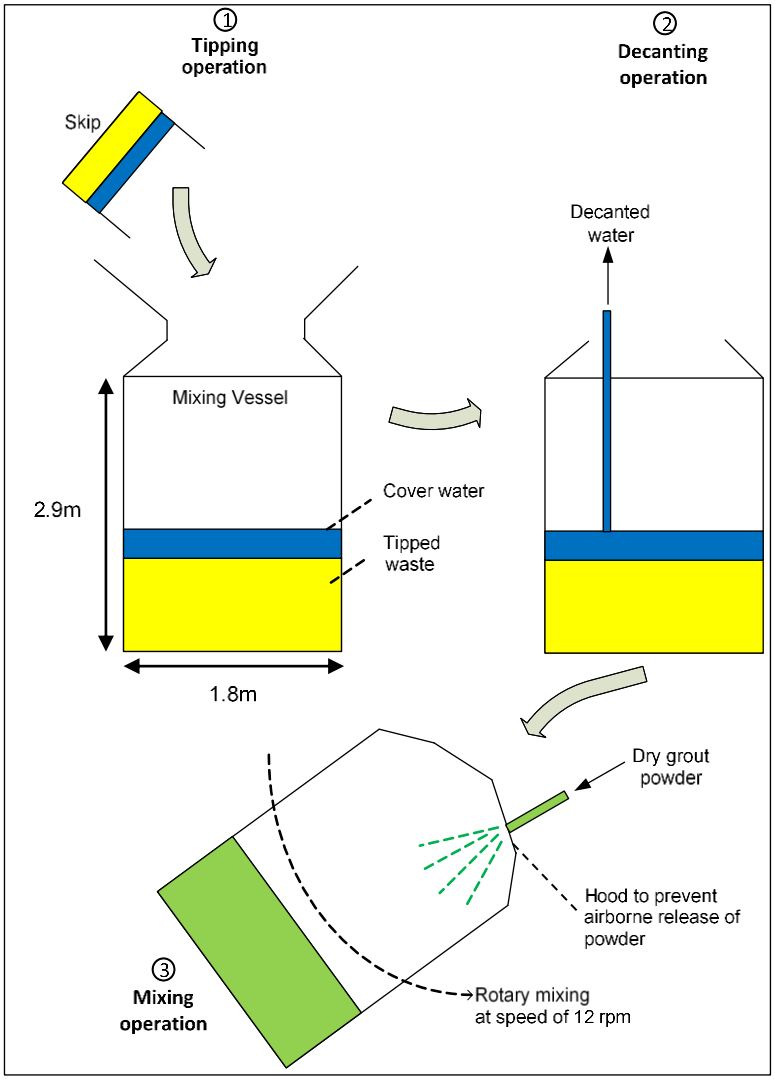

Figure 5-1: Sludge tipping, decanting and grout mixing operation

The key process stages in plant P8 are that the sludge waste initially arrives in the building within a skip which is tipped into the mixing vessel and any excess water is decanted away. During the initial grout powder addition stage, the vessel aperture is

covered with a hood to prevent the spread of airborne dust to the outside. The vessel is mounted on rotational bearings within a hydraulically operated lifting frame to enable the vessel to be lifted to the desired height and angle. The rotational bearings are operated using an electric motor which allow the vessel to be rotated at typical speeds of 12 r.p.m. This has the effect of mixing the vessel contents, similar to an industrial cement mixer operation. Once the dry powder addition is complete the hood is removed, and the mixing operation continues. Following completion of the mixing cycle, the grouted contents of the vessel are tipped into a waste encapsulation drum using the lifting frame.

A key plant operability requirement is that the mixed product within the vessel should be sufficiently mobile to enable it to be tipped into the waste encapsulation drum without any significant adherence. This is primarily dependent on the water to solids ratio and the fluidity of the grouted sludge.

The ILW sludge arising from plant P5 varies in terms of the solids and water content as well as rheology. These are the essential characteristics that dictate how the sludge will mix with grout in the mixing vessel. The variability in these parameters potentially leads to an uncertainty around the required cement and water grout formulation and hence the water to solids ratio. Addition of excessive quantities of cement grout or insufficient water to a particular type of sludge are typical examples of the operability issues encountered during the mixing process. These issues could result in a low fluidity and hence an inability to remove the mix from the vessel, ultimately leading to a significant plant downtime. Conversely, addition of excessive quantities of water in the mixing vessel could result in a high fluidity of the mix such that it is runny, potentially resulting in a non-compliant product matrix.

This case study applies the Bayesian Belief Network (BBN) method to examine the interactions between the various sludge characteristics and mixing parameters. It aims to explore the uncertainty on whether the mixed sludge could be easily removed from the mixing vessel. A further aim is to identify parameters which have a significant impact on this uncertainty. The impact of any parameters of uncertainty on the BBN results will also be investigated by means of a sensitivity analysis. The overall aim is to identify an optimum set of operating conditions that enable removal of the sludge mix from the vessel while ensuring that the product quality is acceptable. The output of the research based on this case study has also been published by the candidate in the IChemE Chemical Engineer magazine as summarised in Appendix H, Table H-1.

5.2 Derivation of BBN variables and CPT data

A series of meetings were held with a team of specialists on the behaviour of Magnox sludge, referred to as the 'Characterisation, Inventory, Sludge, Waste Group' (CISWG), to identify the main variables that affect sludge mobility [*Ahmed,2015*]. Based on the variables and the associated interactions identified at the CISWG meetings, a concept BBN was established, which is shown in Figure 5-2.

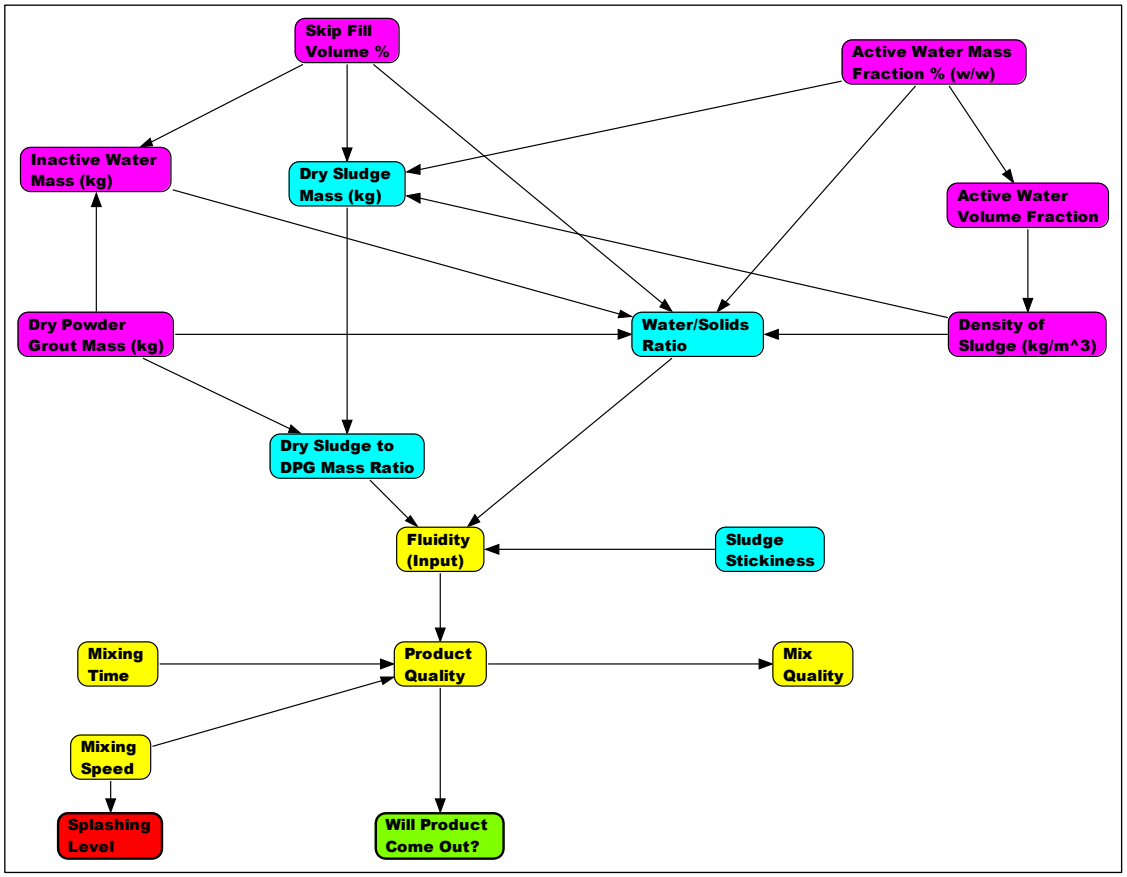

Figure 5-2: Concept model for the sludge mixing hypothesis

In Figure 5-2 the parent nodes coloured purple represent the variables which affect the water to solids ratio of the grouted sludge, while the cyan nodes affect the mix fluidity. The yellow coloured nodes affect product quality, which in turn dictate whether the sludge will tip out of the vessel. The red coloured node represents the potential for the mixing vessel contents to splash during the process which must be minimised in order to prevent a spread of contamination from the radioactive sludge.

The use of a lid over the mixing vessel aperture to prevent the contents splashing out was considered by the mixing vessel design team. However, this would require the lid to be washed and decontaminated each time it needs to be removed from the vessel to prevent the grout material setting on the lid surfaces. The need for frequent washing and decontamination of the lid meant that this option was non-practical. A hood for

prevention of the spread of airborne dust, during the initial dry powder grout addition stage was however considered reasonably practical, which is included in the mixing process as shown in Figure 5-1.

A detailed description of each of the concept model variables, the associated interactions and derivation of the CPTs is given in the following subsections.

5.2.1 Sludge Components

As discussed in the meeting minutes by *Ahmed, 2015,* the expert opinion of the CISWG, based on a historic sampling of the active sludges from plant P5, is that the sludge has three main components, as follows:

- Radioactive water, referred to as 'active water' hereafter.
- A mixture of corrosion products including magnesium hydroxide.
- Uranium dioxide which gives the sludge a 'sticky' characteristic due to its low particle size.

The sludge stickiness can lead to operational difficulties in terms of the product adhering to the mixing vessel internals. Since the sludge comprises coarse material as well as fines, the CPT for sludge stickiness considers that there is a 50% chance that the material is sticky. Whilst there is an uncertainty on the probability distribution of sludge stickiness, the sensitivity to changes in this distribution are explored in this case study. Assuming that any excess water from the sludge has been decanted before starting the mixing operation then, based on the previous trial work, the CISWG suggested that the active water content of the sludge ranges from 30 to 90% weight of the total amount [*Ahmed,2015*].

5.2.2 Quantity of Inactive Feeds

A review of the previous sludge mixing trial work has shown that the fluidity of the grouted mix is a main parameter which affects the likelihood of the sludge coming out of the mixing vessel. The fluidity of the sludge mix is dependent on the water to solids ratio. This ratio is affected by the quantity of active contents of the sludge including active water carryover and inactive feeds added to the sludge mix. These feeds are inactive water, cement powder and organics. Organics are often added to improve the flow properties of the mix. Accordingly, the water to solids ratio of the grout mix is defined by the following relationship:

$$Water\ to\ solids\ ratio\ = \frac{free\ water\ content + \ sludge\ internal\ water}{Quantity\ of\ dry\ cement + dry\ sludge\ solids} \qquad (5\text{-}1)$$

Based on a knowledge from the previous sludge mixing trial work, the CISWG advised that water/solids ratios have ranged from 0.8 to above 1.3 for successful mixing campaigns [*Ahmed, 2015*]. Therefore, the likelihood of the water to solids ratio being in this range will determine whether the sludge mix will come out of the mixing vessel.

The water to solids ratio can be calculated knowing the active and inactive water mass and the dry mass of the sludge. Each of these parameters can be derived based on the principles of mass and volume fractions as detailed in Section 5.2.3.

5.2.3 Active Water Volume Fraction

The volume fraction of active water V_{AW} in the sludge can be derived based on the principles of density, weight and volume fractions of composites in mixtures. Knowing the weight fraction of water, W_{AW}, the density of water, ρ_{AW}, the density, mass and volume of the sludge ρ_S, W_S ,V_S respectively, V_{AW} can be derived as follows:

Density, ρ = Mass W/ Volume V

Hence in terms of weight fractions, $W_{AW} = \rho_{AW} \times V_{AW}$ and $W_S = \rho_S \times V_S$

The weight fraction of water, W_{AW}, and the weight fraction of sludge, W_S, must add to 1, i.e.

$$W_{AW} + W_S = 1 \tag{5-2}$$

Equally the volume fractions V_{AW} and V_S must also add to 1.

$$V_{AW} + V_S = 1 \tag{5-3}$$

The weight fraction of water in a mixture of water and sludge can be expressed as (weight of water)/ (weight of water + weight of sludge) as follows:

$$W_{AW} = \frac{\rho_{AW} \times V_{AW}}{(\rho_{AW} \times V_{AW} + \rho_S \times V_S)} \tag{5-4}$$

Re-arranging equation 5-3 gives:

$$V_S = 1 - V_{AW} \tag{5-5}$$

Hence substituting equation 5-5 into equation 5-4 gives:

$$1 = V_{AW} \times \left(\frac{\rho_{AW}}{\rho_S} \times \left(\frac{1}{W_{AW}} - 1\right) + 1\right) \tag{5-6}$$

Therefore, solving for V_{AW} gives:

$$V_{AW} = \frac{1}{1 + \left(\frac{\rho_{AW}}{\rho_S} \times \left(\frac{1}{W_{AW}} - 1\right)\right)} \tag{5-7}$$

On the basis of equation 5-7, the Active Water Volume Fraction in Netica is calculated by equation 5-8

$$V_{AW} = \frac{1}{1 + \left(\frac{1000}{2345} \times \left(\frac{1}{\left(\frac{W_{AW}}{100} \right)} - 1 \right) \right)} \quad (5\text{-}8)$$

Where:

The numerical values 1000 and 2345 are the densities of active water, ρ_{AW} and wet sludge, ρ_S, respectively with the units Kg/m^3.

As discussed previously, the active water mass fraction is known to be in the range 30 to 90% weight and is assumed to follow a normal distribution. On this basis the CPT Active Water Volume Fraction was derived by Netica as given in Table B-1.

5.2.4 Density of Sludge (Kg/m^3)

The density of the sludge for a mixture of Active water and sludge can be expressed as a function of the active water volume fraction V_{AW}. This is the summation of the density of pure active water and pure wet sludge. However, the actual density of the active water and sludge mixture is also proportional to the volume fraction of active water V_{AW} and the volume fraction of the sludge (1- V_{AW}) as shown in equation 5-9.

$$Density\ of\ sludge = \rho_{AW} \times V_{AW} + \rho_S (1 - V_{AW}) \quad (5\text{-}9)$$

Where:

ρ_{AW} is the density of pure active water, 1000Kg/m^3.

ρ_S is the density of pure wet sludge which is known to be 2345Kg/m^3.

Based on equation 5-9, the density (DS) of sludge in a mixture of active water and wet sludge in Netica is expressed as follows:

$$DS\ (V_{AW}) = V_{AW} \times 1000 + (1 - V_{AW}) \times 2345 \quad (5\text{-}10)$$

Where:

DS is the density of sludge (Kg/m^3) in a mixture of active water and wet sludge.

V_{AW} is the volume fraction of active water.

Based on equation 5-10, the CPT for sludge density (DS) was calculated by Netica as shown in Appendix B, Table B-2.

5.2.5 Inactive Water Mass (Kg)

The mass of inactive water in a skip is dependent on the volume of skip contents. This can be determined knowing the skip fill volume and the total volume of the inactive contents of the skip, including inactive water and dry powder grout mass.

It is known that the skip internal volume is 1260L. The volume of skip occupied by the skip waste contents, i.e., wet sludge and active waste, is the product of the skip internal

volume and the skip fill volume fraction, Vskip (%), i.e., 1260 x Vskip/100. The probability distribution of the skip fill volume fraction is unknown. However, the CPT for this variable, based on best judgment, assumes that the fraction ranges are uniformly distributed.

It is also known that the total volume of the skip contents is 2100 litres. This includes the volume occupied by the skip waste content, i.e., wet sludge and active water as well as the inactive water and dry grout powder. The density of the dry grout is 2.925 kg/l, therefore the grout volume is DPG/2.925. Hence the volume of inactive water (IW) added to the skip is the total volume of the skip contents, minus the volume of dry grout, minus the volume of the skip occupied by the waste (equation 5-11).

$$IW = 2100 - \frac{DPG}{2.925} - 1260 \times \left(\frac{Vskip}{100}\right) \quad (5\text{-}11)$$

Using a density of 1kg/l for inactive water, the equation applied in Netica for the calculation of the mass of inactive water is:

$$IW(Vskip, DPG) = \left(2100 - \frac{DPG}{2.925} - 1260 \times \left(\frac{Vskip}{100}\right)\right) \times 1.0 \quad (5\text{-}12)$$

Using equation 5-12, the CPT for inactive water mass was calculated by Netica, as shown in Appendix B, Table B-3.

5.2.6 Dry Sludge Mass (kg)

The Dry Sludge Mass is calculated knowing the volume of sludge and the weight fraction of dry sludge. The total volume of sludge waste content is 1260L/1000 m^3. However, the actual volume of sludge in the skip is dictated by the skip fill volume fraction, Vskip (%), which is given by equation 5-13.

$$Volume\ of\ sludge\ = \left(\frac{Vskip}{100}\right) \times \frac{1260}{1000} \quad (5\text{-}13)$$

The weight fraction of dry sludge can be determined knowing the weight fraction of active water, $W_{AW.}$ From equation 5-2, the weight fraction of the sludge, W_S, is:

$$W_s\ =\ 1 -\ \mathrm{W_{AW}} \quad (5\text{-}2)$$

The mass of dry sludge can be calculated knowing the volume of sludge as discussed above, and the weight fraction of dry sludge, Ws, and the dry sludge density, ρ_S. Since W_{AW}, is expressed as a percentage in Netica, the actual weight fraction of dry sludge is 1- W_{AW}/100. The dry sludge density, ρ_S, is the product of the weight fraction of dry sludge i.e., 1- W_{AW}/100 and the density of the sludge and active water mixture, DS.

$$\rho_S = DS \times \left(1 - \frac{W_{AW}}{100}\right) \quad (5\text{-}14)$$

Using equation 5-13 for the volume of sludge and equation 5-14 for the fractional density of the dry sludge, the mass of dry sludge is calculated in Netica using equation 5-15.

$$DSM\ (Vskip, DS, AW) = \left(\frac{1260}{1000}\right) \times \left(\frac{Vskip}{100}\right) \times DS \times \left(1 - \frac{AW}{100}\right) \quad (5\text{-}15)$$

Using equation 5-15 and the CPTs for the nodes Vskip, DS, AW, Netica automatically calculates the CPT for the Dry Sludge Mass (DSM).

5.2.7 Water to Solids Ratio

Based on equation 5-1, the water to solids ratio (WS) can be expressed as:

$$WS = \frac{Inactive\ Water\ Mass\ (IW) + Active\ water\ mass(AW)}{Dry\ Powder\ Grout\ \ Mass\ (DPG) + Mass\ of\ dry\ sludge(DSM)} \quad (5\text{-}16)$$

Where:

- Active water mass is the product of active water mass fraction in wet sludge and the mass of wet sludge.
- Mass of wet sludge is the product of the density of wet sludge (DS) and volume of the skip contents.
- Volume of skip contents is the product of the skip fill volume fraction (Vskip %/100) and the skip internal volume (1260 litres/1000 m^3).

Hence:

$$Volume\ of\ skip\ contents = \left(\frac{1260}{1000}\right) \times \frac{Vskip}{100} \quad (5\text{-}17)$$

and:

$$Active\ Water\ Mass = DS \times \left(\frac{1260}{1000}\right) \times \frac{Vskip}{100} \quad (5\text{-}18)$$

From equation 5-2, $W_{AW} + W_S = 1$

Where:

W_{AW} is the Active Water mass fraction = AW/100

Therefore:

$$Dry\ sludge\ mass\ fraction, W_S = 1 - \frac{AW}{100} \quad (5\text{-}19)$$

As shown in equation 5-15, the mass of dry sludge is expressed as:

$$Mass\ of\ dry\ sludge, DSM = \left(\frac{1260}{1000}\right) \times \left(\frac{Vskip}{100}\right) \times DS \times \left(1 - \frac{AW}{100}\right) \quad (5\text{-}15)$$

Hence, by substituting the equations above into equation 5-16, the water to solids ratio, WS, is calculated in Netica using equation 5-20.

$$WS = \frac{IW + \left(\frac{AW}{100}\right) \times \left(\frac{DS}{1000}\right) \times 1260 \times \left(\frac{Vskip}{100}\right)}{\mathrm{DPG} + \left(1 - \frac{\mathrm{AW}}{100}\right) \times \left(\frac{\mathrm{DS}}{1000}\right) \times 1260 \times \left(\frac{\mathrm{Vskip}}{100}\right)} \quad (5\text{-}20)$$

5.2.8 Dry Sludge to DPG Mass Ratio

The main factor that affects the likelihood of the sludge mix being removed from the mixing vessel is the fluidity. This is dependent on the ratio of the Dry Sludge Mass to Dry Powder Grout (DPG) Mass and the water to solids ratio.

From previous trial work, the CISWG advised that the Dry Powder Grout mass ranged from 700 to 1200 Kg [*Ahmed, 2015*]. Based on a uniform distribution of the DPG mass being in this range, and the calculated probability distribution of the Dry Sludge Mass (DSM), Netica calculates the CPT for the DPG to DSM ratio as shown in Appendix B, Table B-4.

5.2.9 Fluidity

Although the water to solids and dry sludge to DPG mass ratios are the main variables that affect fluidity, it is considered that sludge stickiness also has a significant effect. This is on the basis that the magnesium hydroxide sludge is likely to consist of size fractions <20μm which can adhere to vessel surfaces.

In Netica, fluidity is modelled as a discrete node, with DPG, DSM and sludge stickiness as the parent nodes. For sludge stickiness, three possible likelihood states have been identified i.e., high, medium or low. The derivation of the CPT for fluidity was based on expert judgment and knowledge from the previous trial work. For example, if the water to solids ratio is small i.e., in the range 0 to 0.7 and DSM to DPG mass ratio is also small, i.e., between 0 to 1 then, irrespective of the sludge stickiness, it was judged that there is a 100% chance that the fluidity of the sludge is low. If on the other hand, the water to solids ratio increases to mid-range, i.e., 0.7 to 1.3, then with high stickiness and low DSM to DPG Mass ratio the fluidity level would increase to medium. A full set of the CPT data for the fluidity node is given in Appendix B, Table B-5.

5.2.10 Mixing Time

The sludge mixing time is dependent on a number of factors including mix batch size, fluidity, sludge type and design of the mixing vessel. Excessive mixing times can cause the grouted mix to start curing within the mixing vessel and therefore prevent the mix from being discharged. Based on the previous trial work, the CISWG view was that the

mixing times ranging from 60 to 90 minutes would result in an acceptable mix quality [*Ahmed,2015*]. For the purpose of this case study the mixing time is modelled as a discrete node with three possible states i.e., short, medium or long.

5.2.11 Mixing Speed

The ability of the sludge mix to be removed from the mixing vessel is also dependent on the mixing efficiency, which is affected by the mixing speed. The mixing speed also needs to be controlled to avoid splashing of the mix. Based on previous trial work with Helix mixing vessel designs, the CISWG advised that a maximum mixing speed of 12rpm is desired to prevent splashing [*Ahmed,2015*]. For this case study the mixing speed is also modelled as a discrete node with three possible states i.e., Slow, Medium or Fast.

5.2.12 Product Quality

An important requirement for the mixing operations is that the mixed sludge product quality must be acceptable. This would enable successful waste encapsulation and allow safe storage of the waste packages. The main variables that affect product quality are product fluidity, mixing time and speed. In Netica the product quality node is also modelled as a discrete variable with three possible states i.e., 'Good', 'Hard' or 'Runny'. With excessive water, there is a high chance that the mix will be runny irrespective of the mixing speed and time. If the fluidity, mixing time and speed are maintained at Medium levels, then there is a100% chance that the product quality is good. Full details of the CPT for the product quality node are given in Appendix B, Table B-6.

The CPT for the Bayesian Network hypothesis, i.e., whether the mixed product will come out, is given in Appendix B, Table B-7. A probability of 100% is assigned for the 'no' eventuality if the product quality is hard. For a good or a runny product, a 100% probability is assigned to the 'yes' eventuality.

5.3 Results from the Bayesian Belief Network Analysis

Based on the Prior values of the parent input nodes, i.e., skip fill volume %, active water mass fraction and dry powder grout Mass, Figure 5-3 provides the BBN for the uncertainty on whether the mixed product will come out of the vessel. The results show that there is approximately an 81% chance that the mixed sludge will come out.

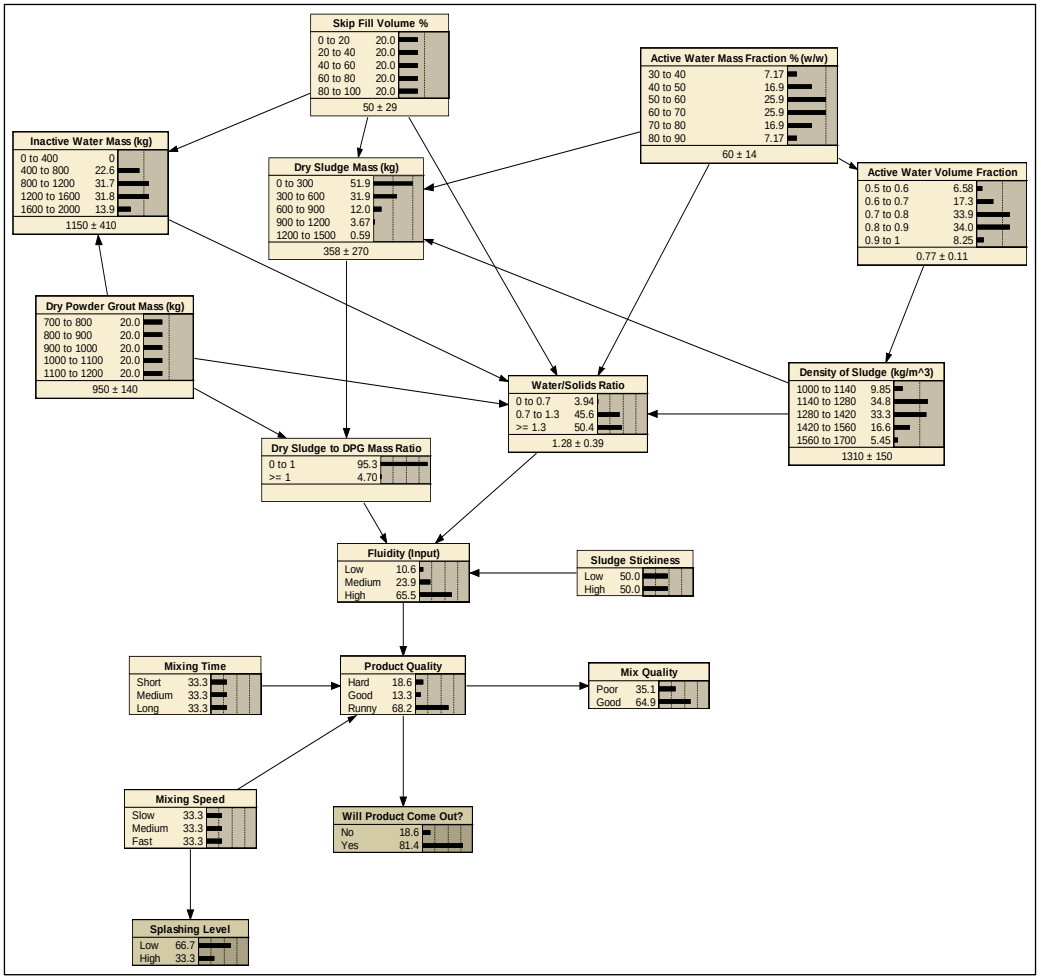

Figure 5-3: Fully developed BBN based on Prior probabilities

To test and verify the BBN given in Figure 5-3, the calculated key parameter values can be compared with previous experimental observations by replicating the values of the relevant Parent Nodes with the trial values.

One previous trial was based on a mix consisting of 58% weight dry sludge, i.e., 42% weight of this sludge constituted the active water mass fraction. The skip fill volume % and the dry powder grout mass (DPG) values were 65% and 1170Kg, respectively. For this trial, the water to solids ratio was known to be 0.74. Using the Netica 'Findings' function the trial values of the input parameters were replicated in the BBN and the model was re-run. The predicted water to solids ratio by the BBN is 0.742, as shown in Figure 5-4, which compares well with the actual experimental value of 0.74.

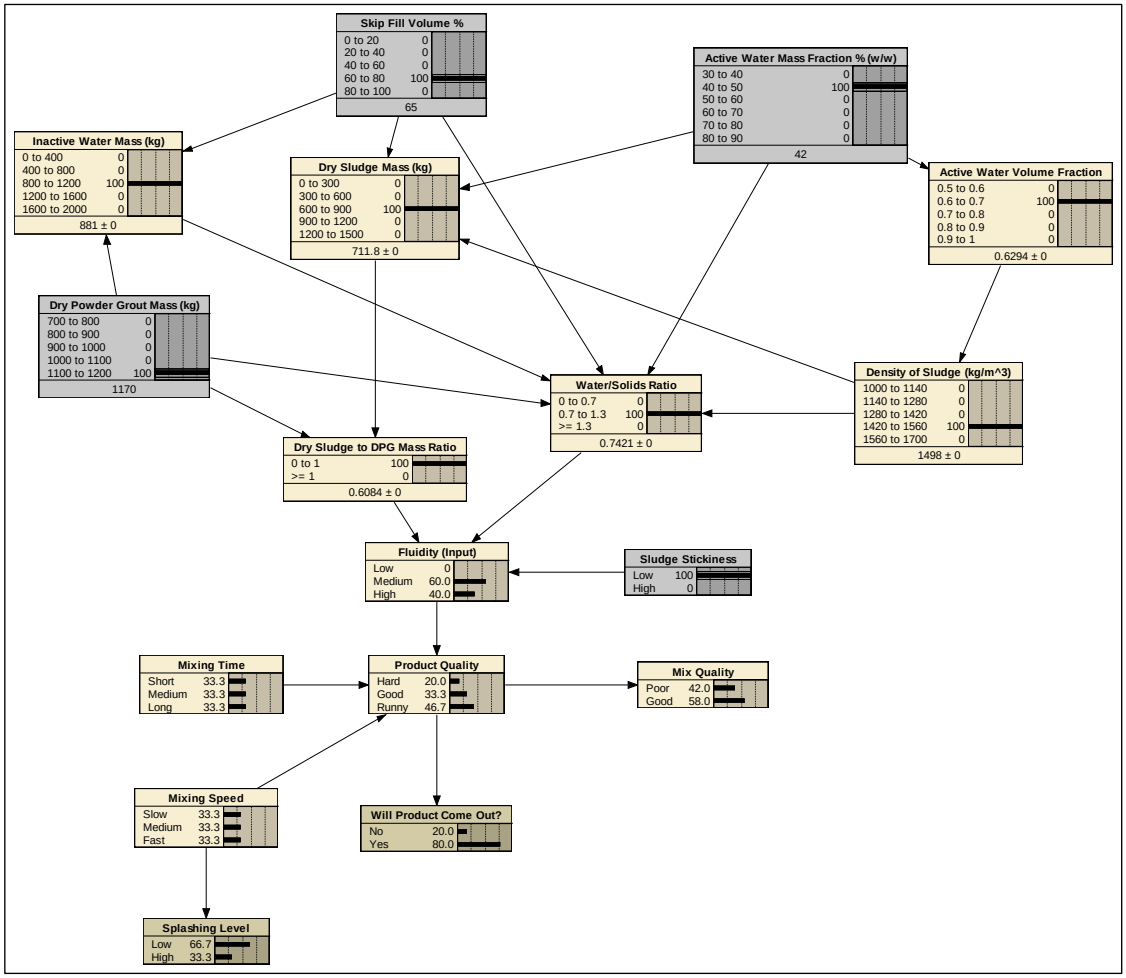

Figure 5-4: Updated BBN for sludge mixing uncertainty to replicate trial with 58%w/w dry sludge

A further previous trial used the active water mass fraction and the DPG mass of 42% and <800kg, respectively. These trial values were replicated in the BBN as shown in Figure 5-5. The predicted water to solids ratio by the BBN is 0.776 which agrees well with the trial value of 0.78. The comparison of the water solids ratio with the experimental observations given here verifies that the BBN model agrees with the expected behaviour. The concept model is therefore verified.

5.4 Sensitivity Analysis

Having established the concept BBN and its validity in terms of agreement with previous experimental work, further analysis can now be undertaken to determine new information which is not already known. For instance, the BBN could be used to investigate the influence of input node uncertainty on the product quality and determine their relative sensitivities. Sections 5.4.1 to 5.4.5 detail the sensitivity analysis undertaken using the BBN updating feature. An optimum configuration of the parameters, for ensuring that good quality sludge comes out of the vessel, is then identified.

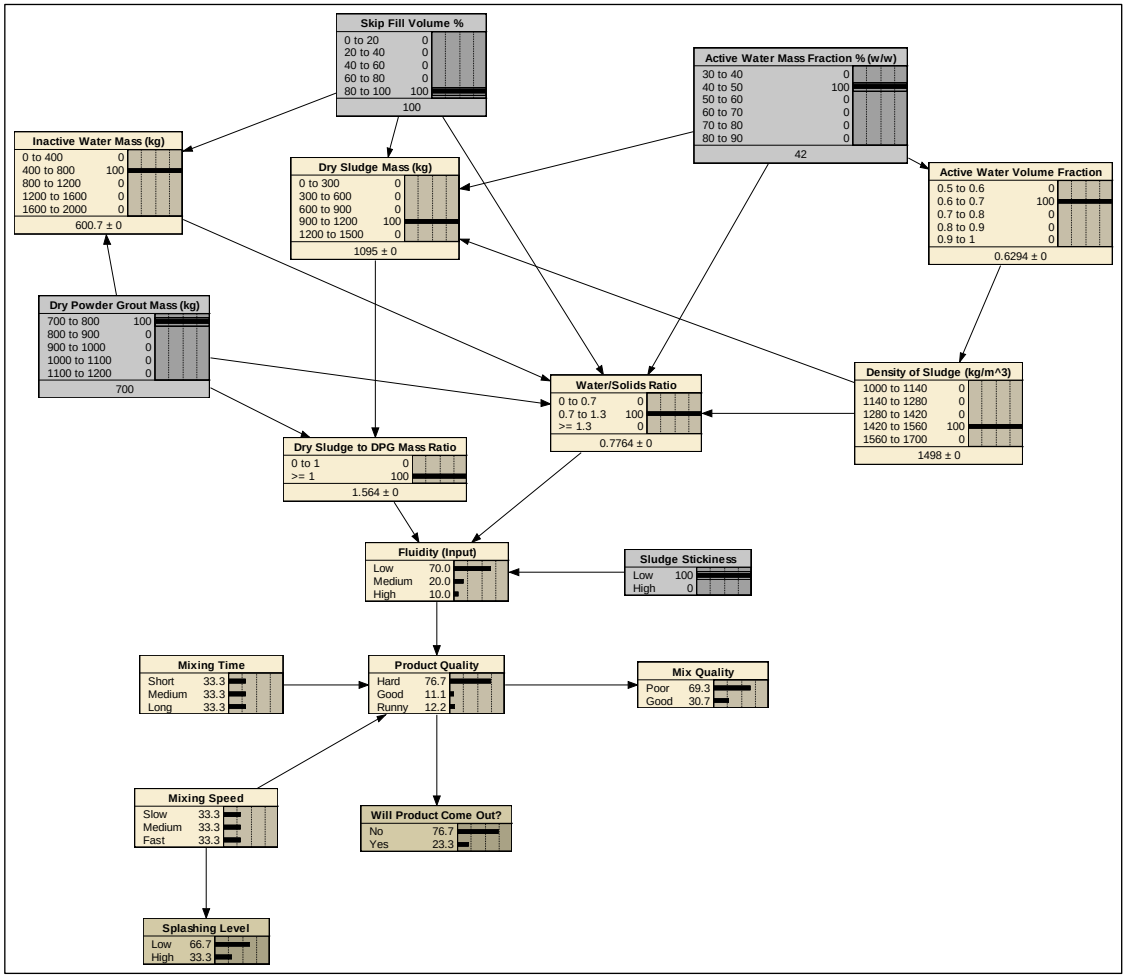

Figure 5-5: Updated BBN for sludge mixing uncertainty to replicate trial with Dry Powder Grout mass <800Kg

5.4.1 Sensitivity to water to solids ratio

The comparison of the BBN prior results with the previous trial work would indicate that the water to solids ratio is a key variable that affects the ability of the sludge being removed from the vessel. Intuitively with high water to solids ratios a fluidic behaviour would be expected whilst at low ratios the sludge is likely to be hard and adhere to the vessel surfaces. The effect of changing the water to solids ratio on the likelihood of sludge removal and good product quality was explored by instantiating each of the ratio ranges to 100% probability. Figure 5-6 provides a comparison of these results.

It can be seen in Figure 5-6 that by increasing the water to solids ratio, the probability of sludge coming out also increases as expected. A water to solids ratio range of >=1.3 leads to a peak probability of 80% for the sludge coming out of the vessel. The likelihood of obtaining a good product quality however reduces with increasing water to solids ratios . This trend agrees with the expected behaviour as high ratios would result in a runny product which is unsuitable for the downstream encapsulation process.

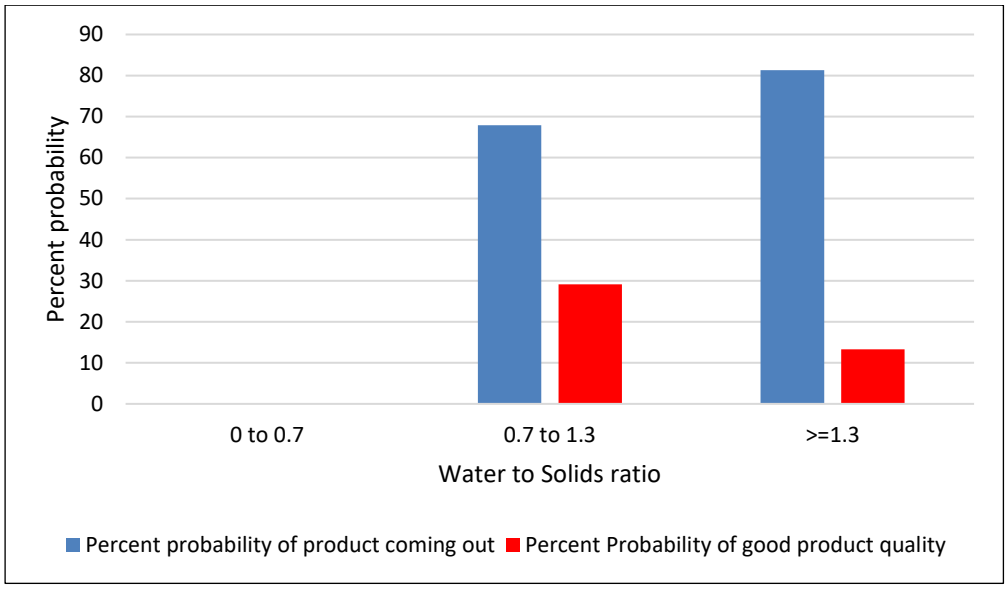

Figure 5-6: Effect of water to solids ratio on likelihood of product removal and quality

At low water to solids ratios of 0 to 0.7, the probabilities of the sludge coming out and obtaining a good product quality are both zero. Again, this agrees with the expected behaviour as low ratios would result in a hard product which would be difficult to encapsulate.

The BBN results based on the most effective water to solids ratios of >=1.3 show that the following conditions for the input parent nodes will be needed to ensure that the sludge comes out of the vessel:

- The active water mass fraction is in the range 50 to 70% weight at a probability of approximately 50%.
- A mean dry powder grout (DPG) mass of 990 kg.
- A mean skip fill fraction of 50% volume.

5.4.2 Sensitivity to Dry sludge to DPG mass ratio

Although the conditions listed in Section 5.4.1 enable an effective water to solids ratio and hence a high probability that the sludge comes out, the observation from Figure 5-6 is that at these conditions the probability of achieving a good product quality is still relatively low. From this trend it is depicted that in addition to the water to solids ratio, other parameters play a key role in achieving a high product quality. As shown in the concept model (Figure 5-2), the sludge fluidity, which in turn is affected by the dry sludge to DPG mass ratio, has a direct impact on product quality. Hence the effect of changing the dry sludge to DPG mass ratio on the product quality was determined by

instantiating each of the states for this node to 100% probability. Figure 5-7 gives a comparison of these results with the Prior probabilities of sludge coming out and obtaining good product quality, based on Figure 5-3.

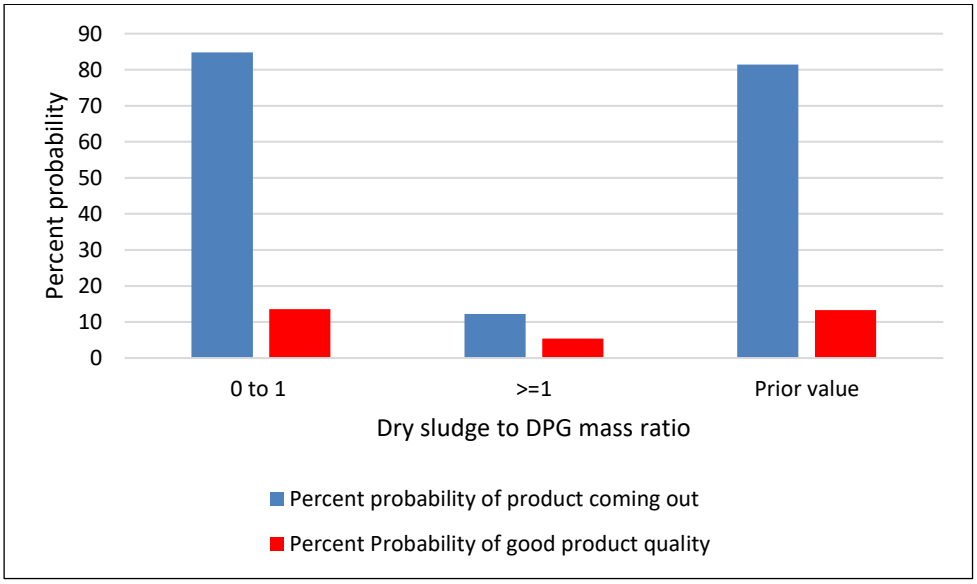

Figure 5-7:Effect of Dry sludge to DPG mass ratio on likelihood of product removal and quality

Figure 5-7 shows that a low dry sludge to DPG mass ratio will lead to a high probability, i.e., above 80%, that the sludge will come out. This is due to the low dry sludge content which leads to the product fluidity being high, thus resulting in the sludge being easily removed from the vessel. The runny mixture due to the low dry powder solids content however means that the product quality is low. Figure 5-7 also shows that at the ratio >=1, there is a sharp fall in the probability of the product coming out, to around 10%. This suggests that the preferred condition would be to keep the dry sludge to DPG mass ratio in the 0 to 1 range. However, controlling the ratio in the 0 to 1 range alone is still not the ideal condition as the probability of achieving a good product quality is still low.

5.4.3 Conditions leading to sludge coming out and good product quality

The success criterion for the hypothesis is that as well as the mixed sludge being easily removed from the vessel, the product quality is also good. The analysis in terms of changing the water to solids and the dry sludge to DPG mass ratios shows that controlling either of these parameters alone will not lead to both the sludge coming out and obtaining a good product quality. This would suggest that a combination of multiple parent nodes being in the ideal state would be needed to achieve the success criteria.

One way of determining the conditions necessary to meet the success criteria is to instantiate the product quality node to the ‘Good’ state as shown in Figure 5-8.

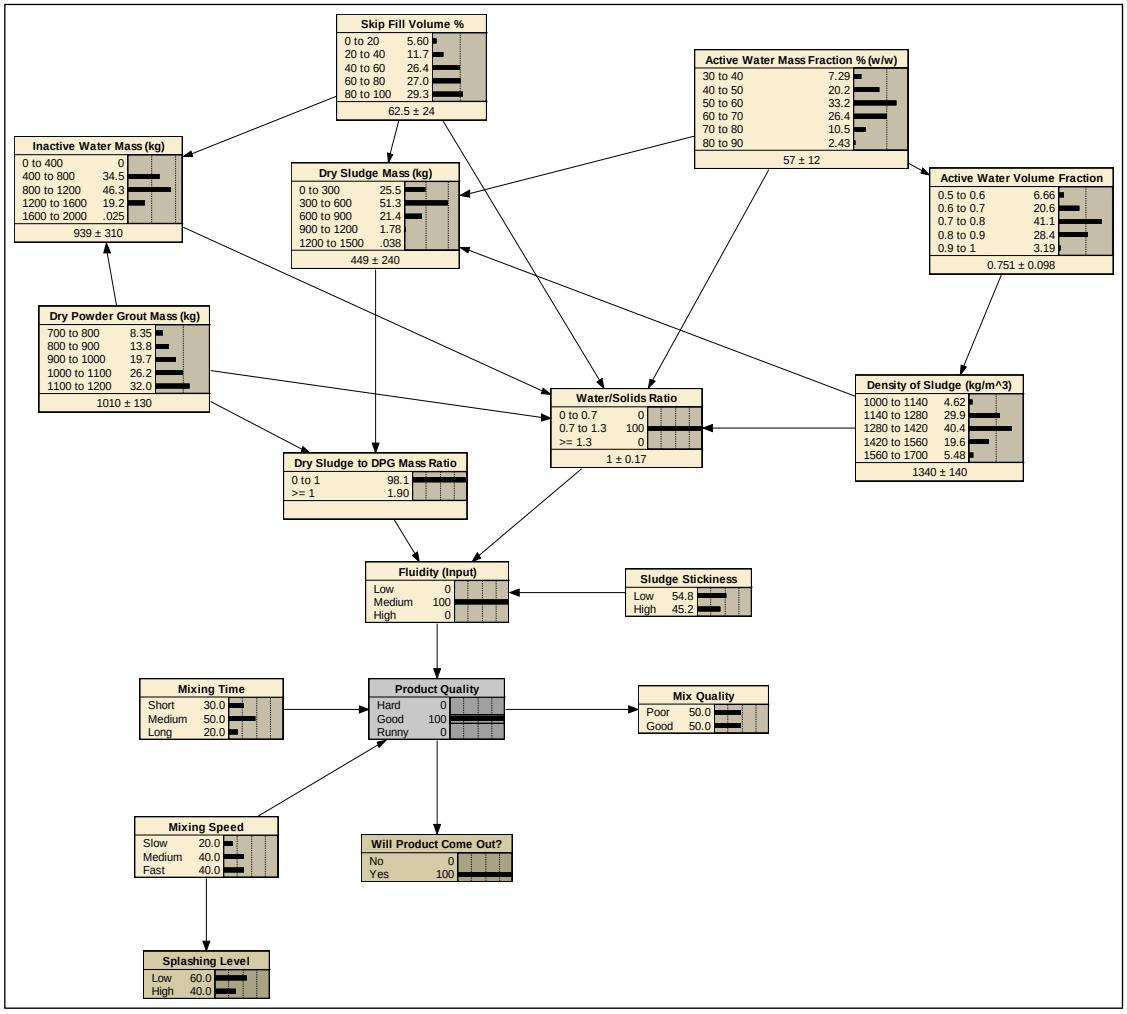

Figure 5-8: Conditions leading to good product quality and sludge comes out

A comparison of the updated results in Figure 5-8 with the BBN based on Prior probabilities (Figure 5-3) shows that the conditions necessary for a good quality product coming out are that the probability of the fluidity being medium would need to increase from 24% to 100%. This in turn requires a small increase in the probability of the dry sludge to DPG mass ratio being in the 0 to 1 range but over a 50% increase in the probability of the water to solids ratio being in the 0.7 to 1.3 range. A significant reduction in the probability of the water to solids ratio being >=1.3, i.e., from 50% to zero, is required to achieve this ideal state. Clearly these results suggest that in order to achieve a good product quality while ensuring that the product comes out, the water to solids ratio needs to be kept in the 0.7 to 1.3 range.

In addition to the need for a significant change to the probability distribution of the water to solids ratio, a further comparison of the Prior and updated probabilities is given in Figure 5-9, which can be summarised as follows:

- The probability of fluidity being low would need to decrease from a Prior value of 11% to zero.
- The probability of mixing time being long, i.e., above 90 minutes, would need to decrease from 33% to 20%.
- The probability of mixing speed being medium, i.e., around 12rpm, would need to increase to 40%.
- The probability of sludge stickiness being low, i.e., which leads to an insignificant sludge adherence to the vessel walls, would need to increase from 50% to around 55%.

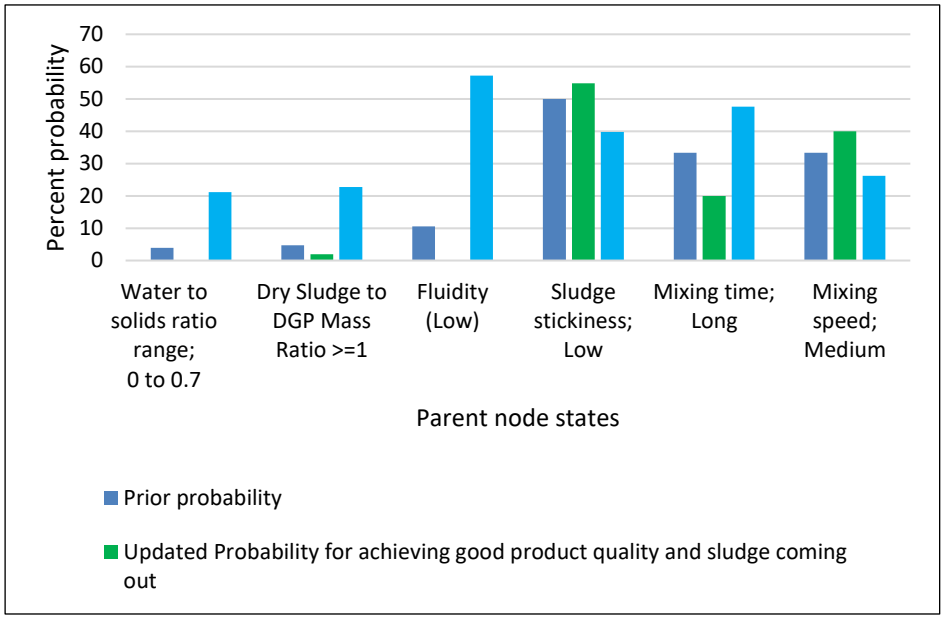

Figure 5-9: Comparison of updated probabilities of parent node states with Prior values

5.4.4 Conditions leading to an inability to remove the sludge and poor product quality

Having determined the conditions needed to meet the success criteria, it is also considered beneficial to identify the mixing parameter states at which the product fails to meet the desired requirements. Thus, by avoiding such conditions the risk of a rejected mix and a subsequent loss of operability time and resources could be reduced. These conditions can be determined by setting the product coming out and product quality nodes to 100% 'No' and 'Hard' states, respectively. The results of this updated BBN are presented in Figure 5-10.

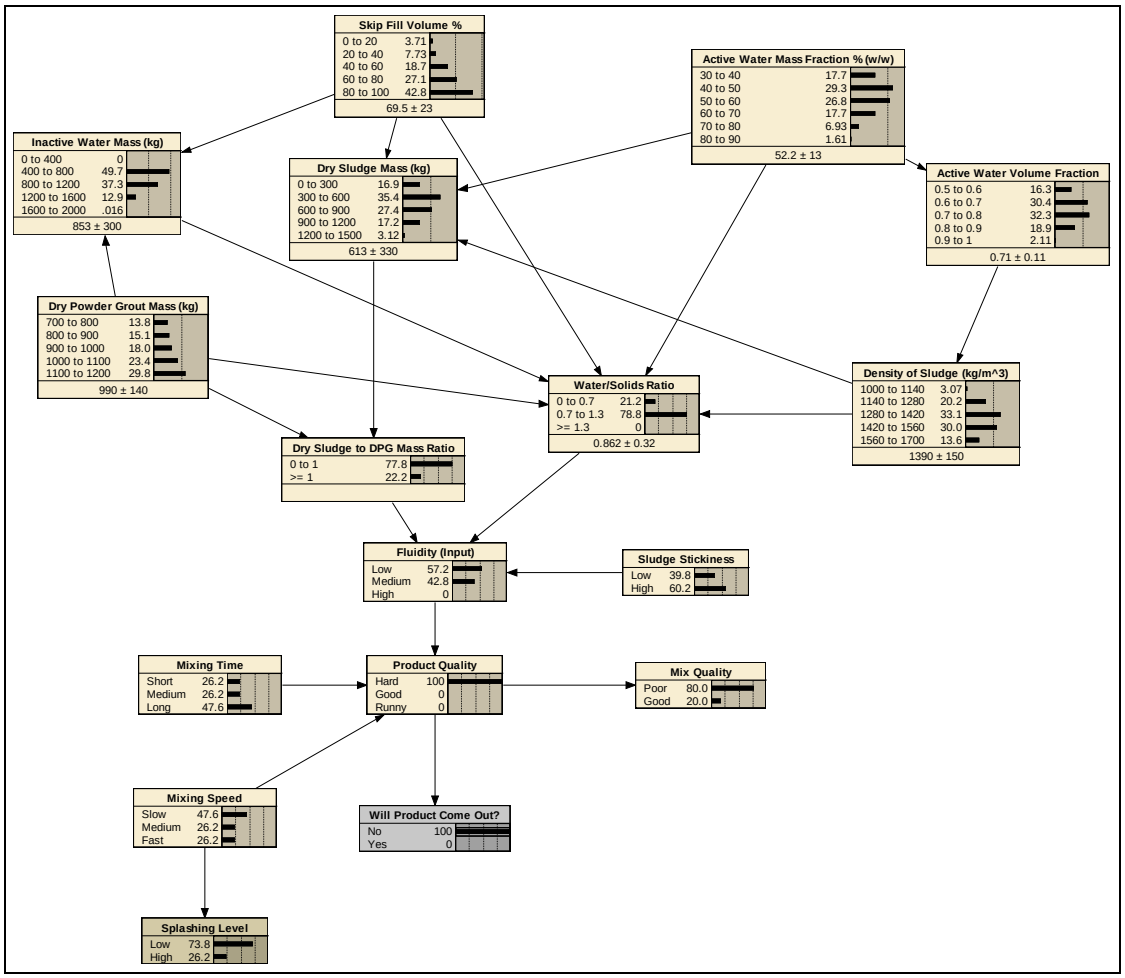

Figure 5-10: Conditions leading to an inability to remove the sludge and poor product quality

A comparison of the results in Figure 5-10 with the BBN based on Prior probabilities (Figure 5-3) can be carried out. This shows that the conditions leading to a failure to meet the mixing success criteria are that the probability of the water to solids ratio being in the low range of 0 to 0.7 would need to increase significantly from 4% to over 20%. Furthermore, the probability of the dry sludge to DPG mass ratio being in the high range of >=1 would need to increase from 4% to over 22%. These results relate to the product mix consisting of excessive solids and insufficient water. A further comparison in terms of the mixing and sludge stickiness parent node states with the Prior values leading to a product which fails to meet the criteria is also given in Figure 5-9. This is summarised as follows:

- The probability of mixing time being long, i.e., well above 75minutes, would need to increase from 33% to almost 50%.
- The probability of mixing speed being medium, i.e., below 12rpm, would need to decrease from 33% to 26%.

- The probability of sludge stickiness being low, i.e., which leads to an insignificant sludge adherence to vessel walls, would need to reduce from 50% to around 40%.

5.4.5 Derivation of optimum plant operating conditions

Sections 5.4.3 and 5. 4.4 have analysed the general trends in relation to product quality and sludge coming out based on the Prior probability values of the input parent nodes; skip fill volume, active water mass and dry powder grout mass. These parameters are likely to vary as part of the normal process. For a given mixing campaign, represented by a set of values for these three input parameters, the resulting effect on the Child nodes and the likelihood of a good quality product coming out can determined using the BBN updating feature. Hence, an optimum set of conditions required to achieve the success criteria for a given operational scenario can be determined.

Suppose an operational scenario requires processing of waste from a skip with a known skip fill volume of 50% and an active water mass fraction of 65 %. Accordingly, these two values were fixed using the Netica 'Findings' function and the effect on the product quality and sludge coming out nodes was determined for a variation in the values for DPG mass. This comparison is shown in Figure 5-11.

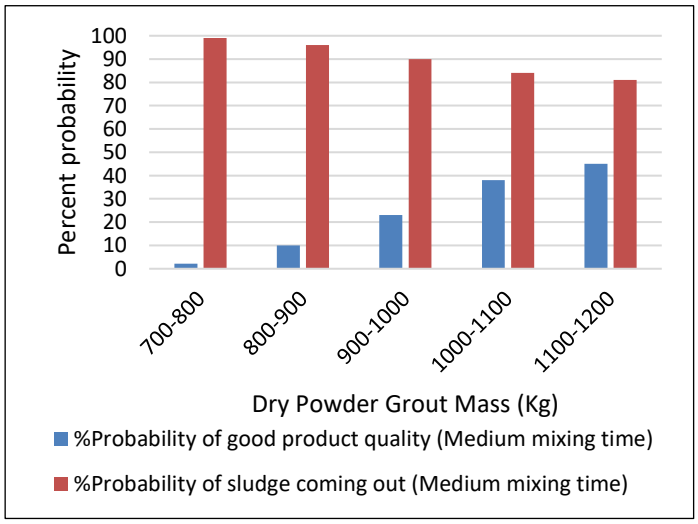

Figure 5-11: Effect of variation in DPG Mass (Skip Fill Volume = 50%, Active Water Mass Fraction = 65%)

It can be seen in Figure 5-11 that for a medium mixing time and low DPG mass values, the probability of the sludge coming out is very high, but the product quality is poor, owing to a runny mix. At a high DPG mass, there is a relatively small reduction in the probability of the sludge coming out but a substantial increase in the likelihood of achieving a good product quality. This result suggests that for medium mixing time the optimum DPG mass is 1100-1200Kg.

The effect of a variation on the mixing time was also tested for the same operational scenario as shown in Figure 5-12. For all DPG mass ranges, increasing the mixing time results in a lower probability of achieving the success criteria. This trend confirms that for an operational scenario requiring a skip fill volume of 50% and an active water mass fraction of 65%, the optimum ranges for DPG mass and mixing time are 1100 -1200Kg and medium, respectively.

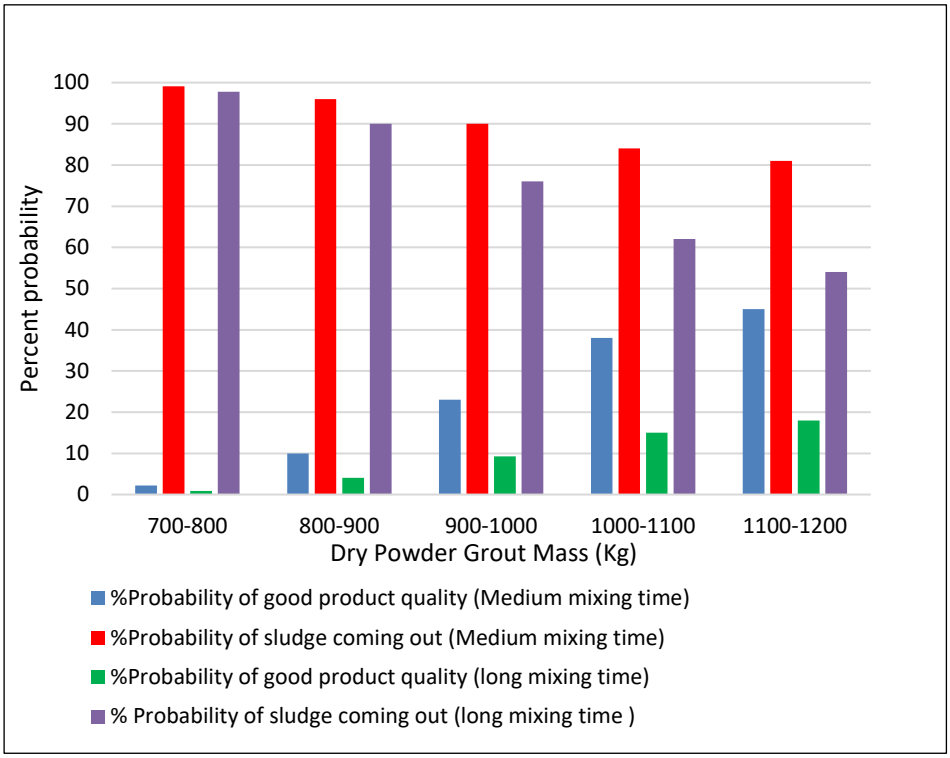

Figure 5-12: Effect of variation in DPG mass and mixing time (Skip Fill Volume = 50%, Active Water Mass Fraction = 65%)

Since sludge stickiness also affects the likelihood of a good quality product coming out of the vessel, the effect of a variation in this parameter was tested for the 50% skip fill volume and 65% active water mass fraction. This comparison is shown in Figure 5-13. It can be observed that provided the sludge stickiness is low, the optimum DGP mass range required to achieve the highest probability of a good quality product coming out of the vessel is still 1100-1200 kg.

In summary the analysis presented in Figure 5-11, Figure 5-12 and Figure 5-13 has determined the optimum conditions necessary for an operational scenario involving a skip fill volume of 50% and an active water mass fraction of 65%. The optimum conditions are a DGP mass range of 1100-1200 kg, a medium mixing time of around 75 minutes and low sludge stickiness.

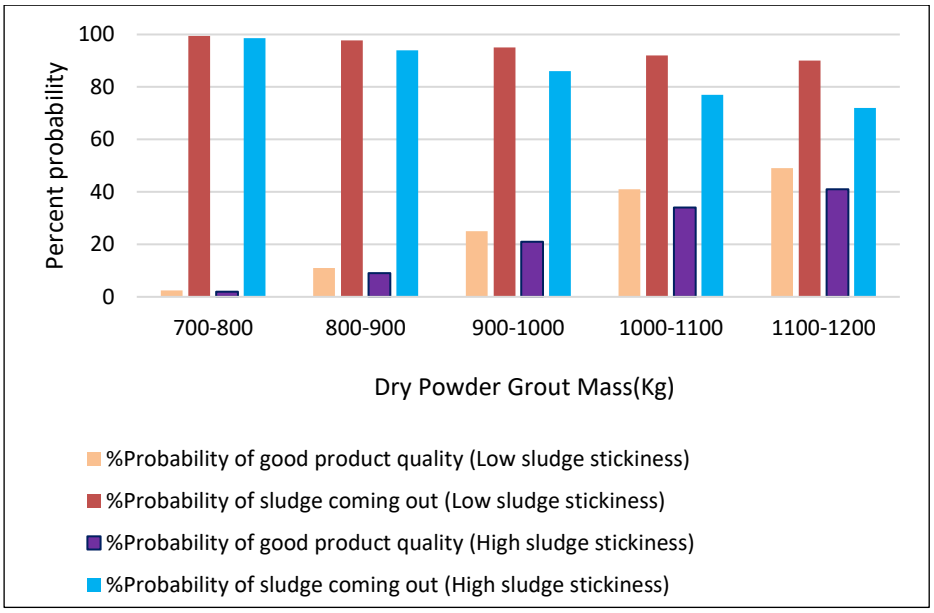

Figure 5-13: Effect of variation in DPG mass and stickiness (Skip Fill Volume = 50%, Active Water Mass Fraction = 65%)

5.5 Conclusions for Chapter 5

This case study has applied the BBN technique to explore the interactions between the radioactive sludge mixing parameters and the resultant uncertainty associated with the sludge behaviour. The overall aim was to identify an optimum set of operating conditions that enable removal of the sludge mix from the vessel while ensuring that the product quality is acceptable for downstream waste encapsulation.

The BBN analysis shows that the water to solids ratio of the sludge and cement grout formulation is a key parameter that affects sludge fluidity and hence the likelihood of the mixed sludge, with acceptable product quality, being removed from the vessel. Other parameters including mixing time and speed also affect product quality, however to a lesser extent.

The BBN model based on prior probability distributions of the key variables has shown that with an equal 50% chance of the water to solids ratio being in the mid (0.7 to 1.3) and high ranges (>=1.3), there is a high probability of 80% that the sludge will come out of the vessel. However, the likelihood of obtaining a good product quality under these conditions is still relatively low. It has been demonstrated that controlling just the water to solids ratio alone will not lead to both success criteria being met.

Using the BBN updating feature a sensitivity analysis has shown that the success criteria for obtaining a good quality product which can be removed from the vessel without significant adherence is that the water to solids ratio needs to be kept in the 0.7

to 1.3 region. Achieving the success criteria also requires a significant reduction in the mixing time such that the likelihood of operating the mixing vessel over a long duration, above 90 minutes, is relatively low.

A BBN sensitivity analysis has also been carried out to determine the operating conditions at which neither the sludge will be easily removed from the vessel nor a good quality product will be obtained. This would require a significant increase in the probability distributions of the water to solids ratio being in the low range of 0 to 0.7 and operating over a long mixing time.

A key insight obtained from the analysis for this case study is that the BBN provides a convenient method to represent the process and determine the optimum outcome. For example, the best outcome was determined in terms of the highest probability of a good quality product being removed from the mixing vessel for a given set of observed input conditions. This is a clear illustration of how the BBN uncertainty analysis technique can be used to optimise a plant and process, thus enabling operational decision making without the need for additional cost and time consuming experimental work.

CHAPTER 6 : CASE STUDY 3 - MONTE CARLO SIMULATION OF A FORCED VENTILATION SYSTEM FAILURE TO DILUTE RADIOLYTIC HYDROGEN IN THE ULLAGE SPACE OF A VESSEL AND COMPARISON WITH BAYESIAN NETWORK ANALYSIS

6.1 Introduction to Chapter 6

The continuous generation of hydrogen gas due to radiolysis of stored radioactive liquors in nuclear reprocessing plants is a well-known mechanism [*Ingram et al, 2001*]. The evolved hydrogen gas has the potential to accumulate in the storage vessel ullage space. For such processes, a typical hazard management strategy is to dilute the hydrogen in air atmosphere within the vessel. This is achieved using a forced ventilation system consisting of an air purge and an extract fan (Figure 6-1).

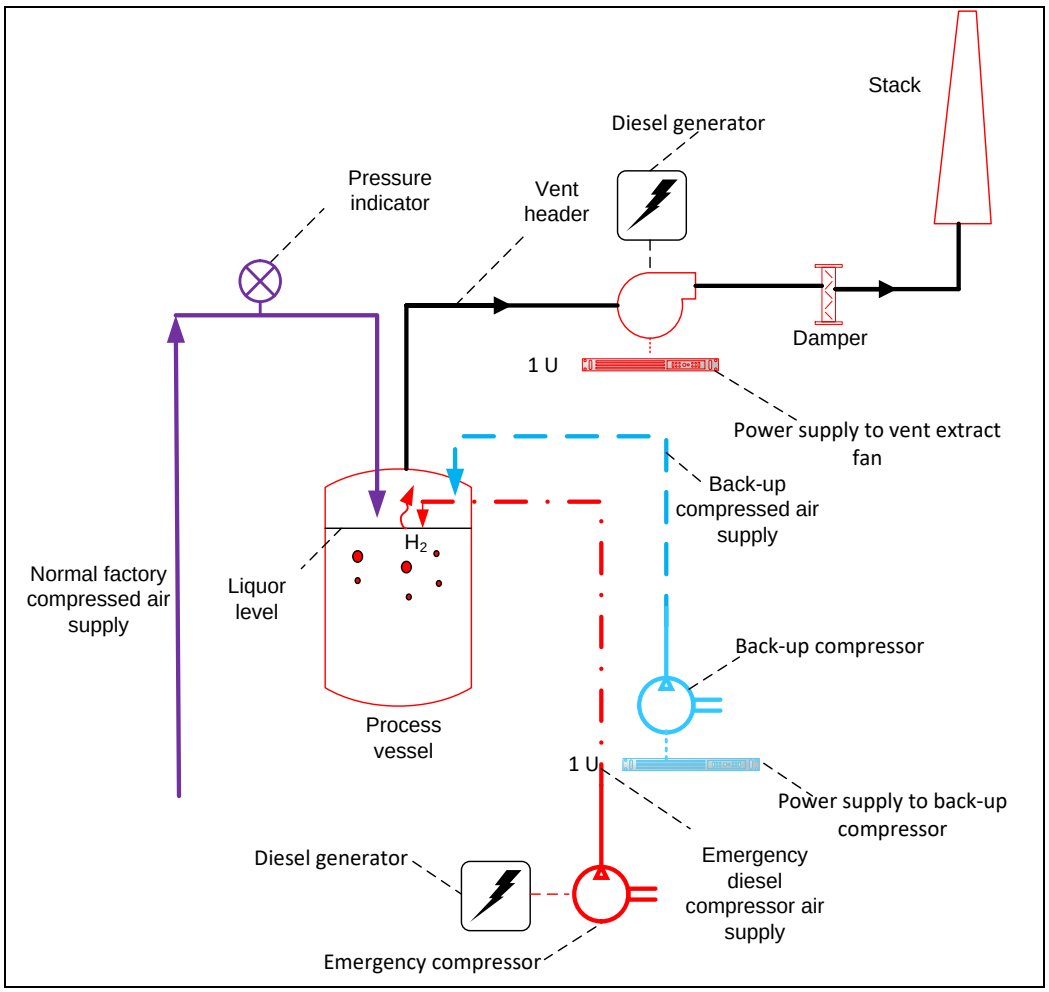

Figure 6-1: Ventilation extract system for removal of hydrogen from a process vessel [*Ahmed, 2019b*]

In the event of a failure of the forced ventilation system, the hydrogen in air concentration in the vessel ullage space will increase over time. This gives the potential for exceeding the 4% Lower Flammable Limit (LFL) or even the 8% limit for 'resilience'. As discussed in Chapter 2, Section 2.6, the term resilience relates to the robustness of process plants against extreme events such as hydrogen explosions, which is based

on the concept detailed by *Hollnagel and Yushi, 2013.* Section 2.6 discusses that given the age of the existing nuclear chemical plants, a hydrogen concentration above 8% could potentially lead to an explosion with damage to containment structures. For instance, in accordance with the Hydrogen Technical Guide, at such high concentrations, particularly in vessels or enclosures where the initial pressure is also above atmospheric, potentially a hydrogen explosion pressure as high as 10barg could be reached. This could be a concern for existing aged vessels which are not designed to withstand such overpressures, thus leading to a loss of containment. To demonstrate resilience against such an eventuality, reliable ventilation systems would be needed.

Exceeding the 4% or 8% hydrogen concentration limits is particularly relevant to fault scenarios which lead to the ventilation system remaining unavailable in vessels with high hydrogen generation rates. This case study applies the Monte Carlo (MC) Simulation method to a Fault Tree Analysis (FTA), as an enhanced means of assessing the uncertainty associated with the reliability of the forced ventilation system. This mapping of MC simulations on to a fault tree is based on the methodology discussed in Chapters 2 and 3 and illustrated in Figure 2-14. For comparison purposes, a Bayesian Belief Network analysis of the same model is also carried out.

6.2 Case Study objectives

As shown in Figure 6-1, the forced ventilation system comprises a diverse compressed purge air supply into the ullage space and an extract fan which provides the driving force for continuous removal of the hydrogen. Back-up and emergency compressed air supply systems are also provided to improve the reliability of the ventilation system. The case study model considers failures of each of these subsystems in order to determine the unavailability, i.e., overall failure probability, of the whole system. For this model, the MC simulation method is applied to the fault tree logic discussed in Section 6.3. Specific objectives of the case study are to:

i) Determine the uncertainty associated with key parameters affecting the ventilation system reliability.

ii) Determine the time required to repair the ventilation system following a failure.

iii) Compare the repair time distribution with the time taken to reach the 4% LFL and 8% limit for resilience.

iv) Use the results from objective iii to determine any improvements necessary to enhance the vent system reliability and hence reduce the risk of exceeding the 4% and 8% hydrogen concentration limits.

6.3 Failure logic for forced ventilation system

The methodology used for determination of the probability of failure of the forced ventilation system is to undertake an MC simulation of each of the primary events that lead to the Top Event. This yields a Probability Density Function (PDF) for the failure of each of the primary events. The PDFs are subsequently used in the MC simulation to determine the probability of the Top Event, i.e., failure to dilute the hydrogen in air atmosphere in the vessel ullage space.

The logic used for calculation of the Top Event probability in the MC simulation is based on an FTA of the same hypothesis, as presented in Figure 6-2. The FTA relies on the appropriate application of the Boolean AND and OR logic gates between the various events. A detailed description of each of the primary events listed in Figure 6-2, the failure logic and the Boolean gates used in this analysis is given in Appendix C, Table C-1. The probability values listed in the FTA are derived as detailed in Section 6.6 and Appendix C, Table C-2.

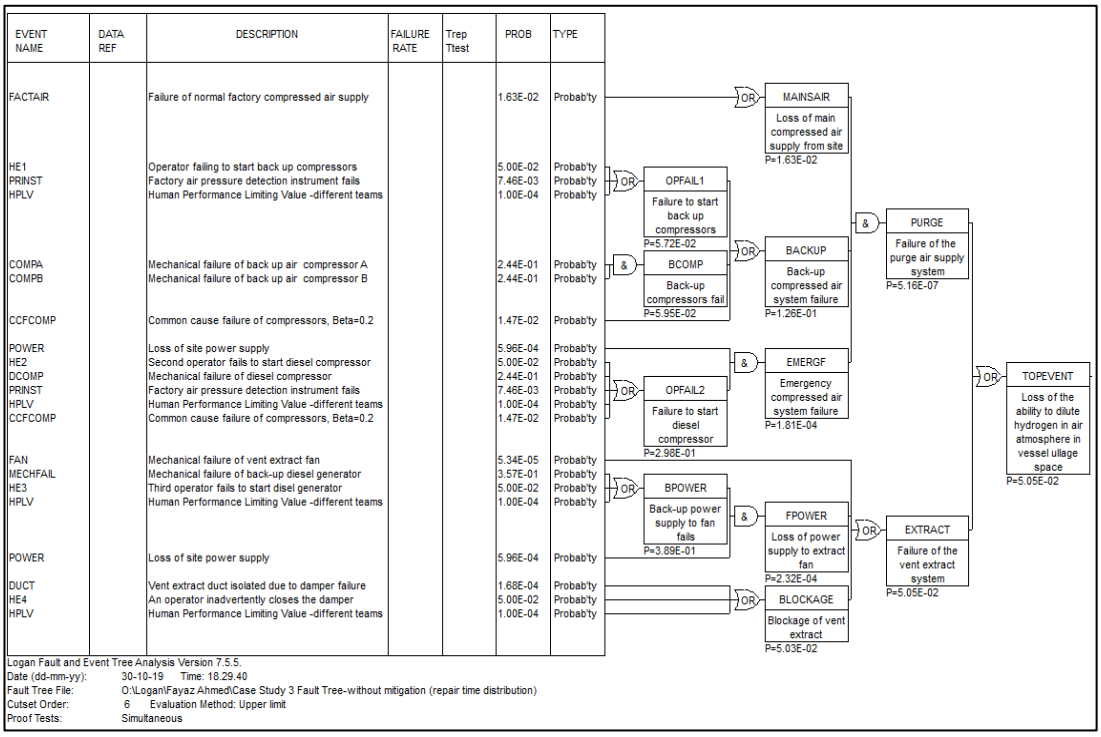

Figure 6-2: Fault Tree Analysis of the process vessel forced ventilation system

6.4 Monte Carlo Simulation of the likelihood of ventilation system failure

6.4.1 Analysis of equipment failure probability data

For the MC simulation, the probabilities of failure of each of the events given in Figure 6-2 requires prediction. This is achieved based on the following concepts of equipment reliability, which are discussed in more detail in Chapter 2.

For revealed failures of repairable plant items, i.e. vent extract fan, power supply system and the vent duct damper, the failure probability P(t) is given by equation 2-11 from Chapter 2.

$$P(t) = 1 - e^{-\lambda t} \quad (2\text{-}11)$$

Where P(t) is the probability of failure within a time period t and λ is the failure rate, per year.

For plant items which are in standby mode i.e. back up air compressors, air pressure alarm and diesel generators, their failures are only revealed following a proof test. For such unrevealed events, the failure probability is given by equation 2-10 discussed in Chapter 2.

$$P = 1 - \left(\frac{1 - e^{-\lambda_s T_s}}{\lambda_s T_s}\right) \quad (2\text{-}10)$$

Where λ_s is the failure rate per year of the standby equipment and T_s is the proof test interval, typically yearly.

The failure probabilities of each of the events were predicted using equations 2-10 and 2-11 in Appendix C, Table C-2. This is based on the failure rate data for each of the primary events listed in Figure 6-2. The failure rate data are obtained from the International Atomic Energy Agency (IAEA) database for nuclear applications [*IAEA, 1997*]

6.4.2 Modelling of common cause failures and human error probabilities

For plant items consisting of multiple components, such as the compressed air system comprising compressors A and B, a potential dependability exists between the components. In other words, a common root cause due to identical design, manufacturer or location on plant, could lead to a failure of both components. In reliability engineering such dependent failures are referred to as 'Common Cause Failures' (CCFs). Cross multiplication of these failures in an FTA, via the AND logic gate, can often lead to an unrealistically low probability which must be avoided. This is achieved through appropriate modelling of CCFs for multiple components. The most widely used approach for modelling of CCFs is the Beta Factor method, detailed by *Summers et al, 1999* and *Lees, 1992.*

Similar to the dependent failures of plant components, when multiple operating teams lead to more than one operator error, the cross multiplication of different human error probabilities can lead to a misleadingly low unavailability value. In order to limit the effects of such cross multiplication to a realistic value in practice, the human error

assessment methodology by *Kirwan et al, 2008* suggests the use of a Human Performance Limiting Value (HPLV).

As shown in the failure logic diagram (Figure 6-2), the reliability of the forced ventilation system also models dependent failures of multiple plant items and operators performing the same function. Appendix C, Table C-3 provides a justification of the Common Cause Failures (CCF), the human error probabilities (HEP) and HPLVs associated with the forced ventilation system failure (Figure 6-2).

6.4.3 Derivation of primary event probability distributions

The MC simulation uncertainty analysis relies on the application of appropriate probability distributions of the primary events. The justification for the choice of the distributions for the various items listed in Figure 6-2 is given below.

Vesley et al, 1981 considers that mechanical plant items which are susceptible to wear, i.e., vent fan, vent duct dampers, diesel generator and mechanical plant components associated with power supplies, their failure probability distribution is reasonably close to the Normal Gaussian Distribution. Furthermore, this distribution is also advantageous in terms of modelling variability. The concept of the Central Limit Theorem states that the sum of many identically distributed random variables, each with a finite mean and variance, is normally distributed. Given that the identified mean failure rates from *IAEA, 1997* could potentially be based on large sample sizes, the application of the Normal Distribution is considered prudent in this analysis.

The primary event failure rates obtained from *IAEA, 1997* are based on mean values. For the Normal Distribution, a low Standard Deviation relative to the mean has been used assuming that there is a high level of confidence in the mean failure rate data. This assumption is on the grounds that the mean failure rate data given by *IAEA, 1997* are based on many years of operational experience which would imply that the data are reliable.

In accordance with *RiskAmp 2007*, the Triangular distribution is applied to parameters with a known range. The operator error probabilities discussed in Appendix C Table C-3 are based on known ranges, hence a Triangular distribution is considered the most appropriate for these events.

Based on the primary event distributions discussed above and using the mean failure rates from Appendix C Table C-2, Appendix C Table C-4 derives the revealed and unrevealed failure probability distributions for each of the vent plant items. The operator error probability distributions and the CCFs for plant items are derived in Table C-5.

6.5 Monte Carlo simulation results

Based on the data derived in Appendix C, Table C-4 and Table C-5, using RiskAmp software [*RiskAmp, 2007*], MC simulations were performed on the Top Event, i.e. the probability of failure of the forced ventilation system. Multiple MC simulations with 10000, 100000 and 1000000 trials were undertaken to determine the sensitivity of the Top Event with increasing number of trials. For each trial the MC simulation utilised failure probabilities from the primary event distributions, P_1 to P_{18} which are derived in Table C-4 and Table C-5. These distributions were then applied to the calculation in the MC simulation, in accordance with the AND and OR gates logic shown in Figure 6-2.

The fault tree equations used in the MC simulation for each of the secondary events and the Top Event as well as the associated probabilities calculated by RiskAmp are summarised in Appendix C Table C-6. The equations listed in Table C-6 are based on the AND and OR logic, utilising the failure probabilities from Table C-4 and Table C-5 for each of the primary events denoted by identifiers P_1 to P_{18}.

6.5.1 Analysis of results from MC Simulation with 1000 trials

By repeating the MC simulation based on 10000, 100,000 and 1000,000 trials, the output from the analysis was a probability distribution of the Top Event. The results from these simulations are summarised in Table 6-1. The probability distribution of the Top Event entails the peak probability and the 95% and 5% values. These 95% and 5% values represent the upper and lower extremes of the Top Event probability distribution, respectively.

Number of simulations	Peak probability of vent failure	95% level probability of vent failure	5% level probability of vent failure
10000	5.60E-02	8.57E-02	2.33E-02
100,000	5.50E-02	8.58E-02	2.41E-02
1000,000	5.50E-02	8.56E-02	2.40E-02

Table 6-1: Statistical summary of MC simulation for vent failure probability

For 100,000 and 1000,000 runs, Table 6-1 shows that the peak failure probability is 5.5E-2 in both cases. However, there is a slight variation in the values for the 95% and 5% levels. For the smaller number of simulations, i.e., 10,000, the variation in the peak, 95% and 5% failure probabilities is slightly greater. In this analysis no significant

difference has been observed in the results for the 10,000 and higher number of simulations. However, research in the field of statistics by *Marco, 2021,* indicates that generally the MC simulation output is improved, particularly for complex systems, if the number of iterations is a minimum of 100,000 but preferably higher. Hence based on the results from 1000,000 simulation runs, it is concluded that the forced vent failure probability range is 2.4E-02 to 8.6E-02 at 5% and 95% levels, respectively. The peak failure probability is 5.50E-02.

In terms of the MC simulation output of failure probabilities of secondary events in RiskAmp, the general trend is that the Top Event probability is dominated by the vent extract failure (event EXTRACT) with a mean failure probability of 3.9E-2. In comparison faults leading to failure of the purge air system (event PURGE), with a mean probability of 5E-7, result in a relatively minor contribution to the occurrence of the Top Event. A further trend observed from the output in RiskAmp is that the event which dominates the failure probability of event EXTRACT is blockage of the vent duct (event BLOCKAGE). Thus, if the likelihood of vent duct blockage can be reduced, the overall Top Event failure probability would decrease proportionally.

6.6 Comparison of MC simulation results with Fault Tree Analysis

A standalone Fault Tree Analysis for the Top Event, without the MC simulation, was also undertaken to determine any differences in the results from the two methods. The standalone FTA is presented in Figure 6-2.

The FTA software LOGAN [*Logan, 2018*] provides the capability of modelling single values as well as distributions of the primary events hence enabling an uncertainty analysis. The failure probabilities of each of the primary events modelled in Figure 6-2 are based on the mean failure rates given in Appendix C Table C-2 and the most likely human error probabilities given in Table C-3. The purpose of the FTA in Figure 6-2 was to determine how the performance of MC simulation using RiskAmp (Table 6-1) compares with the analysis based on single values.

The FTA and MC with 1000,000 runs results for the vent system failure probability are 5.05E-2 and 8.56E-02 respectively. The reason for the slightly lower Top Event probability predicted by the FTA with mean values is that this model uses a lower fixed probability of 0.05 for the human error probability HE4 which dominates the vent duct blockage event. In comparison, the MC simulation uses a Triangular distribution for event HE4 with maximum and minimum values of 0.1 and 0.01, respectively. Thus, by accounting for the maximum possible human error probability, the MC simulation has

enabled a more realistic analysis of the Top Event. Hence an underestimate of the risk due to averaging has been avoided.

The validity of the MC simulation output from RiskAmp Table 6-1) was also compared with the MC analysis of the FTA model using LOGAN. Based on the Normal and Triangular distributions of the primary events given in Table C-4 and Table C-5, Figure 6-3 illustrates the output of the MC simulation with 1000,000 runs using LOGAN.

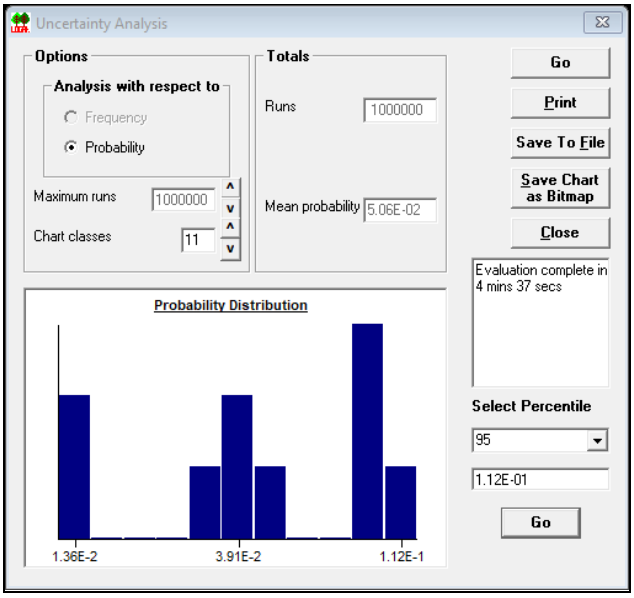

Figure 6-3: MC simulation of forced ventilation system failure probability using LOGAN

In the LOGAN MC simulation model, the results are displayed as a mean probability of the Top Event, i.e., 5.06E-2 and a histogram of the probability distribution which ranges from 1.4E-2 to 1.1E-1. In comparison, the RiskAmp MC simulation with 1000,000 runs gives the Top Event peak probability of 5.50E-02, with the 5% and 95% percentile values of 2.40E-02 and 8.56E-02 respectively (Table 6-1).

Whilst the simulation results from RiskAmp and LOGAN are broadly similar, the minor differences are attributed to the way in which the repair time for revealed failures is modelled in the two software systems. There is a limitation in LOGAN as it does not provide the ability to model repair time as a distribution. Instead, it assigns a single value for the repair time. A further explanation for the minor differences between LOGAN and RiskAmp MC simulation results is the way in which the Triangular Distribution is modelled. The Triangular distribution modelled in RiskAmp is based on the minimum, most likely and maximum values, whereas LOGAN uses the mean and the range.

6.7 MC simulation with additional mitigation for the forced ventilation system

6.7.1 Identification of additional mitigation measures

The peak Top Event probability determined by the MC simulation in RiskAmp is 5.5E-2 with the maximum and minimum values of 8.6E-2 and 2.4E-2 at 95% and 5% levels respectively. As the peak probability is approaching 0.1, from a risk perspective this could be classed as a high likelihood of occurrence. This would indicate that additional mitigation is needed to reduce the risk. The MC simulation, as well as the standalone FTA results show that the extract duct blockage is the dominant failure. Therefore, if the onset of occurrence of this event can be detected and corrective action undertaken, a reduction in the Top Event probability could be achieved. The extract failure probability could also be reduced through an improvement to the extract fan power supply by introducing an additional diesel generator. Accordingly, the standalone fault tree was expanded with these additional measures. An explanation of the failure logic based on these additional mitigating measures is given in Appendix C Table C-7.

Appendix C Table C-3, Table C-4, and Table C-5 provide the details on the derivation of the failure probabilities of the primary events associated with the additional mitigation. On this basis, Figure 6-4 presents the standalone FTA for the forced vent system with additional mitigation.

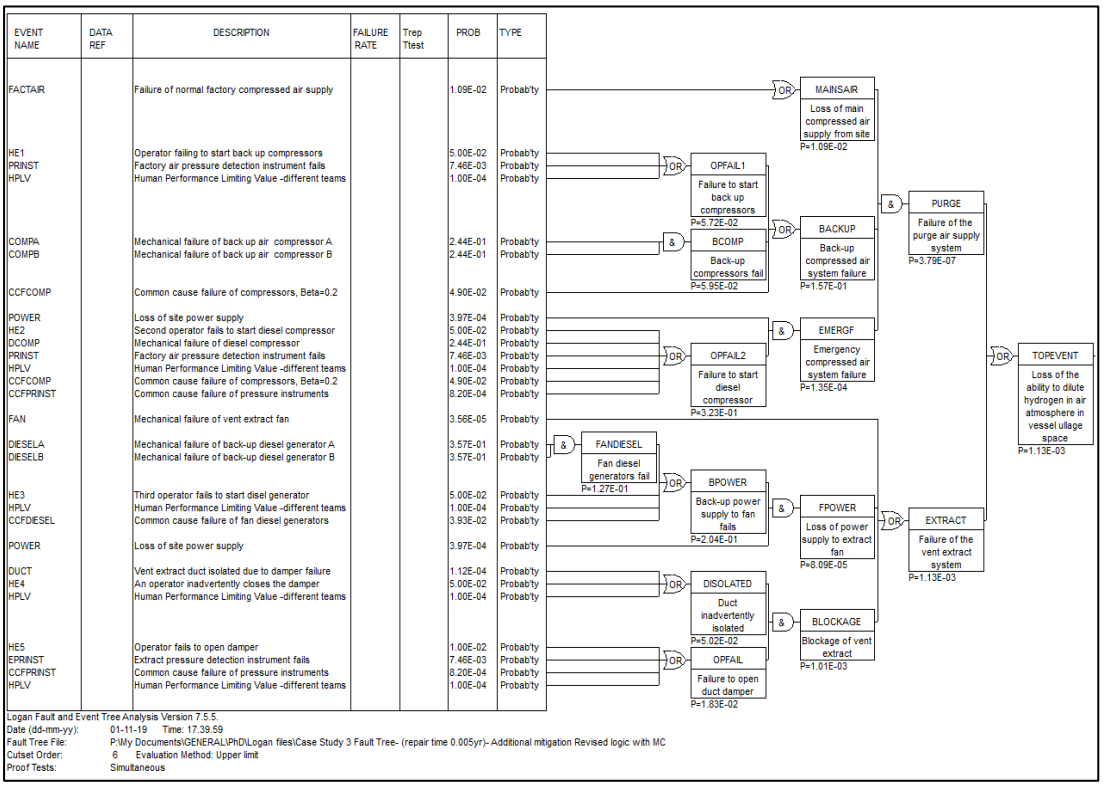

Figure 6-4: Expanded fault tree analysis of forced ventilation system failure with additional mitigation

The standalone FTA in Figure 6-4 shows that by introducing the additional mitigation, the failure probability of the extract (event EXTRACT), reduces to 1E-3. Hence, in comparison with the original model in Figure 6-2, a reduction in the extract failure probability by over an order of magnitude has been achieved. The decrease in EXTRACT failure probability has occurred because of the additional operator failure (event OPFAIL) that now has to take place before the duct blockage can occur.

6.7.2 Analysis of results from MC simulation with 1000000 trials

For the vent system with additional mitigation, an MC simulation with 1000,000 trials was carried out to determine the Top Event failure probability. The results were compared with the standalone FTA (Figure 6-4). The fault tree equations used in the MC simulation for each of the secondary events and the Top Event, taking account of additional mitigation, are summarised in Appendix C, Table C-7.

6.7.3 Analysis of results from RiskAmp MC simulation with 1000000 trials

Using the equations for derivation of the failure probability distributions of the secondary events given in Appendix C Table C-7, Figure 6-5 presents the results of MC simulation in RiskAmp for the forced ventilation system failure probability based on 1000000 runs. With additional mitigation, the peak failure probability is now 2E-3 at a PDF of 19.5%. The associated maximum and minimum failure probabilities of the vent system at 95% and 5% percentile levels are 5.6E-3 and 7.8E-4, respectively.

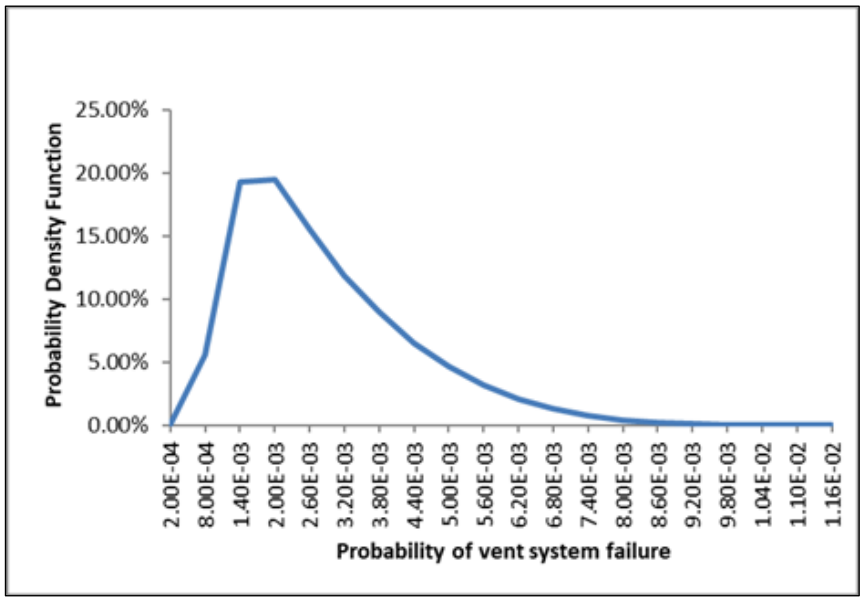

Figure 6-5: MC simulation for failure probability of vent system with additional mitigation

In comparison with the standalone FTA for the same model (Figure 6-4), the MC simulation has also resulted in a reduction of the Top Event peak probability. This

demonstrates that the additional mitigation has resulted in an improvement on the availability of the vent system. However, similar to the previous model presented in Figure 6-2 and Table 6-1, the Top Event failure probability with MC simulation is slightly higher than the probability in the standalone FTA. This is due to the Top Event probability being dominated by the secondary event BLOCKAGE, which is primarily affected by the human error probabilities, HE4 and HE5. Both human errors are based on a Triangular distribution that allows for the maximum probability of 0.1. The standalone FTA is however based on the most likely human error probabilities, thus resulting in a slightly lower value of the Top Event probability.

An MC simulation of the ventilation system failure probability with additional mitigation based on 1000000 runs was also undertaken in LOGAN, which is presented in Figure 6-6. The results show that the mean, 95%, and 5% level probabilities are 1.1E-3, 6E-3 and 1.15E-4 respectively. The mean and 95% level probabilities based on RiskAmp and LOGAN are broadly the same. However, the difference in the 5% level values of 7.8E-4 and 1.1E-4 is possibly attributed to the revealed failure probabilities being limited to single values of repair time in LOGAN. RiskAmp, on the other hand, provides the ability to model the repair time as a distribution.

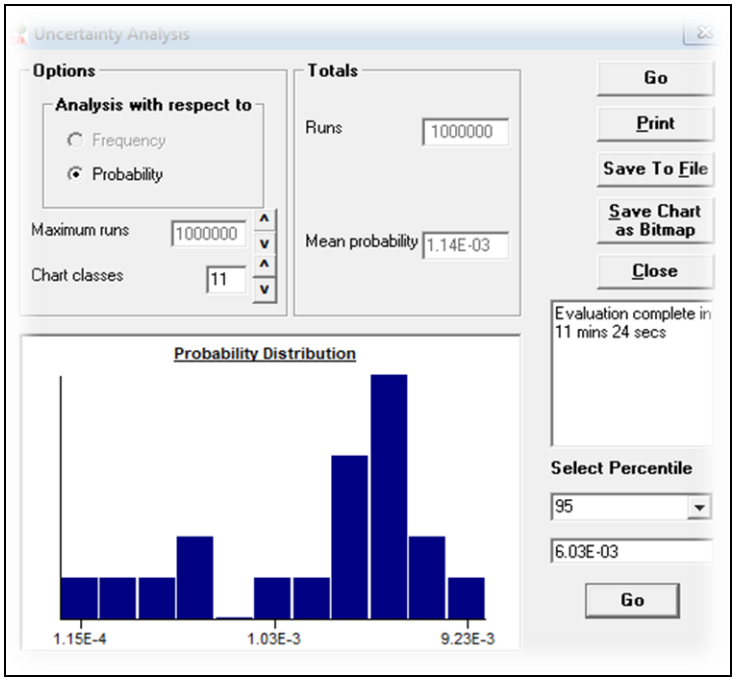

Figure 6-6: MC simulation in LOGAN with 1000,000 runs for failure of vent system with additional mitigation

The RiskAmp MC simulation and the standalone FTA results based on additional mitigation are in agreement when comparing the order of failure probabilities of the secondary events. For example, the RiskAmp MC simulation results show that a loss

of power to the fan (FPOWER) and duct blockage (BLOCKAGE) are still the dominant secondary events. Whilst the addition of the second diesel generator for the fan backup power supply has resulted in a reduction in the FPOWER probability in both models, the common cause failure of the diesel generators has resulted in only a slight net reduction of this probability. The introduction of the additional mitigation has enabled a significant reduction in the duct blockage and hence the extract failure probability, which is evident in both the FTA and MC simulation. Hence it is clear that the additional mitigation has enabled an improvement in the availability of the forced ventilation system.

6.8 Comparison of FTA and MC simulation results with Bayesian Belief Network Analysis

As discussed in Chapter 3, one of the main features of the Bayesian Belief Network methodology is that it recognises Boolean algebra. Similar to a Fault Tree Analysis, it also enables modelling of failure modes using the AND and OR logic gates. Hence using the failure logic for the forced ventilation system as detailed in Section 6.3, a standalone Bayesian Belief Network (BBN) analysis was also undertaken for the same model. The purpose of the BBN analysis was to determine how the performance of this methodology compares with FTA and MC simulation and whether it provides any additional benefits. Based on the same primary event failure probabilities as those derived for the standalone FTA, Figure 6-7 presents the quantified BBN for a failure of the vent system, without the additional mitigation.

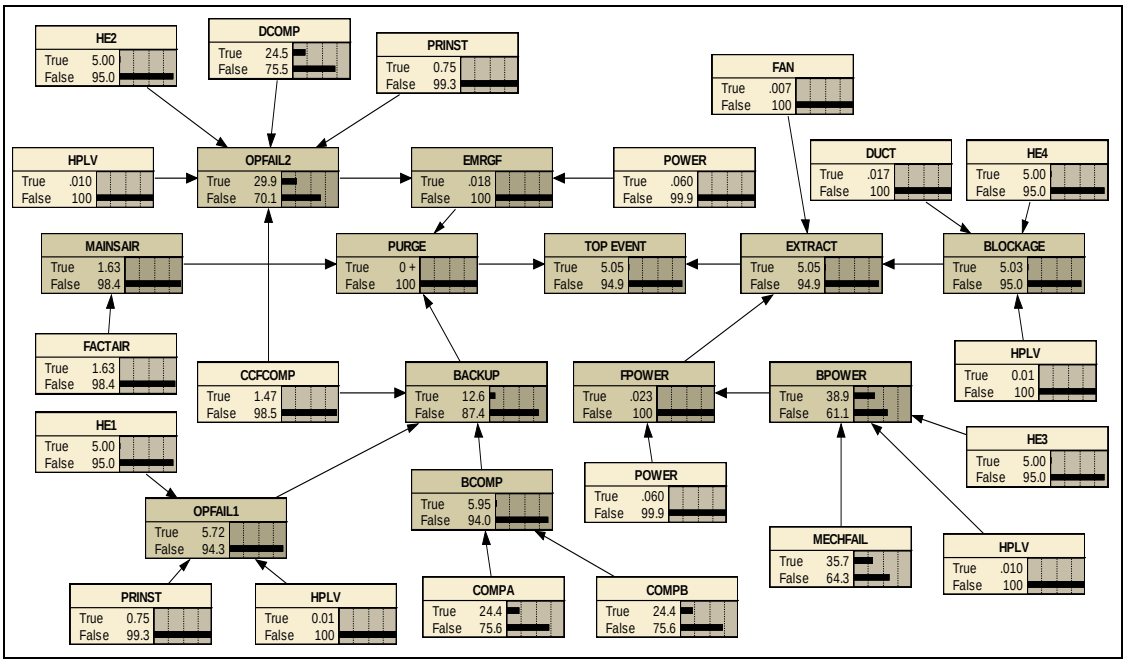

Figure 6-7: Bayesian Belief Network analysis of forced ventilation system failure

6.8.1 Comparison with standalone FTA

Figure 6-7 shows that the Top Event, i.e., forced ventilation system failure probability is 5.05E-2, noting that all numerical probability values stated this BBN are percentages. This result is the same as for the standalone FTA presented in Figure 6-2. A further agreement between the two models is that the Top Event probability is dominated by the vent extract failure (secondary event EXTRACT) with a failure probability of 5.05E-2. The contribution by the purge system failure is insignificant. This confirms that the logic used in the BBN is consistent with the FTA and MC simulation.

One of the distinct features of the Bayesian Network methodology is that it is able to determine the maximum posterior probability of a set of variables based on the evidence obtained for the remaining nodes. In other words, the 'Most Probable Explanation' (MPE) of the observed hypothesis can be determined [*Kwisthout, 2011*]. The MPE functionality identifies the key sensitivities for the occurrence of the Top Event by identifying all 'true' states in the BBN which are either at a 100% or close to this value. Effectively the larger the true state MPE probability, the greater is the sensitivity on the occurrence of the Top Event. In order to identify the key sensitivities affecting the Top Event, i.e., failure of the forced ventilations system, the Bayesian Network in Figure 6-7 was updated, with a value of 100% using the Netica 'Findings' function. Subsequently the MPE function in Netica was activated to yield the most probable configuration. The results of the updated BBN are given in Figure 6-8. It can be seen that the events which yield an MPE probability of 100% are EXTRACT and BLOCKAGE, which are the dominant factors affecting the Top Event probability.

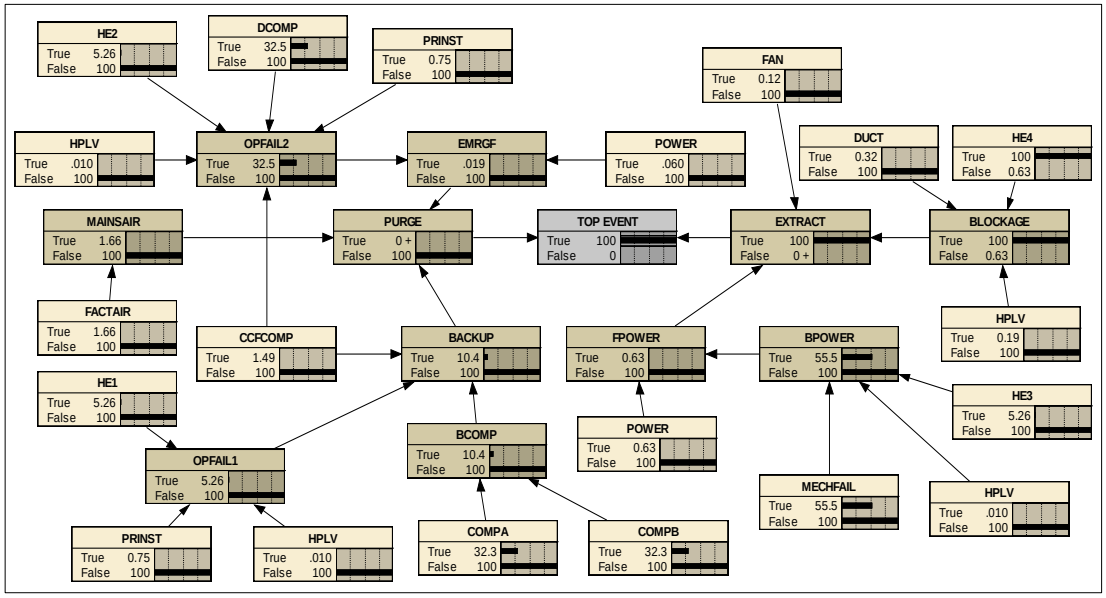

Figure 6-8: Updated BBN for ventilation system failure with Most Probable Explanation (MPE)

6.9 Analysis of hydrogen concentration in the ullage space following vent system failure

6.9.1 Identification of vessels exceeding the hydrogen Lower Flammability Limit

The normal operational limit for hydrogen concentration in the ullage space of a vessel in nuclear chemical plants is 25% of the 4% Lower Flammability Limit, i.e., 1%. The LFL is adopted as a limit for assessment against fault conditions. Plant resilience is often assessed against a hydrogen concentration limit of 8%. This section uses the MC simulation method to determine likelihood of exceeding each of these concentration limits following a failure or unavailability of the forced ventilation system. Upon introduction of the purge air to the vessel, the objective is to ensure that the equilibrium hydrogen concentration, C_{eq} (%v/v) in the ullage space is always below the 1% and 4% limits. The equilibrium hydrogen in air concentration as a function of radiolytic hydrogen generation rate, Q_H, and purge air flow rate, Q_{air}, can be determined using equation 6-1:

$$C_{eq} = \frac{100 \times Q_H}{Q_H + Q_{air}} \quad (6\text{-}1)$$

Hence a high Q_{air} value will ensure that a low equilibrium concentration is achieved. Reprocessing process plant operation experience suggests that the radiolytic hydrogen generation rate ranges from very low values of 0.0527 L/hr to a maximum of 30.6 L/hr. The high hydrogen generation rates from 10 to 30.6L/hr arise in storage vessels with large quantities of radioactive liquor, typically above $10m^3$ with ullage space volumes of up to 15000L.

For smaller vessels, the hydrogen generation rate is typically 3L/hr and the ullage space volume is approximately 7400L. The normal hydrogen hazard management strategy generally for vessels of this size is to control the purge air flow rate such that the C_{eq} value is approximately 0.1%v/v. Based on the Hydrogen Technical Guide, in the event of a failure of the purge air supply, the time, t, to reinstate the purge air before a concentration X% v/v is reached in an ullage space volume, U, can be calculated using equation 6-2.

$$t = \left(\frac{U}{Q_H}\right) \ln\left(\frac{100 - C_{eq}}{100 - X}\right) \quad (6\text{-}2)$$

Using equation 6-2 with X set to 4%v/v, radiolytic hydrogen generation rates of 3 to 30.6L/hr for medium to large vessels and C_{eq} values of 0.17 %v/v, Table 6-2 shows the associated time taken for the hydrogen concentration in the vessel to reach the 4% LFL.

Radiolytic hydrogen generation Q(L/hr)	Equilibrium hydrogen concentration (%/v/v) Ceq	Ullage space volume, U (L)	Time taken to reach LFL, t (hr)
30.6	0.17	15000	19.2
12.23	0.17	15000	48.0
10.7	0.17	15000	54.8
3	0.17	7400	96.5

Table 6-2: Calculation of time taken to reach the LFL with varying hydrogen generation rates

Table 6-2 shows that for large vessels with the ullage volume of 15000L, the longest time taken to reach the LFL is 54.8 hours, i.e., just over 2 days. This is based on a hydrogen generation rate of 10.7L/hr. In medium sized vessels with a typical hydrogen generation rate of 3L/hr the time taken to reach the LFL is 96.5 hours, i.e., almost 4 days. Based on the probability distribution of equipment repair times derived in section 6.9.3, it is considered that equipment repairs can normally be undertaken within a period of less than 2 days. On this basis, it is considered that the potential for unavailability of the ventilation system leading to a hydrogen concentration exceeding the 4%LFL arises only in large vessels with hydrogen generation rates greater than 10L/hr. Hence this case study uses hydrogen generation rates of 10 to 30.6 L/hr as the bounding basis.

6.9.2 MC simulation of the time taken to reach the hydrogen concentration limits

From the data given in Table 6-2 , it is known that the hydrogen generation rate in most of the large vessels is 12.23 L/hr. The hydrogen generation rate of 10.7L/hr arises in only a small number of the vessels. Given that the range of the hydrogen generation rates is also known, i.e. 10.7-30.6 L/hr, it is considered that the associated probability distribution, and hence the time taken to reach the LFL, is best represented by a Triangular distribution. Therefore, based on Table 6-2, the MC simulation for the likelihood of exceeding any given hydrogen concentration uses the hydrogen generation rates of 10.7, 12.23 and 30.6L/hr as the least likely, most likely, and maximum values, respectively. Using the Triangular distribution of hydrogen generation rates given in Table 6-3, the distributions of the time taken to reach the 4% and 8% hydrogen concentration limits were determined by RiskAmp using equation 6-2.

Least Likely hydrogen generation rate, L/hr	Most Likely hydrogen generation rate, L/hr	Maximum Hydrogen generation rate, L/hr	Distribution of hydrogen generation rate, L/hr
10.7	12.23	30.6	Triangular Value (10.7, 12.23, 30.6)

Table 6-3: Distribution of the hydrogen generation rates in process vessels

An MC simulation with 100,000 trials (Figure 6-9) shows that the time taken to reach the 4% hydrogen concentration (LFL) peaks at 29 hours with a PDF of 8%. The associated 95% and 5% level values for the time taken to reach the LFL are 49.2hours and 22.3 hours, respectively. Figure 6-9 also presents the MC simulation results, based on 100,000 trials, for the time taken to reach the 8% hydrogen concentration limit for plant resilience. In this case, the time peaks at 64 hours with the associated 95% and 5% levels of 102.8 hours and 46.5 hours, respectively.

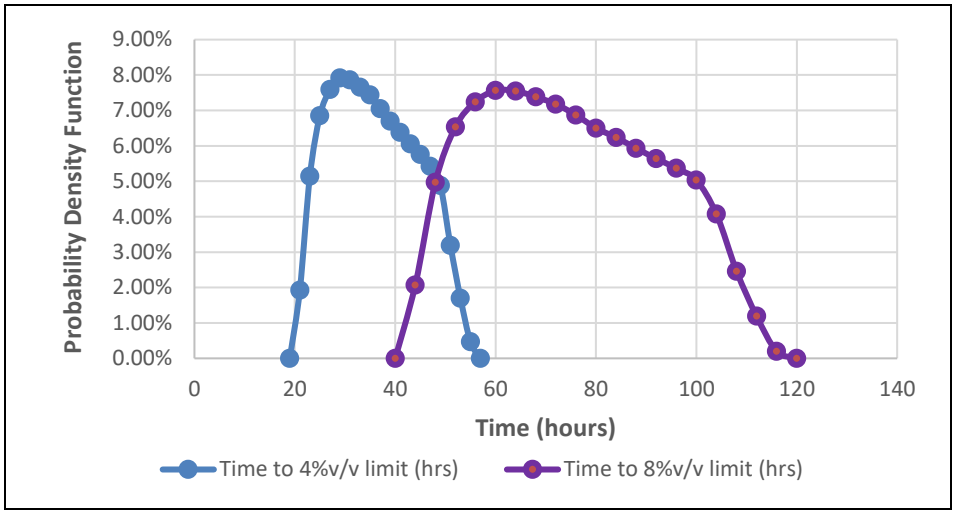

Figure 6-9: MC simulation results for the time taken to reach the 4% and 8% hydrogen concentration limits

6.9.3 MC simulation of the time taken to repair the forced ventilation system

To determine how likely it is for each of the hydrogen concentration limits of 4% and 8% to be exceeded following vent failure, the probability distribution of the time taken to repair the system requires prediction. A comparison of the distribution of the time taken to reach each of the two concentration limits with the distribution of the time taken to repair the system is then undertaken.

The results of the FTA with MC simulation for the likelihood of failure of the forced ventilation, in Section 6.7, show that the Top Event is mainly affected by duct blockage or loss of power. Taking into consideration the additional mitigation, both events are highly revealed. Furthermore, given that equipment spare parts, e.g., additional mobile

diesel generators will be readily available, the most likely repair time for reinstating the duct and the power supply is 24 hours. However, it is considered highly unlikely that these systems could be reinstated in less than a day. Hence a least likely time of 12 hours is considered. To allow for any unforeseen circumstances, i.e., in the unlikely event that the spares for plant repairs are not available, a maximum repair time of 48 hours is possible.

For the model without the additional mitigation for detecting the duct blockage, it is considered that the minimum, most likely and maximum response times would be at least half a day longer due to the added time taken to diagnose the fault. Hence a repair time distribution of 24, 36 and 60 hours as the minimum, most likely and maximum values is considered appropriate.

Since the most likely, least likely and maximum repair times have been estimated based on operational experience, it is considered that the repair time probability distribution is best represented by a Triangular distribution. Applying the Triangular distribution functions 'Triangular Value (24,36,60)' and 'Triangular Value (12,24,48)' for the unmitigated and mitigated cases respectively, an MC simulation with 100,000 trials was carried out using RiskAmp. The resulting distributions for the mitigated and unmitigated cases are presented in Figure 6-10 and Figure 6-11, respectively. These graphs also provide a comparison of the repair time distribution with distributions for the time taken to reach the 4% and 8% hydrogen concentration limits.

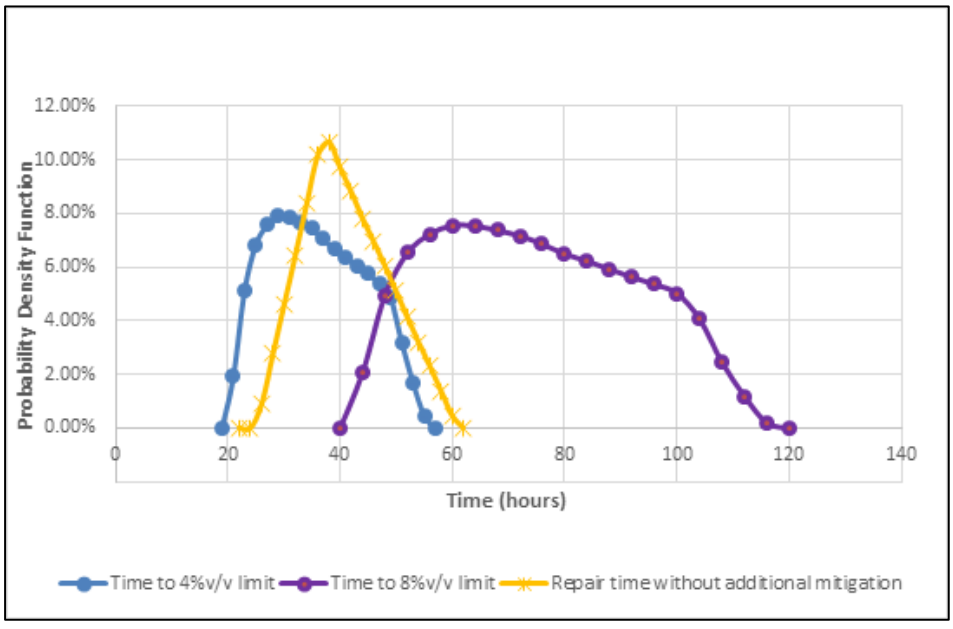

Figure 6-10: Comparison of MC simulation for ventilation system repair time without additional mitigation against time taken to reach 4%v/v and 8%v/v limits

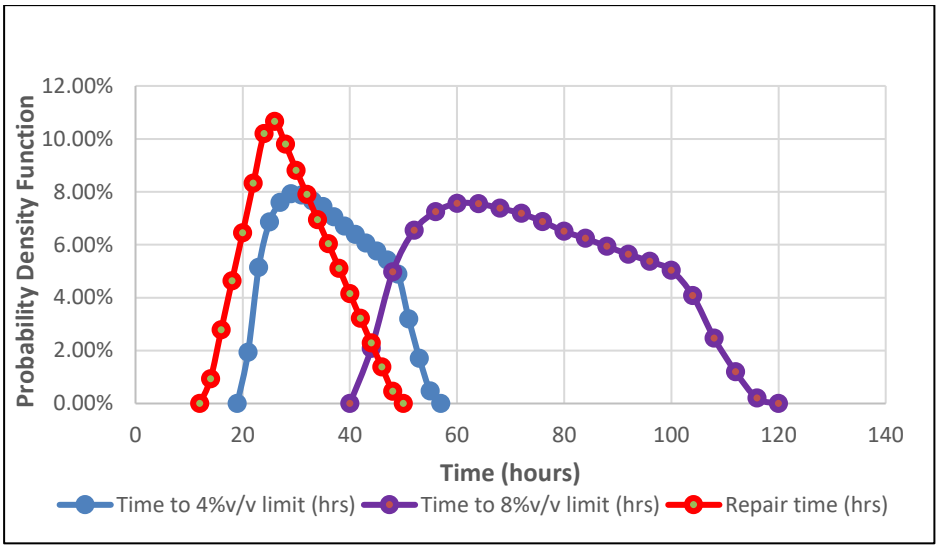

Figure 6-11: Comparison of MC simulation for ventilation system repair time with additional mitigation against time taken to reach 4%v/v and 8%v/v limits

Based on the results from Figure 6-10 and Figure 6-11, Appendix C Table C-8 provides a summary of the comparison of the time taken to reach the hydrogen concentration limits of 4% (LFL) and 8% with the distribution for equipment repair time. The general trend that can be observed from these results is that without the additional mitigation the peak repair time of 38 hours exceeds the peak time of 29 hours for reaching the LFL. Furthermore the 5% and 95% levels of 26 hours and 58 hours for the repair time exceed the time taken to reach the LFL. Thus, without the additional mitigation it is considered that there is the possibility that the LFL could be exceeded before a repair to the ventilation system is undertaken.

A comparison with the distribution for the time taken to reach the 8% hydrogen concentration limit indicates that although the peak value of 64 hours is well above the peak repair time of 38 hours, the lower tail end of the 8% distribution is exceeded by the upper end of repair time. However, a significant proportion of the distribution for the time taken to reach the 8% limit is well above the repair time. This indicates that without the additional mitigation there is a small possibility that the 8% limit could also be exceeded. With additional mitigation, Figure 6-11 shows that the repair time distribution has shifted more to the left of the distributions for the time taken to reach the 4% and 8% hydrogen concentrations. This shows that the potential for exceeding either of these concentration limits has been reduced because of the additional mitigation.

6.9.4 Comparison of the probability distributions of the time taken to reach the hydrogen concentration limits vs equipment repair time

Section 6.9.3 has shown that the time taken to repair the ventilation system, particularly without the additional mitigation could exceed the time taken to reach the LFL and

potentially the time taken to reach the 8% concentration limit. The probability of these occurrences both with and without the additional mitigation needs to be determined. This will provide a further understanding of the improvements achieved by the additional mitigation. This can be achieved through a comparison of the MC simulations for the 4% and 8% hydrogen concentration time limits and the repair time in terms of number of events, i.e., counts. The results of this analysis based on the MC simulations with 1000,000 runs for the cases without the additional mitigation and with the mitigation are presented in Figure 6-12 and Figure 6-13, respectively.

Figure 6-12 shows that from a total of 1000,000 simulation runs the number of repair time counts which exceed the 50 to 100 percentiles of the distribution for the time taken to reach the 4% limit is 850,105. Hence the probability that the repair time exceeds the time taken to reach the 4% concentration is 850,105/1000,000, i.e., 0.85. This suggests that without the additional mitigation there is a very high probability that the time taken to reach the LFL could be exceeded before the system is repaired.

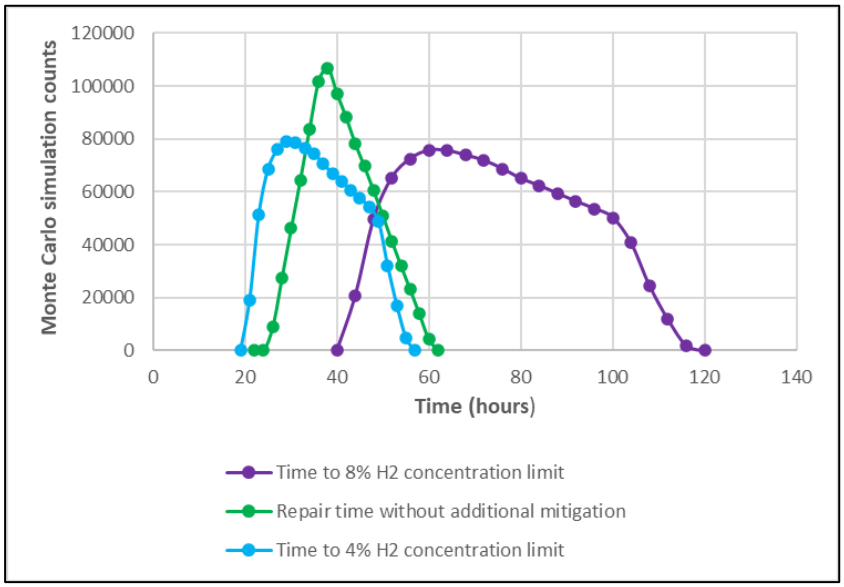

Figure 6-12: Comparison of MC simulation counts for repair time without additional mitigation with time taken to reach the 4%v/v and 8%v/v concentration limits

When comparing against the distribution for the time taken to reach the 8% concentration , it can be seen in Figure 6-12 that a large proportion of the repair time distribution is below the time taken to reach the 8% limit. In this case the total number of repair time counts that exceed the 8% hydrogen concentration is 166,088. Hence without the additional mitigation the probability that the repair time exceeds the time taken to reach the 8% concentration is 0.166. Whilst this probability is much lower than the probability of 0.85 for the time taken to reach the 4% limit, it is still considered

significant. This indicates that an improvement, in the form of additional mitigation, is necessary that would reduce the repair time.

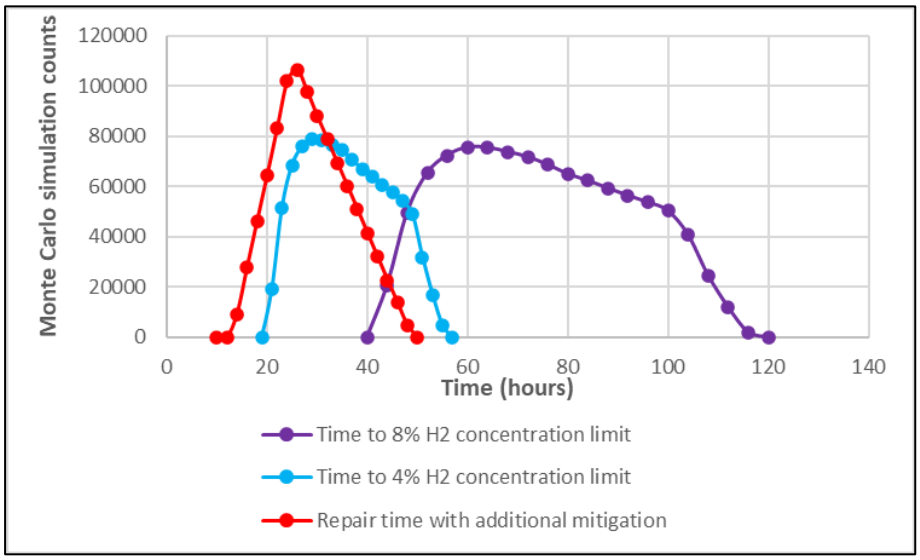

Figure 6-13: Comparison of MC simulation counts for the repair time with additional mitigation with time taken to reach the hydrogen concentration limits

With additional mitigation Figure 6-13 shows that a significant proportion of the repair time distribution has shifted below the distribution for the time taken to reach the 4% hydrogen concentration limit. This leads to only the 70 to 100 percentiles of the repair time distribution exceeding the time taken to reach the 4% concentration. From an MC simulation with 1000,000 runs, Figure 6-13 shows that the number of repair time counts which exceed the time taken to reach the 4% limit is 374449. This equates to a probability of 0.4, which is over a two-fold reduction in comparison with the probability of 0.85 without the additional mitigation.

Figure 6-13 also shows that with additional mitigation, much of the repair time distribution is below the time taken to reach the 8% concentration limit. In this case the number of repair time counts, from a total of 1000,000, which exceed the time taken to reach the 8% concentration is 18,329. Hence with additional mitigation, the probability that the repair time exceeds the time taken to reach the 8% concentration is 0.018. Hence in comparison with the case without the mitigation, there is a reduction in the probability by almost one order of magnitude. This indicates that the additional mitigation has resulted in a significant improvement.

6.10 Conclusions for Chapter 6

The application of the Monte Carlo (MC) Simulation method to a Fault Tree Analysis (FTA), as an enhanced means of assessing the reliability of a forced ventilation system for hydrogen removal has been investigated.

The analysis shows that by introducing additional mitigation in the ventilation system design, overall, there is a significant improvement in the reliability of the system. This is because the additional mitigation system, which consists of a new duct pressure monitoring instrument, enables the vent failure due to duct blockage to be revealed. Corrective action can then be undertaken by the plant operators to reinstate the vent system. By taking account of such risk mitigation measures, the MC simulations show that the probability of a failure to repair the vent system following the initiating fault is very small.

It is the probability distribution handling capability of the MC simulation method that has enabled this uncertainty analysis to be performed and the necessary ventilation system improvements to be identified. A standard FTA based on single values is unable to perform this type of an analysis.

The output of the research based on this case study, in terms of the methodology used for assessment of the reliability of the ventilation system and the time taken to reach the various hydrogen concentration limits has also been published by the candidate and presented at the IChemE Hazards 29 Conference [*Ahmed, 2019b*]. A summary of the published paper is given in Appendix H, Table H-3.

CHAPTER 7 : CASE STUDY 4 - BAYESIAN BELIEF UNCERTAINTY ANALYSIS OF HYDROGEN GENERATION IN TRANSPORTABLE VESSELS CONTAINING INTERMEDIATE LEVEL WASTES

7.1 Introduction to Chapter 7

Chapter 2 discusses in depth the knowledge gap associated with hydrogen hold-up and discontinuous release of the gas from sludgy waste forms in transportable storage skips (Figure 7-1). The design details including the dimensions shown in Figure 7-1, as well as the vent area provided by the filters which allow the hydrogen to escape, are the same for all skips and the outer boxes. This case study investigates the application of the Bayesian Belief Network methodology to identify key sensitivities which would affect the likelihood of a flammable hydrogen in air mixture forming within the skips.

The uncertainties associated with hydrogen hold-up, discontinuous release as well as the effect of skip design features, such as the filtered outlets, on the hydrogen concentration in the skip ullage space are investigated. The overall objective is to use the BBN uncertainty analysis to derive the conditions required to reach the least and most hazardous states in terms of the hydrogen concentration in the skip ullage space. This would enable identification of an effective means of managing the hydrogen hazard.

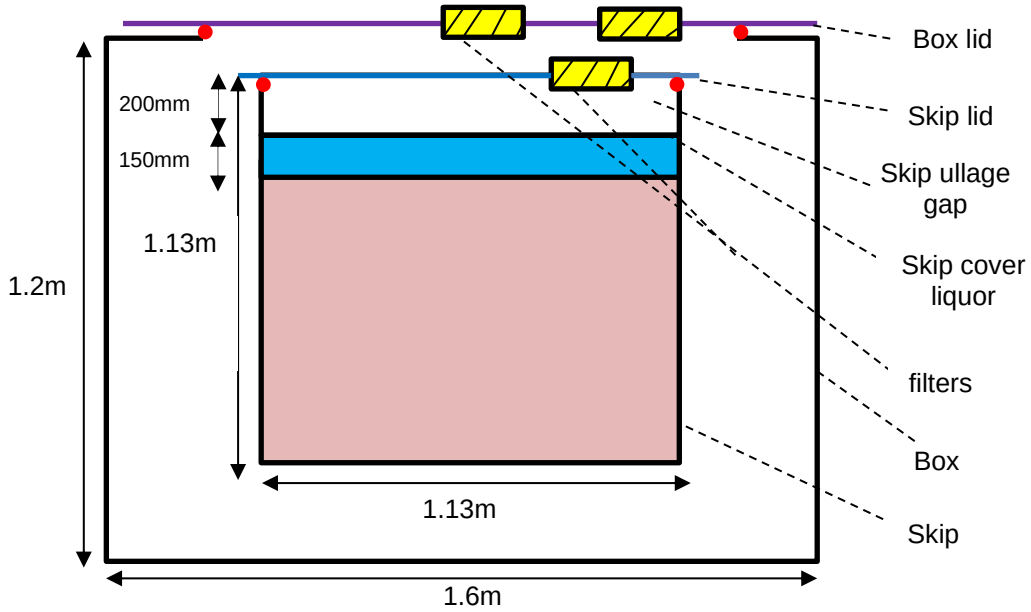

Figure 7-1: Schematic of transportable sludge waste skip and outer box [*Ahmed, 2019a*]

The output of the research based on this case study has been published by the candidate in the Nuclear Future, Journal of the Nuclear Institute [*Ahmed, 2019a*]. This is summarised in Appendix H, Table H-2. Research based on the output from this case study, focussing on the key sensitivities affecting the discontinuous release of hydrogen from sludge waste forms, has also been published and presented by the candidate at

the IChemE Hazards 29 Conference(*Ahmed, 2019b*). A summary of this paper is given in Appendix H, Table H-3.

7.2 Mechanisms of hydrogen gas generation in the storage skip

The main mechanism for hydrogen generation within the skip is the corrosion reaction of Magnox with water, which is dependent on the amount of uncorroded metal. In nuclear chemical plants, the continuous release of hydrogen due to corrosion of the Magnox waste is also referred to as 'chronic' hydrogen release. The continuous corrosion of the waste also results in the formation of magnesium hydroxide sludge. Some of the chronic hydrogen gas can potentially be held within the sludge matrix, leading to swelling or expansion of the waste. Radiolysis of aqueous liquor within the skip is the second main mechanism for hydrogen generation.

Chapter 2 discusses the behaviour of held-up gas released from sludges and from radiolysis. In this respect, the main points that can be identified are:

- Under normal circumstances, a slow release of chronic hydrogen will occur due to continuous corrosion of the Magnox, some of which will be vented via the skip filtered outlets such that an equilibrium concentration is reached in the ullage.
- Some of the hydrogen gas from the corrosion reaction will be held up in the sludge, leading to waste expansion.
- The held-up hydrogen can be released discontinuously from the sludge, leading to a sudden build-up of a large volume of the gas in the skip ullage space.
- Radiolysis of the skip radioactive liquor is primarily affected by the 'G' value and the liquor radioactivity content [*Bibler et al, 2007*].

Under normal operations, i.e., without the discontinuous release scenario, the filtered vents are designed to ensure that the volume of the hydrogen gas that remains in the ullage space is small. This remaining hydrogen in the ullage space is referred to as the 'standing hydrogen'. Typically, a standing hydrogen volume of 3L into an ullage volume of 290L is expected such that the equilibrium hydrogen concentration is around 1%, i.e., below the 4% LFL. A detailed analysis of the hydrogen volumes and concentration in the skip ullage space are given in Section 7.3.

If a discontinuous release occurs into an ullage space with standing hydrogen already present at the equilibrium concentration, then the resultant ullage concentration, C_u, can be expressed as:

$$C_u = \frac{Discontinuous\ hydrogen\ release\ volume\ + Standing\ hydrogen\ volume}{Vessel\ ullage\ volume\ +\ Discontinuous\ hydrogen\ release\ volume} \quad (7\text{-}1)$$

The mode of plant operation assumed in this analysis relates to normal skip handling operations involving planned movements. These skip handling operations could result in disturbance of the skip waste contents and hence increase the likelihood of a discontinuous release of the held-up hydrogen gas in the sludge. The rate of radiolytic hydrogen generation, $Q_{H,}$ can be expressed by equation 2-9, as discussed in Chapter 2.

$$Q_H = kG(H_2)_{(\alpha)}E_{(\alpha)} + kG(H_2)_{(\beta\,\gamma)}E_{(\beta\,\gamma)} \quad (2\text{-}9)$$

Factors affecting radiolytic hydrogen in systems containing radioactive liquors were also investigated in Case Study 1, which are discussed in Chapter 4. However, the context of Case Study 1 was to investigate the uncertainty from radiolytic hydrogen generation in sealed process pipes using a qualitative approach. Hence a significant number of factors affecting radiolytic hydrogen generation in sealed pipes, e.g., penetration of gamma radiation from the surrounding liquor through the pipe metallic structure, are not relevant to this case study. The purpose of this case study for hydrogen generation in vessels containing bulk radioactive liquors is to explore the use of a quantified approach for the derivation of radiolytic hydrogen generation rate using equation 2-9.

7.3 Identification of variables affecting hydrogen concentration in the skip ullage

In support of this case study, a series of meetings and discussions were held with the Characterisation, Inventory, Sludge and Wastes Group of SL (CISWG). These discussions are summarised in the meeting minutes by *Ahmed, 2017a* and *Ahmed, 2018*. The meeting objectives were to identify the key variables for the Bayesian network which affect hydrogen concentration in the skip ullage and how they interact with each other. The CISWG requested that this case study needs to focus on the key sensitivities affecting the discontinuous release mechanism, which could potentially lead to the LFL being exceeded [*Ahmed, 2017a*]. This way the best means of managing the hydrogen concentration in the ullage space could be identified thus preventing a hydrogen explosion. It was considered that by preventing the hazard in the first place, the consequences would also be prevented. The interrelationships between the variables that were identified at the meetings are illustrated in Figure 7-2. This represents the concept model for this case study. Due to the large number of variables associated with the model, for ease of interpretation and cross referencing purposes, groups of parameters are numbered and colour coded in the concept model, as follows:

- Dark green nodes, A1 to A14, represent the radiolytic hydrogen generation rate.
- Pink node B1 represents the chronic hydrogen generation rate.

- Yellow node C1 represents total hydrogen generation rate.
- Purple nodes, D1 to D6, represent skip filter performance.
- Cyan nodes, E1 to E2, represent standing hydrogen concentration and volume.
- Light green nodes, F1 to F3, represent skip ullage volume.
- Blue coloured nodes, G1 to G3, represent waste matrix expansion factors.
- Brown nodes, H1 to H3, represent hydrogen gas retention and discontinuous release volume.
- Red coloured nodes, I1 to I2, represent the total volume of hydrogen and concentration in the skip ullage space.
- Node I2 represents the hypothesis being assessed in this case study, i.e., hydrogen concentration in the skip ullage following a discontinuous release.

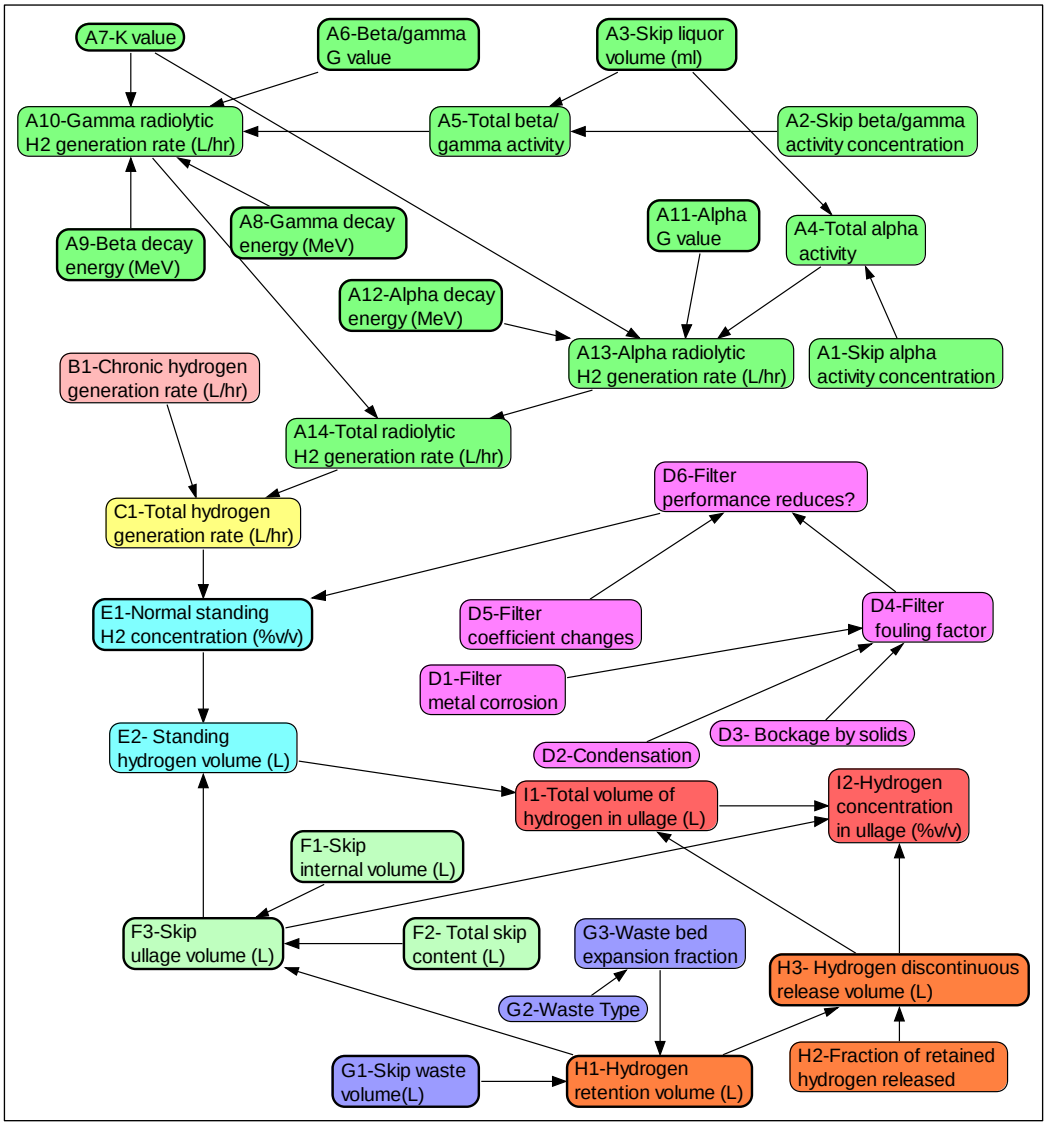

Figure 7-2: Concept model for hydrogen generation in skip ullage

The development of the concept model including the quantification of data for the input variables was based on the discussions with the CISWG [*Ahmed, 2017a, Ahmed, 2018*]. These data are presented in Appendix D Table D-1. Sections 7.3.1 to 7.3.3 identify the key assumptions which form the basis for the concept model.

7.3.1 Hydrogen generation rate

- The hydrogen generation rate due to corrosion of Magnox and radiolysis and the release through the filtered vents affect the total volume of hydrogen present in the skip ullage.
- Corrosion of Magnox waste is the main mechanism for hydrogen generation in the skip, however the uncertainty on the contribution from radiolytic hydrogen generation also needs to be considered.
- A mean chronic hydrogen generation rate of 1.9L/hr, due to corrosion of Magnox, was provided by the CISWG [*Ahmed, 2018*] and similar values have also been reported by *Averill et al, 2018.*
- The radiolytic hydrogen generation rate is primarily dependent on the alpha and Beta-Gamma radioactivity concentration of the skip liquor.

7.3.2 Volume of hydrogen in skip ullage

The total volume of hydrogen accumulating in the ullage space (Node I1) is equivalent to the steady state release volume of hydrogen from the skip sludge matrix, i.e., the 'standing hydrogen volume' plus the volume due to a discontinuous release from the sludge (Node H3). The standing hydrogen volume is primarily affected by the skip filter performance. The discontinuous release volume of hydrogen is dependent on:

- The volume of held-up hydrogen gas (Node H1), which is proportional to the waste volume and waste expansion fraction.
- The fraction of the held-up hydrogen that is released (Node H2) due to waste disturbance.

7.3.3 Hydrogen concentration in the skip ullage space

The derivation of the hydrogen in air concentration in the ullage space is based on equation 7-1. As such, the main variables which would affect the hydrogen flammability of the gaseous mixture in the ullage space are:

- Total hydrogen volume accumulating in the ullage, i.e., standing hydrogen plus the discontinuous release volume.

- The volume of the skip ullage space which can also vary, depending on parameters such as the choice on processing a full skip or part filled skip.

7.4 BBN development and supporting data

Based on the concept model discussed above, a BBN was developed using Netica. As a result of the large number of identified variables, it was realised that the quantified Bayesian network should be developed in stages for each exclusive part of the analysis and then verified. This staged development and verification was necessary in order to ensure that the BBN model was logical and accurate. Each developed stage of the network is presented in the following figures in Appendix D:

- Figure D-1 models and verifies the BBN for radiolytic hydrogen generation rate.
- Figure D-2 models and verifies the BBN for total hydrogen generation rate.
- Figure D-3 models and verifies the BBN for skip ullage volume and hydrogen retention volume.
- Figure D-4 models and verifies the BBN for discontinuous hydrogen release.
- Figure D-5 models and verifies the BBN for hydrogen concentration in the ullage space.

All the numerical values for the BBN input nodes are based on the process data provided by the CISWG at the discussion meeting [*Ahmed,2018*]. The data are detailed in Appendix D, Table D-1. This table also provides a description of each node and explains how the relevant data for the parent node Conditional Probability Tables (CPTs) were derived, making references to the advice provided by the CISWG. The individual CPTs for the main parent nodes are presented in Appendix D, Table D-2 to Table D-10.

7.5 BBN verification

When an equation is used in a continuous node, a verification of the BBN output is carried out to test the equation result using a hand calculation and comparing this with the result from the BBN output. Appendix D, Table D-11 provides the details of the BBN verification, which is supported by Figure D-1 to Figure D-5. The comparison given in Table D-11 shows that the BBN results for the continuous nodes are identical to the hand calculations using the same equations and parameter values. Hence, it was verified that the logic used in the network is accurate. For the purpose of discretisation of the continuous variable range, the maximum and minimum values of the range also needed to be specified. Appendix D, Table D-11 provides the discretisation data for each of the parent nodes.

7.6 BBN results

Figure 7-3 shows the results of the fully developed BBN analysis of the hydrogen concentration in the skip ullage space. This is based on the Prior probability distributions of the input nodes A1, A2, B1, F1, F2, G2 and H2.

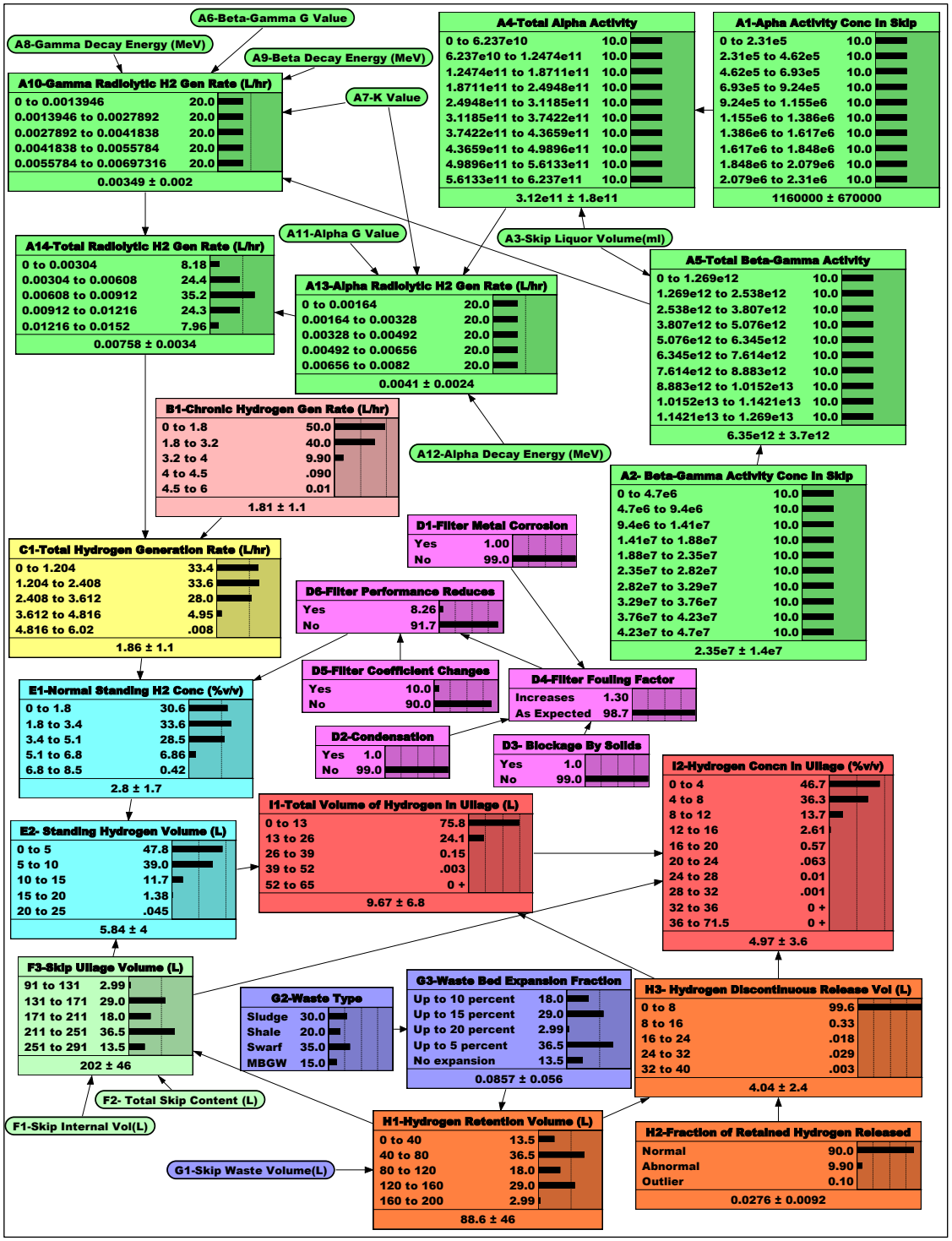

Figure 7-3: Bayesian Belief Network for hydrogen concentration in the skip ullage space

7.6.1 Results for hydrogen generation rate

The predicted probability for the chronic hydrogen generation rate due to corrosion of Magnox waste is that 90% of the distribution lies in the range 0 to 3.2L/hr, while the remaining 10% is in the region of 3.2 to 6L/hr. The general trend observed from Figure 7-3 is that the radiolytic hydrogen generation rate (Node A14) is at least two orders of magnitude lower than the estimated mean hydrogen generation rate of 1.8L/hr due to corrosion (Node B1).

The results above were based on the CPT for total hydrogen generation rate (Node C1). This was derived from the CPTs for chronic hydrogen generation rate due to corrosion of Magnox (Node B1) and the total radiolytic hydrogen generation rate (Node A14). Full details of this derivation are given in Appendix D, Table D-1. The individual CPT matrices for Nodes A14, B1 and C1 are presented in Appendix D, Table D-2,Table D-3 and Table D-4, respectively.

7.6.2 Results for standing hydrogen concentration

The skip standing hydrogen concentration (Node E1) is dependent on the filter size and performance (Node D6) as well as the total rate of hydrogen generation in the ullage space (Node C1). At a high probability of around 92% that the filter performance is satisfactory and the mean hydrogen generation rate is 1.9L/hr, a mean standing hydrogen concentration of 2.8%v/v has been predicted. This result is based on the condition that a discontinuous release does not take place. Hence it is shown that provided that the filter performance is satisfactory, and a discontinuous release does not occur, there is a high chance that the normal standing hydrogen concentration will remain below the 4% Lower Flammable Limit (LFL). This shows that the plant is effective at managing the hydrogen hazard during normal release mechanisms. These results are based on the CPT for Node E1 (Appendix D, Table D-5) as derived in Table D-1.

Whilst the maximum standing hydrogen concentration range that can be reached is 6.8 to 8.5%, Figure 7-3, Node E1 shows that the likelihood of this event is very small. A small probability of only 0.4% has been determined for this occurrence.

7.6.3 Results for skip ullage volume

The skip ullage volume (Node F3) is dependent not only on the initial waste and water volume, but also on the increase in waste volume (Node G1) due to waste bed expansion (Node G3). A prerequisite condition for this BBN analysis that the skip is full, i.e., it contains 1000L of waste and 270L of water. With this condition and a low waste

bed expansion fraction of 0.09, the BBN (Figure 7-3) predicts a probability of around 85% that the ullage volume is in the range 91 to 251L. The probability of the ullage volume being greater than 251L is predicted as less than 14%. The mean ullage volume is predicted as 202L. Since this value is well above the lowest allowable limit of 91L, the general trend from this result is that provided the waste bed expansion fraction is low, the ullage volume will remain relatively high. Hence at these conditions, the hydrogen concentration in the ullage space will be controlled effectively. This result is based on the CPT for the skip ullage volume (Node F3), given in Appendix D Table D-6. The CPT was calculated by Netica using the expression for Node F3 given in Appendix D Table D-1.

7.6.4 Results for standing hydrogen volume

Based on the probability distribution of skip ullage and a mean standing hydrogen concentration of 2.8%v/v, a mean standing hydrogen volume of 5.8L (Node E2) has been predicted by the BBN (Figure 7-3). A probability of nearly 50% for the standing hydrogen volume being less than 5L and only a small probability, below 2%, for the volume being 15L or more has been determined. Hence this demonstrates that under normal operating conditions, assuming a discontinuous release does not take place, the volume of hydrogen that can be present in the ullage space will be close to the lowest range of 0 to 5L. This low hydrogen volume is based on the condition of a high probability that the filter performance is satisfactory, thus demonstrating the importance of this plant item in terms of managing the hydrogen hazard. The CPT for standing hydrogen volume is given in Appendix D, Table D-9, which was calculated by Netica using the expression for Node E2 given in Table D-1.

7.6.5 Results for hydrogen retention and discontinuous release volume

The hydrogen retention volume (Node H1) is affected by the waste volume (Node G1) and the waste bed expansion fraction (Node G3). Based on the condition that the skip is full and the mean waste bed expansion fraction is 0.09, a probability of approximately 37% for the hydrogen retention volume being in the range 40 to 80L has been determined. This result is based on the CPT for Node H1 (Table D-7), which is derived in Appendix D Table D-1.

The hydrogen retention volume determined above does not necessarily mean that this will all release into the ullage space. The actual volume of the gas that will be released into the ullage discontinuously (Node H3) is affected by the fraction of retained hydrogen released (Node H2). The BBN model is based on the normal skip handling operations, assuming faults resulting in a dropped skip will not occur. A release fraction

of 0.025 for normal operations has been recommended by the CISWG [*Ahmed, 2018*]. With a mean release fraction of 0.028, which is broadly within the normal range, the BBN model in Figure 7-3 predicts a mean hydrogen volume of 4L for the discontinuous release mechanism.

The main observation from the result above is that although a discontinuous release would contribute to the total hydrogen concentration in the ullage space, the 4L volume is in the low range of the probability distribution for this mechanism (Node H3). The relatively low discontinuous release volume is due to the low release fraction of 0.028. These results are based on the CPT for Node H3 (Appendix D, Table D-8), which is derived in Table D-1.

7.6.6 Results for hydrogen concentration in skip ullage space

Node I1 predicts that the mean total hydrogen volume in the ullage space due to the standing hydrogen and discontinuous release mechanism is 9.7L. At a mean ullage volume of 202L and a total hydrogen volume of 9.7L, Node I2 shows that there is an equal 40% chance that the hydrogen concentration in the ullage space is in the 0-4%v/v and 4-8%v/v ranges. If this result is compared with the mean normal standing hydrogen concentration of 2.8%v/v for Node E1, it can be seen that the discontinuous release volume makes a significant difference to the hydrogen concentration in the ullage space. These results for Node I2 were based on the CPT for node I1, which was calculated by Netica using the equations derived in Appendix D Table D-1.

7.7 Comparison of BBN output with previous analyses

In terms of the validity of the BBN output, the results can be compared with a previous analysis, provided by the CISWG [*Ahmed, 2018*]. This previous work was undertaken in the form of an Event Tree Analysis (ETA) within an Excel spreadsheet to determine the likelihood of a discontinuous hydrogen release in skips containing sludge. This analysis was based on chronic hydrogen generation rates only, which ranged from 0.1 to 2 L/hr. Depending on the types of waste present within each skip, the potential for hydrogen hold-up, i.e., waste bed expansion fraction was approximated, which ranged from 0 to 20%v/v. The potential for release of the held-up hydrogen, i.e., hydrogen release fraction was also predicted for the waste in each skip. For each event the hydrogen concentration in the skip ullage space was then calculated within the spreadsheet.

The variation in each of the three attributes discussed above and the subsequent hydrogen concentration in each skip was treated as a separate event in the ETA. The

number of skips conforming to the conditions for each event was then summed within the spreadsheet. An extract from the CISWG ETA is given in Figure 7-4.

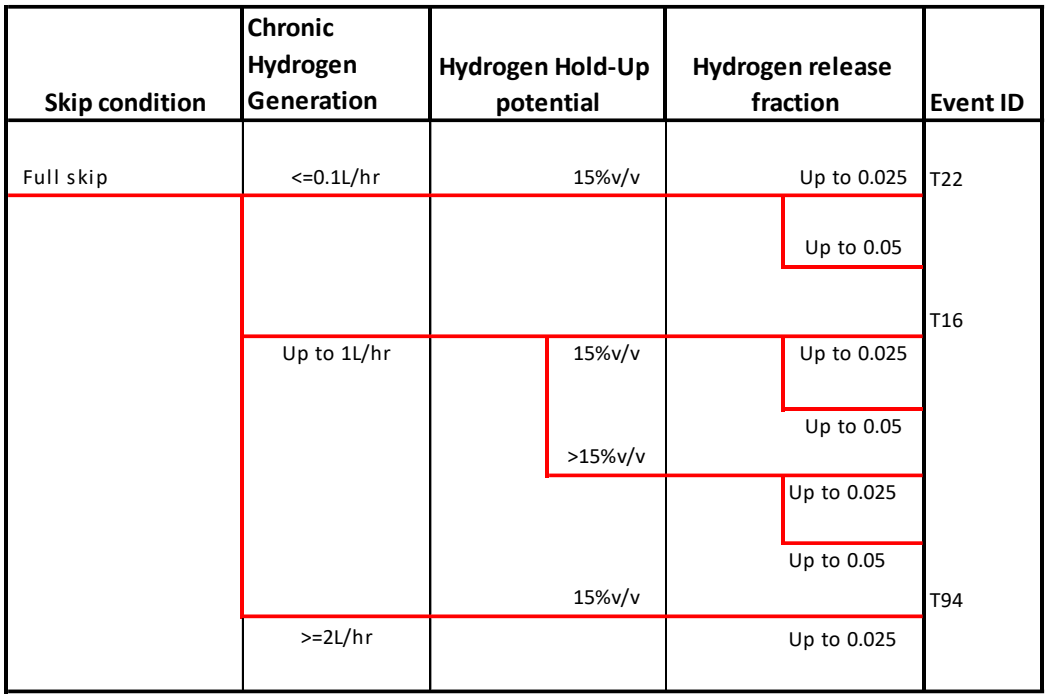

Figure 7-4: Extract from the CISWG Event Tree for hydrogen generation in ILW skips [*Ahmed, 2018*]

Event T16 in Figure 7-4 represents the skips in which the chronic hydrogen generation rate was a maximum of 1L/hr. For this event, the hydrogen hold-up and release fractions were 15% and 2.5% respectively. Based on these conditions, the hydrogen concentration in the skip ullage space was calculated using the same relationship between the discontinuous release volume, standing hydrogen volume and ullage volume as that given by equation 7-1. Similar to the BBN analysis, the discontinuous release volume was determined knowing the percentage of the held-up hydrogen within the sludge, the hydrogen release fraction and the sludge volume, i.e., 1000L for a full skip. For Event T16, the discontinuous release volume was calculated as 1000 x 0.15 x 0.025, i.e., 3.8L.

The previous method for determination of the standing hydrogen volume in the Event Tree was however different to the BBN model. Based on the filter performance curve as shown in Figure 7-5, the standing hydrogen concentration (SC) as a function of hydrogen generation rate (CH) was approximated in the previous analysis. The approximation was achieved by applying the line of best fit of SC = 1.34CH + 0.66 to Figure 7-5 for hydrogen generation rates greater than 1L/hr. Based on extrapolation from Figure 7-5, for hydrogen generation rates less than 1L/hr ,the line of best fit was approximated to SC = 2CH in the previous analysis.

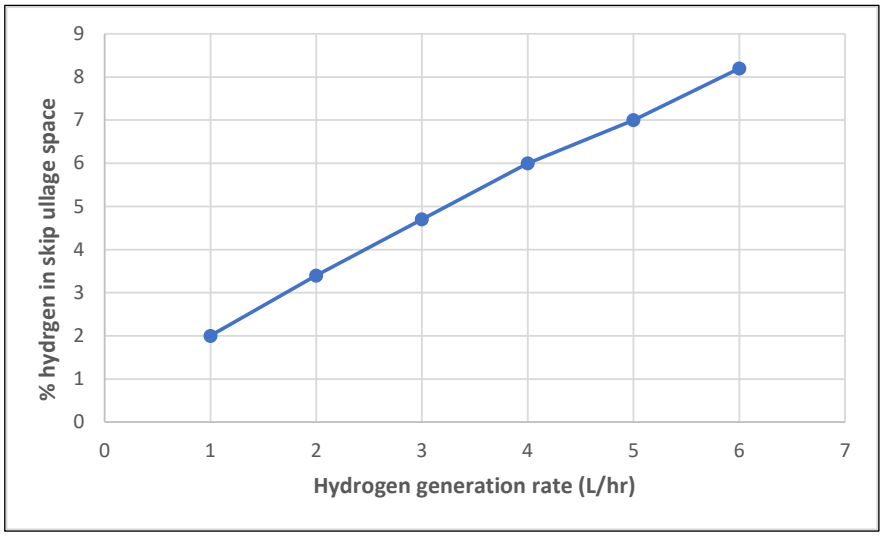

Figure 7-5: Graph of hydrogen concentration in skip ullage vs hydrogen generation rate

Using the approach described above, for a hydrogen generation rate of 1L/hr, a standing hydrogen concentration of 2%v/v was determined in the previous analysis. Event T16 was also based on an ullage volume of 141L, which took account of the 15% waste expansion fraction due to hydrogen hold-up. Hence, the standing hydrogen volume was calculated as (2 x 141)/100, i.e., 2.8L. Using a discontinuous release volume of 3.8L, the hydrogen concentration in the skip ullage space was derived as (2.8+3.8)/(3.8 +141), i.e., 4.6%v/v.

Event T94 was based on a total hydrogen generation rate of 2L/hr, a hydrogen hold-up fraction of 15%, a skip ullage volume of 141L and a release fraction of 2.5%. Using the same approach as for Event T16, the Event Tree spreadsheet yielded a discontinuous release volume of 3.8L, a standing hydrogen volume of 4.7L and a hydrogen concentration of 5.8%v/v.

Using a similar set of values for the key parameters as for Event T94, i.e., a hydrogen generation rate of 2L/hr, waste expansion fraction of 0.15, ullage volume of 141L and a hydrogen release fraction of 0.025, the BBN model was updated as shown in Figure 7-6. It can be seen that the mean volume of hydrogen released discontinuously is 4L. This is similar to the 3.8L volume calculated by the Event Tree Analysis. A further observation from the updated BBN is that when the ullage volume is instantiated to 141L, the waste expansion fraction is automatically updated to 15%. This is the same as the value determined in the Event Tree spreadsheet. This demonstrates that the logic used for the derivation of the skip ullage volume in the BBN is in agreement with the Event Tree Analysis.

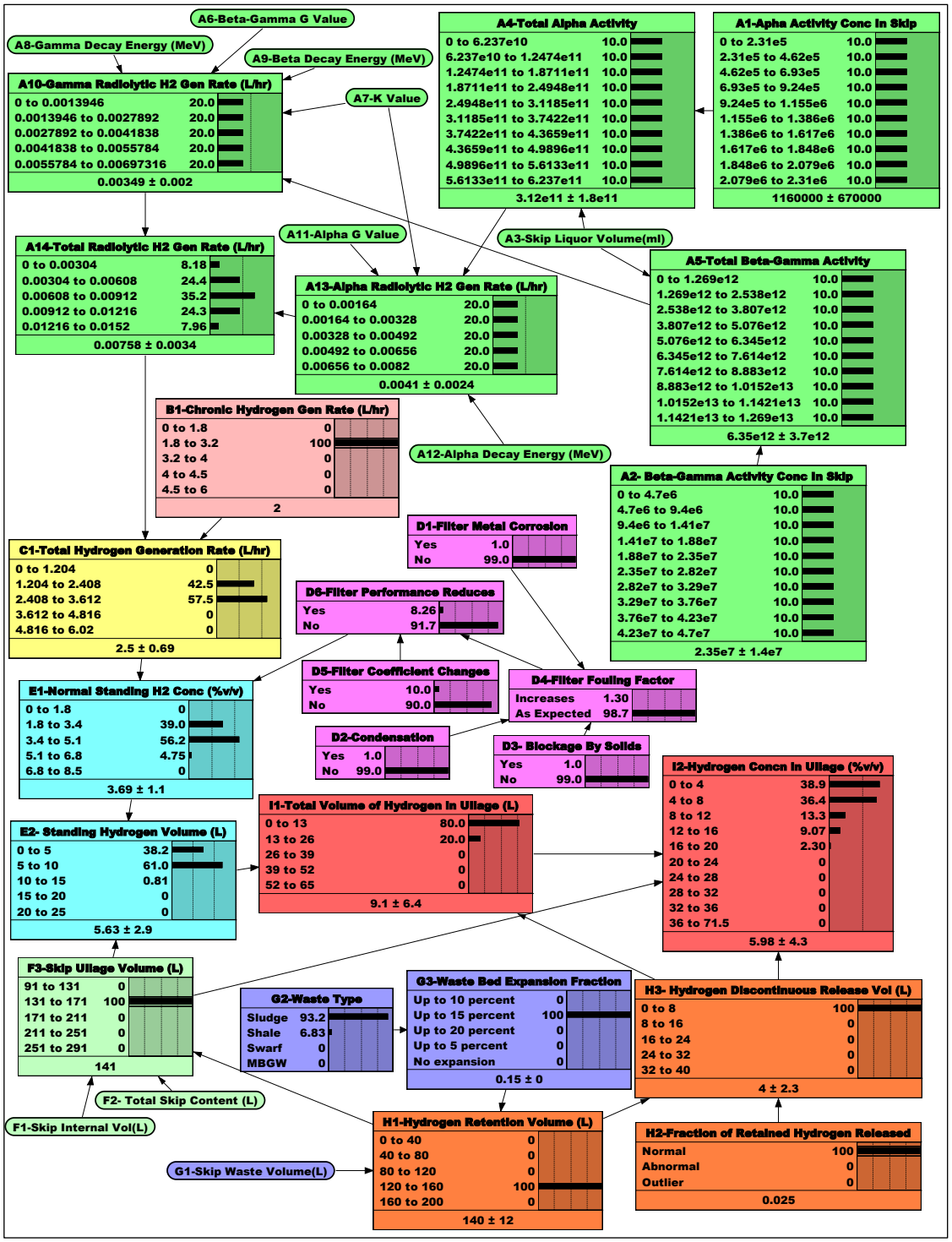

Figure 7-6: Updated BBN to replicate the conditions modelled in event T94 of the Event Tree Analysis

The mean standing hydrogen volume of 5.63L, predicted by the updated BBN, is however slightly higher than the event tree value of 4.7L. The main reason for the difference is that the event tree approximates the standing hydrogen concentration by applying the line of best fit to the filter performance curve as discussed previously. The BBN model (Node E1) on the other hand is based on the standing hydrogen

concentration for each credible band of hydrogen generation rates (Node B1). Accordingly, the BBN determines the mean concentration over the whole range of hydrogen generation rates i.e., 0 to 6L/hr.

A further reason for the difference in the standing hydrogen volumes in the two analyses is that the BBN takes into consideration the reduction in the filter performance (Node D6). The event tree is however based on normal filter performance, thus assuming that more hydrogen will be vented, which leads to a lower hydrogen concentration. If the effects of the filter performance are removed from the BBN analysis, i.e., by setting the likelihood of filter performance reduction to a 100% 'No' state in Node D6, then the mean standing hydrogen volume reduces to 5.4L. Therefore, in this case there is better agreement in the results. Although the two models differ slightly in terms of the standing hydrogen volume, the updated BBN model in Figure 7-6 shows that the probability that the hydrogen concentration is in the range 4 to 8%v/v is 36.4%. The mean value of the hydrogen concentration is 5.98 ± 4.3%v/v, which is similar to the 5.8%v/v calculated by the event tree.

Given that the results from both methods are very similar, the CISWG agreed with the verification of the BBN. They also agreed that the logic used in the BBN is reasonably accurate [*Ahmed, 2018*]. The benefit of the Bayesian technique is that it enables an uncertainty analysis by predicting a distribution of the key variables, which is then used by the network to calculate the distribution of the final output node.

7.8 Sensitivity Analysis

7.8.1 Sensitivity to changes in parent node probabilities

Having demonstrated the validity of the BBN model in Section 7.7, further analysis can now be undertaken to determine new information about the hypothesis, that the BBN provides, which is not already known. This is achieved through the application of the BBN updating feature. Given the uncertainty associated with the BBN input parent nodes, the sensitivity of the hydrogen concentration in the ullage space to changes in the parent node probabilities can be tested.

Intuitively, it is expected that the hydrogen concentration in the skip ullage is likely to be sensitive to the input nodes including hydrogen generation rate, filter performance, ullage volume, hydrogen release fraction and the type of waste in the skip. Hence the most hazardous state of each of these input nodes can be instantiated to a 100% probability to determine the likelihood of exceeding the hydrogen concentration limits of 4% and 8%. For example, in Figure 7-7 the most hazardous chronic hydrogen generation rate of 4.5 to 6 L/hr (Node B1) is instantiated to a 100% probability.

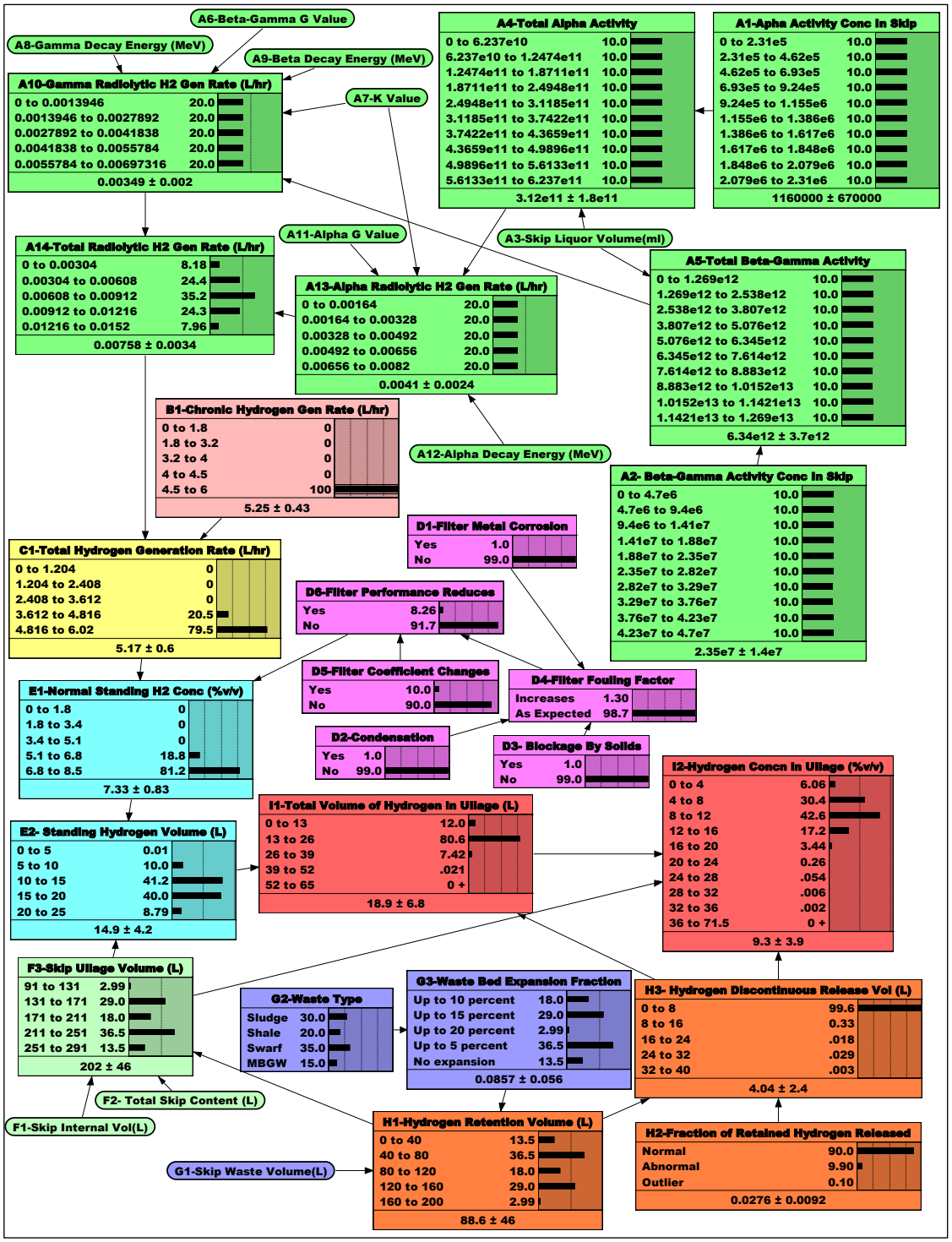

Figure 7-7: Sensitivity to chronic hydrogen generation rate

As shown in Node I2 of Figure 7-7, the instantiation of Node B1 yields a total probability of approximately 94% and 64% for exceeding the 4% and 8% skip ullage concentration limits, respectively. Similarly, the following most hazardous states of each of the other parent nodes were also instantiated to 100% and the results are compared in Figure 7-8.

- D6 - Filter performance reduces? Yes.

- F3 – Skip ullage volume; 91-131L.
- H2 - Hydrogen release fraction; 0.2.
- G2 – Waste type; Sludge.

The actual instantiated BBNs for Nodes D6, F3, H2 and G2 are given in Appendix D, Figure D-6, Figure D-7, Figure D-8 and Figure D-9 respectively.

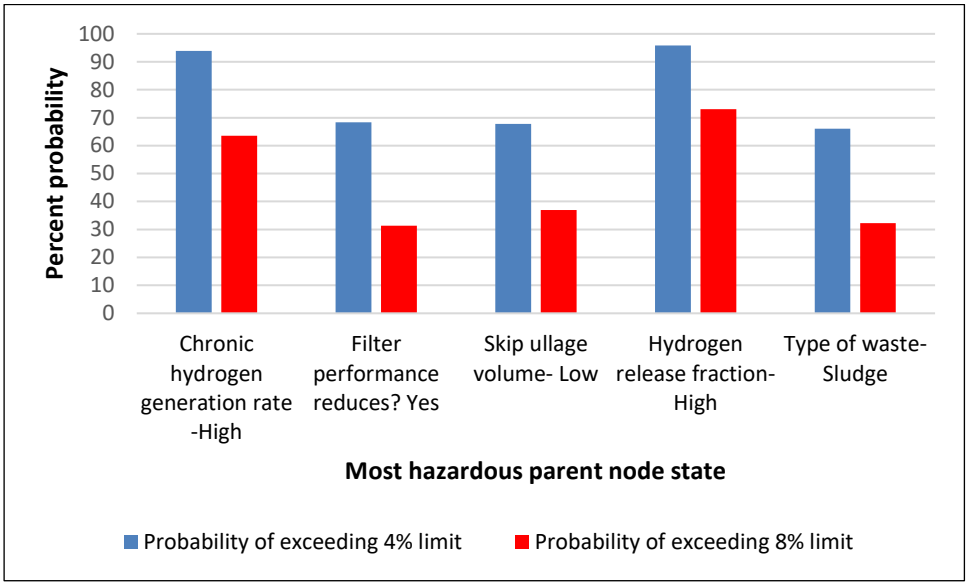

Figure 7-8: Effect of most hazardous parent node states on the likelihood of exceeding the 4% and 8% hydrogen concentration limits

The general trend in Figure 7-8 is that there is a high chance that all five of the parent nodes being in the most hazardous state will lead to the skip hydrogen concentration exceeding the 4% LFL. There is also the potential to exceed the 8% limit, however the likelihood of occurrence of this event is lower. The high chronic hydrogen generation rate and high hydrogen release fraction are the two most dominant states that affect the potential to exceed the 4% and 8% hydrogen concentration limits. The probability of either of these two hazardous states would need to increase to almost 100% in order to exceed the 4% limit. To exceed the 8% hydrogen concentration limit, the probabilities of the high hydrogen generation rate and high hydrogen release fraction would need to be around 60% and 70% respectively.

7.8.2 Conditions required for the least hazardous hydrogen concentration

The BBN updating feature can also be applied to determine the conditions required to achieve the least hazardous state. As the hypothesis for this case study concerns the likelihood of the skip ullage atmosphere being within a given hydrogen concentration band, the preferred conditions would be those that result in a hydrogen concentration below the 4% LFL. Accordingly, the model was updated in Figure 7-9 by instantiating the 0 to 4% state of Node I2 to 100%.

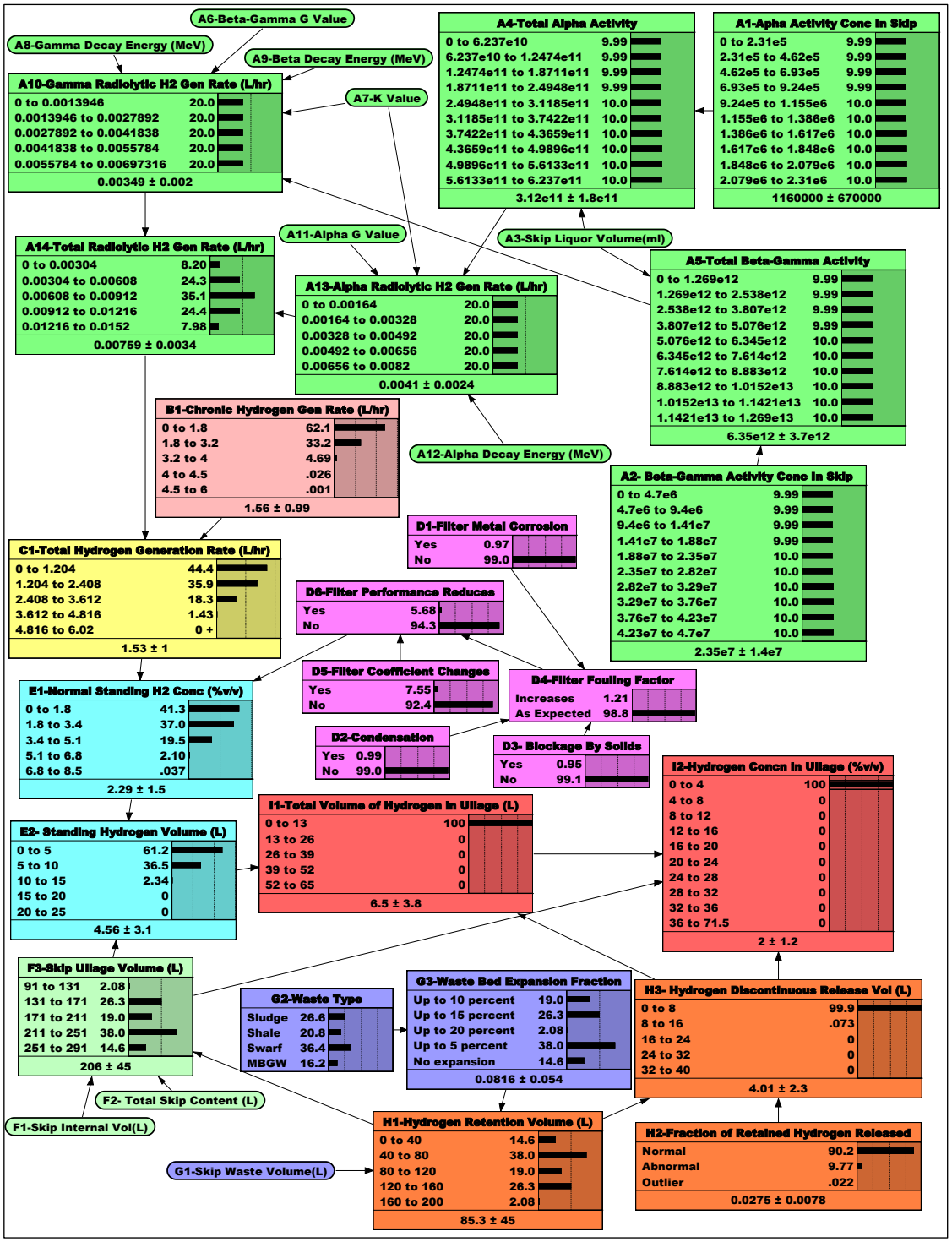

Figure 7-9: Conditions required for the least hazardous hydrogen concentration

A comparison of the updated results in Figure 7-9 with the model based on Prior values in Figure 7-3 shows that, in order to achieve the least hazardous state, the probability distributions for the following input parent nodes would need to change the most:

- The probability of chronic hydrogen generation rate due to Magnox corrosion being in the low range of 0 to 1.8L/hr would need to increase from 50% to 62%.

- The probability of a change in filter coefficient would need to decrease from 10% to around 7%.
- The probability of the ullage volume being above 251L would need to increase from around 13% to almost 15%.

Essentially the results above show that the key control measure in terms of achieving the least hazardous state is to reduce the chronic hydrogen generation rate due to corrosion of Magnox. This could be achieved for instance by reducing the amount of uncorroded Magnox being transferred to each skip.

A further comparison of the BBN results based on the mean Prior values (Figure 7-3) with the mean values in the updated BBN in Figure 7-9 shows that the parent node which needs to change the most is the total hydrogen volume in the ullage space (Node I1). In order to achieve the least hazardous hydrogen concentration range of 0 to 4%v/v, there needs to be a reduction in the mean hydrogen volume in the ullage from around 10L to 6.5L i.e., by 33%.

It is recognised that increasing the vent area of the filtered outlets would also result in a reduction in the hydrogen concentration in the ullage space by increasing the rate of escape of the gas from the skip. However larger vents would also potentially lead to an increase in the quantity of airborne radioactivity being released from the skip and the integrity of the skip lid may be reduced, which would be disadvantageous.

7.8.3 Conditions required for the most hazardous hydrogen concentration

The most hazardous hydrogen concentration that could potentially arise is that which leads to a detonation as this would result in the most physical damage to the vessel. The minimum hydrogen in air concentration at which a detonation could arise is known to be 18%v/v. Hence, as shown in Figure 7-10, the BBN was updated with the hydrogen concentration in the ullage set to 18%v/v. The updated model shows that the conditions which would lead to this hydrogen concentration range are:

- The total hydrogen volume in the ullage increases mainly to the 13 to 26L range.
- The ullage volume decreases mainly to the low range of 131 to 171L.
- The hydrogen retention volume increases to the high range of 120-160L.
- The likelihood of the hydrogen release fraction being high increases two-fold.
- The waste bed expansion fraction increases predominantly to 0.15.
- Filter performance reduction probability increases two-fold.

It is known that the stoichiometric hydrogen in air concentration at which the gas explosion can occur is 29.5%v/v, which could also be regarded as part of the most

hazardous range. The results for the updated BBN which represents this hydrogen concentration value are shown in Appendix D, Figure D-10.

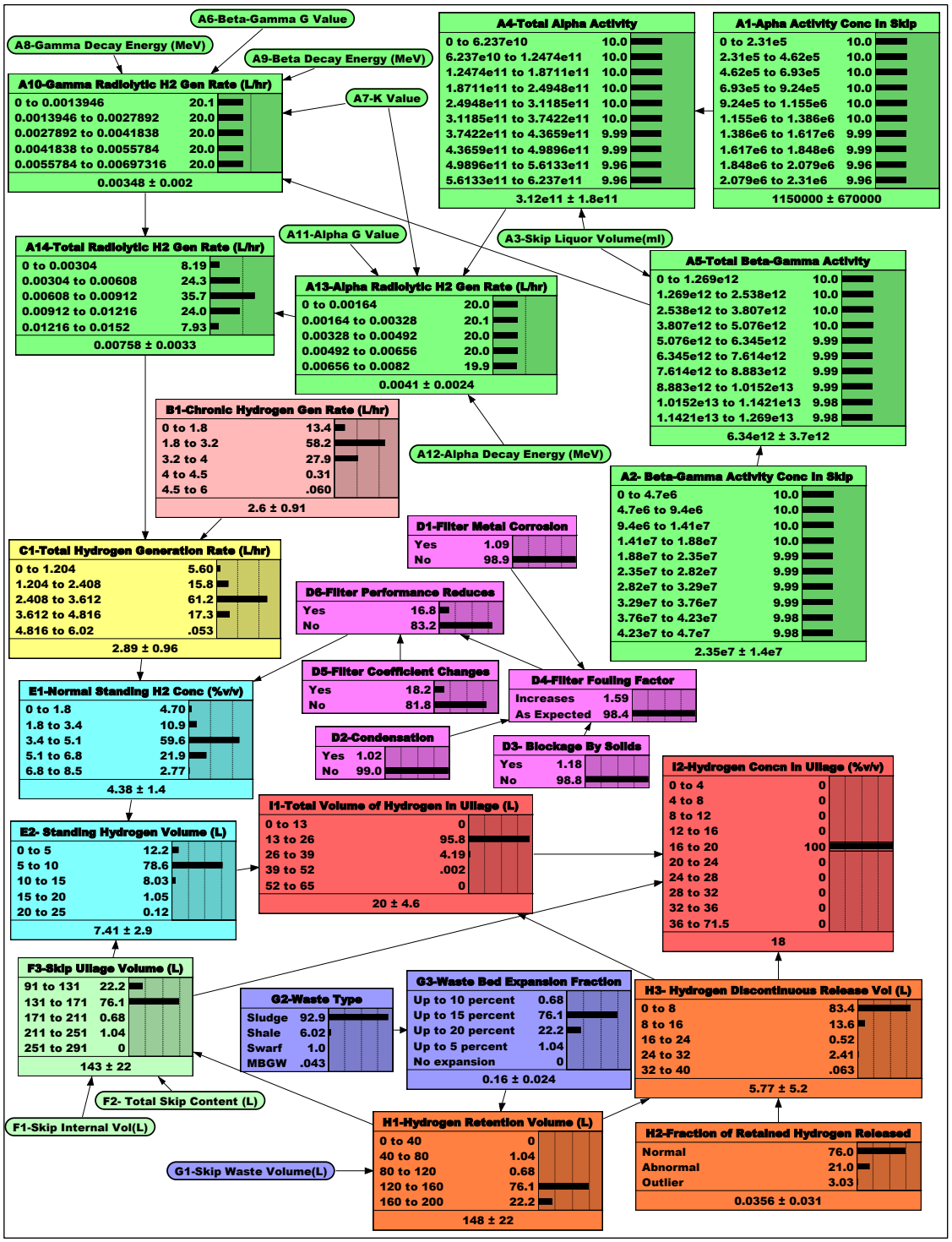

Figure 7-10: Updated BBN for a hydrogen concentration of 18%v/v

Figure 7-11 provides a comparison of the BBN results based on the Prior values (Figure 7-3) with the updated results for the 18%v/v and the 29.5%v/v limits given in Figure 7-10 and Appendix D, Figure D-10, respectively. The comparison is given in terms of

the main variables that affect the hydrogen concentration. These variables are ullage volume, hydrogen retention volume and the total volume of hydrogen in the ullage.

The observation from Figure 7-11 is that the ullage volume decreases whilst the hydrogen retention volume and the total hydrogen volume in the ullage both rise with increasing hydrogen concentration. This trend is as expected because the hydrogen concentration is inversely proportional to the ullage volume, while the hydrogen retention and total hydrogen volumes are directly related.

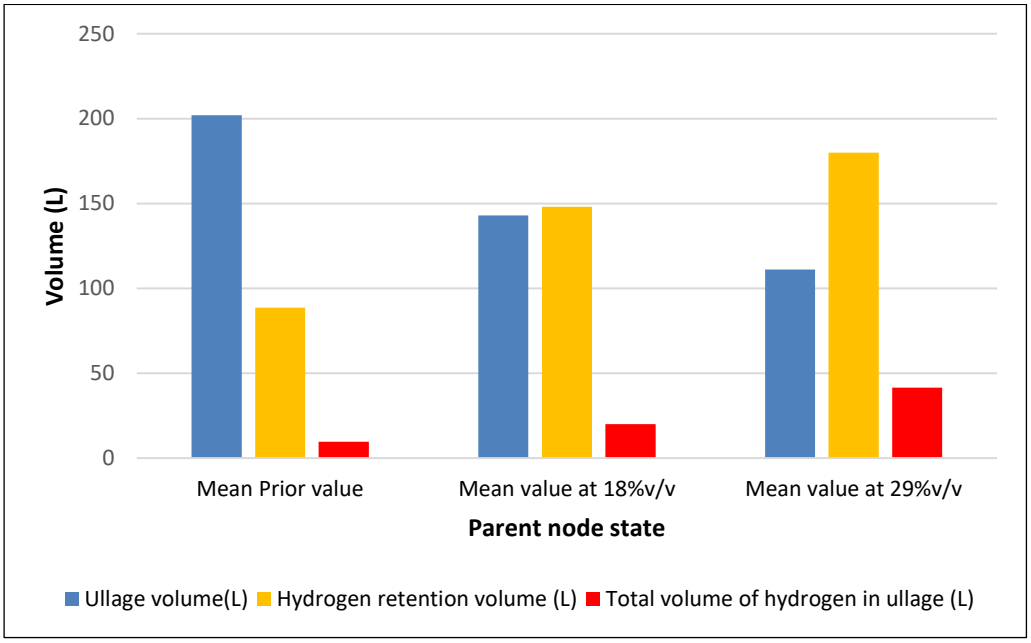

Figure 7-11: Comparison of the most hazardous conditions with Prior values

A further trend observed in Figure 7-11 is that, in comparison with the Prior BBN results, the total hydrogen volume in the ullage and the hydrogen retention volume would need to increase four times and twice, respectively before the 29.5%v/v hydrogen concentration is reached. To reach the 18%/v detonation limit these two variables would need to increase two fold. These increases are considered significant as a substantial change in the probability distribution of the three variables would need to occur before the 18%v/v and 29.5%v/v states are reached. For example, the prior probability of the hydrogen retention volume being in the range 40-80L is 36.5% (Figure 7-3). For the 18%v/v and 29.5%/v/v most hazardous states, the probability of the hydrogen retention volume being in the range 40-80L would need to reduce to under 1% and 0%, respectively and shift to the 120-160L and 160-200L range at 76% and 100% probability.

The prior probability of the ullage volume being above 171L is 68% in accordance with Figure 7-3. The 18%v/v and 29.5%v/v states would require the probability of the ullage volume being above 171L to reduce to just below 2% and 0%, respectively.

Clearly, the significant change to the probability distribution needed to reach the hazardous 18%v/v and 29.5%v/v hydrogen concentration limits suggests that the risk of these events is small. Primarily it is the ullage volume, hydrogen retention volume and hence the discontinuous release volume which are the key sensitivities that affect the risk of reaching these most hazardous states.

7.9 Conclusions for Chapter 7

Hydrogen gas generated from the corrosion of metallic magnesium (Magnox) waste, and to a lesser extent radiolysis of radioactive liquors, can potentially be retained within the sludge waste forms. Disturbance of such waste within transportable storage skips can lead to a sudden discontinuous release of a large volume of hydrogen within the vessel ullage space. A Bayesian Belief Network has been developed to model the uncertainty associated with hydrogen hold-up and sudden release scenarios, and hence the effect on the hydrogen concentration in the vessel ullage space.

The BBN model based on Prior beliefs shows that under normal storage operations, when the potential for vessel disturbance and a discontinuous release of hydrogen is small, there is approximately a 40% chance that the hydrogen concentration will remain below the 4%v/v Lower Flammable Limit. If a discontinuous release of hydrogen occurs, there is approximately a 40% chance that the hydrogen concentration will be in the range 4% to 16%v/v.

An analysis to determine the conditions necessary to reach the least hazardous hydrogen concentration of 4%v/v showed that the parent nodes which present the greatest sensitivity are the total hydrogen volume in the ullage, skip lid filter performance and the total hydrogen generation rate. The contribution from radiolytic hydrogen generation has shown to be insignificant such that corrosion of Magnox is the dominant mechanism.

CHAPTER 8 : CASE STUDY 5 - BAYESIAN BELIEF NETWORK ANALYSIS OF THE LIKELIHOOD OF A CRITICALITY IN CONTAINERS OF MATERIAL MIXED WITH PuO_2

8.1 Introduction to Chapter 8

Nuclear chemical plants handle containers of material mixed with variable quantities of the fissile radionuclide Pu-239 in the form PuO_2. Due to the presence of the fissile radionuclide in the waste material and the likelihood that water is also being present within the containers, there is the potential for a nuclear fission reaction. This is illustrated in Figure 8-1.

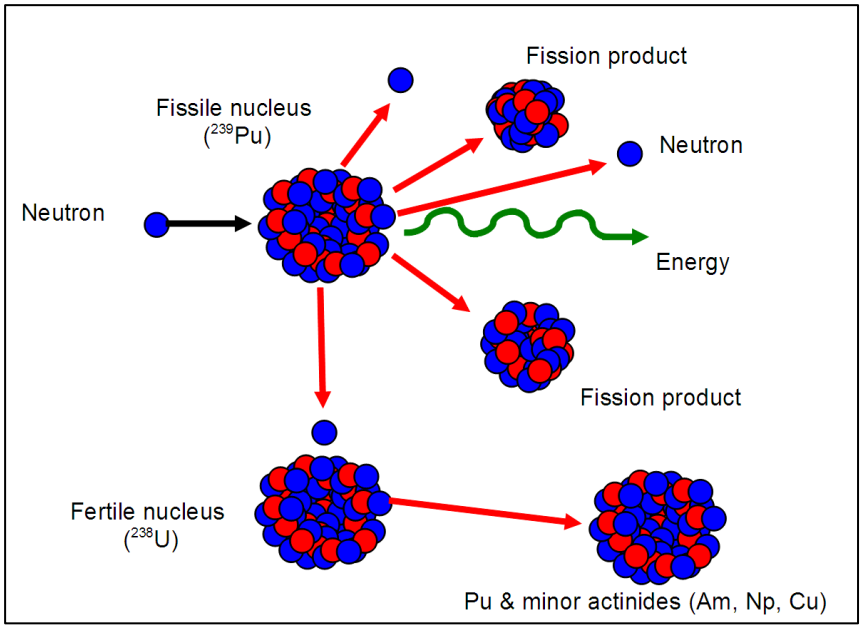

Figure 8-1: Simple illustration of a Pu-239 fission reaction [www.*iync.org website*]

In a typical fission associated with Pu-239, as discussed by *Knief, 2008* and the *Nuclear Power Web, 2019,* the radionuclide absorbs a neutron ($_0n^1$) which leads to splitting of the nucleus into smaller radionuclides, referred to as 'fission products'. The fission products are Zirconium ($_{40}Zr^{103}$) and Xenon ($_{54}Xe^{134}$) and additional neutrons. The fission reaction also results in the release of a large amount of heat energy and gamma (γ) radiation. This reaction can be expressed by the following equation:

$$_0n^1 + {}_{94}Pu^{239} \rightarrow \textit{fission} \rightarrow {}_{54}Xe^{134} + {}_{40}Zr^{103} + 3\ {}_0n^1 + \gamma + \text{Heat}$$

The release of three additional neutrons in the fission process above means that further fissions of other Pu radionuclides can occur, thus leading to a chain reaction. This is commonly referred to as a 'criticality' in nuclear safety. Water within the fissile material behaves as a 'moderator'. This is the medium that reduces the speed of the neutrons thus increasing the potential for them to be absorbed by the recipient nuclide in the fission reaction. Therefore, the moderator mass as well as the amount of fissile material

within a given volume are the key factors when determining the likelihood of a criticality. This is acceptable in a nuclear power reactor where controlled heat production within a shielded environment is desirable. However, an uncontrolled criticality event leading to a release of gamma radiation in an operating environment in nuclear chemical plants is obviously detrimental to the workforce and must be avoided.

As part of the process for handling the plutonium contaminated material (PCM) arising in nuclear chemical plants, the material is required to be containerised within drums and compacted. This case study applies the Bayesian Belief Network methodology to develop a model to assess the likelihood of a criticality event occurring in containers of material mixed with PuO_2 within nuclear chemical plants. The BBN will take into consideration factors of uncertainty, e.g., the distribution of the moderator and fissile material mass as well as other variables such as operational control failures that lead to unsafe waste conditions.

In support of the Nuclear Decommissioning Authority (NDA), *Hicks, 2007* carries out a criticality safety assessment to identify safe limits in terms of the moderator and fissile material masses for different types of wastes from nuclear facilities and subsequent transportation and long-term storage. By identifying safe limits, *Hicks, 2007*, demonstrates how a criticality could be prevented. However, an uncertainty analysis of the factors affecting the likelihood of a criticality and the application of the BBN approach to identify the best means of managing the hazard has not been previously undertaken for nuclear chemical plants.

8.2 Factors affecting the likelihood of a criticality

A meeting was held with the SL Criticality Subject Matter Experts (SMEs) in 2017 to discuss the criticality issues experienced in nuclear chemical plants and to identify a hypothesis which could be modelled in a BBN. *Ahmed, 2017c* provides the minutes of the meeting. The meeting with the SMEs also aimed to identify the key factors affecting the likelihood of a criticality. The hypothesis for this BBN concerns a drum containing a certain mass of water, W_i, and a mass of PuO_2, M_j, which is required to be compacted. The previous criticality safety assessments, e.g., by *Hicks, 2007* and *Hicks, 2009*, show that the greater the amounts of fissile Pu and moderator in a container, the greater is the likelihood of a criticality. The ratio of the fissile mass to moderator is also a key factor that affects the likelihood of a criticality. Therefore, the potential for a criticality arises if operations accidentally lead to addition of excess quantities of fissile material and moderator to the container beyond the safe specified limits, and subsequently allowing the material to be compacted.

It is known that the geometry of the fissile material and moderator in a container, particularly during compaction of the waste, becomes a significant factor that dictates the likelihood of a criticality. It is also known that spherical geometries of the fissile material including the moderator increase the likelihood of a criticality. Figure 8-2 provides an illustration of the relationship between the fissile material in a spherical geometry and the moderator within a container of waste.

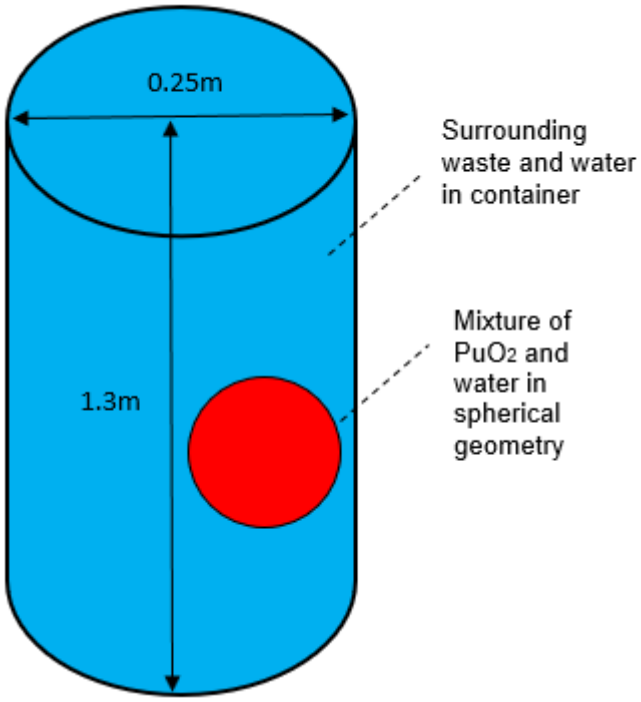

Figure 8-2: Illustration of a waste container of fissile material and water moderator in spherical geometry

For spherical geometries, there are existing data on the critical mass, as given in the Criticality Handbook, an extract from which is reproduced in Appendix E, Table E-1. The Criticality Handbook, Appendix E, lists the ratios of the moderator to the actual mass of fissile material and the corresponding masses of PuO_2 at which a criticality will occur (SM). Often the relationship between the critical mass of PuO_2 (SM) and ratio of moderator mass to the mass of PuO_2 in the waste material is represented graphically as shown in Figure 8-3. This is based on the Criticality Handbook, given in Appendix E, Table E-1. It is emphasised that all data used in this case study are based on the previously published generic criticality safety assessments and is not specific to any particular nuclear chemical plant.

The curve given in Figure 8-3 represents mixtures of water and waste consisting of the PuO_2 compound containing 100% Pu-239 isotope, which is based on the MONK 9A JEF 2.2 code. This is a well-recognised program for criticality assessments undertaken

by organisations such as SERCO, as reported by *Putley and Prescott*, 2007). Essentially the curve shows that the mass of PuO_2 required for a criticality reduces significantly as the moderator to PuO_2 mass ratio is increased. The critical mass reaches a minimum at the moderator to PuO_2 mass ratio of around 30 and then increases sharply for larger ratios. Similar Criticality Handbook data for waste mixtures containing other Pu isotopes, e.g., Pu-240, have also been established as shown in Appendix E, Table E-1.

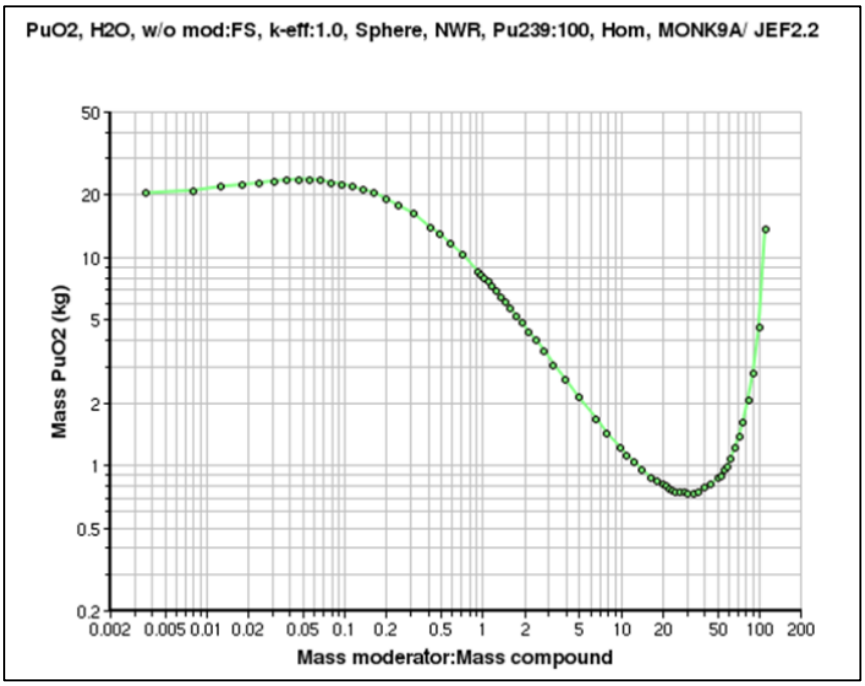

Figure 8-3: Relationship between Mass of Compound, PuO_2 (100% Pu239), and Ratio of Mass Moderator to compound [*obtained from Criticality Handbook*]

The distinct shape of the curve in Figure 8-3 can be explained by first considering the main processes involved in nuclear fission. At times, instead of a neutron being captured by the nucleus of another atom and initiating a fission reaction, it can collide with the nucleus but without reacting with it, and subsequently scatter away at a lower kinetic energy. Moderators such as water provide an ideal medium for enabling scattering and reducing the neutron energy. The scattered neutron with the reduced energy is also referred to as a 'thermal neutron', which has a much higher chance of colliding and reacting with another radionuclide than a non-thermal or fast neutron.

The thermalisation of neutrons subsequently increases the likelihood of a fission propagating to a chain reaction or a criticality. An increase in the number of thermalised neutrons also leads to a reduction in the critical mass, which is the minimum quantity of fissile material needed for a fission to propagate to a criticality. Therefore, the left hand side of the curve in Figure 8-3 shows that at low quantities of the moderator relative to fissile mass, the mass of fissile material needed for a criticality, i.e., the

critical mass, is high. As the amount of moderator relative to the fissile mass is gradually increased, the number of thermalised neutrons within the system also increases, hence reducing the critical mass. Therefore, there is a fall in the critical mass with increasing moderator to mass ratio.

An interesting feature of the water moderator is that the hydrogen atom in the water molecule also has a good ability to absorb the neutrons due its high cross-sectional area for absorption. By absorbing a neutron, the hydrogen atom transitions to form the isotope Deuterium. Therefore, when a system contains relatively large quantities of water, a point is reached where absorption begins to dominate moderation. The gradual absorption of the neutrons by the hydrogen atom leads to a reduction in the number of thermalised neutrons, such that the fissile mass needed for a criticality increases. Hence, as shown in Figure 8-3, at very high moderator to fissile mass ratios, there is an increase in the critical mass.

While compaction of waste within a single drum will lead to concentration of fissile material in a given volume, this does not necessarily mean that the likelihood of a criticality is significant. This is because some wastes consist of very small quantities of fissile material while others are high in content. Nevertheless, it is acknowledged that compaction will potentially lead to rearranging the material shape ideal for a criticality, i.e., a spherical geometry, which is illustrated in Figure 8-2.Therefore, compaction represents the bounding case condition in terms of the likelihood of a criticality. The BBN uncertainty analysis assesses the likelihood of criticality across the whole distribution of the mass of PuO_2 and moderator volume, i.e., from very small to large values.

If the critical mass limit for a particular moderator and waste fissile content is expressed as SM and the actual mass of fissile material in the drum is M_i, then the expert opinion of the Criticality Subject Matter Experts (SMEs) suggests that for a ratio of M_j/SM less than 1.00, the likelihood of a criticality is zero [*Ahmed, 2017c*]. Previous experience also suggests that if the ratio of M_j/SM is equal to 1.00, the probability of a criticality is typically 0.001. The Criticality SMEs also advised that the probability of criticality increases linearly with increasing M_j/SM ratio until the ratio reaches 1.3 [*Ahmed, 2017c*]. For an M_j/SM ratio greater than 1.3, the probability of criticality is 1. The criticality probability criteria detailed here are representative of compacted material resulting in an ideal spherical geometry of the fissile material mixed with the water moderator.

The likelihood of a criticality is also dependent on the fissile radionuclide composition of PuO_2. The two isotopes of Pu present in the waste mixture are Pu-240 and Pu-239. It is the Pu-239 isotope which is fissile and therefore the relative make-up of this form of Pu affects the likelihood of a criticality. Various compositions of these two forms of Pu can exist in the waste material. This model assumes the presence of two compositions, i.e., up to 15% weight or zero quantities of Pu-240 within the same container. Waste material without any Pu-240 is assumed to be mixed with 100% Pu-239. It is postulated that the weight fraction split between the 15% Pu-240 and 100% Pu-239 compositions is 0.8 and 0.2, respectively.

The potential for a criticality only arises if there is a failure in the plant operating regime leading to addition of waste with excessive fissile and moderator mass to the drum such that the critical mass limit is exceeded. However, the risk from such failures leading to unsafe waste conditions is managed through radiometric assay systems. These are neutron and gamma radiation detection systems, as well as operational controls including gamma dose monitoring and prevention of water addition to drums. Provided that such controls are in place, unsafe waste conditions would be detected in the early stages of the waste processing operations before allowing the material to be compacted. The BBN analysis therefore takes into consideration a failure of these operational and engineered controls on the overall risk of a criticality.

Figure 8-4 provides an illustration of the interrelationships between the key factors affecting the overall risk of a criticality. This conceptual model is colour coded to distinguish the factors leading to a criticality (cyan nodes A to F) and the operational control failures (yellow nodes G to R).

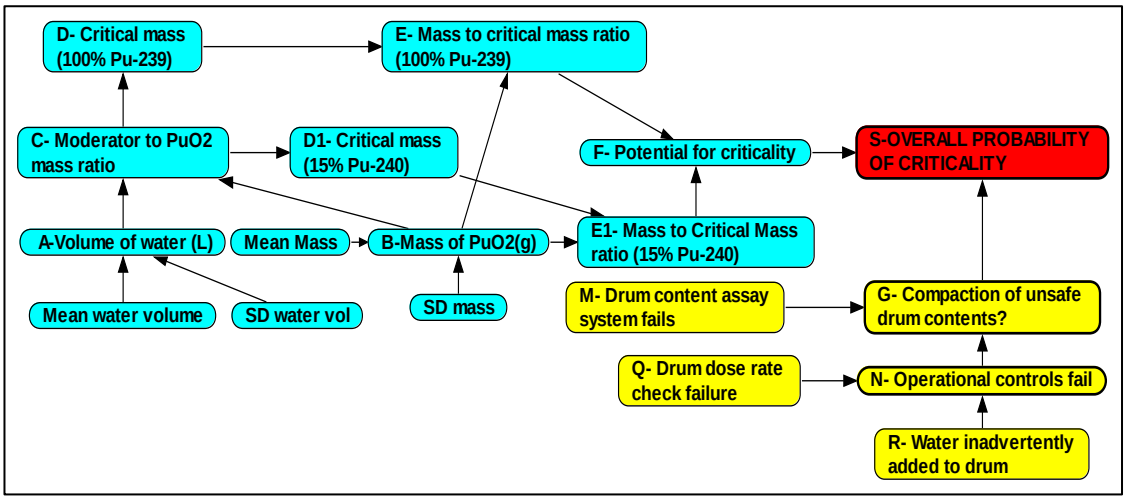

Figure 8-4: Concept network for the likelihood of a criticality in container of waste mixed with fissile PuO_2

The general logic is that a failure in the operational controls would need to occur that leads to unsafe waste conditions within the drum, allowing the material to be compacted. The operational failures in conjunction with the factors leading to the potential for a criticality give rise to the overall probability of a criticality, represented by Node S. In terms of the logic associated with the factors affecting the potential for a criticality, it is hypothesised that a drum contains solid waste material contaminated with water volume (Node A) and PuO_2 mass (Node B). As discussed in Section 8.2, whilst there are many isotopic compositions of Pu associated with the PuO_2 compound in the drum, the likelihood of a criticality is bound by two particular compositions which are 15% weight Pu-240 and 0% Pu-240. The 0% Pu-240 composition is assumed to be 100% Pu-239. This case study considers the presence of both these compositions within a single drum.

The likelihood of a criticality is dependent on Nodes E and E1, which are the ratios of the mass of PuO_2 in the drum to the safe critical mass of the compound with 0% Pu-240 (Nodes D) and with 15% weight Pu-240 (Node D1). The probability distribution of the safe critical mass given in Nodes D and D1 is dependent on Node C which is the ratio of the moderator mass (Node A) to PuO_2 mass (Node B).

8.3 Derivation of probability distributions for Nodes A, B and C

The main objective of this case study is to determine the probability of a criticality event across the whole distribution of the fissile PuO_2 mass and moderator volume. However, the probability of a criticality for a low drum water content and a low PuO_2 mass also needs to be assessed. This is to ascertain whether the risk from these conditions is still significant and if protection systems are needed to reduce the risk further.

For the reason above the starting conditions for the BBN analysis are that the mean water volume and PuO_2 mass are very low. Values of 8E-5L of water and 0.1g PuO_2 mass were used in agreement with the Criticality SMEs. However, as part of the overall uncertainty analysis, the maximum value of each of these parameters was considered to be 40L and 25 kg, respectively. These maximum values were also accounted for in the distribution. A lognormal distribution was assigned for both nodes A and B based on the advice from the criticality team.

Node C, i.e., the ratio of moderator mass to PuO_2 mass, is a continuous variable with the probability distribution derived using the equation:

$$C\ (A, B) = \frac{998 * A}{B} \tag{8-1}$$

Where the value 998 is the density of water(g/L), A is the water volume (L), B is the mass of PuO_2 in the drum(g). Using equation 8-1, the minimum and maximum values for discretisation of Node C were calculated. Twenty equal discretisation intervals were assigned for Node C.

8.4 Derivation of probability distribution for Nodes D and D1

Since Node C is a Parent to Node D, the BBN methodology requires the probability distribution for Node D to be expressed as a function of Node C. The safe critical mass values for Pu listed in the Criticality Handbook are only relevant to specific moderator to Pu mass ratios (Appendix E, Table E-1). Therefore, the handbook data cannot be directly applied to Node C. To derive the safe critical mass as a function of Node C, the criticality handbook data for each of the two compositions i.e., 15% weight Pu-240 and 0% Pu-240, as listed in Appendix E Table E-1, were plotted in Figure 8-5 and Figure 8-6. Trendlines were then fitted to the graphs using Excel.

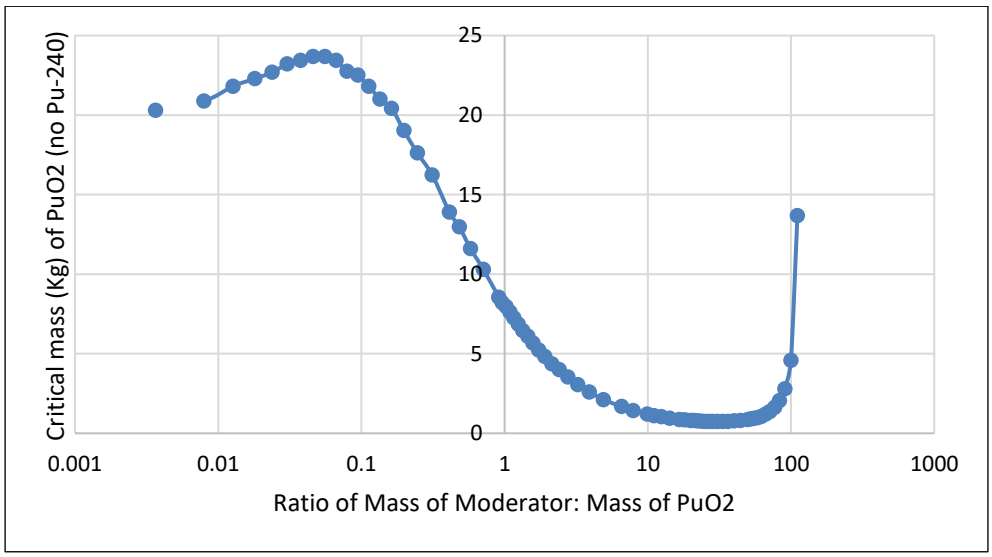

Figure 8-5: Critical mass curve for PuO_2 with 0% Pu-240

Using the Excel trendline function it was observed that some sections of the curves in Figure 8-5 and Figure 8-6 are exponential whilst others are polynomial or logarithmic in character. Therefore, a single trendline fitted to the whole of the curve did not yield the highest R^2 value. However, if each curve is split into discrete sections highly representative trendline equations for the safe critical mass, y, as a function of Node C, i.e., ratio of moderator mass to PuO_2 mass, with R^2 values of 0.9 or higher were derived.

The optimum trendline functions for both compositions of PuO_2 are tabulated in Appendix E Table E-2. Each of the equations for specific ranges of the ratio of moderator mass to PuO_2 mass were entered into Nodes D and D1 of the BBN using

the IF function. For example, for the ratio of mass of moderator to mass of PuO_2 of 0 to 0.04, the first equation in Table E-2 was entered in Node D as if(C<=0.04,20.042*exp(4.8139*C).

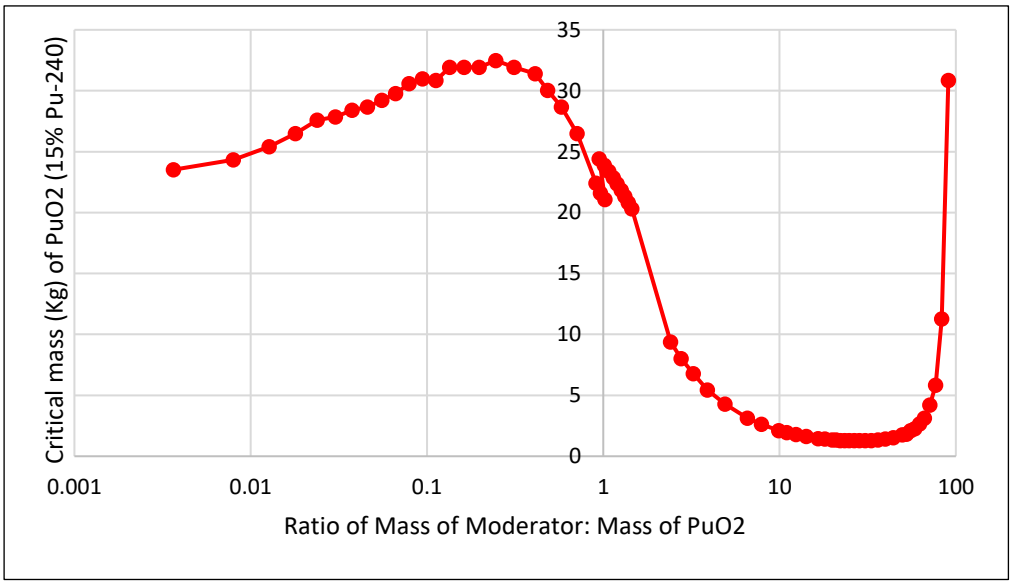

Figure 8-6: Critical mass curve for PuO_2 containing 15%weight Pu-240

8.5 Derivation of probability distribution for Nodes E and E1

Nodes E and E1 are continuous variables, which represent the ratio of PuO_2 mass (Node B) to critical mass for the 0% Pu-240 and 15% weight Pu-240 compositions, respectively. Since both compositions are assumed to be present within the same drum, a single probability distribution is assigned for the overall PuO_2 mass (Node B). However, the actual probability distributions of Nodes E and E1 are specific to the composition of the PuO_2 compound, which are affected by Nodes D and D1, respectively. Hence, the following equations are applied in Netica to derive the probability distributions for Nodes E and E1, where the factor 1000 represents the conversion of Node D and D1 values from kg to g:

$$E\ (B,D) = \frac{B}{1000 * D} \tag{8-2}$$

$$E\ (B,D1) = \frac{B}{1000 * D1} \tag{8-3}$$

Nodes E and E1 were discretised over the range 0 to 1.3 or higher as the criticality probability is affected by this range (see discussion on Node F below).

8.6 Derivation of Conditional Probability Table for Node F

Node F calculates the overall probability of criticality assuming both compositions of PuO_2 are present within the drum. Unlike the other preceding nodes, Node F is a

discrete variable since the occurrence of a criticality can only result in two possible outcomes i.e., true or false. Hence the derivation of the Conditional Probability Table for this node was based on a calculation using Excel spreadsheet as discussed below.

The criticality probability is calculated as a function of Nodes E and E1 based on a set of known criteria. As discussed earlier, it is known that for the ratio of mass to critical mass of less than 1, the likelihood of a criticality is zero and for values above 1.3 the criticality probability is 1. For the ratios between 1 and 1.3, the probability of criticality grows linearly in accordance with the function P(x) = 3.33x – 3.329, such that if E is set at 1.3 and 1, the probability of criticality would equate to 1 and 0.001, respectively. Compaction of the fissile material also has an impact on the likelihood of a criticality. Based on the discussions with the Criticality SMEs, this linear function has already accounted for the compaction condition.

In agreement with the Criticality SMEs, the weight fractions of the 100% Pu-239 and 15% weight Pu-240 compositions in the overall mass of PuO_2 are set at 0.2 and 0.8, respectively. Hence, to calculate the probability of criticality for each discretised value, a factor of 0.2 and 0.8 is applied to the Node E and Node E1 values, respectively. Based on these criteria, Appendix E, Table E-3 calculates the probability of criticality as a function of the Node E and E1 values, using the lower bound value for each range. For instance, based on the range 1 to 1.05 in Node E, the probability of criticality is calculated in Table E-3 as 0.2*(1*3.33-3.329), i.e., 0.0002.

The CPT matrix for Node F was generated using the probability of criticality values given in Appendix E Table E-3. This CPT is presented in Appendix E, Table E-4. Since Node F determines the overall probability of criticality based on the presence of both compositions of PuO_2, the individual probabilities for the two compositions were added together. For example, with a Node E1 value in the range 1 to 1.05, the probability of criticality calculated in Table E-3 is 8E-4. For a Node E value in the range 0 to 1, Table E-3 determines a criticality probability of 0. Hence the overall probability of criticality calculated in Table E-4 is 8E-4 + 0, i.e., 8E-4. Similarly, Table E-3 was used within an Excel spreadsheet to generate the probability values for all the other combinations in the CPT matrix in Table E-4.

8.7 Overall risk of criticality

It is emphasised that the probability of criticality determined in Node F cannot be considered in isolation as a fault would have to occur coincidentally that leads to unsafe drum contents and subsequent compaction of the waste. To reduce the overall risk of a criticality, there are a number of plant operational and engineered controls in place

that would detect the unsafe waste conditions at the early stages of the process. Following this detection, the compaction operation will be prevented and further remedial actions, such as removal of the suspect material, will be undertaken. Therefore, for a criticality event to occur these controls would also need to fail. The specific engineered and operational control measures that would need to fail are:

i) Safety Integrity Level (SIL) 1 rated drum assay system (Node M). This system detects neutrons and gamma radiation from the fissile material, thus providing a warning of abnormal waste contents before the material is compacted. In accordance with the standard *IEC 61508,* a worst case probability of failure on demand (Pfd) of 0.1 is considered appropriate for SIL 1 rated equipment.

ii) Independent supervisory checks of the gamma dose rates from the drums to reveal any abnormal waste material (Node Q). For independent supervisory checks, a Human Error Probability (HEP) of an order of magnitude less than the most conservative value of 0.1, specified by *HSE, 2017,* is considered reasonable.

iii) Operational controls requiring prevention of water addition to the drums (Node R). For a failure of this control measure, a more conservative HEP of 0.03 is applicable as this does not assume any supervisory checks.

In terms of the logic for the overall fault sequence, Node N represents the total probability of failure of both operational preventative measures (Nodes Q and R). Therefore, a Boolean AND logic gate is applied to calculate the probability of Node N. Node G represents the failure of the radiometric assay system (Node M) and the operational controls (Node N) leading to compaction of the unsafe drum contents. Hence a Boolean AND logic gate is applied between these two nodes to calculate the probability of Node G.

Nodes A to F of the Bayesian Network determine the likelihood of a criticality without taking account of the protection systems listed above. Node S represents the overall probability of criticality coincident with a failure of the protection systems. Therefore, to calculate the final fault probability in Node S, the criticality probability given by Node F is combined with the total probability of failure of the protection systems via a Boolean AND gate.

8.8 BBN results

Based on the derivation of the Prior probability distributions for nodes A to S given above, Figure 8-7 shows the fully developed BBN. All results are presented as percent probability in Figure 8-7. The BBN assesses the overall probability of criticality within

drums of fissile waste material due to a failure of the protection systems for detection of unsafe waste conditions and subsequent compaction of the waste. The probability of criticality without taking credit for any protection systems is predicted as 0.17% in Node F, i.e., 1.7E-3. However, when taking credit for all the protection systems represented by Node G, the final probability of the event reduces significantly to 4.9E-8 (Node S). This is presented as a very low probability of '0+' in Figure 8-7. However, the precise value of 4.9E-8 was obtained for Node S in Netica by using the 'Findings – Calibration' function.

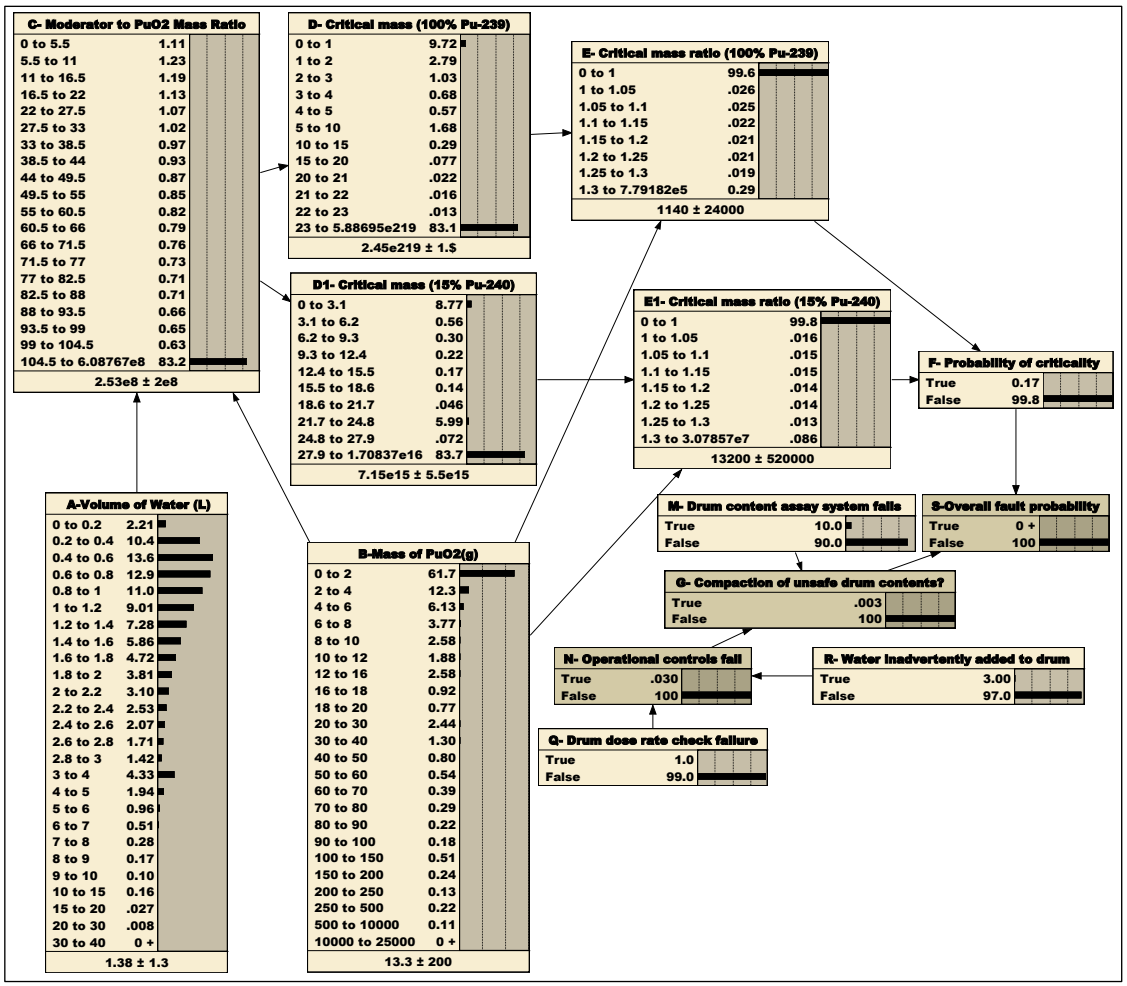

Figure 8-7: BBN for failure of operational controls leading to a criticality

8.9 Comparison of BBN results with expected trends

To demonstrate the validity of the BBN, the results based on specific conditions were compared with expected trends given in the Criticality Handbook. As shown in Appendix E, Table E-1, the Criticality Handbook lists the critical mass values for specific Moderator to PuO_2 mass of the waste for both compositions. The BBN Node C was updated with specific values of the Moderator to PuO_2 mass ratio given in the handbook.

The updated BBN values for the critical mass determined in Nodes D and D1 were then compared with those listed in the handbook. The results of this comparison for the 0% Pu-240 and the 15% Pu-240 compositions are presented in Figure 8-8 and Figure 8-9, respectively.

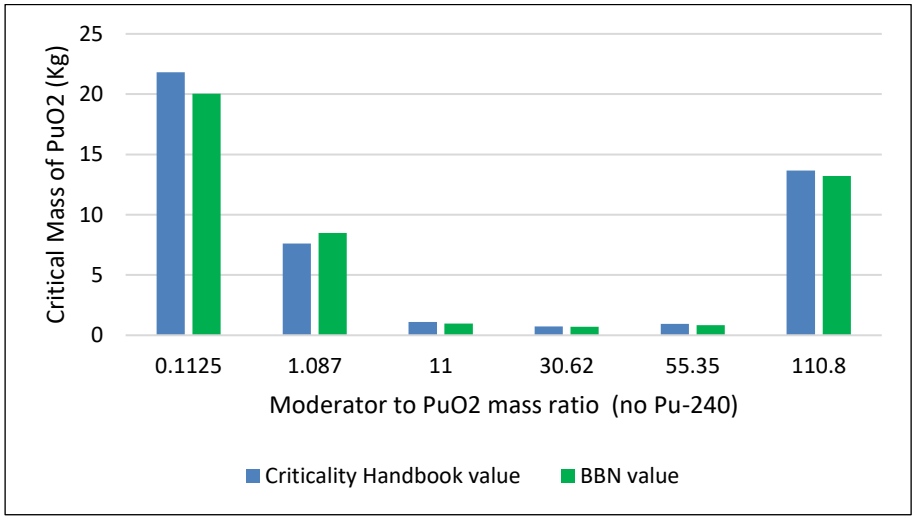

Figure 8-8: Comparison of BBN critical mass values with the Criticality Handbook for the 0% Pu-240 composition

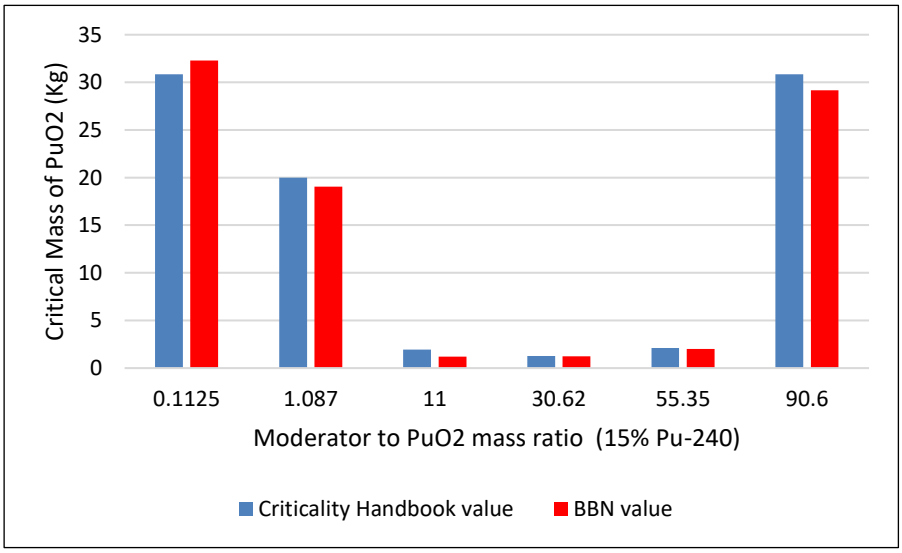

Figure 8-9: Comparison of BBN critical mass values with the Criticality Handbook for the 15% Pu-240 composition

The comparison in Figure 8-8 and Figure 8-9 clearly shows that the results for the critical mass values as a function of the moderator to PuO_2 mass ratio derived by BBN are very similar to the Criticality Handbook values.

A further observation from the comparison given in Figure 8-8 and Figure 8-9 is that for both compositions, at small moderator to PuO_2 mass ratios of less than 1, the critical mass decreases steadily. The critical mass then plateaus at the mid-range of the

moderator to mass ratios of around 11 to 55 and rises sharply at high ratios of above 90. This trend also agrees with the expected behaviour illustrated in Figure 8-5 and Figure 8-6 for the critical mass curves based on the Criticality Handbook data. This agreement confirms that the functions used in Node D and D1 are reasonably accurate.

8.10 Analysis of conditions required for the least hazardous state

The probability of criticality of 1.7E-3 in Figure 8-7 is based on a low mean PuO_2 mass and water volume. However, as part of the overall distribution, the analysis still takes account of the maximum values of these parameters, i.e., 25kg and 40L, respectively. This subsequently leads to the relatively high probability of 1.7E-3. To test the effect on the probability of criticality, when the PuO_2 mass and water volume are fixed to the lowest ranges, Nodes A and B were instantiated to 0.1L and 0.1g, respectively. These lowest range values represent the least hazardous conditions and the updated results based on these states are presented in Figure 8-10.

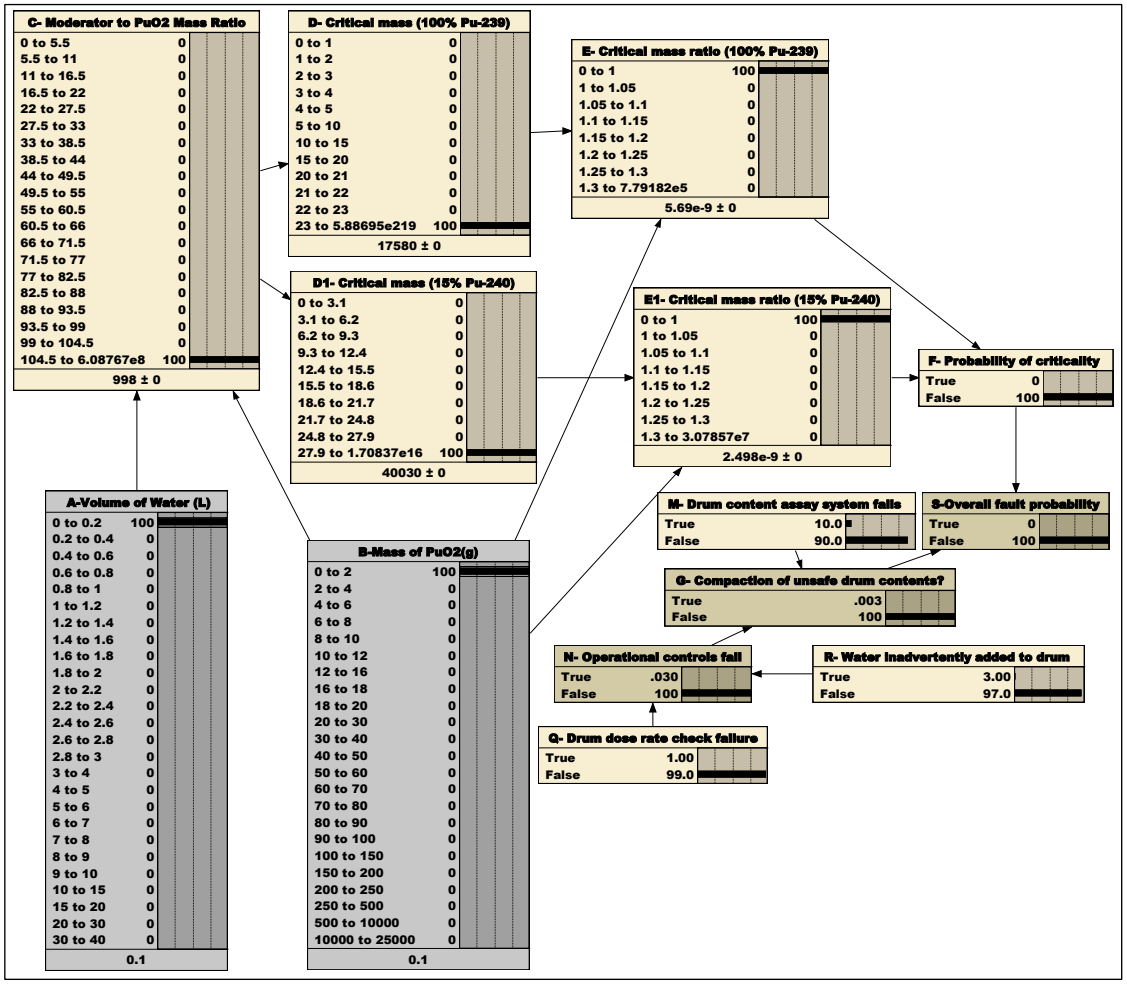

Figure 8-10: BBN results for water volume =0.1L, PuO_2 Mass = 0.1

The updated results in Figure 8-10 show that due to the low mass of PuO_2 in the drum, the probability distribution of the moderator to mass ratio in Nodes D and D1 being in

the high ranges of > 23 and 27.9 respectively, increases to 100%. This subsequently leads to a probability of nearly 100% for the mass to critical mass ratios being in the 0 to 1 range and hence a probability of criticality of zero. As illustrated in Figure 8-5 and Figure 8-6, this trend agrees with the expected behaviour when comparing with the Criticality Handbook. The Criticality Handbook data show that at very high moderator to mass ratios for both compositions, the mass of PuO_2 required for the system to become critical would also need to be high. Typically, these high masses would equate to 30kg and 14kg for the15% Pu-240 and 0% Pu-240 compositions, respectively.

8.11 Probability of criticality under abnormal operating conditions

It is considered that under fault conditions abnormally high quantities of PuO_2 and water could potentially be added, resulting in an increased probability of criticality. The worst case conditions would be those that lead to a probability of criticality of 1. To determine the minimum quantities of water and PuO_2 mass needed in the drum for a criticality probability of 1, Node S was instantiated to the 100% True state, as shown in Figure 8-11.

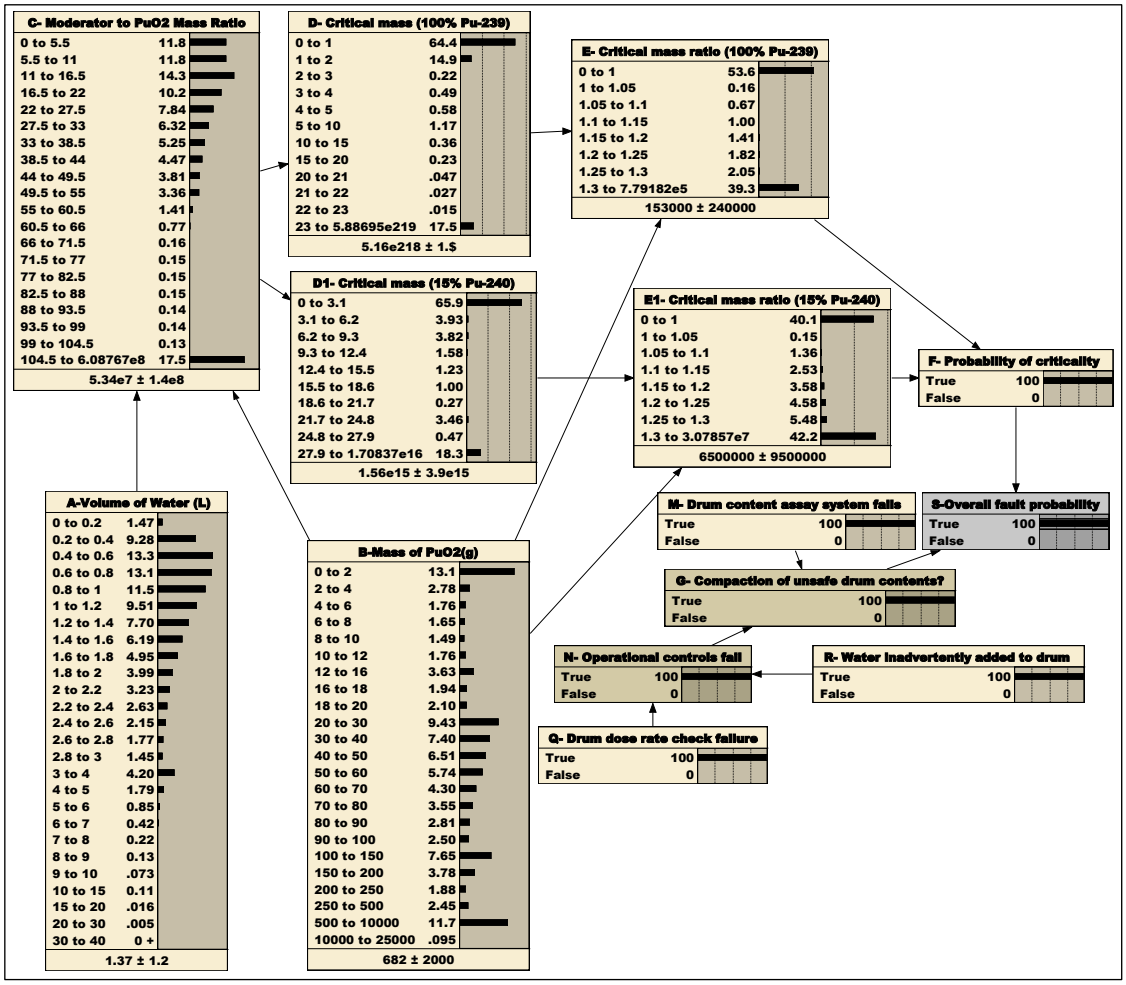

Figure 8-11: Conditions leading to a probability of criticality of 1

It can be seen in Figure 8-11 that the probability of the PuO_2 mass being in the low range of 0 to 2g (Node B) would need to reduce significantly from the Prior value of 62 % (Figure 8-7) to 13%. The probability of the PuO_2 mass being in the high range of 500 to 10000g would need to increase from negligible to almost 12%. This increase leads to a probability distribution of over 75% for the moderator to PuO_2 mass ratio being less than 50.

Essentially, the results in Figure 8-11 suggest that the probability of criticality is highly sensitive to the PuO_2 mass in the drum being in the range 500 to 10000g. Thus, provided that the PuO_2 mass is kept below this range, and the water volume distribution is broadly the same as the Prior distribution, the probability of criticality would reduce significantly. This expected behaviour is confirmed in Figure 8-12. When the PuO_2 mass in the drum is instantiated to less than the 500g, the criticality probability reduces by two orders of magnitude to a value of 0.018.

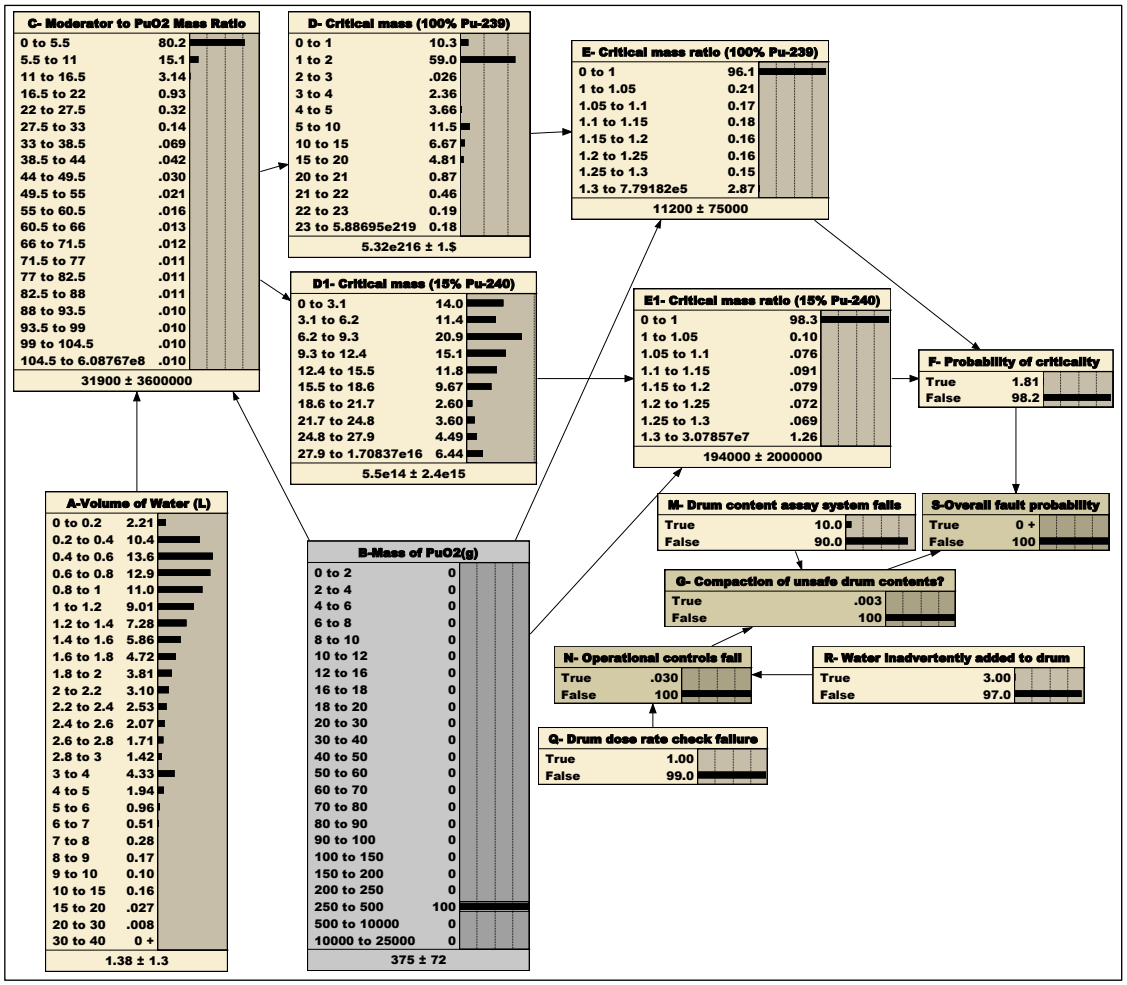

Figure 8-12: Effect of controlling the PuO_2 mass to less than 500g on criticality probability

8.12 Sensitivity to failure of protection systems

The Prior probability distributions of the water volume and PuO_2 mass are such that these two variables are predominantly in the low range. Therefore, it could be argued that such low values may lie below the detection range of the drum content assay system (Node M) or the drum dose rate monitoring system (Node Q). To assess the effect of a failure of these detection systems on the overall fault probability, the true states of Nodes M and Q were instantiated to 100%. The results of this updated BBN are presented in Figure 8-13.

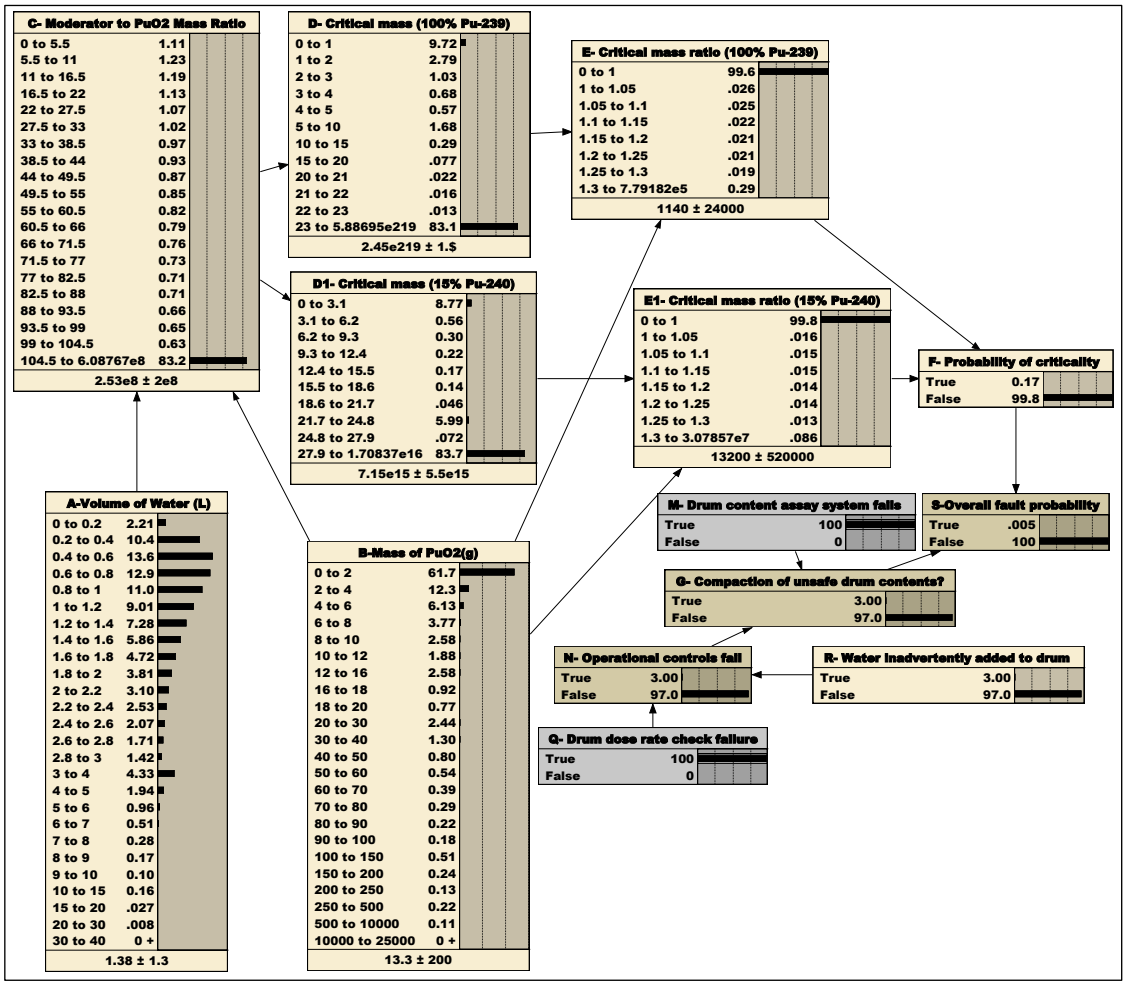

Figure 8-13: Updated BBN for drum dose rate monitoring and content assay system failures

Figure 8-13 shows that when the drum assay and dose monitoring systems are in a 100% failed state, the overall fault probability in Node S increases significantly from the Prior value of 4.9E-8 to 5E-5. This shows that the overall fault probability is highly sensitive to the performance of the protection systems against the criticality event.

8.13 Conclusions for Chapter 8

This case study applies the Bayesian Belief Network methodology as an enhanced approach for assessing the likelihood of a criticality event in containers of nuclear waste material mixed with PuO_2 and water. Furthermore, the BBN approach has enabled an uncertainty analysis of the key factors contributing to the likelihood of a criticality, which has not been previously undertaken for nuclear chemical plants.

In summary, the sensitivity analysis using the Bayesian updating feature has revealed the following additional information from the model that was not previously known:

i) The least hazardous plant configuration, which results in a negligible probability of criticality, could be achieved by ensuring that the PuO_2 mass and the water volume in the container are below 500g and 2L, respectively.

ii) Based on the Prior distributions of the water volume and PuO_2 mass, it has been demonstrated that the typical values of these parameters under normal operating conditions are very low, i.e., <0.1L and <0.1g, respectively. Under these normal operating conditions, the uncertainty analysis shows that the risk of a criticality is negligible.

iii) The overall fault probability is highly sensitive to the performance of the drum assay and dose monitoring systems. A failure of these protection systems will result in an increase in the criticality probability by almost three orders of magnitude.

The BBN analysis has enabled an assessment of the risk of a criticality across the whole probability distribution of the key variables. It has also allowed the impact of changes to the operating conditions to be analysed. Through Bayesian inference, the model has used abductive reasoning to enable identification of safe limits for plant operating conditions. These capabilities clearly indicate the benefits of the BBN methodology as a useful tool for undertaking criticality assessments and aid key decision making in nuclear plants.

CHAPTER 9 : CASE STUDY 6 - BAYESIAN DECISION NETWORK ANALYSIS FOR INSTALLING A COMPRESSED AIR SUPPLY TO MITIGATE THE RISK OF HYDROGEN EXPLOSIONS IN ANCILLARY PROCESS VESSELS

9.1 Introduction to Chapter 9

Compressed air for the management of radiolytic hydrogen generation within process vessels in nuclear chemical plants, is normally introduced via the liquor level monitoring instruments i.e., the pneumercator pipework (Figure 9-1). A blockage or an inadvertent isolation of this pipework, particularly where it dips into the liquor, would result in a reduction in the air supply to the vessel. Hence this could lead to an increase in the hydrogen concentration in the vessel ullage space. If the pneumercator blockage is not cleared and the air supply to the vessel is not reinstated a flammable atmosphere within the ullage space could form. This could potentially lead to an ignition of the hydrogen in air mixture and a release of radioactivity from the vessel, which must be avoided.

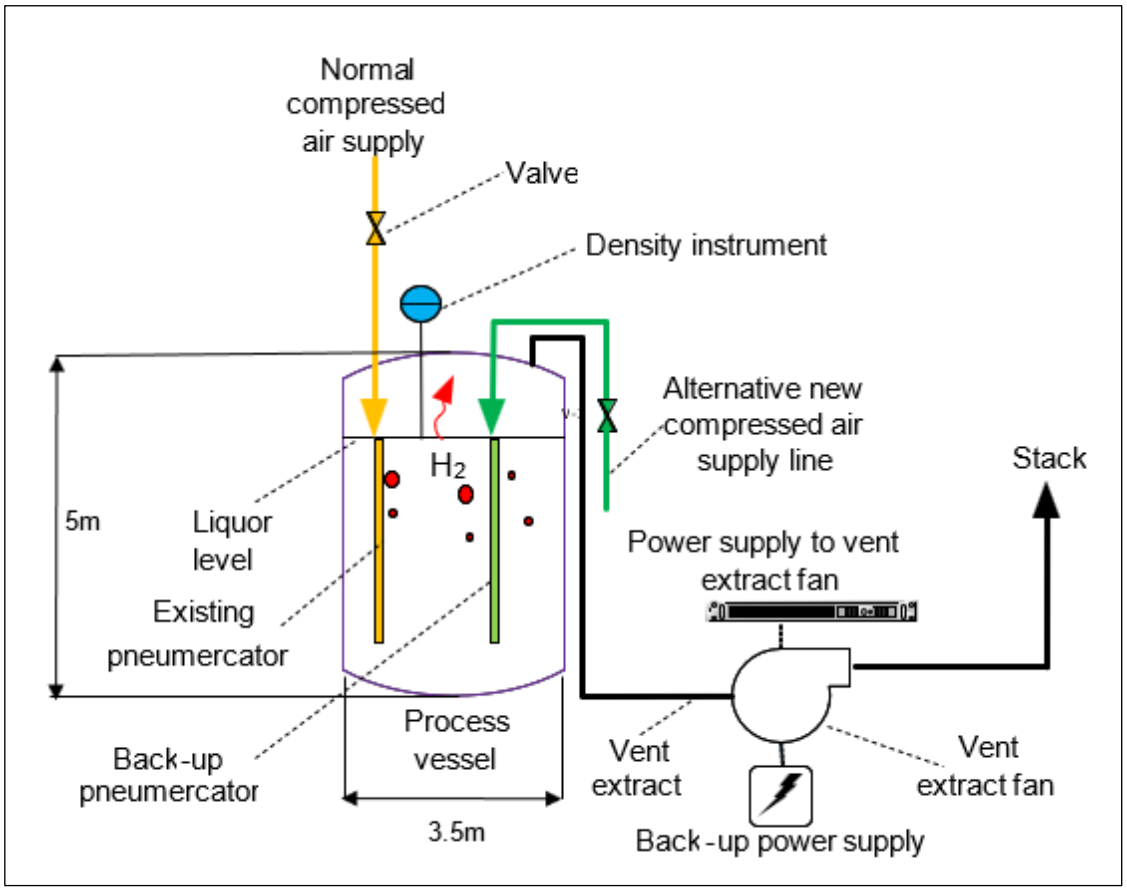

Figure 9-1: Pneumercator air supply and extract system

It is a legal requirement that the accident risk in nuclear chemical plants is shown to be As Low As Reasonably Practicable (ALARP). The ALARP principle requires a demonstration of the best practicable improvements to the plant and process that can be achieved against any shortfalls in the design or operational regime [*Jones-Lee and Aven, 2011*]. As discussed by *French et al, 2005* and in accordance with the *HSE Cost*

Benefit Analysis (CBA) website, most ALARP decisions about making improvements are based on qualitative arguments, supported by a CBA. It is considered that a detailed quantified approach to ALARP decision making could be used to further strengthen the choices on making improvements. The Bayesian Decision Network is a technique that enables decision making in a quantified and structured manner. Such a technique has not been previously applied to safety cases for nuclear chemical plants.

This case study investigates the application of Decision Networks to decide whether an improvement to the plant design for managing the radiolytic hydrogen hazard in nuclear chemical plants is justifiable. The Bayesian Decision Networks use a Decision node and a Utility node linked to the standard Bayesian Belief Network. By assigning quantified monetary values to the various decision outcomes in the Utility node, a quantitative decision can be reached within the Decision Network analysis. The ability to link the risk factors to the decision uncertainty is a unique feature of the Bayesian Decision Networks which is not provided by other decision analysis techniques.

9.2 The hypothesis

The hypothesis for the Decision Network is that a blockage in the pneumercator pipe occurs which leads to an obstruction in the normal compressed air supply to the ullage space of an ancillary process vessel. The reduced air flow due to the pneumercator blockage results in hydrogen accumulation within the ullage space. Effective operation of the pneumercator system is also dependent on the vessel vent extract system being functional. This is because a continued supply of air via the pneumercator with the extract system being in a failed state will result in tripping of the air supply to prevent vessel pressurisation. Therefore, the hypothesis also takes into consideration a failure of the vent extract system.

For the hydrogen concentration in the vessel ullage space to reach the 4% LFL, a coincident failure to re-instate the pneumercator or the vent extract system within the required time limit would need to occur. For any significant consequences from a hydrogen explosion to arise, a failure of the protection systems against pneumercator blockages or the vent extract system would also need to occur. The actual decision uncertainty is whether the risk of a hydrogen explosion due to pneumercator blockages or a failure of the extract system is significant enough to warrant the installation of an alternative air supply system. More specifically, the benefits of installing an alternative compressed air supply against the risk of the duty pneumercator blockages are explored.

9.3 The Decision Network

A concept model for the Decision Network is shown in Figure 9-2. The Decision Network comprises nature nodes numbered 1 to 25. The yellow coloured nodes 1 to 8 model the failure of the hydrogen dilution system due to a loss of the pneumercator system. The green coloured nodes 9 to 17 are nature nodes which model the ventilation extract system failure. Nodes 1 to 17 are collectively modelled with the red coloured nature nodes, 18 to 25, to determine the overall radiological risk of a hydrogen explosion in the vessel. The Nature nodes link to the Utility node 26, represented by the elongated pink hexagon, and the Decision node 27. Collectively these nodes model the monetary value for the decision on whether to install an alternative compressed air supply.

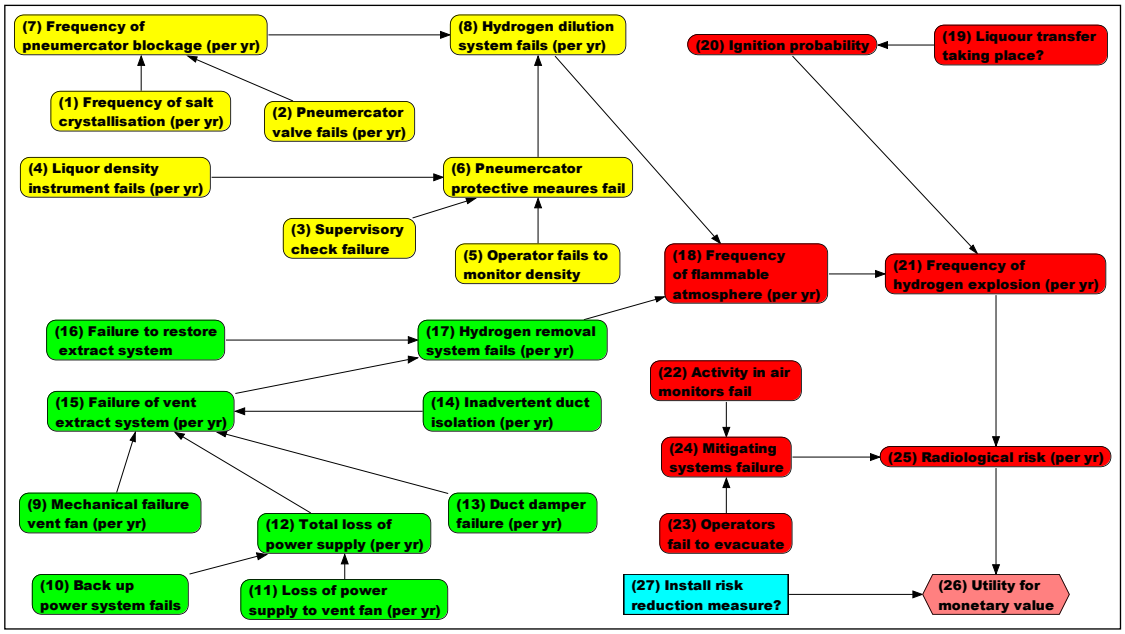

Figure 9-2: Concept model for the decision network

A description of each of the nodes 1 to 26 together with the justification of the Prior probabilities is given in Appendix F, Table F-1.

9.4 Methodology for modelling frequency of hydrogen explosion

9.4.1 Boolean logic gates

For this case study, the frequency of a hydrogen explosion event is expressed as a hazard rate, i.e., events per year, as opposed to a dimensionless probability value. This is necessary in order to derive the cost benefit utility values for the decision analysis, which requires the risk to be expressed as a frequency. Further details about this requirement are given in Section 9.8. The standard approach for modelling frequencies and probabilities of events is Fault Tree Analysis (FTA) which applies the following rules

based on Boolean algebra, explained in the user manual for the FTA software, LOGAN, [*LOGAN, 2018*]:

i) Event A (frequency) OR Event B (frequency) = Event C (frequency).

ii) Event D (frequency) AND Event E (probability) = Event D (frequency).

iii) Event F (probability) AND Event G (probability) = Event H (probability).

iv) Event I (probability) OR Event J (probability) = Event K (probability).

v) Event L (frequency) AND Event M (frequency) is forbidden.

Whilst the FTA software is capable of modelling frequencies of events using the logic above, Bayesian Networks can only apply Boolean algebra to probability values. The principles for replication of the Boolean algebra for modelling frequencies within the Bayesian Networks are discussed below.

In accordance with the set theory, the Boolean OR logic gate between two events A and B can also be expressed as the union of the sets A and B, i.e., A U B. This is based on the concept that if two events, A and B, are not independent their probability area will coincide so that they cannot be simply added together. In this case, as shown in equation 9-1, *Bolstad, 2007* states that the intersection between the events A and B must be subtracted from the summed probabilities of A and B:

$$p(A\ OR\ B) = p(A \cup B) = p(A) + P(B) - p(A \cap B) \tag{9-1}$$

The intersection of A and B is equivalent to the product of the two events (equation 9-2).

$$p(A \cap B) = p(A) \times p(B) \tag{9-2}$$

Substituting equation 9-2 into equation 9-1 gives:

$$p(A\ OR\ B) = P(A \cup B) = p(A) + p(B) - p(A) \times p(B) \tag{9-3}$$

If on the other hand the probabilities of the two events are small, then the probability p(A) x p(B) becomes relatively insignificant and can be ignored.

Based on the same principles used for deriving equation 9-3, for three events A, B and C, the probability of A OR B OR C can also be expressed as the probability of the union of three sets, i.e., A U B U C. As demonstrated by *Taylor, 2019,* this probability is equivalent to the expressions given by equations 9-4 and 9-5.

$$\begin{aligned} p(A \cup B \cup C) = {} & p(A) + p(B) + p(C) - p(A \cap B) - p(A \cap C) - p(B \cap C) \\ & + p(A \cap B \cap C) \end{aligned} \tag{9-4}$$

$$p(A\ OR\ B\ OR\ C) = p(A) + p(B) + P(C) - p(A) \times p(B) - p(A) \times p(C) - p(B) \times p(C) + p(A) \times p(B) \times p(C) \quad (9\text{-}5)$$

When modelling two or more frequencies, i.e., a hazard rate per year, via an OR gate, the same rules as those given by equations 9-3 and 9-5 apply.

For modelling AND logic gates, the relationship between a probability p(A) and a frequency f(B) can simply be equated to the intersection between the two events:

$$p(A)\ AND\ f(B) = p(A) \times f(B) \quad (9\text{-}6)$$

As stated in in Boolean rule number (v) above, equation 9-6 cannot be applied when events A and B are both frequencies.

9.4.2 Derivation of BBN child node failure probabilities and frequencies

To enable calculation of frequencies of the Child nodes within the Bayesian Network equations 9-2, 9-3, 9-5 and 9-6 were applied using continuous nodes. From Figure 9-2 the following main Child nodes can be identified which affect the frequency of the Top Event, i.e., radiological risk of a hydrogen explosion in the vessel:

- Frequency of pneumercator blockage (Child node 7).
- Failure probability of pneumercator protective measures (Child node 6).
- Frequency of failure of hydrogen dilution and removal systems (nodes 8 and 17)
- Flammable atmosphere and hydrogen explosion frequencies (nodes 18 and 21).
- Radiological risk of a hydrogen explosion in the vessel (Child node 22).

For each of the above Child nodes, Appendix F Table F-1 provides an explanation of the logic applied to determine the associated probability or frequency. A detailed derivation of the data used are also given. For example, as illustrated in Figure 9-2, parent nodes 1 and 2 are both frequencies with maximum values of 0.38 and 0.6 failures per year respectively (Appendix F Table F-1). As discussed in Table F-1, either of these two events must occur for the Child node 7 to arise such that an OR gate applies. Hence using equation 9-1, the maximum frequency for node 7 was calculated as 0.38+0.6, i.e., 0.98/year. Similarly, by applying equations 9-2, 9-3, 9-5 and 9-6 to all the remaining Child nodes, the associated CPTs were determined using Netica. The main CPTs are listed in Appendix F Table F-2 to Table F-5.

9.5 Key insights obtained from the BBN analysis

Based on the fault progression logic shown in the concept network (Figure 9-2) and the derivation of the CPTs for the nature nodes given in Appendix F Table F-1, Figure 9-3 presents the quantified BBN.

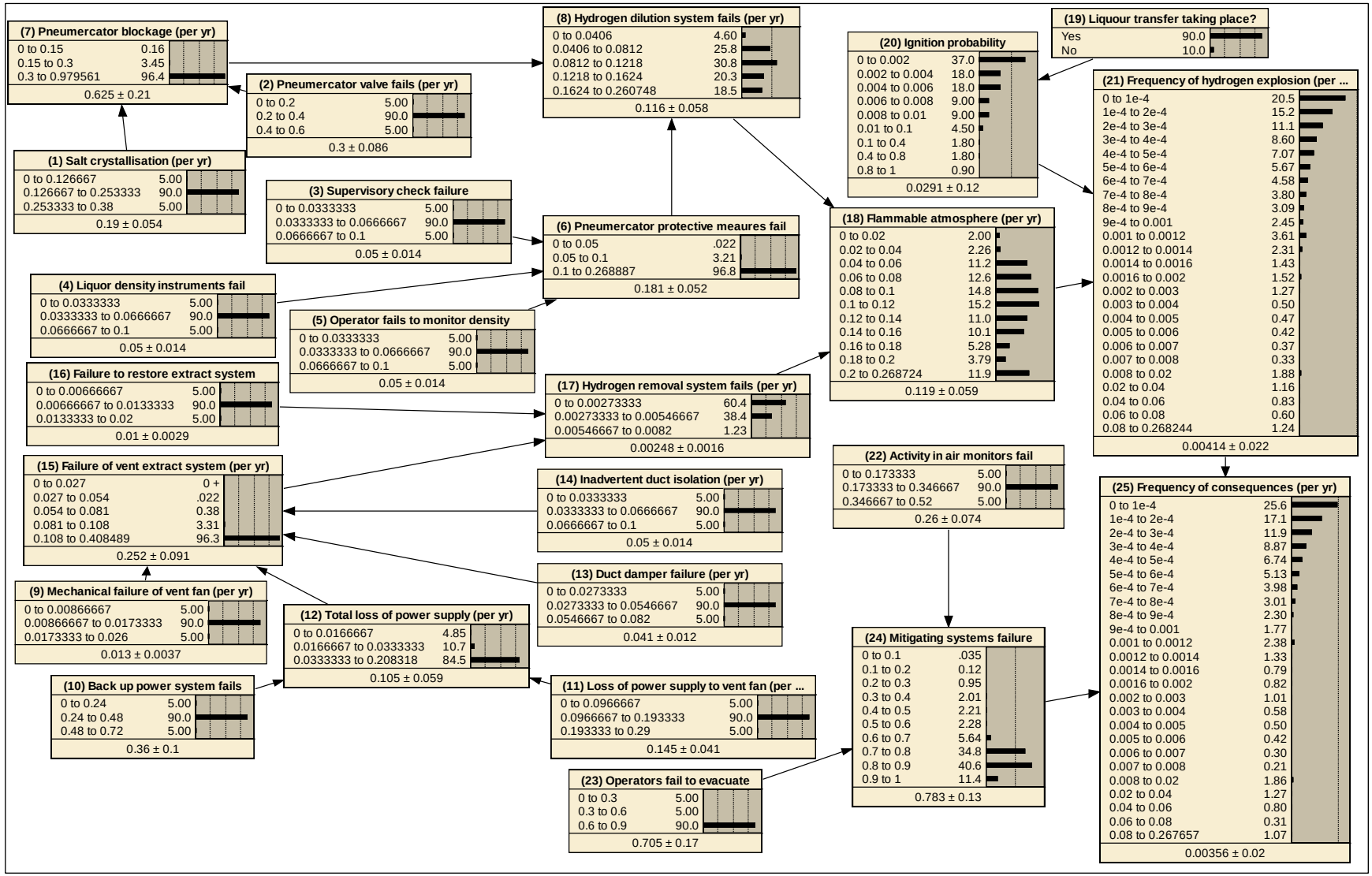

Figure 9-3: Overall quantified BBN for frequency of vessel hydrogen explosion

The results presented in Figure 9-3 are based on only the nature nodes for the derivation of the risk of radiological consequences of a hydrogen explosion in the ancillary vessel. The development of the Decision Network based on Figure 9-3 is detailed in Section 9.8. Figure 9-3 shows that the radiological risk frequency ranges from values as low as 1E-4/year to a maximum of 0.27/year. The distribution of the radiological consequence frequency (Node 25) being in these ranges is approximately 26% and less than 1% respectively. The probability distribution within the BBN also shows that the mean frequency of radiological consequences is 3.6E-3/year.

To ascertain if the risk values determined above are acceptable, a comparison can be made with the risk criteria for faults leading to a high consequence. Chapter 2, Section 2.3.1 specifies that for a high radiological consequence to the workforce, an acceptable level of risk is 1E-3/year or less. The consequence to the workforce in relation to this case study is 1000mSv, which is classed as high. Also, the upper bound and mean risk values of 0.27/year and 3.6E-3/year respectively, have exceeded the 1E-3/year risk target. This suggests that a decision analysis is required to show if the risk can be reduced practicably.

Further observations from the BBN are that the main contributing mechanism for the flammable hydrogen atmosphere arising in the vessel ullage is the failure of the hydrogen dilution system, due to pneumercator blockage. The mean fault frequency of the hydrogen dilution system failure is 0.1/year (Node 8). In comparison, the failure frequency of the hydrogen removal system, i.e., vent extract, is approximately two orders of magnitude lower, with a mean value of 0.002/year (Figure 9-3, Node 17). These results therefore suggest that the governing factors that would affect the decision on whether to install a risk reduction system would be the failures associated with the pneumercator system.

Of course, the other main factor that affects the risk of a hydrogen explosion in the vessel is the ignition probability. This is evident in Figure 9-4 when the ignition probability (Node 20) is set to the lowest range of 0 to 0.002. This results in a reduction in the mean frequency of hydrogen explosion by over an order of magnitude to 1.2E-4/yr. Note that for clarity purposes, Figure 9-4 presents only parts of the BBN that have a direct impact on the hydrogen explosion frequency. Appendix F, Table F-1 discusses that the ignition probability is directly affected by the likelihood of liquor transfers in the vessel, which must remain fixed as it is a plant operational constraint. On this basis the results from the BBN analysis would suggest that any risk reduction improvements would be those that link to the reliability of the hydrogen dilution (pneumercator system).

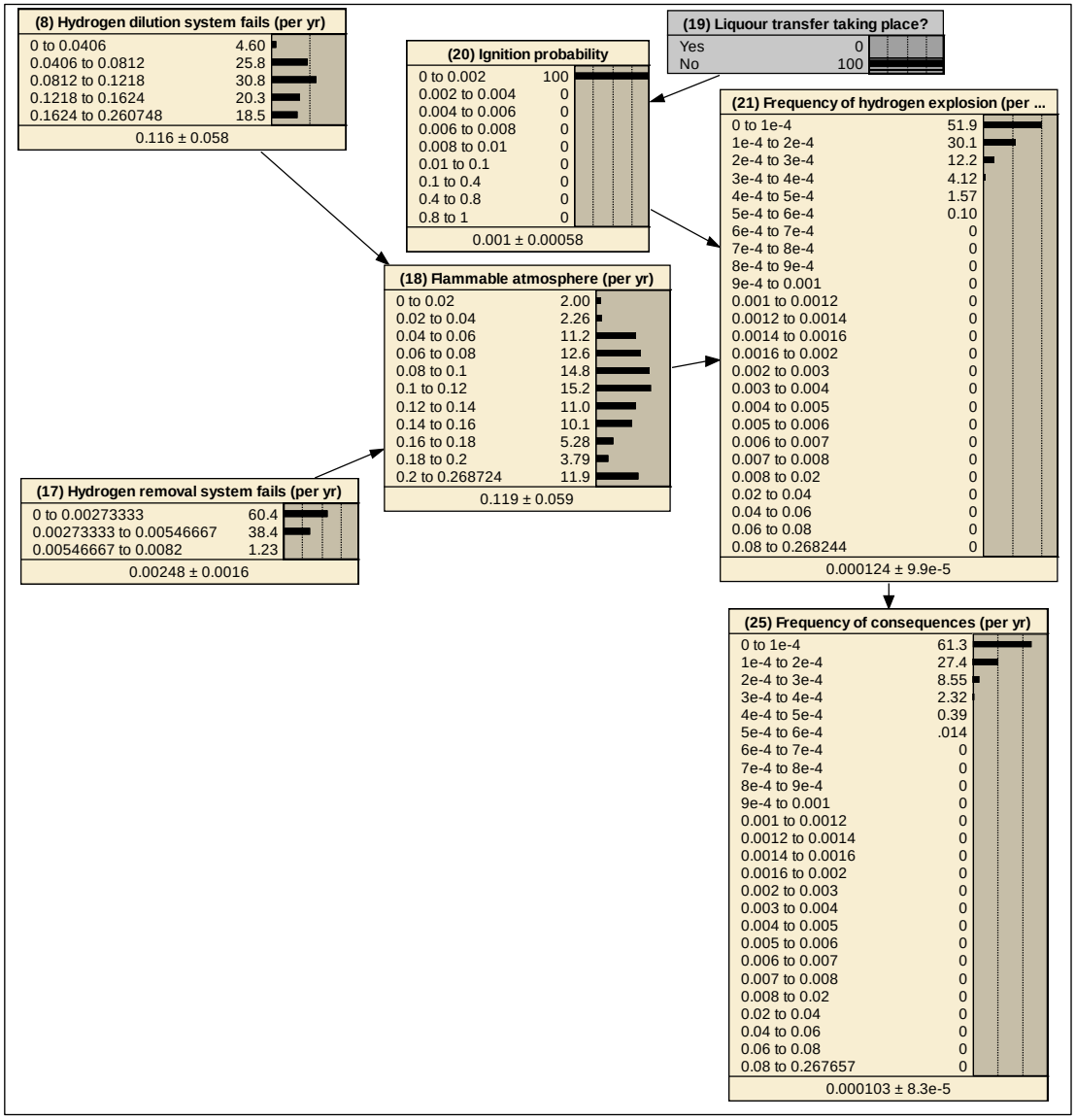

Figure 9-4: Effect of reduced ignition probability on risk of hydrogen explosion

9.6 Comparison of the BBN output with fault tree analysis

The validity of the output from the Nature Nodes of the Bayesian Network can be tested by undertaking a Fault Tree Analysis (FTA) of the same fault scenario using the Logan software (Figure 9-5). The logic used in the BBN model, as detailed in Section 9.4 and Appendix F Table F-1 was replicated in the FTA.

Based on the mean values of each of the primary input nodes, the FTA in Figure 9-5 shows that the Top Event frequency of the radiological consequences is 1.63E-3/year. If each of the input parent nodes is instantiated to the single mean values used in the FTA, then Figure 9-6 shows that the resultant values for all the Child nodes 6,7,8, 12, 15, 17,18, 21 and 25 are exactly the same as those predicted by the FTA in Figure 9-5. This demonstrates that the BBN logic is consistent with the FTA.

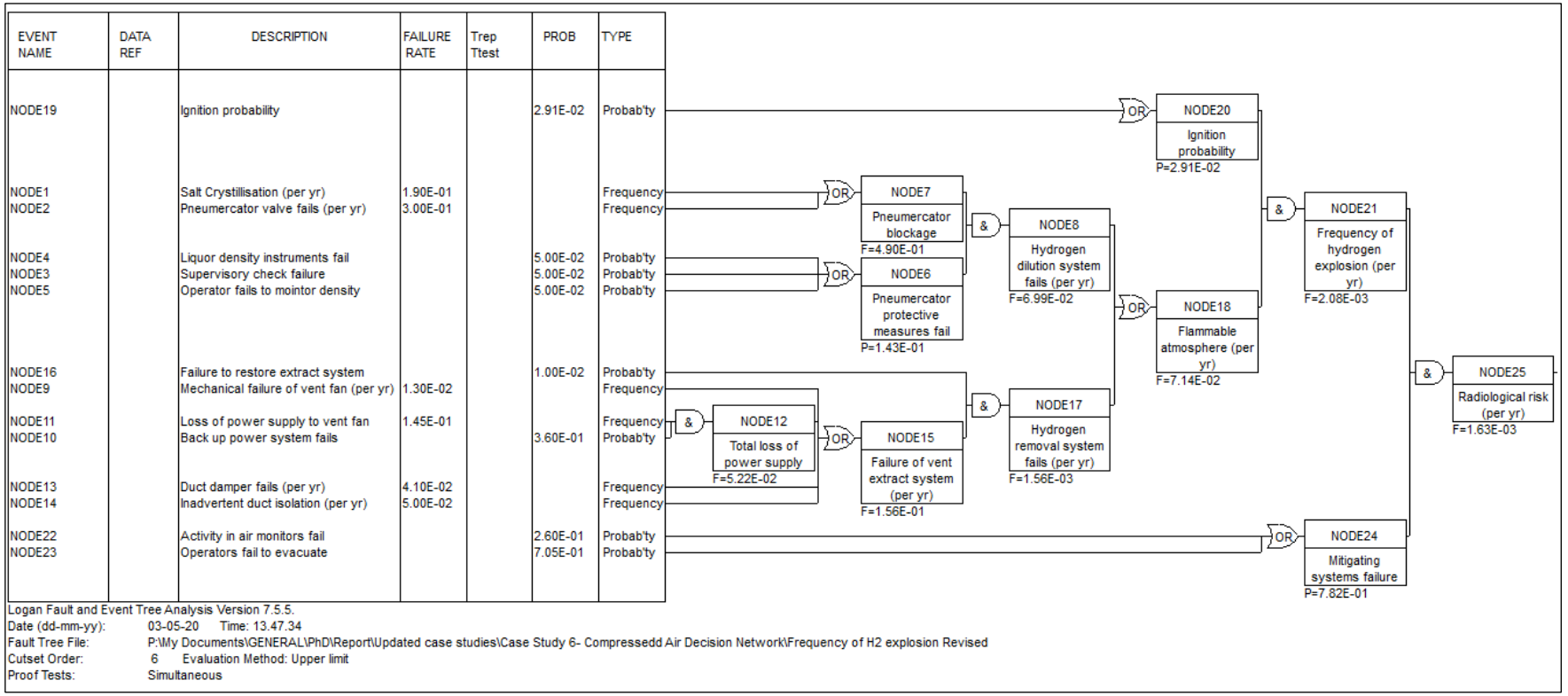

Figure 9-5: Fault Tree Analysis of radiological risk from a hydrogen explosion in the ancillary vessel

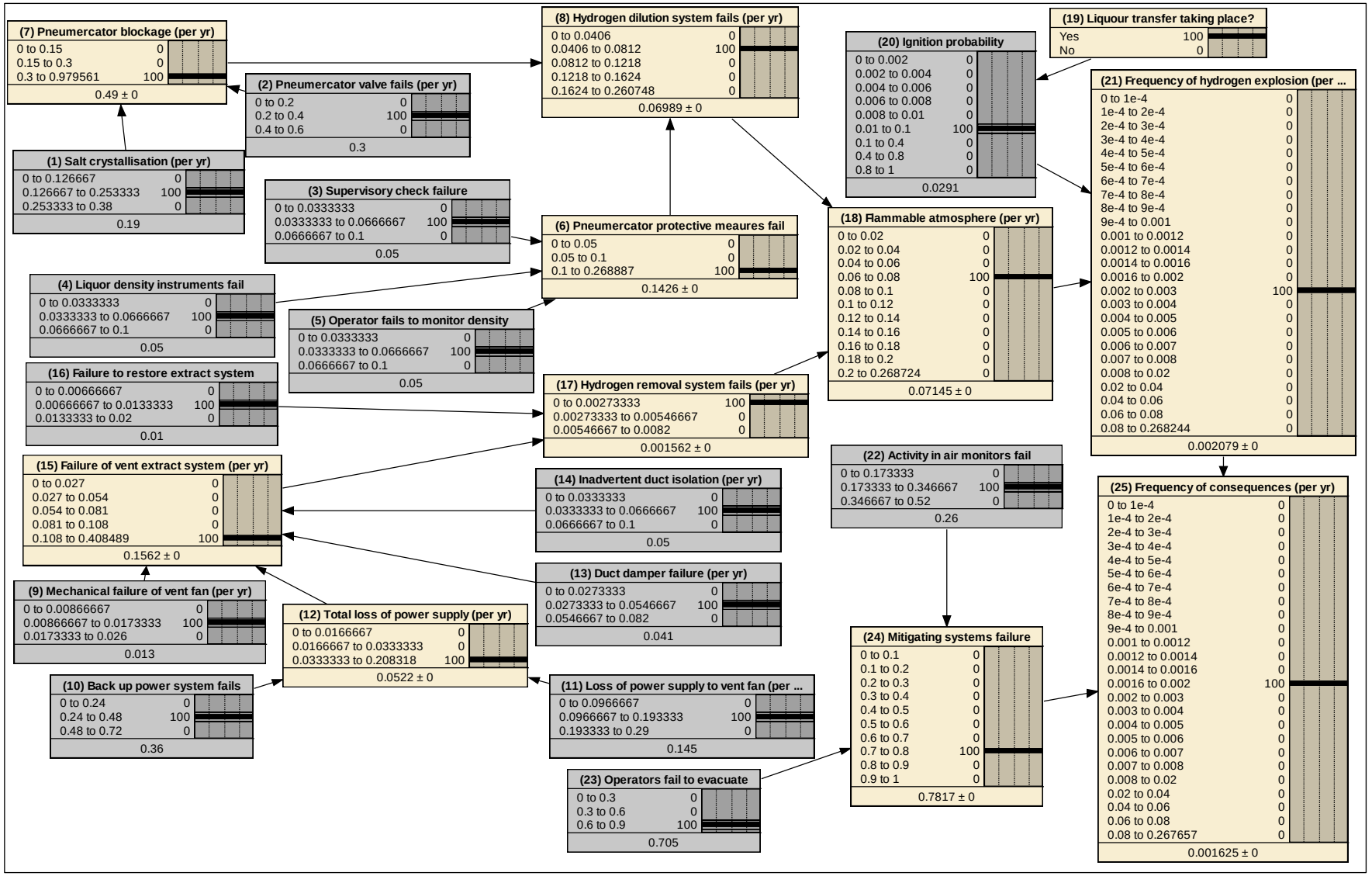

Figure 9-6: Updated BBN for radiological risk with mean input parent values

Whilst demonstrating the consistency between the BBN and the FTA, the former method provides additional information in terms of the probability distribution of the radiological risk. The FTA on the other hand calculates the final risk as a single value based on mean values of the primary events. For instance, from the BBN in Figure 9-3 shows that the probability distribution of the radiological risk being in the low and high ranges 0 to 1E-4/yr and 0.08 to 0.27/year, i.e., 27% and 1% respectively. This is useful information which can be accounted for in the overall quantified decision analysis.

9.7 Determination of hydrogen explosion hazard key sensitivities

Whilst the results from the BBN are similar to the FTA, the former technique is considered superior as it allows updating of the analysis with new evidence. This enables the effect on individual parent nodes to be observed within the same network, thus providing information on the key sensitivities. For example, if future evidence suggests that no further liquor transfers take place, then Figure 9-4 shows that the mean frequency of a hydrogen explosion (Node 21) reduces by over an order of magnitude in comparison with the Prior model (Figure 9-3).

The updating function of the Bayesian analysis also enables the effect on the Parent Nodes to be determined. Figure 9-7 demonstrates this by instantiating the lowest possible radiological risk range of 0 to 1E-4/year, in Node 25, to a probability of 100%.To achieve this desired state, Figure 9-7 shows that the following reductions in the likelihood of the associated Parent nodes would be required:

- Ignition probability reduced by over an order of magnitude.
- Mean hydrogen dilution system failure frequency reduced by 23%.

Further analysis in Appendix F Figure F-1 shows that if the mitigating systems failure probability is reduced to the 0.1 range, the radiological risk (Node 25) will again reduce to predominantly the 0 to 1E-4/year range. This suggests that the mitigating system failure also has a significant impact on the overall risk.

Effectively the updated BBN results above have enabled determination of the key sensitivities, i.e., ignition probability, hydrogen dilution system and the mitigating system failures. The updated BBN has also enabled a direct analysis of the required reduction in the likelihood of these variables. This updating of the child nodes to determine the impact on the parent nodes is not achievable in FTAs.

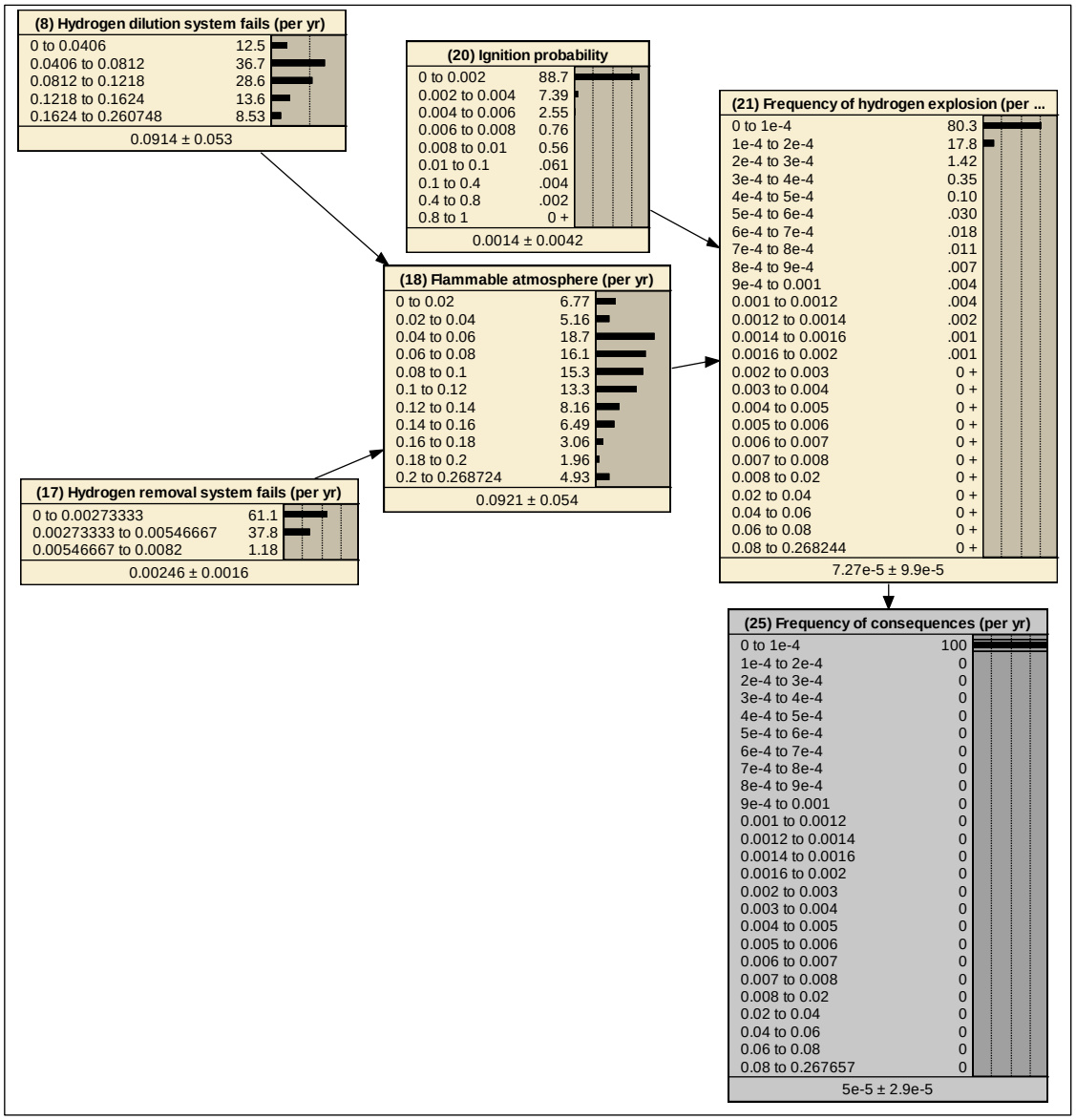

Figure 9-7: Updated BBN the conditions needed for the lowest radiological risk

It is acknowledged that the FTA software, i.e., LOGAN [*Logan, 2018*], can apply Boolean algebra to calculate the frequency of events. However, the analysis given above shows that this is also achievable in BBNs by replicating the OR and AND logic gates using equations 9-2, 9-3, 9-5 and 9-6 within the continuous node functionality. The BBN methodology is still considered beneficial as it can handle any given distribution of the primary input parent nodes to determine the distribution of the child nodes, thus enabling an uncertainty analysis.

9.8 Decision Analysis

The quantified BBN (Figure 9-3) for the radiological risk of a hydrogen explosion in the ancillary vessel shows that the hazard is primarily sensitive to the failure of the hydrogen dilution, i.e., air supply via the pneumercator system. Taking into consideration the existing protective measures and mitigating systems against the

hydrogen explosion hazard, the mean accident frequency has been determined as 3.6E-3/year. To comply with the ALARP principle, this section carries out a decision analysis to determine whether further risk reduction measures, e.g., an alternative pneumercator air supply, are warranted.

9.8.1 Analysis of total detriment from the accident

To decide whether the installation of an alternative air supply is justified on ALARP grounds, the overall detriment of the hydrogen explosion accident in terms of the radiological dose to the workforce needs to be evaluated. This dose detriment would then require comparison with the cost of the improvement. However, the utility node in a decision network can only recognise variables with a 'common currency'. Therefore, the dose detriment requires conversion to a cost or monetary value.

The HSE guidance on ALARP improvements, as detailed in the *HSE, Cost Benefit Analysis (CBA)* website, suggests that the net detriment to the workforce can be equated to a cost of around £1.3E6 per fatality. The cost from potential cancers arising due to a release radioactivity from a plant is suggested as twice this value, i.e., £2.6E6. This value was based on the year 2003 prices. However, allowing for inflation, the guidance also suggests that the value of preventing a fatality should be increased by an annual value of 2%. Hence over the 16 year period the cost of a fatality for year 2019 would increase by 32%, i.e., to £3.43E6.

Based on the studies of the effects of ionising radiation to members of the public, the HSE guidance on tolerability of risk [*HSE, 1992*] states that the risk of a fatal cancer to a person is 5 in 100 000 for every millisievert (mSv) of dose received. This can be equated to a risk of 0.05 for every 1000mSv. The ancillary process vessel contains radioactive liquor which is classed as high active waste in accordance with the categorisation of radioactive wastes by *IAEA, 2009*. As part of the long-term waste storage strategy, this liquor is required to be immobilised by conversion to a glass product. *Dunnett, 2007* provides a detailed review of the glassification process. The high level waste category of this liquor is akin to the understanding that if released, a high workforce consequence in the range 20-1000mSv [*ONR, 2020*] could potentially arise following a hydrogen explosion fault. This assumption is further qualified based on a review of the hazard reduction strategy for high active wastes, undertaken by *ONR, 2015*. It is stated that the potential consequences from a release of this type of liquor are high. Therefore, in terms of monetary value, the maximum workforce dose detriment of 1000mSv is:

£3.43E6 x 0.05 = £1.72E5

In addition to the radiological dose, the hydrogen explosion would also result in the following detriments which must be accounted for when evaluating the overall cost:

- Lost production due to plant shut down and cost of plant repairs including site remediation.
- Cost of emergency services for workforce rescue from the accident scene.

In terms of lost production, it is considered that the plant will be shut down following the hydrogen explosion. This would lead to a cessation of the downstream processes, i.e., immobilisation of the radioactive liquor within product containers. The production frequency of the containers in a normally operating plant is approximately 1 per week. Also, from discussion with plant operators, it is known that the production of each product container has a monetary value of £60,000. Given the significant implications of the hydrogen explosion event, a minimum site shut down period of 3 months would be likely. Effectively this would result in a lost production cost of £60,000 x 3 x 4, i.e., £720,000. Cost of plant repairs and site remediation, i.e., decontamination, involving deployment of resources such as purpose-built robotics, would easily amount to a minimum of £200,000. A further £100,000 is considered realistic for site emergency services, rescue of personnel and provision of a temporary safe environment until permanent repairs are undertaken.

On the basis above a total detriment of £172,000+ £720,000+£200,000+£100,000, i.e., £1.192E6 will have incurred following the hydrogen explosion event. The £1.192E6 value determined above represents the minimal detriment based on current best judgement. However, it is considered that there is still an uncertainty associated with each of the contributory factors. For example, there is an uncertainty on the total timescale for lost production. Depending on the scale of the damage caused by the incident, the timescales for plant outage could potentially be longer than the current estimate. Equally the costs for plant repairs and site remediation could increase. To account for these uncertainties and include a reasonable bounding case against unforeseen eventualities, it is considered that the total detriment could potentially increase twice in value to £2.384E6. The worst case detriment for this case study is therefore considered to be £2.384E6.

9.8.2 Comparison of total detriment with the gross disproportionate factor

The overall ALARP decision for making an improvement is also dependent on the actual cost of the improvement. The cost of the improvement requires a consideration of the alternative compressed air supply design, procurement, installation, and future

maintenance. When all these phases are costed, an overall cost of the improvement is likely to be £300,000.

The current standard technique applied to ALARP assessments in safety cases is the HSE guidance on Cost Benefit Analysis (CBA) given in the *HSE CBA website*. The CBA guidance requires a comparison of the net detriment of an accident, in terms of monetary value, with the cost of the improvement or modification. Effectively the CBA guidance stipulates that a decision for not implementing an improvement would only be warranted if the cost is grossly disproportionate to the benefits. If D = the net detriment that could be saved, C = the full cost of implementing the improvement and the Disproportionate Factor, X = C/D; then the CBA guidance lists the following criteria:

- If X > 10, the improvement is typically indicated as not justified.
- If X < 1, the improvement is typically indicated as justified.
- X values between 1 and 10 represent an area of uncertainty and the Duty Holder is required to justify the decision for not implementing the improvement (*HSE CBA website*).

In accordance with the *HSE CBA website*, the total benefit that could be saved is given by equation 9-7:

$$D = Summed\ detriment\ (£) \times frequency\ of\ accident\ (/y) \times plant\ life(y) \qquad (9\text{-}7)$$

Based on the current stocks of the radioactive liquor wastes, it is considered that the liquor glassification plant and process will be required for a minimum of 20 years. The standard CBA methodology normally applies the fault frequency calculated by the FTA to the total detriment and the plant life to determine the total benefit that could be saved. The FTA for the radiological risk, based on mean failure rates, calculates that the accident frequency is 1.63×10^{-3} per year (Figure 9-5). Using the summed detriment of £2.384E6 derived in Section 9.8.1, the total benefit that could be saved in terms of the monetary value over the remaining lifetime of the plant, in accordance with the CBA method, is:

$$£2.384E6 \times 1.63 \times 10^{-3} \times 20 = £77718$$

For this case study, the full cost of the improvement, i.e., design, procurement, installation and future maintenance of the alternative pneumercator air supply is £300,000. Hence X = 300000/77718, i.e., 3.9. As discussed above an X value between 1 and 10 represents the region of uncertainty. Hence, the gross disproportionality argument would be difficult to make in this instance. As such the decision for installing the alternative compressed air supply would not be straight forward using the standard

CBA methodology, which applies the fault frequency to the decision analysis based on single values. It is considered that the Bayesian Decision Network methodology could be usefully applied to address the uncertainty discussed above and reach an appropriate decision. This is detailed in Section 9.8.3.

9.8.3 Decision network analysis

A unique feature of the Bayesian decision networks is that the decision uncertainty is directly linked to the variables which affect the overall likelihood of the accident i.e., Nodes 1 to 25. Hence the impact of a change in these variables on the final decision can be determined. The CBA technique on the other hand is not linked to the fault variables. This leads to single values of the total benefit that could be saved, thus potentially resulting in an underestimate. As shown in Figure 9-3, Node 25, the accident risk of a hydrogen explosion ranges from frequencies as low as 0 to as high as 0.27/year. Therefore, in line with equation 9-7 the total benefit and hence the final decision outcome will vary accordingly. The Decision Network method can predict the final decision across the whole distribution of the accident risk, hence enabling a more accurate decision analysis, as detailed below.

The decisions to install the alternative air supply or to reject the installation are represented by the states with titles 'Install' and 'Don't Install', respectively in Node 27 of the decision network. For these decisions appropriate utilities need to be derived for the utility Node 26. For the 'Install' decision, the utility, U, is the total benefit as a function of the risk minus the cost of the improvement (£300,000). Therefore, as shown in the concept diagram (Figure 9-2), the risk Node 25 is a parent to the utility Node 26. Hence using equation 9-8 and the risk values predicted by the BBN Node 25 (Figure 9-3), the third column of Table F-6 in Appendix F determines the utilities for Node 26. This is based on the summed detriment value of £2.384E6, which is derived in Section 9.8.1.

$$U = ([Summed\ \ detriment\ ] \times [frequency\ of\ accident\ ] \times [plant\ life]) - 300000 \qquad (9\text{-}8)$$

For the 'Don't install' decision, since no money is being spent, the utility is 0 minus the total benefit that could have been saved in the event of the hydrogen incident. Hence the fifth column in Appendix F Table F-6 determines these utilities using equation 9-9.

$$U = 0 - ([Summed\ \ detriment\ ] \times [frequency\ of\ accident\ ] \times [plant\ life]) \qquad (9\text{-}9)$$

Using the utility values derived in Appendix F Table F-6, Figure 9-8 provides a Decision Network for the uncertainty on the installation of the alternative pneumercator air supply as an improvement against the risk of a hydrogen explosion in the vessel.

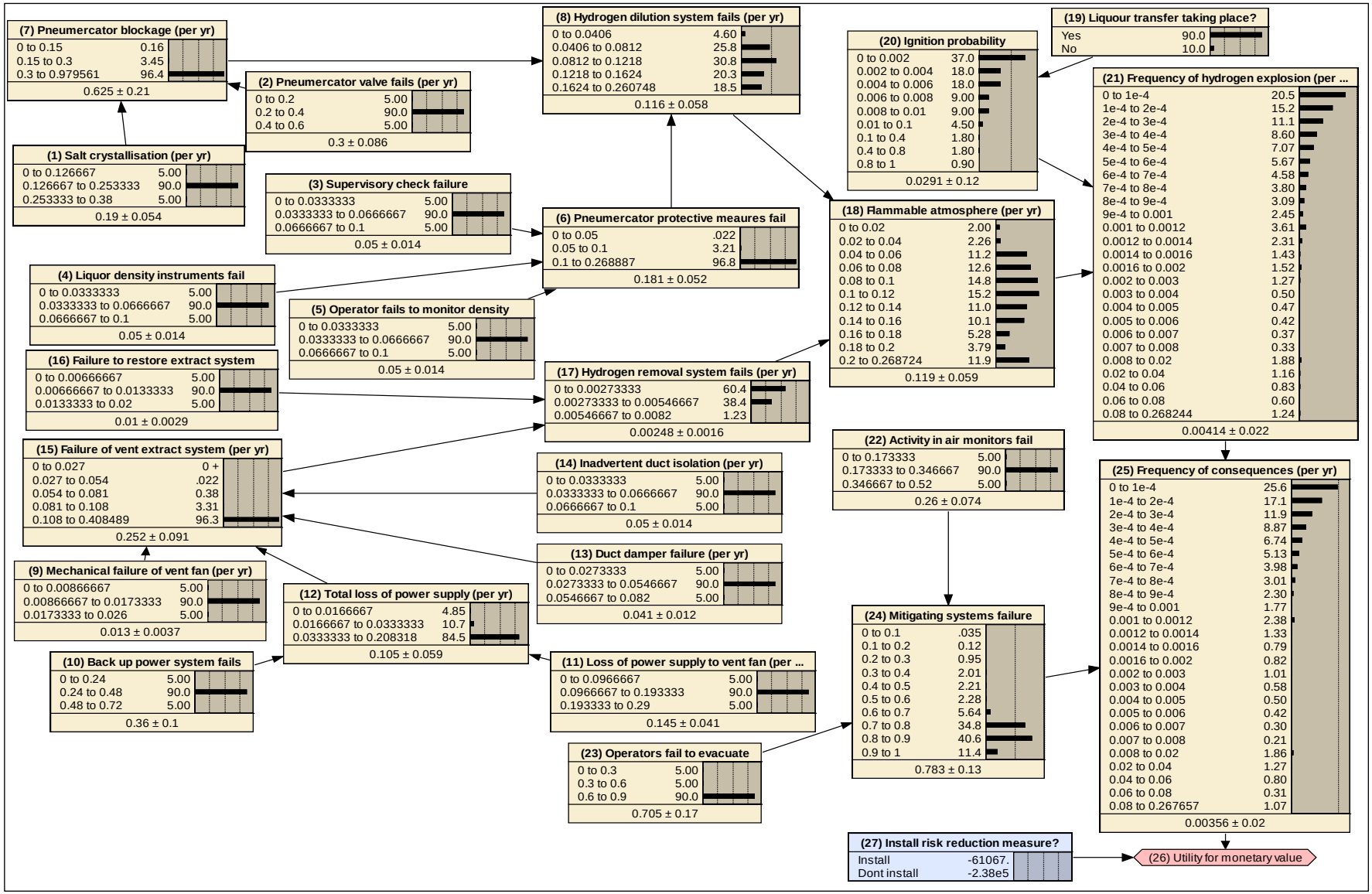

Figure 9-8: Decision network for the installation of a new compressed air supply

Based on the utilities derived across the whole distribution of the risk of a hydrogen explosion, Figure 9-8 (Node 27) shows that the utilities for the decisions to install the alternative air supply or to reject the installation are -£61067 and -£2.38E5, respectively. Although the negative utility values indicate that the decision would lead to a detriment as opposed to a benefit, the actual decision in Netica is indicated as 'Install'. This is because numerically the utility of -£61067 to install the air supply is still higher than -£2.38E5.

9.8.4 Sensitivity analysis

A sensitivity analysis was also undertaken to determine the risk at which the decision changes to a positive benefit, which is presented in Figure 9-9.

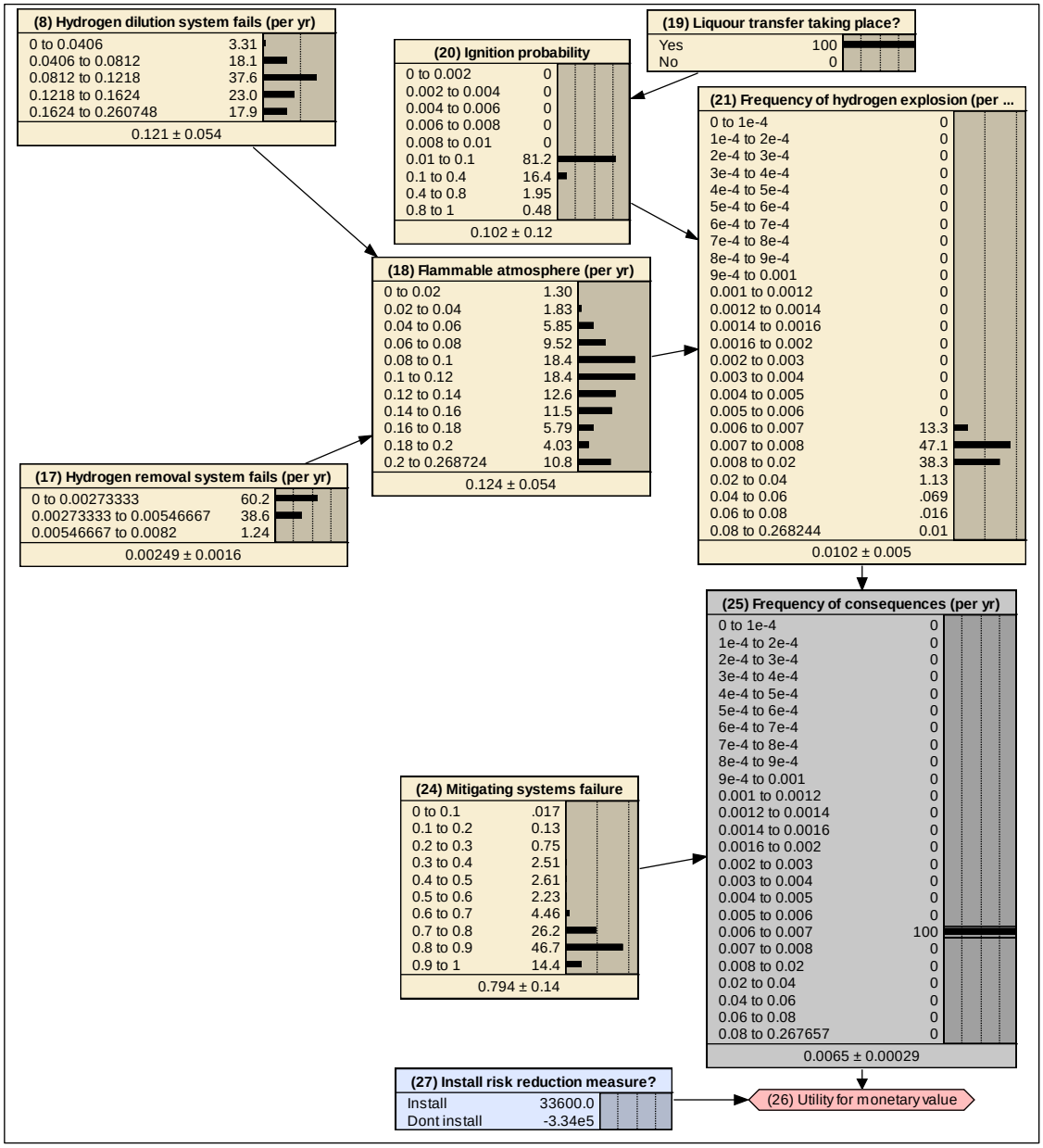

Figure 9-9: Conditions required to achieve a benefit from the improvement

For the sensitivity analysis, each of the discretised risk bands in Node 25 of the Decision Network was instantiated to a 100% probability and the resultant effect on the decision outcome in Node 27 was observed. The sensitivity analysis showed that the 'Install' decision changed to a positive benefit value of £33600 for the radiological risk values $\geq$ 0.006 per year (Figure 9-9). For the risk ranges less than 0.006 per year, the 'Install' decision was negative.

The percentage increase in the Parent node likelihood that would be needed to gain a positive benefit can also be observed from the updated results in Figure 9-9. This comparison is given in Table 9-1 which shows that the main parent node probabilities only need to increase by a relatively small factor that would lead to the radiological risk value >0.006 per year and give a positive benefit for the 'Install' decision. For example, to exceed the 0.006/year risk value, the mean hydrogen dilution system failure rate and the likelihood of a liquor transfer only need to increase by factors of 1.04 and 1.11, respectively. This signifies that the risk of a hydrogen explosion in the vessel, and hence the final decision, is highly sensitive to these variables.

Parent Node ID	Prior mean value	Updated mean value	Factor increase
(6) Pneumercator protective measures fail	0.181	0.182	1.01
(8) Hydrogen dilution system fails (per year)	0.116	0.121	1.04
(17) Hydrogen removal system fails (per year)	2.49E-3	2.49E-3	1
(18) Flammable atmosphere (per year)	0.119	0.124	1.04
(19) Liquor transfer taking place?	0.9	1	1.11
(20) Ignition probability	0.029	0.102	3.5
(21) Frequency of hydrogen explosion (per year)	4.4E-3	0.01	2.3
(24) Mitigating systems failure	0.783	0.794	1.01
(25) Radiological risk (per year)	3.6E-3	6.5E-3	1.8

Table 9-1: Comparison of prior and updated parent node probabilities

Given the uncertainty associated with the variables affecting the hydrogen dilution system failure frequency and the ignition probability, the possibility of small increases in the likelihood of these variables leading to a radiological risk $\geq$ 0.006 per year cannot be ruled out. Based on this sensitivity and on the balance of risk argument, the decision to install the alternative compressed air supply as a risk reduction measure is justified and considered ALARP.

9.9 Decision sensitivity to changes in total detriment

The decision analysis in the preceding sections is based on an estimated total detriment of £2.38E6. This takes into consideration the potential rise in costs e.g., due to increased plant outage time leading to lost production. The actual detriment without any increases in costs was estimated as half the £2.384E6 value, i.e., £1.192E6. This results in a Disproportionate Factor, X, of £300000/(£1.192E6 x $1.63x10^{-3}$ x 20), i.e., 7.7. If on the other hand the total detriment is three times the £1.192E6 value, i.e., £3.576E6, this would equate to an X value of 2.6. Thus, changes in the total detriment to either extreme of £2.384E6 still leads to an X value between 1 and 10, i.e., in the uncertainty region such that the decision is not straight forward.

The decision uncertainty due to changes in the total detriment was analysed by undertaking further Decision Network analyses for total detriments of £1.192E6, and £3.576E6. The results are presented in Appendix F Figure F-2 and Figure F-3, respectively.

The detriment of £1.192E6 results in a utility of -1.93E5 and -1.06E5 for the 'Install' and 'Don't Install' decisions respectively, thus indicating that the latter decision is more favourable. The detriment of £3.576E6 however, leads to the utility values of 57541.4 and -3.57E5 for the 'Install' and 'Don't Install' decisions, respectively. As such, the overall decision in this case is to install the alternative air supply. This sensitivity analysis using the Decision Network approach has therefore enabled a clear understanding of the detriment limits above which the installation of the alternative air supply is justified.

9.10 Conclusions for Chapter 9

The current standard practice for decision making processes is the HSE Cost Benefit Analysis (CBA) technique, which uses the quantified risk assessed in separate Fault Tree Analyses. The standalone FTAs are then used to determine the net benefit that could be saved by the proposed improvement. This case study demonstrates that the Decision Network method provides the ability to link the variables that affect the risk from the hydrogen explosion to the actual decision nodes. Hence the decision outcome is directly affected by the analysed risk. The standalone FTA in support of the CBA technique does not provide this link and consequently the prediction of the decision outcome as a function of risk is not possible with this standard approach.

A further benefit of the Decision Network methodology demonstrated in this Chapter is that the Bayesian analysis within the network provides the ability to model the final decision across the whole distribution of the accident risk. Hence this enables an uncertainty analysis such that an accurate decision can be made. The CBA technique

on the other hand uses single values of the risk, without the uncertainty analysis, thus leading to potential inaccuracies in the analysis.

The Bayesian Decision Network for this case study shows that the two main variables that affect the risk from a hydrogen explosion within the vessel are ignition probability and hydrogen dilution system failure frequency. A sensitivity analysis, based on a comparison of the prior and updated results, shows that for the decision to install the alternative air supply, the mean radiological risk frequency would need to be 0.0065/year.

To exceed the risk of 0.0065/year the mean hydrogen dilution system failure rate and likelihood of liquor transfer, which has a direct impact on the ignition probability, only need to increase by factors of 1.04 and 1.1, respectively in comparison with the Prior values. Based on this sensitivity and on the balance of risk argument, the decision to install the alternative compressed air supply as a risk reduction measure is justified and considered ALARP.

In conclusion, the uncertainty analysis and the updating features of the Bayesian Decision Network methodology have enabled key sensitivities to be identified, through a comparison of the prior and updated results. Accordingly, an appropriate judgement was made with respect to the likelihood of exceeding the risk band at which the decision to install the air supply provided a positive benefit. The decision based on the standard CBA approach on the other hand, resulted in an uncertainty. The uncertainty was that the gross Disproportionate Factor was in the range 1 and 10 such that the decision without the Bayesian Decision Network was not straight forward.

CHAPTER 10 : CASE STUDY 7- APPLICATION OF BAYESIAN NETWORKS TO ASSESS RELIABILITY OF ROBOTS FOR PROCESSING OPERATIONS IN RADIATION ENVIRONMENTS

10.1 Introduction to Chapter 10

Robots are deployed in the process industry to aid routine operations primarily to reduce the time, labour, and strain from repetitive tasks. In radiation environments robotics provide a further advantage of undertaking remote operations thus protecting the workforce from the harm potential of ionising radiation.

Many nuclear waste processing operations require treatment and safe storage of material that is categorised as Intermediate Level Wastes (ILWs) in accordance with the International Atomic Energy Agency (IAEA) safety guide, and classification of radioactive wastes, *IAEA, 2009*. As discussed by *IAEA, 2009,* the ILWs consist of long lived alpha and beta gamma emitting radionuclides that require a high degree of containment and isolation for the purpose of protecting the workforce and members of the public. Hence to meet the required radiological safety standards, the application of robotics is becoming increasingly popular for decommissioning and processing operations in nuclear chemical plants. Journal articles published by *Tsitsimpelis et al, 2019, Bloss, 2010, Bogue, 2011, Fuji et al, 1976, Carteret et al, 1997 and Fischetti, 1985* discuss the effectiveness of robotics in nuclear applications.

Whilst radiation protection and economics due to an increase in plant throughput are the key benefits, a failure or breakdown of robots in nuclear environments can be detrimental. The main detriments would be the need for plant recovery and perhaps even replacement with a new robot. This would potentially lead to a radiation exposure of the recovery workforce which must be avoided. Hence demonstration of high reliability of robot components in nuclear environments is essential.

This case study applies the Bayesian Belief Network methodology to assess the reliability of robotics used for handling of radioactive ILWs in a nuclear reprocessing plant, referred to as the Waste Processing Cell hereafter. Ultimately a breakdown of the robot system would lead to a reduction of plant throughput and the need for recovery. If key sensitivities affecting the likelihood of robot breakdown can be identified, then relevant design improvements could be undertaken to improve the overall reliability of the system.

10.2 Description of robot operations in the waste processing cell

The ILW material generated from nuclear processing and decommissioning operations requires safe storage and disposal in accordance with guidelines given by *IAEA, 2009.* The safe disposal and storage strategy requires the ILWs to be covered by water in robust storage vessels until a long-term geological waste repository becomes available.

Each storage vessel will be housed in a secondary containment box and the annulus between the inner vessel and the box filled with cement grout to prevent mobilisation of the inner vessel. This case study focusses on operations within the Waste Processing Cell (WPC), where the ILW material from the donor plants is imported, inspected for the type of material, size reduced if necessary and exported to the next part of the process for grout filling. The main processes involving the use of robots in the WPC are outlined below.

A transportable storage vessel referred to as the 'skip', as illustrated in Chapter 7 Figure 7-1, is imported from the donor plant used for storage of solid radioactive waste into the waste processing facility. The skip contents are metallic magnesium and magnesium hydroxide sludge which is categorised as ILW in accordance with the criteria given by *IAEA, 2009.* Robot automated sequences are used to carry out the following tasks:

1) Top-up of the skip contents with water to ensure complete immersion of the contents under water, thus providing a safe condition for transfer of the skip for next part of the process. The robot is required to pick up the water top-up nozzle from the nozzle park stand using a hydraulic gripper tool. Once the water top-up is complete, the robot has to return the nozzle and the gripper to their original location in the cell.
2) The ILW is extracted from the skip, inspected, disrupted, and characterised as required using the robot. This requires operator decision on whether liquor from the skip needs decanting prior to extracting the waste. If so, the robot Auto Sequence is used to pick up hydraulic gripper from the tool stand and the decant nozzle from the nozzle park stand. The decant nozzle is submersed and the liquor removal pump is activated using the manual mode. Once the liquor has been removed, the nozzle and gripper are returned to their park stands using the robot Auto Sequence. Disruption is a process of size reduction of the waste so that the final box package contains the desired type of material and meets the conditions for acceptance for safe interim storage. Waste disruption is carried out using the operator joystick control.
3) The robot system is also used for the consolidation of waste at the Waste Treatment Table (WTT) from two skips and transfer the waste into a single box liner. This process requires the waste to be picked out from the skip and released on to the WTT. Once the waste is characterised and size reduced if necessary, it is transferred into the box liner. The liner is fitted with an Anti-Floatation Plate, which prevents waste material rising above the water surface during interim safe storage. The box is then transferred to the next part of the process for grouting.

The actual waste characterisation and consolidation into the box liner is carried out using manual joystick control of the robot. The robot automated sequences are used to return the secondary tools to the tool stations.

10.3 Identification of robot key components

The type of robot used in the WPC is a cylindrical arm with six degrees of freedom to enable rotational movements along each of the six axes. Effectively the robot flexibility increases with the number of axes, allowing a wide range of tasks to be performed in a variety of rotational directions. Figure 10-1 illustrates a typical six axes cylindrical arm robot and the direction of rotation about each axis [*Machine Design*, *2020*].

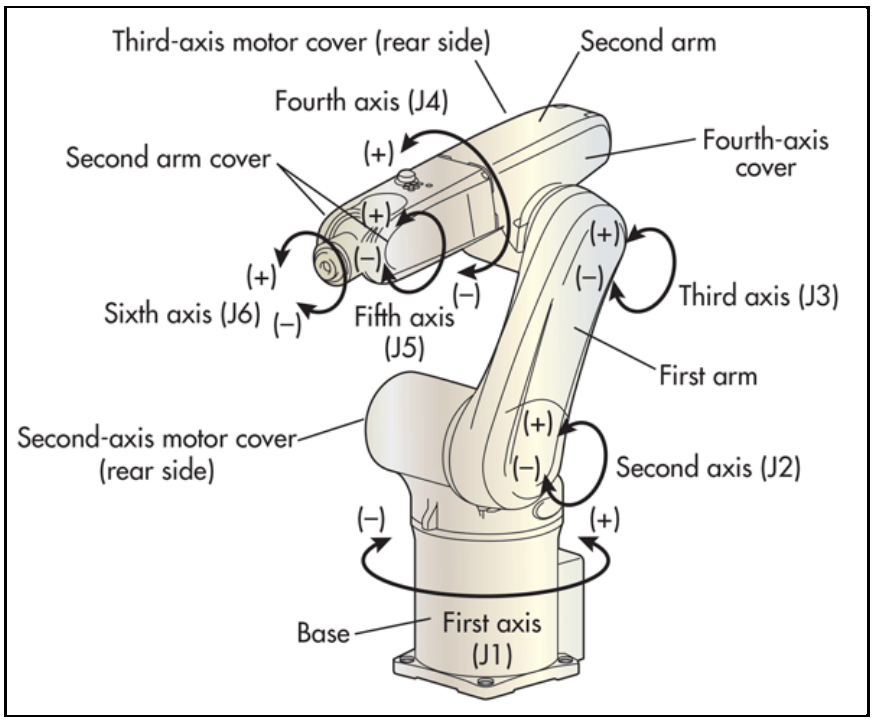

Figure 10-1: Industrial cylindrical arm robot with six axes [*Machine Design*, *2020*]

The main components of the six axes robot can be outlined as follows:

10.3.1 Control Unit

The control unit encodes the automatic sequences of the tasks that the robot arm and its supporting features need to perform. Joystick control can also be deployed as part of the control unit to enable operator intervention to perform certain manual tasks.

10.3.2 Axis Motor

Each of the six axes consists of a motor drive that rotates for the required number of revolutions as set by the sequence code. This has the effect of moving the robot arm to the desired location.

10.3.3 Gearbox

The gears receive and transmit rotational forces between the axes, as well the ability to change speed of rotation of the motor. A reduction of motor speed has the effect of increasing the axis torque.

10.3.4 Robot Arms and Joints

The six axis robot consists of two arms with six articulated joints (Figure 10-1, joints J1 to J6) that enable rotary movements about each axis. With two arms and six joints, the robot can perform the function of an arm, shoulder, elbow, and the wrist. Effectively, this provides the same function as a human limb.

10.3.5 End Effector

The end of the second arm, which is joint J6 in Figure 10-1, is attached to a hydraulic tool that serves the same function as a human hand, i.e., to pick and place items at their designated location. The ‘hand’ is referred to as the ‘end effector’ in robotics. Other equipment, such as a drill or cutting tools can also be attached to the end effector to perform specific tasks.

10.3.6 Force Torque Sensor and Resolvers

The force torque sensor is a key component that enables the robot to sense the force being applied, particularly to the sixth axis i.e., the wrist. This is required to manoeuvre the end effector in the 3 dimensional X, Y and Z direction. The wrist axis is programmed to operate within the defined force torque limit. The force torque sensor detects excessive forces applied at the axis and prevents further movement, thus reducing the risk of a mechanical breakdown. A robot needs to be able to measure the degrees of rotation at each axis so that it can decide if the required extent of movement has taken place. Resolvers are rotary transformers which can measure the degree of rotation.

10.3.7 Brakes

Brakes are primarily used in robotics to stop the arm movement at the specified point. Brakes are also necessary to stop arm movements following an electrical power failure, thus preventing arm collapse or catastrophic damage to the adjacent equipment.

10.4 BBN analysis of WPC robot equipment failure and loss of functionality

10.4.1 Identification of Failure Modes and Effects

The main objective of the case study is to apply the Bayesian Belief Network technique to identify key failure modes and sensitivities of the robot system which could lead to a failure to carry out the required operations.

Initially a fault identification review with the SL Equipment Reliability team was undertaken to identify and agree the main failure modes and effects that could lead to a failure to process the waste in the Waste Processing Cell (WPC) [*Ahmed 2018b*]. It was considered that a failure to process the waste could occur either due to a loss of the robot secondary tools or due to a direct loss of the robot functionality. The agreed failure modes and effects associated each of these two main groups of faults are illustrated in Figure 10-2.

Figure 10-2: Cause and effect diagram for failure to process waste in the WPC

The identified causes and effects were replicated in the Bayesian Network for robot tool and equipment failure (Figure 10-3) and loss of robot functionality (Figure 10-4).

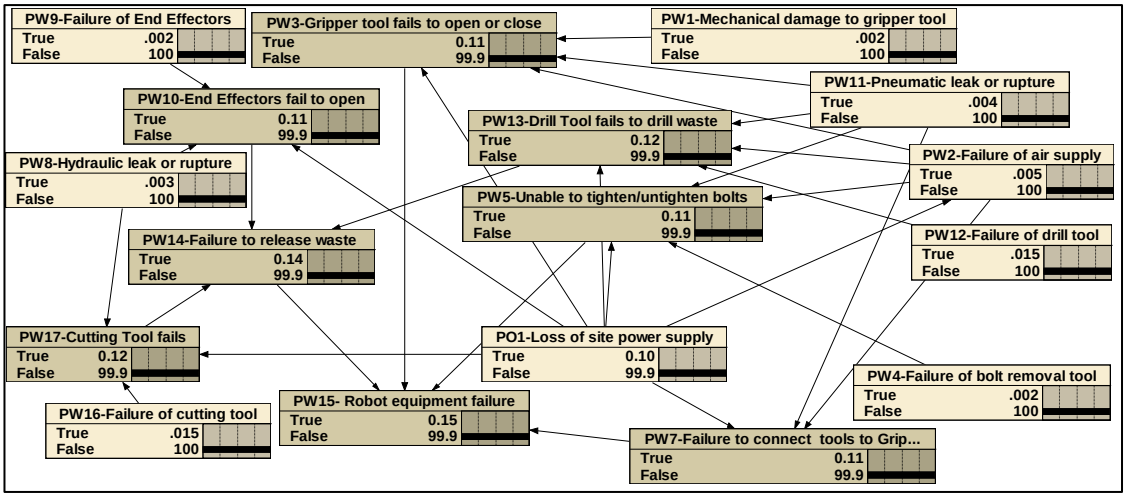

Figure 10-3: BBN for robot secondary equipment failures

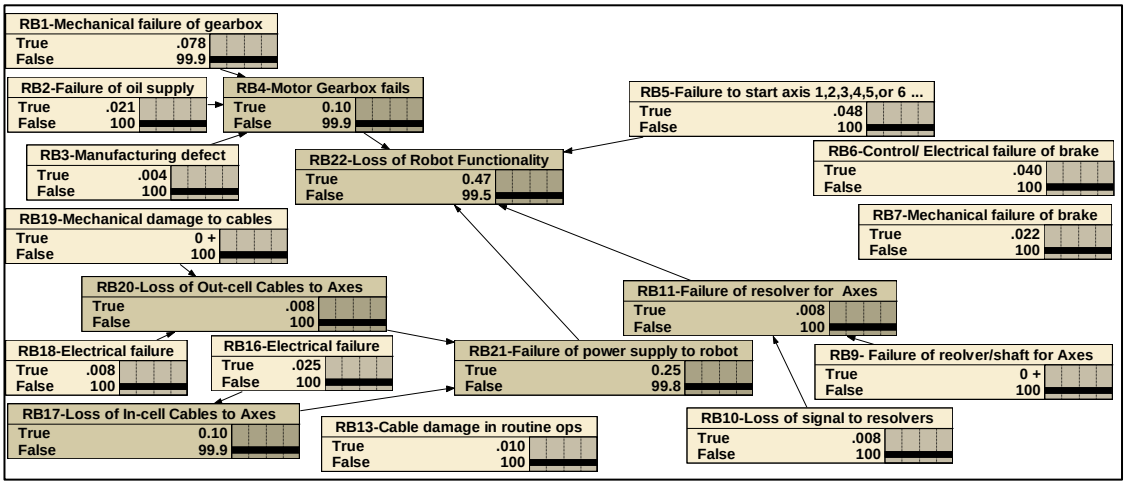

Figure 10-4: BBN for failures leading to loss of robot functionality

Each of the nodes in Figure 10-3 and Figure 10-4 was assigned an identification number, PW1 to PW17 for tool equipment failures and RB1 to RB22 for loss of robot functionality. Given that the purpose of this case study is to model failures of the robot components and secondary tools, it was considered that each item can be either in a failed or operational state. Hence the Bayesian Network for this case study models all the Parent and Child nodes as discrete Boolean variables with the failures being either in a 'true' or 'false' state.

The true and false probability values presented in Figure 10-3 and Figure 10-4 are based on the input parent node failure probabilities and the Conditional Probability Tables (CPTs) for each of the discrete child nodes. The CPTs can be derived using the Boolean AND and OR logic gates. The following sections detail the identified failure modes and effects associated with equipment failures and a loss of robot functionality. A description of the Boolean logic for each of the failure modes as well as the methodology used to derive the CPTs is also given.

10.4.2 Derivation of Conditional Probability Tables for failure modes leading to loss of functionality of robot and secondary tool equipment

Manual waste characterisation, size reduction and consolidation into the box liner require the use of the robot in the manual mode by means of manipulator and joystick control outside the cell. Such operations in the manual mode require attachment of secondary tools to the robot end effector including:

- Jaw type gripper tool used for various activities, including waste disruption and unloading from the WTT.
- Bolt removal tool for unscrewing the bolts from the skip features.
- Drill tool for drilling holes in skips to drain and remove the fluids from the skips.
- Cutting tools such as shears for cutting the waste to the correct size and reduce the voids in the waste.
- Grab type end effectors are used to transfer the waste from the skip unloading position to the WTT and from the WTT to the liner load position.

A loss of functionality of the grab type end effectors would lead to a failure to release the waste on to the WTT or into the liner and hence ultimately causing a failure to process the waste. Operation of the bolt removal, drill and waste cutting tools requires connection to the gripper tool. The fault identification session considered that a loss of functionality of either of these four tools would also lead to a failure to process waste in the WPC.

The gripper, bolt removal and drilling tools as well as the process of connection of the tools to the gripper are all pneumatically driven operations by means of a common compressed air supply. The loss of compressed air represents a common mode that could lead to a failure of all this equipment. A further common mode is the loss of site power supply to this equipment. Therefore, it was considered that a loss of functionality of each of these four items of equipment (Nodes PW3, PW5, PW7 and PW13) could occur either due to a loss or leakage of the compressed air supply, a mechanical failure of the tools or due to loss of power. Hence a Boolean OR gate was applied to model these failures.

Similarly, the end effector and the cutting tool are hydraulically operated by a common hydraulic supply. Either mechanical damage or a hydraulic leak, or a loss of electrical power supply to the hydraulic system would lead to their failure. Hence, the CPT of the child nodes PW10 for end effectors failing to open and PW17 for cutting tool failure, was determined by applying an OR gate between each of the respective parents.

The methodology for mapping the Boolean AND and OR logic gates into Bayesian Networks, is detailed by *Bobbio et al, 2001* and *Portinale and Bobbio, 2013*. They show

that for each child node in the Bayesian Network generated from an OR gate, the CPT for the child node is such that the node is true with a probability of 1 if at least one parent node is true. For instance, in the case of node PW10 for end effector failure, as shown in Figure 10-3, this can occur either due to node PO1, OR PW8, OR PW9. This leads to a CPT which is a 4 x 8 matrix (Table 10-1).

PW10- End Effectors fail to open	PW9- Failure of end effectors	PW8- Hydraulic leak or rupture	PO1- Loss of site power supply
TRUE	TRUE	TRUE	TRUE
TRUE	TRUE	TRUE	FALSE
TRUE	TRUE	FALSE	TRUE
TRUE	TRUE	FALSE	FALSE
TRUE	FALSE	TRUE	TRUE
TRUE	FALSE	TRUE	FALSE
TRUE	FALSE	FALSE	TRUE
FALSE	FALSE	FALSE	FALSE

Table 10-1: CPT for Node PW10, end effectors fail to open

An alternative way of modelling the OR gate relationship is to use the Netica Boolean function or (b1, b2,… bn)". To determine the CPT for node PW10 the following expression would be applied which will yield the same results as those given in Table 10-1:

p (PW10 | PO1, PW8, PW9) = or(PO1,PW8, PW9)

This function can be applied to any given number of parent nodes. Thus, for more than three parents modelled as an OR gate, the CPT matrix would be larger. Application of the OR gate functionality in Netica allows the CPT to be generated automatically, therefore allowing a significant amount of effort to be saved and avoiding potential errors when populating the tables manually. On this basis for all the remaining child nodes coloured dark grey in Figure 10-3 and Figure 10-4, the CPTs are generated using the Boolean logic gates and equations given in Appendix G Table G-1.

10.4.3 Derivation of primary node failure probabilities

After determining the CPTs of all the Child nodes, the failure probabilities of the primary input nodes, in Figure 10-3 and Figure 10-4 were derived. Initially a review of the failure rates of the components associated with the primary nodes was undertaken. This was based on the data given by *NPRD11, 2011, IEEE Standard 500,1984, Dexter and Perkins,1982.* A list of the primary nodes and the failure rates based on these references is given in Appendix G, Table G-2.

At the cause and effect identification review meeting [*Ahmed, 2018b*], it was considered that all the primary node failures would be revealed i.e., detected via automatic

feedback to the operators in the control room. The time taken for the operators to reveal the fault, diagnose and undertake repairs, is referred to as the 'repair time' in reliability engineering. Given that sufficient spare parts will be available to minimise the downtime due to primary node failures, it is considered that each of the identified failure modes will be rectified within a single plant shift. Hence a repair time of 8 hours, i.e., 0.001year for each failure mode is considered appropriate for this analysis. For revealed faults rectified within a specific repair time, *Beurden, and Goble 2016,* suggest that the probability of failure (P) equates to the product of failure rate, λ, and repair time, T_R, (equation 10-1). Hence, the failure probability values in Appendix G Table G-2, column D are derived using equation 10-1 with a repair time of 0.001year and the failure rate values given in column B.

$$P = \lambda T_R \tag{10-1}$$

10.5 Analysis of BBN results

Based on the input parent node Prior probabilities and the CPTs discussed above, by combining the BBNs for equipment failure (Figure 10-3) and loss of robot functionality (Figure 10-4), Figure 10-5 presents the overall BBN for a failure to process the waste.

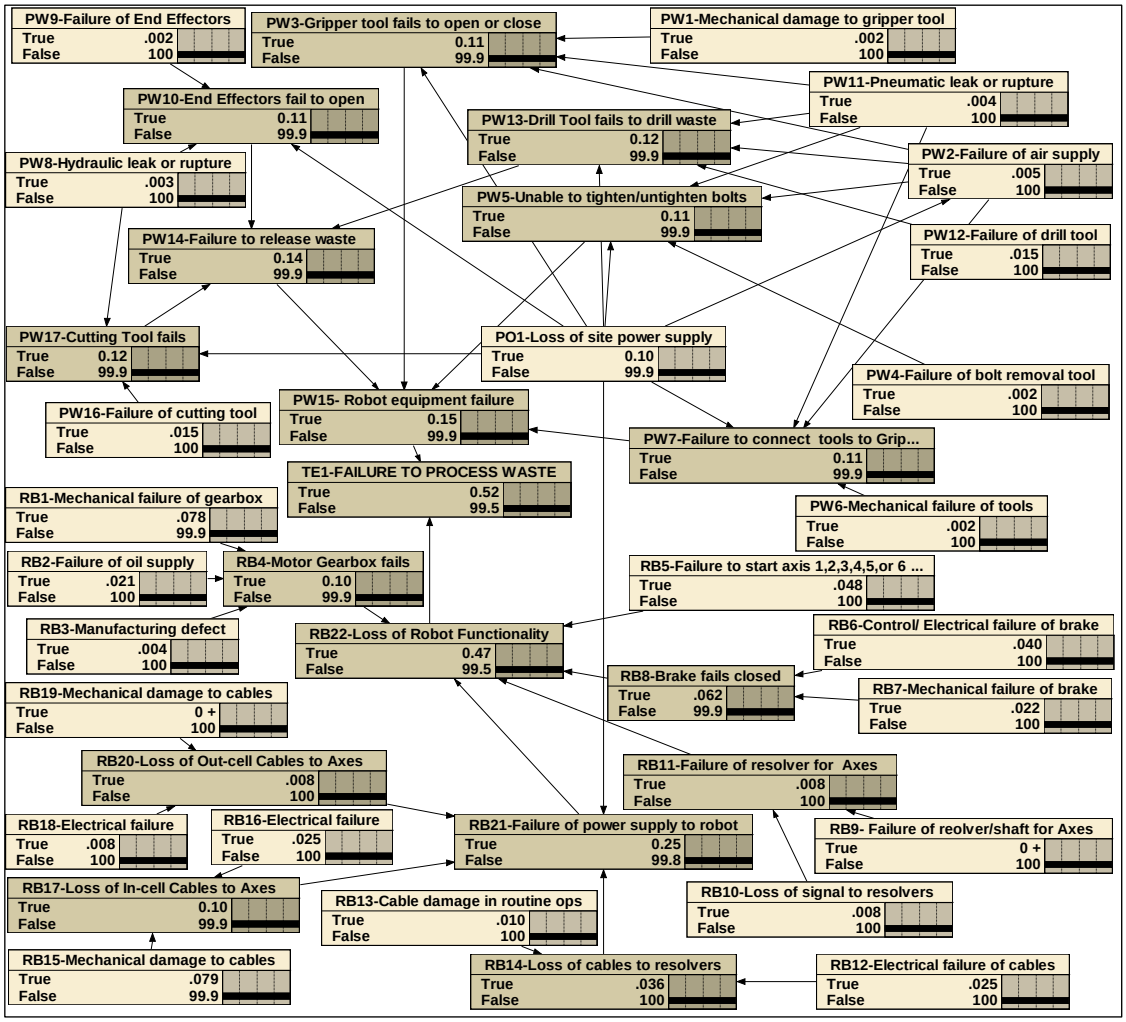

Figure 10-5: Fully Developed BBN with Prior failure probabilities

10.5.1 Comparison with standard Fault Tree Analysis

To test the validity of the BBN in terms of the logic used for determination of the CPTs, a Fault Tree Analysis (FTA) of the same model was carried out using the LOGAN software. The FTA results are presented in Figure 10-6.

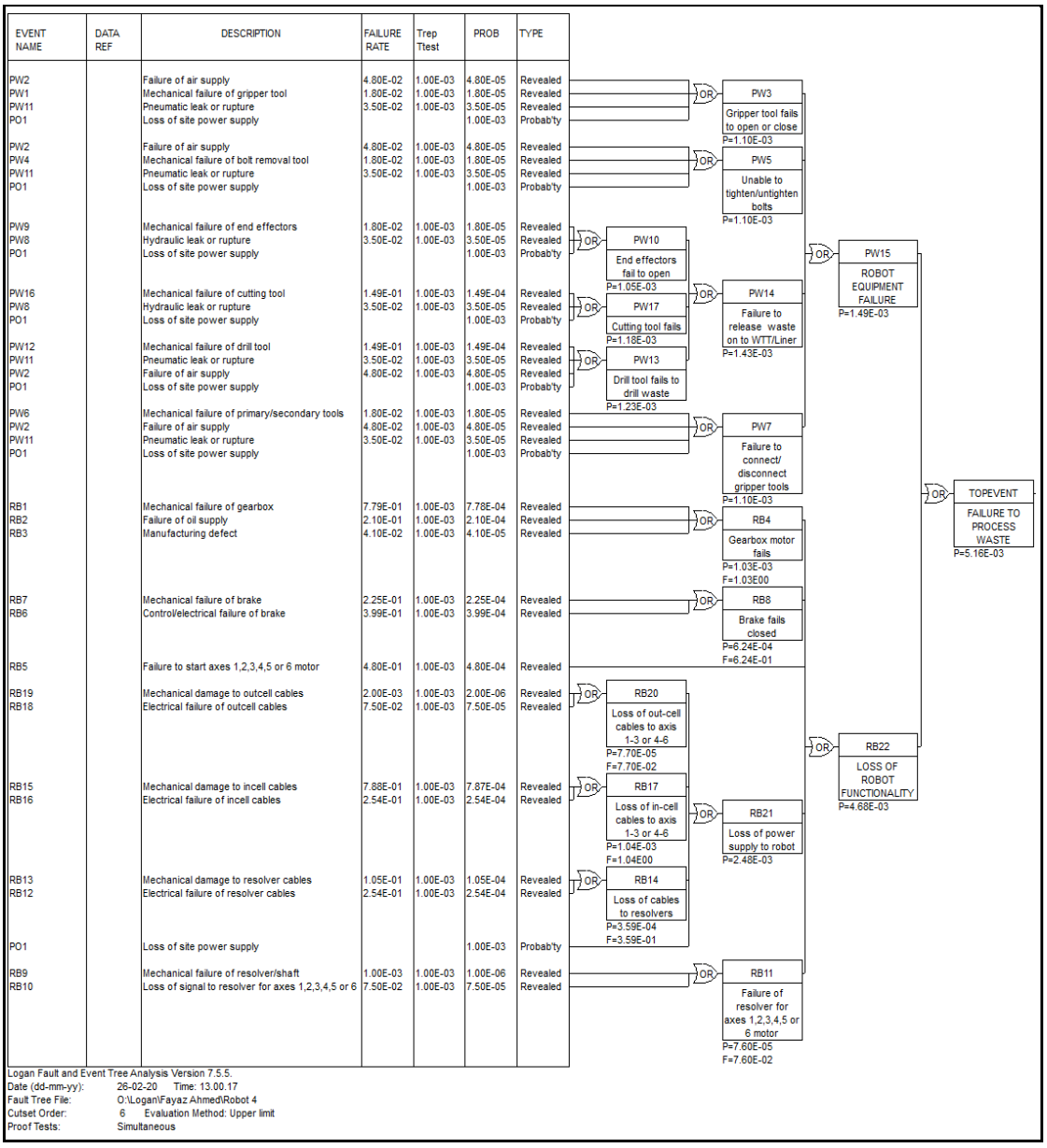

Figure 10-6: Fault Tree Analysis for failure to process waste

A comparison of the BBN and FTA results in terms of the failure probabilities of each node is given in Appendix G Table G-3. The comparison shows that the FTA failure probability results for the nodes PW15 and RB22, and the Top Event are exactly the same as those for the BBN (Figure 10-5), thus confirming that the Bayesian network has been modelled correctly.

10.5.2 Sensitivity Analysis of Top Event

One of the objectives of this case study is to identify the main failure modes contributing to the Top Event and to determine how significantly the individual failures would need to increase if the Top Event probability is increased. The first of these two objectives has been achieved by undertaking a sensitivity analysis in the Bayesian Network. The Bayesian Network methodology can determine the maximum posterior probability of a set of variables given the evidence obtained for the remaining nodes. In other words, the 'Most Probable Explanation' (MPE) of the observed hypothesis can be obtained. *Kwisthout, 2011* provides a comprehensive review of the Bayesian MPE functionality.

To identify the key sensitivities affecting the Top Event for this case study, i.e., failure to process the waste, the Bayesian Network in Figure 10-5 was updated, with a value of 100% using the Netica 'Findings' function. Subsequently the Netica 'Most Probable Explanation' function was activated to yield the most probable configuration. The updated BBN without the MPE analysis and with the same is given in Figure 10-7 and Figure 10-8, respectively.

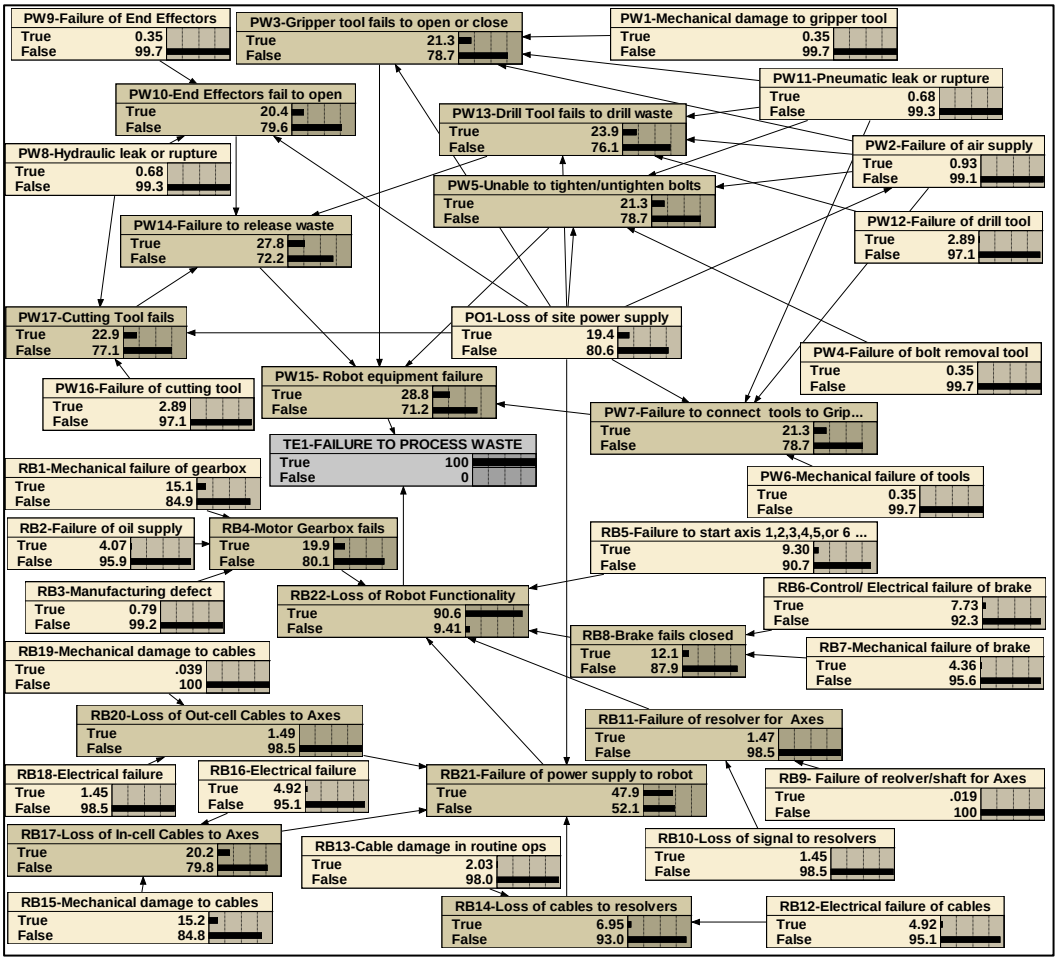

Figure 10-7: Updated BBN with Posterior failure probabilities

The most probable configuration in Figure 10-8 was obtained by identifying the state in each node with a 100% probability. Thus all 'true' states in Figure 10-8 which are either

at 100% or close to the 100% probability indicate the most probable failure modes resulting in the occurrence of the Top Event. Effectively the sensitivity on the occurrence of the Top Event is proportional to the MPE probability of the true states.

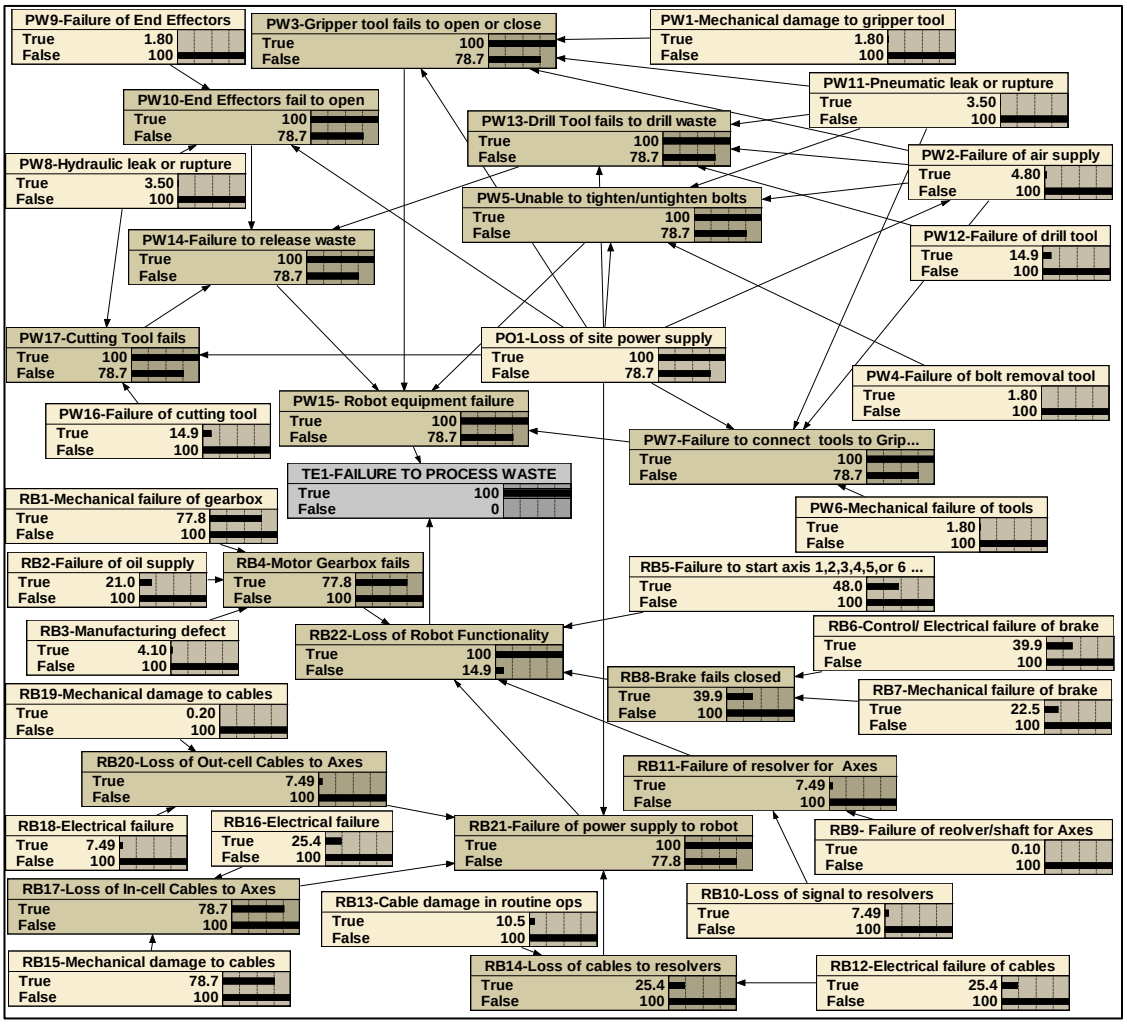

Figure 10-8: Updated BBN using Maximum Probable Explanation

Full details of the MPE results from Figure 10-8 in descending order of true state probabilities are tabulated in Appendix G Table G-4. A summary of the results for events with the highest true state probabilities is given in Table 10-2.

The MPE results show that the primary nodes RB15, for mechanical damage to in-cell cables and RB1, for mechanical failure of gearbox, present the highest sensitivity to the occurrence of the Top Event. Accordingly, Figure 10-8 and Table 10-2 suggests that the Top Event is more likely to occur due to a loss of robotic functionality than due to a secondary equipment failure.

Primary Event ID	Description	BBN MPE Sensitivity Analysis (percent probability)	FTA Sensitivity Analysis (probability)
PO1	Loss of site power supply	100	1.93E-01
RB15	Mechanical damage to in-cell cables	78.7	1.52E-01
RB1	Mechanical failure of gearbox	77.8	1.50E-01
RB5	Failure to start axis 1,2,3,4,5 or 6 motor	48.0	9.27E-02
RB6	Control electrical failure of brake	39.9	7.71E-02
RB12	Electrical failure of resolver cables	25.4	4.91E-02
RB16	Electrical failure of in-cell cables	25.4	4.91E-02
RB7	Mechanical failure of brake	22.5	4.35E-02
RB2	Failure of oil supply	21.0	4.06E-02
PW16	Mechanical failure of cutting tool	14.9	2.88E-02

Table 10-2: MPE results for key sensitive events affecting robot system failure

To test the validity of the above MPE analysis, a sensitivity analysis in the FTA model was also undertaken. The LOGAN software sensitivity analysis is based on the concept of Fusel-Vesely Importance Measure (IM) which is expressed as:

$$\text{IM} = \frac{\text{Percent change in Top Event value}}{\text{Percent change in basic event}} \tag{10-2}$$

The equation above uses the concept that the importance of a primary node is 0.7 if the primary node failure probability increases by 10% such that the Top Event probability changes by 7%. Using this concept, the FTA sensitivity analysis is also tabulated in Appendix G Table G-4 and the top ten entries are listed in Table 10-2. Whilst the MPE and FTA sensitivity analysis methods differ completely, it can be seen from Table G-4 and Table 10-2 that the order of sensitivity of the primary nodes is exactly the same in both cases i.e., node RB15 followed by RB1, which represent the key sensitivities.

It is observed that the order of sensitivity is directly proportional to the magnitude of the Prior failure probabilities of the primary nodes. The reason for this trend is that the logic used in the model requires an application of the Boolean OR gates to all the Parent nodes. If on the other hand the model required some Parent nodes to be modelled with an AND gate, then the cut set order and hence the sensitivities would not necessarily be proportional to the Prior failure probabilities.

10.5.3 Analysis of the Bayesian Probability Updating Results

The results discussed in sections 10.5.1 and 10.5.2 have shown that the Bayesian technique is able to meet all the functionalities of a standard Fault Tree Analysis in terms of the Boolean logic gates and the sensitivity analysis. In addition to these

capabilities, the Bayesian updating technique can apply abductive reasoning to determine the posterior probability of the primary nodes which are conditional to the occurrence of the Top Event [*Khakzad et al, 2011*]. In other words, the Bayesian technique can perform reverse inference to determine the effect on the primary node probabilities conditional to the Top Event probability. Such information is extremely beneficial in reliability engineering, as it provides information on how significantly the failures of system components would need to increase for the Top Event to occur. This probability updating feature is unique to the Bayesian technique which is lacking in FTAs.

Thus, by instantiating the Top Event probability to 100%, Figure 10-7 shows the posterior probabilities of the primary nodes. Based on Figure 10-7 and Appendix G Table G-3, a list of the top five entries in terms of sensitivity is given in Table 10-3. The general trend is that the posterior probabilities of the primary nodes PO1, RB15 and RB1 would need to increase almost two fold for the Top Event to occur at a 100% probability. From a design substantiation perspective, these posterior probabilities provide useful information which the designers could use to improve the overall reliability of the system.

Primary Event ID	Description	Prior probability	Posterior probability
PO1	Loss of site power supply	0.1	0.194
RB15	Mechanical damage to in-cell cables	0.08	0.152
RB1	Mechanical failure of gearbox	0.08	0.151
RB5	Failure to start axis 1,2,3,4,5 or 6 motor	0.05	0.09
RB6	Control electrical failure of brake	0.04	0.08

Table 10-3: Prior and Posterior probabilities for loss of robot functionality

10.6 Effect of additional protection on robot system reliability

Using the Netica Updating and Most Probable Explanation functionalities, it has been demonstrated that the primary nodes PO1 for loss of site power supply, RB15 for mechanical damage to in-cell cables and RB1 for mechanical failure of gearbox present the greatest sensitivity. Taking account of these key failures an overall failure probability of 0.52% i.e., an unavailability of 5.2E-3 for the Top Event has been determined.

If the probability of a loss of site power supply can be reduced, e.g., through the introduction of a local diesel power generator, the overall reliability of the system could be improved. Accordingly, the effect of a back-up power supply system consisting of two standby diesel generators on the robot unavailability was analysed within the BBN.

The BBN analysis uses two additional input parent nodes for each of the diesel generators, i.e., DE1 and DE2, respectively. Both diesel generators would need to fail for a complete failure of the back-up power supply system (Node DE3). Hence the CPT for Node DE3 was determined by applying the Boolean AND gate to nodes DE1 and DE2 using equation 10-3.

$$\mathrm{p}\,(\mathrm{DE3}\,|\mathrm{DE1},\mathrm{DE2}) \;=\; \mathrm{and}(\mathrm{DE1},\mathrm{DE2}) \qquad (10\text{-}3)$$

Using a failure probability of 0.357 for the diesel generators as derived in Chapter 6, the probability of loss of both diesel generators was calculated by Netica. For a total loss of power to occur, both diesel generators as well as the normal site power supply (Node PS1) would need to fail. Hence the Boolean AND gate was applied between Nodes DE3 and PS1 to determine the new failure probability for a total loss of power supply (Node PO1). The BBN results with this additional protection provided by the diesel generators, represented by green coloured nodes, are shown in Figure 10-9.

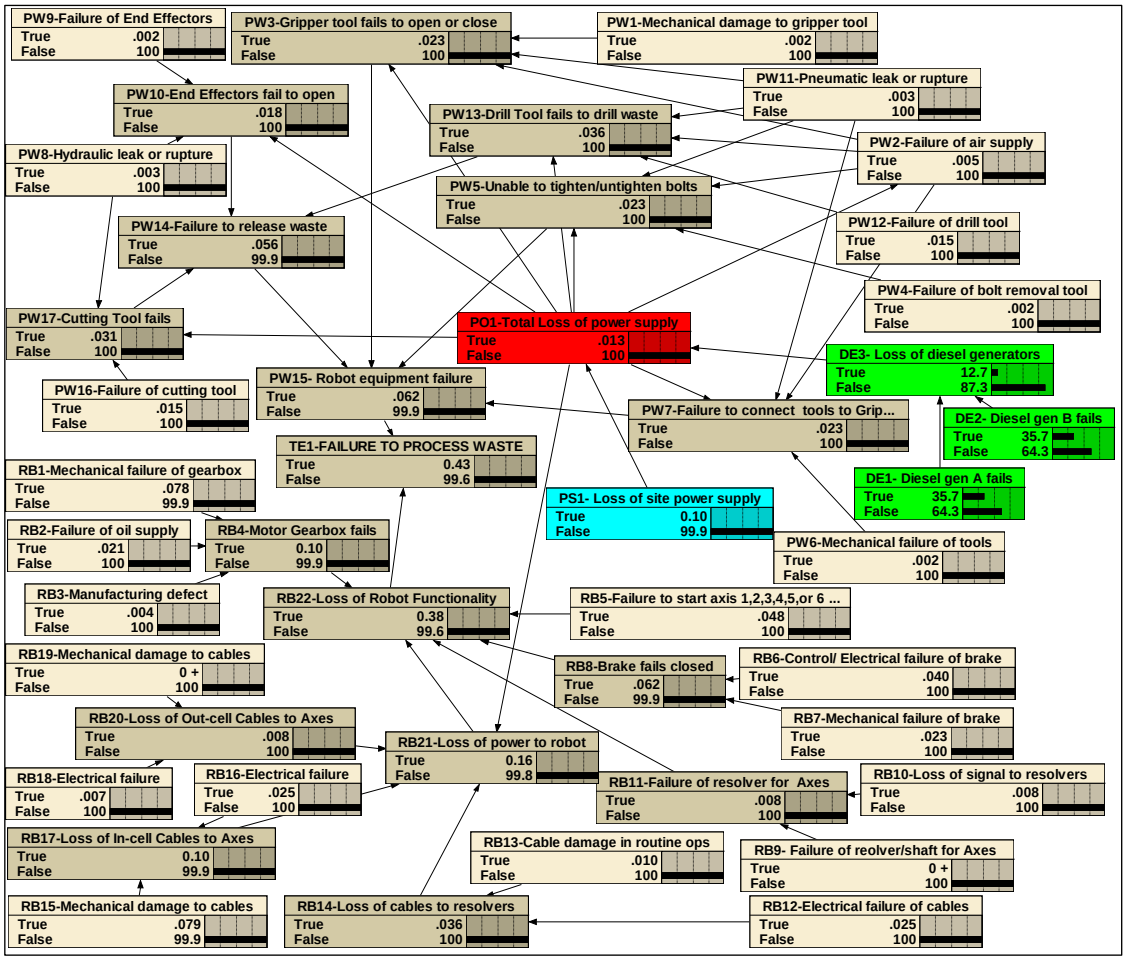

Figure 10-9: BBN for additional mitigation by the diesel generator power supply

Figure 10-9 shows that with the additional protection provided by the diesel generators, the probability of total loss of power reduces from 0.1% (Figure 10-5) to 0.013%, i.e., an order of magnitude reduction in the unavailability of this system. The overall effect

of this additional protection system against power loss is that the Top Event (TE1) probability reduces from 0.5% to 0.4% which is equivalent to a 17% reduction in the overall system unavailability.

10.7 Effect of increased reliability of robot functionality nodes

Whilst a loss of power supply is the most significant contributor to the occurrence of the Top Event, as discussed previously, the next most important parameters are those which affect the robot functionality i.e., mechanical damage to in-cell cables (Node RB15) and failure of the motor gearbox (Node RB1). Therefore, if the failure probabilities of these input nodes are also decreased, the overall system unavailability could be reduced further. Hence the BBN model with the additional protection provided by the diesel generators (Figure 10-9) was modified with the failure probabilities of Nodes RB1 and RB15 reduced by an order of magnitude to 0.008. These modifications are represented by the yellow and purple colour nodes, as shown in Figure 10-10.

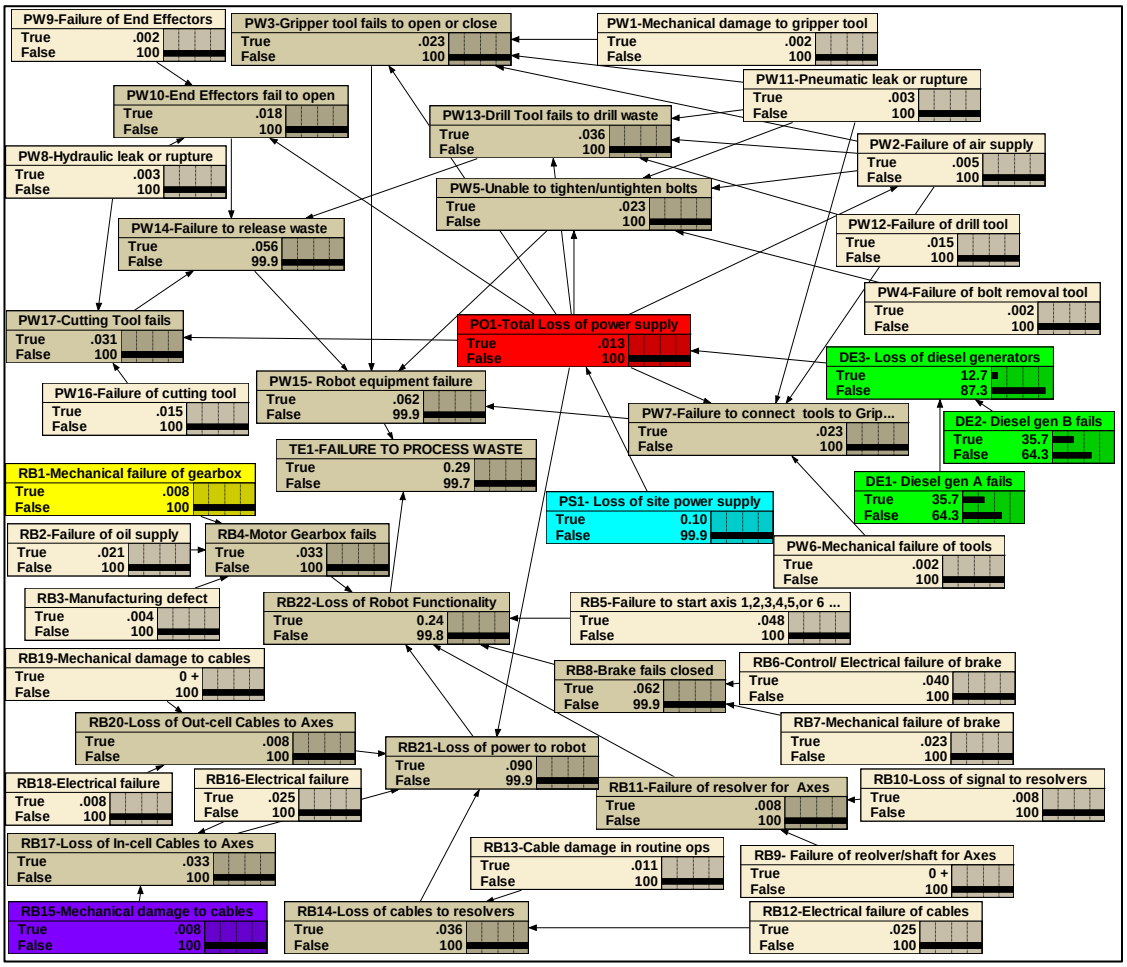

Figure 10-10: BBN showing effect of increased reliability of plant components

Figure 10-10 shows that the overall effect of increasing the reliability of the key sensitive parent nodes RB15 and RB1, by an order of magnitude, is that the Top Event probability is approximately halved to 0.29%. Since an order of magnitude reduction in these

parent probabilities corresponds to very low values of 8E-5, it is acknowledged that design substantiation to achieve such high reliabilities may be difficult to achieve. Nevertheless, the improvement of the power supply by means of the additional diesel generators is considered beneficial and reasonably practicable to achieve.

10.8 Conclusions for Chapter 10

This case study has applied the Bayesian Belief Network methodology to assess the reliability of robotics used for remote handling of radioactive Intermediate Level Wastes. The robots enable performance of repetitive waste processing tasks including characterisation, sorting and size reduction. The BBN methodology as a means of assessing robot system reliability and sensitivity is a technique which has not been previously applied to nuclear chemical plants.

Ultimately a breakdown of the robot system would lead to a reduction of plant throughput and the need for plant recovery. The case study aimed to identify key sensitivities affecting the likelihood of robot breakdown. The objective of the sensitivity analysis was to identify design improvements that could be undertaken to enhance the overall reliability of the system, thus minimising the radiological dose uptake to workers due to plant recovery operations.

The BBN model based on Prior probabilities of the primary events, has shown that there is less than 1% chance that the robot will fail to process the waste. The sensitivity analysis, based on the Bayesian Maximum Probable Explanation (MPE) concept, has shown that the unavailability of the robot system is dominated by the loss of power supply. To a lesser extent, the robot axis motor gearbox failures and damage to in-cell cables also affect the system reliability. The sensitivity analysis also shows that if the reliability of the power supply is improved through the addition of back-up diesel generators, the robot system unavailability reduces further.

CHAPTER 11 : DISCUSSION, CONCLUSIONS AND RECOMMENDATIONS

11.1 Research case studies

Chapter 2 Section 2.6 has identified knowledge gaps and uncertainties associated with hydrogen generation and operability issues in nuclear chemical plants, which need to be managed effectively. Specific knowledge gaps that have been identified are the quantified risk associated with:

- Radiolytic hydrogen explosions in sealed process pipes.
- Failure of ventilation systems used to dilute radiolytic hydrogen in process vessels.
- Failure of reprocessing vessel hydrogen purge and removal systems and the subsequent impact on the decision uncertainty in installing additional hydrogen purge systems to reduce the risk.

The uncertainty in hold-up of hydrogen in radioactive sludges and the effect of a subsequent sudden release of the gas on the hydrogen concentration in the vessel ullage space presents a further significant knowledge gap. There are also knowledge gaps associated with operational risks in nuclear chemical plants including the mixing behaviour of radioactive sludges, performance of robotics during nuclear waste characterisation and control of nuclear fission products associated with solid wastes.

From a literature review of modern Quantified Risk Assessment (QRA) techniques, Bayesian Belief Networks (BBN) and Monte Carlo (MC) simulations have been found to be the most appropriate methods for modelling uncertainty and dependability between multiple variables in complex systems. The BBN and MC techniques also help to address the knowledge gaps identified.

Through the application of the BBN and MC simulation methods to a series of plant case studies, new knowledge on decommissioning and reprocessing operations has been generated. The new knowledge relates to establishing a realistic quantified risk from hydrogen explosions and nuclear plant operability issues. New knowledge has also been gained in terms of the key factors contributing to the quantified risk as well as areas where the greatest uncertainties lie. Furthermore, in relation to the risk from hydrogen explosions, Bayesian inference has been used to identify the least and most hazardous plant conditions. This has enabled identification of fit for purpose solutions for managing the uncertainty, for instance mitigation measures specific to the key sensitivities. The main conclusions drawn from each of the plant case studies are given below.

11.1.1 Case study 1

In Case Study 1, detailed in Chapter 4, the BBN technique was applied to identify the key sensitivities affecting the likelihood of radiolysis leading to a hydrogen deflagration or detonation in sealed pipes.

It has been demonstrated that ignition source probability and hydrogen flammability present the greatest sensitivity to the likelihood of a deflagration or a detonation and subsequent consequences. This suggests that any modification work to the pipes must be carefully controlled to minimise ignition sources. For example, any pipe cutting or grinding operations could be undertaken in an inert atmosphere, thus reducing ignition probability.

Expert judgement of the SL Hydrogen Working Party (HWP) suggests that the oxygen concentration of the sealed pipework is negligible. On this basis the probability of a high flammability reduces significantly.

11.1.2 Case study 2

Case study 2 in Chapter 5 carries out a BBN analysis to explore a plant operability issue concerning the uncertainties associated with radioactive sludge mixing parameters. Through the derivation of probability distributions of the key variables, an optimum set of operating conditions that enable effective removal of the mixed sludge from the vessel, while ensuring that the product quality is acceptable, have been identified.

The sludge water to solids ratio is a key parameter that affects the fluidity and hence the likelihood of the material, with acceptable product quality, being removed from the vessel. To a lesser extent, other parameters, including mixing time and speed, also affect product quality.

The results from this case study as outlined above provide a clear illustration of how BBNs can be used to optimise a plant and process. Thus, an operational decision is reached without the need for additional cost and time-consuming experimental work.

11.1.3 Case study 3

Chapter 6 investigates the application of the Monte Carlo (MC) simulation method to a Fault Tree Analysis (FTA), to determine the likelihood of a failure of the hydrogen dilution mechanism in a process vessel. The ability of the MC simulation technique to model probability distributions, as opposed to single values in a standard FTA, has enabled key uncertainties to be identified and managed effectively.

By comparing the probability distribution of plant repair time with the distributions of the time taken to reach the LFL and the 8% hydrogen concentration limit for plant resilience,

it has been demonstrated that the risk of not undertaking repairs in a timely manner is small. Effective management of the risk is demonstrated through the identification of additional mitigation, in the form of a new duct pressure monitoring instrument, which enables the vent failure due to duct blockage to be revealed.

11.1.4 Case study 4

Hydrogen gas generated from corrosion of metallic magnesium (Magnox) waste, and to a lesser extent radiolysis of radioactive liquors, can potentially be retained within the sludge waste forms. Disturbance of such waste within transportable storage skips can lead to a sudden transient release of a large volume of hydrogen within the vessel ullage space. A BBN has been developed in Chapter 7 to model the uncertainty associated with hydrogen hold-up and sudden release scenarios, and the effects they have on the hydrogen concentration in the vessel ullage space.

Under normal storage operations, the potential for skip disturbance and hence a sudden transient release is small. Based on this condition, the BBN analysis shows that the main proportion of the probability distribution of hydrogen concentration in the ullage space lies in the 0 to 4%vol and 4 to 16%vol ranges, with equal chance. The likelihood of the hydrogen concentration being higher than 16%vol is shown to be negligible.

An analysis to determine the conditions necessary for the least hazardous hydrogen concentration showed that the input parent nodes which present the greatest sensitivity are skip lid filter performance, the total hydrogen generation rate and the type of waste present in the skip. The contribution from radiolytic hydrogen generation has been shown to be insignificant such that the corrosion of Magnox waste is the dominant mechanism.

The main contributor to the total volume of hydrogen in the ullage is the transient, or ‘discontinuous’, release of the held-up gas. If the amount of sludge waste in a skip is reduced then the volume of hydrogen releasing discontinuously would decrease proportionally. This is identified as an effective means of managing the hazard.

11.1.5 Case study 5

Case study 5 in Chapter 8 applies the BBN method to develop a generic model as a novel means of assessing the likelihood of a criticality event occurring in containers of material mixed with PuO_2 and moisture, which behaves as the reaction moderator.

The sensitivity analysis using the Bayesian updating feature has revealed additional information from the model that was not previously known. Based on the developed distributions of the water volume and PuO_2 mass, the BBN uncertainty analysis shows

that the plant conditions are already within the limits for these two parameters such that the likelihood of a criticality is negligible.

The BBN analysis also shows that the overall fault probability for accidentally adding large quantities of PuO_2 and water to a container is highly sensitive to the performance of the drum assay and dose monitoring protection systems. The high integrity of these protection systems leads to the overall risk from criticality being extremely low.

11.1.6 Case study 6

Case Study 6 in Chapter 9 investigates the application of the Bayesian Decision Network (DN) methodology as an alternative new means of analysing decision uncertainties on making improvements in nuclear plants and demonstrating that the risk is ALARP. The decision for introducing improvements against the risk of hydrogen explosions is analysed using the Bayesian DN method and compared against the standard Cost Benefit Analysis (CBA) technique. The Bayesian DN methodology is one which has not been previously applied to hydrogen safety cases for nuclear chemical plants.

More specifically, the case study explores the decision uncertainty associated with the installation of a new compressed air supply in a process vessel. This would enable a reduction in the risk of a hydrogen explosion following a failure of the vessel's hydrogen dilution and extract systems.

The DN analysis has enabled factors affecting the risk of a hydrogen explosion in the process vessel to be linked directly with the decision utilities, which is not possible in the standard CBA approach. Accordingly, the DN analysis has demonstrated that decision is particularly sensitive to the ignition probability and the hydrogen dilution system failure frequency. Based on this sensitivity and on the balance of risk argument, the DN analysis shows that the decision to install the alternative compressed air supply is justified. On this basis the risk is ALARP.

11.1.7 Case study 7

Case study 7 in Chapter 10 applies the BBN methodology to assess the reliability of robotics used for remote handling of radioactive wastes to enable repetitive waste processing tasks including characterisation, sorting and size reduction. The BBN methodology as a means of assessing robot system reliability and sensitivity is a technique which has not been previously applied to nuclear chemical plants.

The BBN sensitivity analysis, using the Maximum Probable Explanation (MPE) concept, has shown that the unavailability of the robot system is dominated by the loss of power supply and to a lesser extent, axis motor gearbox failures and damage to in-cell cables. Based on this sensitivity analysis, an improvement to the reliability of the

power supply, through the addition of back-up diesel generators, has been identified. This improvement ensures that the robot system unavailability reduces further.

11.2 Performance of BBNs and MC simulations against standard practice

Current standard practice for risk quantification in nuclear chemical plants is to apply Fault Tree and Event Tree analysis which are binary systems, limited to AND or OR gates. Only single value data are used in such techniques. BBNs and MC simulations on the other hand allow an uncertainty analysis to be undertaken by providing the ability to model probability distributions of the primary variables. This leads to the result of the hypothesis also in the form of a probability distribution thus enabling an uncertainty analysis.

In the context of hydrogen safety, the uncertainty analysis capability of BBNs has shown to be extremely beneficial particularly in Case Study 4. The benefits gained were a better understanding of the credibility of the likelihood of hydrogen concentration being in the flammable range or less. Thus, the uncertainty analysis allows more realistic risk values to be determined. Also, over-conservatism is prevented in safety cases which are particularly sensitive to the probability of exceeding the Low Flammable Limit of 4%v/v.

The BBN updating feature has been shown to be an exceptionally powerful tool for identifying the key sensitivities. As stated in the conclusions for each of the case studies in section 11.1, this tool has been used to derive the optimum operating strategies whilst managing the uncertainty and hence the risk.

11.3 LFE from research and recommended best practice

Whilst the best means of managing the uncertainty from hydrogen hazards and plant operability issues using BBNs and MC simulations has been identified in the case studies, some important LFE was also gained through the course of this research. Accordingly, the following best practice is recommended when applying these techniques.

11.3.1 LFE and best practice for initial stages of BBN and MC development

BBN analysis is a collaborative technique and must not be undertaken in isolation by one individual assessor, otherwise there is the risk of misinterpretation of the problem in question. At the conceptual stage of the model, relevant team members acquainted with the problem must be involved in the identification of the key variables and the associated interactions. For instance, in this research project the hydrogen explosion and the sludge mixing cases studies involved participation by the SL HWP and CISWG members.

The accuracy of the MC and BBN methods is primarily dependent on the quality of the input data in the analysis. For example, the probability distributions of important parameters such as ignition probability, hydrogen generation rates and equipment failure rates should be supported by sufficient evidence such as previous experimental work and existing literature. In such cases it would be useful to apply the relevant existing research data, for instance the HTG, to BBNs and MC simulations.

11.3.2 Modelling of BBN Discrete Vs Continuous nodes

When modelling discrete nodes with multiple states in a BBN, the best practice is to avoid the use of more than three Parent nodes linking a single Child node as this leads to large Conditional Probability Tables (CPTs), which are difficult to complete manually. For instance, if a child node is affected by three parent nodes, each comprising three possible states, then the resulting CPT for the Child node would be a matrix with 3^3, i.e., 27 entries. This issue was experienced in Case Study 2 for sludge mixing, which showed that with more than three discrete parent nodes, the resulting Conditional Probability Tables (CPTs) were large matrices. Since the CPTs for discrete nodes are populated manually by the user, there is the potential for errors and inconsistencies arising when undertaking such a task. Where application of multiple parent nodes is unavoidable, use of Continuous nodes with equations, to derive the CPTs automatically by the BBN software, should be considered.

For large complex BBNs such as Case Study 4 for hydrogen generation in transportable storage skips, to prevent inconsistencies between various parts of the network, it was established that the best practice is to split the model into manageable sections. The individual smaller BBNs, once verified, were then amalgamated into a fully developed network. This staged development is illustrated in Appendix D Figure D-1 to Figure D-5.

11.3.3 Trending and verification

The input parameter data as well as the BBN results should be verified. For example, the input data for the BBN model in support of Case Study 1 for hydrogen explosions in sealed process pipes were compared with historical plant trends on parameters such as presence of oxygen and ignition sources. Accordingly, appropriate probability distributions for these variables were identified.

In terms of verification, the BBN model should be tested to demonstrate that it agrees with expected behaviour. This can be achieved through the instantiation of various parent nodes and observation of the effect on the associated Child node. For instance, in Case Study 1, instantiation of the ignition probability to zero resulted in the expected

behaviour, i.e., the likelihood of a hydrogen explosion reduced to nil. The sensitivity of the model to changes in the CPT data, as well as the discretisation of continuous nodes should also be tested to see the impact on the end results. An inappropriately discretised continuous node, e.g., lumping the distribution into one large range instead of splitting the range into smaller intervals, will potentially lead to misleading end results. In terms of the verification of MC simulations, comparison should be made with standalone FTAs to confirm that there are no major inconsistencies.

11.4 Recommendations

11.4.1 Application of BBNs and MC simulations to hydrogen safety and equipment reliability assessments

The evidence gathered from this research, as summarised in the preceding sections, demonstrates that the quantification of the risk from hydrogen gas explosions must take into consideration the uncertainty associated with the key variables. In comparison with the existing roadmap, FTA, ETA and CBA approaches, the BBN and MC techniques provide significant benefits in terms of the uncertainty analysis and identification of best means of managing the uncertainty. Whilst it is acknowledged that the existing QRA techniques cannot be completely replaced, they could be applied in conjunction with BBNs and MC simulations for analysing and managing uncertainty. On this basis, it is recommended that the SL Hydrogen Technical Guide (HTG) is updated to reflect the need for uncertainty analysis using the BBN and MC simulation methods, taking on board the suggested best practice in Section 11.3.

Research associated with case studies 2 and 4 has demonstrated that BBNs are not limited to fault analysis. They can also be used to solve process engineering problems and operational decision uncertainties. It is therefore recommended that the HTG illustrates the application of BBNs as a tool for process engineering analysis.

BBNs provide the same functionalities as a standard FTA in terms of modelling the Boolean And and OR logic gates. However, this research project has demonstrated that due to the additional updating features, BBNs are superior in terms of modelling reliability and unavailability of systems such as robotics in nuclear chemical plants. It is therefore recommended that the SL Reliability Engineering section applies BBNs as an additional means of assessing system reliability to improve plant performance.

11.4.2 Future development work

11.4.2.1 Hydrogen gas hold-up

Corrosion of Magnox waste due to storage under water leads to the generation of hydrogen and formation of magnesium hydroxide sludge as a secondary product. This could potentially lead to hold-up of hydrogen in the sludge and expansion of the waste

in storage skips. Ultimately waste expansion could result in a reduction in the volume of the skip ullage space. The BBN analysis performed in Case Study 4 has shown that any subsequent sudden release of the held-up hydrogen gas into the reduced ullage space could result in a hydrogen concentration exceeding the 4% LFL.

A key factor of sensitivity in the sudden release of hydrogen from sludge wastes is the degree of waste expansion in the storage skips. It is recommended that the hydrogen hold-up fractions currently applied in the BBN analysis should be confirmed by experimental work specific to the type of sludge waste being stored in the skips. This would reduce the uncertainty on the volume of the held-up hydrogen.

11.4.2.2 Monitoring filter performance

The Bayesian model for hydrogen generation in the storage skips is also based on the understanding that the skip filters are correctly sized. It would be beneficial to monitor the filter performance and the rate of hydrogen accumulation in the skip ullage space during the actual skip transfer operations on plant. This way the current BBN results for the hydrogen concentration in the ullage space being less than 4%, during normal operations, could be confirmed through a comparison with measured plant data. Although this plant condition monitoring cannot take place at the current time since the skip handling process is still at the design stage, it is recommended that the monitoring is undertaken when the skip operations commence on plant.

11.4.2.3 Oxygen depletion rate

The radiolytic hydrogen generation rates assessed in the BBN analyses for Case Studies 1 and 4 are primarily based on the predicted 'G' values for radioactive aqueous and nitrate based liquors. However, it is known that there are other contributory factors that affect radiolysis. For instance, it is known that radiolysis in sealed pipework can be prevented due to ferritic contaminants in the pipes leading to consumption of oxygen in the ullage space. However, there is still an uncertainty associated with the precise level of oxygen depletion in such environments. It is therefore recommended that further experimental development work is undertaken to determine the rate of oxygen depletion in specific nuclear environments such as aged and sealed process pipes. This would result in an improvement in the accuracy of the conditional probability of oxygen depletion in the BBN analysis for hydrogen explosions in sealed pipes.

11.4.2.4 Effect of waste compaction on criticality

In terms of the likelihood of a criticality in containers of solid radioactive material, it is considered that under certain conditions the criticality can be self-terminating. One possible condition is where the water moderator associated with the waste drains out

during the compaction process. Although compaction would lead to concentration of the fissile material, the drainage of water from the waste would mean that there is negligible moderator available for a criticality. It is therefore recommended that the Bayesian model is further developed to address this uncertainty. Hence the BBN model accuracy could be improved.

11.4.2.5 Improvement of the BBN modelling technique

When modelling a continuous variable which has a range of values, the BBN methodology requires the range to be discretised into equal discrete intervals. The probability of each discretised interval is then calculated by the BBN software based on the probability distribution assigned to the variable. The current technique for modelling continuous variables relies on the BBN modeller to input the appropriate number of discretised intervals. An insufficient number of intervals can lead to inaccuracies in the application of the probability distribution which could lead to an incorrect quantification of the BBN result. Conversely an excess number of discretised intervals could cause an inability to calculate a probability for all the cells in the CPT matrix, again leading to an inaccurate result.

The current technique relies on a sensitivity analysis to identify an optimum number of discretised intervals for continuous variables, hence reducing the inaccuracies. If the discretisation could be automated, the methodology for modelling of continuous variables could be improved. Therefore, it is recommended that further work is undertaken to identify possible methods for automation of continuous variable discretisation.

REFERENCES

Ackroyd, G. Bailey, M. and Mullins, R. (2009) The effect of reduced oxygen levels on the electrostatic ignition sensitivity of dusts, *Institution of Chemical Engineers Hazards XXI Conference,* Manchester, 10-12 November 2009.

Ahmed F. (2015) *Minutes of the meeting to review sludge mixing parameters in support of Bayesian network for research case study 2, 12 February 2015,* Conference Room2, NSG, Chorley.

Ahmed, F. (2016) *Minutes of the meeting for the development of a Bayesian Belief Network for hydrogen detonations and deflagrations in sealed process pipes, 2 February 2016,* Sellafield Ltd, Hinton House, Warrington.

Ahmed, F. (2017a) *Minutes of the meeting for the development of a Bayesian Belief Network for hydrogen generation during box handling operations, 16 February 2017*, Sellafield Ltd, Hinton House, Warrington.

Ahmed, F. (2017b) Bayesian Belief Networks - A robust approach to quantified risk and uncertainty analysis, *Institution of Chemical Engineers*, *The Chemical Engineer,* 911, pp. 28-32.

Ahmed, F. (2017c) *Minutes of the meeting to identify Bayesian network variables for research case study 5, criticality in waste storage containers, 21 December 2017,* Sellafield Ltd, Albion House, Whitehaven/ Hinton House Video Link.

Ahmed, F. (2018a) *Minutes of the meeting for the presentation of the fully developed Bayesian Belief Network for hydrogen generation during box handling operations, 22 March 2018*, Sellafield Ltd, Hinton House, Warrington.

Ahmed, F. (2018b) *Minutes of the meeting to identify the causes and effects associated with robot system failures during waste handling operations, 30 August 2018*, Sellafield Ltd, Hinton House, Warrington.

Ahmed, F. (2019a) Managing hydrogen gas hazards, *Nuclear Future, The Professional Journal of the Nuclear Institute*, 15(2), pp.46-50.

Ahmed, F. (2019b) Application of Bayesian Belief Networks to assess hydrogen gas retention hazards and equipment reliability in nuclear chemical plants, *Proceedings* of the *Institution of Chemical Engineers Hazards 29 Conference, Symposium Series No.166*, Birmingham, 22-24 May 2019.

Ahmed, F. (2019c) *Minutes of the meeting to discuss historical trends on radiolytic hydrogen in sealed process pipes, 11 November 2019,* Sellafield Ltd, Hinton House, Warrington.

Ahmed, F. *(2020) Minutes of the meeting to present the finalised BBN results for criticality in drums of solid wastes, 8 June 2020*, Sellafield Ltd. Microsoft Teams Meeting.

arXiv, (2014) *How statisticians found Air France flight 447 two years after it crashed into Atlantic*. Available from: https://www.technologyreview.com/2014/05/27/13283/how-statisticians-found-air-france-flight-447-two-years-after-it-crashed-into-atlantic/ [Accessed 28 March 2021].

Averill, A. F. Ingram, J. M. Battersby, P. and Holborn, P. G. (2014) Ignition of flammable hydrogen mixtures by mechanical stimuli. Part 1: Ignition with clean metal surfaces sliding under high load conditions, *International journal of hydrogen energy*, 39, pp.18472-18479.

Averill, A. F. Ingram, J. M. Battersby, P. and Holborn, P. G. (2015) Ignition of flammable hydrogen mixtures by mechanical stimuli. Part 3: Ignition under conditions of low sliding velocity (<0.8m/s), *International journal of hydrogen energy*, 40, pp. 9847-9853.

Averill, A. F. Ingram, J. M. Holborn, P. G. Battersby, P. and Benson, C. M. (2018) Application of Bayesian methods and networks to ignition hazard event prediction in nuclear waste decommissioning Operations, *Process Safety and Environmental Protection*, 116, pp. 396-404.

Baig, A. A. Ruzli, R. and Buang, A. (2013) Reliability analysis using fault tree analysis: A review, *International Journal of Chemical Engineering and Applications*, 4, pp. 169-173.

Bayes Server. (2018) 32 Bit, Version 8.3. Available from: https://www.bayesserver.com. [Accessed 28 March 2021].

Bedford, T. and Cooke, R. (2001) *Probabilistic Risk Analysis – Foundations and Methods*. Cambridge: Cambridge University Press.

Beurden, I. and Goble, W. M. (2016) The key variables needed for PFD avg Calculation, Exida, Update 1.2. Available from: https://www.exida.com/articles/White-Paper-Key-Variables-Needed-for-PFDavgCalculationSep-2016-rev1.pdf [28 March 2021].

Bibler, N. E. Pareizs, J. M. Fellinger, T. L. and Bannochie, C. J. (2007) Measurement and Prediction of Radiolytic Hydrogen Production in Defence Waste Processing Slurries at Savanah River Site, *WM 07 Conference*, 2007.

Bilgic, I. Onder, M. and Yesin, O. (1994) Uncertainty Analysis for the Maximum Credible Accident Probability of the TR-2 Research Reactor, *International Meeting: PSA/PRA and Severe Accidents 94*, Slovenia, April,1994.

Bloss, R. (2010) How do you decommission a nuclear installation? Call in the robots, *Industrial Robot: An International Journal*, 37(2), pp.133-136.

Bobbio, A. Portinale, L. Minichinob, M. and Ciancamerlab, E. (2001) Improving the analysis of dependable systems by mapping fault trees into Bayesian networks, *Reliability Engineering and System Safety,* 71, pp.249–260.

Bogue, R. (2011) Robots in the nuclear industry: a review of technologies and applications, *Industrial Robot: An International Journal*, 38 (2) pp.113-118.

Bolstad, W.M. (2007) *Introduction to Bayesian Statistics*, 2nd Ed. Hoboken, New Jersey: John Wiley and Sons.

British Standards Institute. (2010) *Functional safety of electrical/ electronic/ programmable electronic safety-related systems (E/E/PE, or E/E/PES), IEC 61508*.

British Standards Institute. (2011) *BS EN 62502:2011, Analysis techniques for dependability – Event Tree Analysis (ETA)*.

British Standards Institute. (2019) *BS EN 1127-1:2019*, *Explosive atmospheres - Explosion prevention and protection. Part 1: Basic concepts and methodology.*

Cain, J. (2001) *Planning improvements in the natural resource management. Guidelines for using Bayesian networks to support the planning and management of development programmes in the water sector and beyond*, Centre for Ecology and Hydrology, Gromwarsh Gifford, U.K.

Carteret, B. A. Holliday, M.A. and Jones, E.D. (1997) Needs Assessment for Remote Systems Technology at the Chornobyl Unit 4 Shelter. Available from: https://inis.iaea.org/collection/NCLCollectionStore/_Public/29/040/29040418.pdf?r=1. [Accessed 28 March 2021].

Cashdollar, K. L. Zlochower, I. A. Green, G. M. Thomas, R. A. and Hertzberg, M. (2000) Flammability of methane, propane, and hydrogen gases, *Journal of Loss Prevention in the Process Industries,* 13, pp.327-340.

Chengyan, T. Jing, L. Zixiang, Z. Zeng L.Cheng Z. and Hui, R. (2019) How to optimize ecosystem services based on a Bayesian model: a case study of Jinghe river basin, *Sustainability*, 11(15), 4149; https://doi.org/10.3390/su11154149

Ciccarelli, G. and Dorofeev, S. (2008) Flame acceleration and transition to detonation in ducts, *Progress in Energy and Combustion Science,* 34, pp.499–550.

Coward H. F. and Jones G. W. (1952) Limits of flammability of Gases and Vapours, US Bureau of Mines Bulletin 503. Available from: https://shepherd.caltech.edu/EDL/PublicResources/flammability/USBM-503.pdf. [Accessed 28 March 2021]

Dahoe, A. E. (2011). Tutorial on deflagrations and detonations, University of Ulster. Available from: http://www.hysafe.org/science/eAcademy/JSSFCH/.JSSFCH2011/DahoeAE_TutorialOnDeflagrationsAndDetonations.pdf [Accessed 28 March 2021].

Dexter, A. H. and Perkins, W. C. (1982) Component failure-rate data with potential applicability to nuclear fuel reprocessing plant, Du Pont de Nemours (E.I.) and Co. Aiken, SC (USA). Available from: University of North Texas Digital Library, https://www.osti.gov/biblio/5296365 [Accessed 28 March 2021].

Dunnett, B. F. (2007) Review of the development of UK high level waste vitrified product, Nexia Solutions (06) 7926, Issue 4. Available from: https://rwm.nda.gov.uk/publication/review-of-the-development-of-uk-high-level-waste-vitrified-product/?download [Accessed 28 March 2021].

Ellis, G.R. (2008) Practical application of static hazard assessment and DSEAR compliance, *Institution of Chemical Engineers Hazards XX Conference,* Symposium Series No. 154, Manchester, 2008.

Fenton, N. and Neil, M. (2001) Making Decisions using Bayesian Nets and MCDA, *Knowledge-Based Systems*, 14, pp.307-325.

Fenton, N. E. Neil, M. and Caballero, J.G. (2007) Using ranked nodes to model qualitative judgments in Bayesian networks', *IEEE Transactions of Knowledge Data Engineering* 19(10), pp.1420-1432.

Fischetti, M. A. (1985) Robots do the dirty work: some walk, some roll as they go about their tedious, hazardous chores in nuclear-power plants, *IEEE Spectr* ,22(4), pp.65–73.

French, S. Bedford, T. and Atherton, E. (2005) Supporting ALARP decision making by cost benefit analysis and multi-attribute utility theory, *Journal of Risk Research* 8 (3), pp.207–223.

French Republic, Ministry of ecology, energy, sustainable development and town and country planning. (2009) Accidentology involving hydrogen, Available from: www.aria.developpementdurable.gouv.fr/wp.../SY_hydrogen_GB_2009.pdf. [Accessed 28 March 2021].

FrontlineSolvers. (2020) Risk Solver software. Available from: https://www.solver.com/ [Accessed 28 March 2021].

Fujii, M. Kimura, T. and Sadakane, K. (1976) A Robotic approach to reduction of personnel radiation exposure in nuclear power plants, *Journal of Nuclear Science and Technology*, 13(8), pp.462-46.

Galassi, M. C. Papanikolaou, E. Baraldi, D. Funnemark, E. Håland, E. Engebø, A. Haugom, G. P. Jordan, T. and Tchouvelev, A. (2010) HIAD, Hydrogen Incidents and Accidents Database, *European Commission, Institute for Energy.* Available from: https://h2tools.org/sites/default/files/ICHS_import/paper%20(HIAD).pdf [Accessed 28 March 2021].

Gharari, R. Kazeminejad, H. Mataji, N. Kojouri, A. and Hedayat A. (2018) A review on hydrogen generation, explosion, and mitigation during severe accidents in light water nuclear reactors, *International Journal of Hydrogen Energy*, 43, pp.1939-1965.

Gibson, N. and Harper, D. J. (1988), Parameters for assessing electrostatic risk from non-conductors- A discussion, *Journal of Electrostatics*, 21, pp.27-36.

Grossel S. S. (2002) *Deflagration and detonation flame arresters*. New York: American Institute of Chemical Engineers, Centre for Chemical Process Safety.

Gummer, J. and Hawksworth, S. (2008) Spontaneous ignition of hydrogen, literature review. HSE Research Report RR615. Available from: http://www.hse.gov.uk/research/rrpdf/rr615.pdf [Accessed 28 March 2021].

Gupta, S. and Langer, G. (2019) Experimental research on hydrogen deflagration in multi-compartment geometry and application to nuclear reactor conditions, *Nuclear Engineering and Design,* 343, pp.103-137.

Hanea, D. and Ale, B. (2009) Risk of human fatality in building fires: A decision tool using Bayesian networks. *Fire Safety Journal*, 44, pp.704-710.

Haugom, G. P. and Friis-Hansen, P. (2011) 'Risk modelling of a hydrogen refuelling station using Bayesian network. *International Journal of Hydrogen Energy*, 36, pp. 2389 - 2397.

Health and Safety Executive (HSE). (1992) *The tolerability of risk from nuclear power stations*, London: Her Majesty's Stationary Office.

Health and Safety Executive (HSE). (1998) *Principles and guidelines to assist HSE in its judgments that duty holders have reduced risk as low as reasonably practicable*. London: HMSO.

Health and Safety Executive (HSE). (2001) *Reducing risks protecting people*, ISBN 0 7176 2151 0, London: Her Majesty's Stationary Office.

Health and Safety Executive (HSE). (2017) Failure rates and event data for use within risk assessments. Available from: https://www.hse.gov.uk/landuseplanning/failure-rates.pdf [Accessed 28 March 2021].

Health and Safety Executive (HSE). (2020) Cost Benefit Analysis (CBA) checklist, Available from: http://www.hse.gov.uk/risk/theory/alarpcheck.htm [Accessed 28 March 2021].

Hicks, T. W. (2007) *Criticality safety assessment for waste packages containing separated plutonium, Version 1.1*, Nuclear Decommissioning Authority. Available from: https://rwm.nda.gov.uk/publication [Accessed 28 March 2021].

Hicks, T.W. (2009) The general criticality safety assessment. Available at: https://rwm.nda.gov.uk/publication/the-general-criticality-safety-assessment/. [Accessed 28 March 2021].

Holborn, P. G. Battersby, P. Ingram, J. M. Averill, A. F. and Nolan, P. F. (2013) Modelling the effect of water fog on the upper flammability limit of hydrogen-oxygen-nitrogen, *International Journal of Hydrogen Energy*, 38, pp.6896-6903.

Hollnagel, E., and Yushi, F. (2013) Fukushima disaster- Systematic failures as the lack of resilience, *Nuclear Engineering and Technology*, 45(1), pp.13-20.

Hong, E. Lee, I. Shin, H. Nam, S. and Kong, J. (2009) Quantitative risk evaluation based on event tree analysis technique, *Tunnelling and Underground Space Technology,* 24, pp. 269-277.

Hugin Expert A/S. (2018) Version 8.6, Available from: http://www.hugin.com/ [Accessed 28 March 2021].

Institute of Electrical and Electronics Engineers (IEEE). (1983) *Standard 500-1984: IEEE Guide to the collection and presentation of electrical, electronic, sensing component, and mechanical equipment reliability data for nuclear-power generating stations,* pp.1-1424, ISBN: 978-0-7381-4379-8.

International Atomic Energy Agency (IAEA). (1997) *Generic component reliability data for research reactor PSA, IAEA-TECDOC-930, ISSN 1011-4289*. Available At: https://www-pub.iaea.org/MTCD/Publications/PDF/te_0930_scr.pdf [Accessed 28 March 2021].

International Atomic Energy Agency (IAEA). (2003) Guidelines for radioelement mapping using gamma ray spectrometry data, ISBN 92–0–108303–3. Available from https://www-pub.iaea.org/mtcd/publications/pdf/te_1363_web.pdf. [Accessed 11 March 2021].

International Atomic Energy Agency (IAEA). (2009) *Safety standards for protecting people and the environment, Classification of Radioactive Waste, General Safety Guide No. GSG-1*. ISBN 978–92–0–109209–0. Available from: https://www-pub.iaea.org/MTCD/Publications/PDF/Pub1419_web.pdf [Accessed 28 March 2021].

International Electrotechnical Commission (IEC). (2010) *Standard IEC 61508:2010: Functional Safety of Electrical/Electronic/Programmable Electronic Safety-related Systems (E/E/PE, or E/E/PES)*.

International Youth Nuclear Congress (2013) *Interview with Mr François GAUCHÉ, CEA*. Image. Available from: https://www.iync.org/interview-with-mr-francois-gauche-cea/. [Accessed 28 March 2021].

Ingram, J. M. Kempsell, I.D. Wakem, M. J. and Fairclough, M. P. (2001) Hydrogen explosion – An example of hazard avoidance and control, *IChemE Hazards XVI Conference*, Symposium Series No. 148, pp.523-539.

International Organisation for Standardisation (ISO), (2015) Basic considerations for the safety of hydrogen systems, ISO/TR15916: 2015.

Jensen, F. V. and Nielsen, T. D. 2007*. Bayesian Networks and Decision Graphs*, ISBN 9780387682815, New York: Springer.

Jones, S. Averill A. F. Ingram, J. M. Holborn, P. G. Battersby P. Nolan P. F. Kempsell, I. D. and Wakem, M. J. (2006a). Mitigation of hydrogen-air explosion mixtures. IChemE *Hazards XIX conference*, Manchester 27-30, March 2006.

Jones, S. Averill A. F. Ingram, J. M. Holborn, P. G. Battersby P. Nolan P. F. Kempsell, I. D. and Wakem, M. J. (2006b). Impact ignition of hydrogen air mixtures. IChemE *Hazards XIX conference*, Manchester, 27-30, March 2006.

Jones-Lee, M. T. and Aven, T. (2011) ALARP- What does it really mean, *Reliability Engineering and System Safety*, 96, pp.877-882.

Khakzad, N. Khan, F. and Amyotte, P. (2011) 'Safety analysis in process facilities: Comparison of fault tree and Bayesian network approaches', *Reliability Engineering and System Safety,* 96, pp.925-932.

Khan, F. Rathnayaka, S. and Ahmed, S. (2015) Methods and models in process safety and risk management: past, present, and future. *Process Safety and Environmental Protection*, 98, pp.116-147.

Kirwan, B. Umbers, I. Edwards, J. and Gibson, H. (2008) Quantifying the unimaginable human performance limiting values. Available from: https://www.hkarms.org/ASUS_Server/psam9.sytes.netweb_resources_20080518_PSAM9/Parallel_Session/D_Harbour_III/Wed_7-9/D7_1030-1200/Quantifying_the_Unimaginable_Human_Performance_Limiting_Values.pdf [Accessed 28 March 2021].

Kleemann, J. Celio, E. and Fürst, C. (2017) Validation approaches of an expert-based Bayesian Belief Network in Northern Ghana, West Africa, *Ecological Modelling,* 365, pp.10-29.

Knief, R. A. (2008) *Nuclear Engineering, Theory and technology of commercial nuclear power*, 2nd Ed. ISBN- 10-89448-458-3, Illinois: American Nuclear Society, Inc.

Kuo, K. K. (2005) *Principles of Combustion*, 2nd Ed., Wiley.

Kwisthout, J. (2011) Most probable explanations in Bayesian networks: Complexity and tractability, *International Journal of Approximate Reasoning*, 52, pp.1452-1469

Kotchourko, A. Baraldi, D. Benard, P. Jordan, T. Kessler, A. and LaChance, J. (2013) State-of-the-art and research priorities in hydrogen safety, *5th International Conference on Hydrogen Safety*, 9-11 September, Brussels.

Le Caer, S. (2011) Water Radiolysis: Influence of oxide surfaces on H_2 production under ionizing radiation, *Water*,3, pp. 235-253.

Lee J. H. (1987) A summary of hydrogen in air detonation experiments, Office of Nuclear Regulatory Research, U. S. Nuclear Regulatory Commission. Available At: https://inis.iaea.org/collection/NCLCollectionStore/_Public/20/071/20071936.pdf. [Accessed: 28 March 2021].

Lees, F. P. (1992) *Loss Prevention in the Process Industries*, 1st Ed., Volume 1, ISBN 0 7506 1522 2, Butterworth-Heinemann Ltd.

Lewis, B. and von Elbe, G. (1961) *Combustion, Flames and Explosions of Gases*, 2nd ed., New York: Academic Press, Inc. p. 535.

Logan. (2018) *Logan Fault Tree and Event Tree Analysis*, User Manual *Version 7.5.6, Issue I*, Available at: www.loganfta.com [Accessed 28 March 2021].

Machine Design. (2020) Six Axes Cylindrical Robot, Image Available from: https://www.machinedesign.com/robotics/what-s-difference-between-industrial-robots. [Accessed 28 March 2021].

Marco, L. (2021) Optimum number of trials for Monte Carlo Simulation. Available at https://www.valuationresearch.com/wp-content/uploads/kb/SpecialReport_MonteCarloSimulationTrials.pdf [Accessed 17 February 2021.

Miki, K. Prudencio, E. E. Hung, S. and Terejanu, G. (2013) Using Bayesian analysis to quantify uncertainties in the H + O2 → OH + O reaction, *Combustion and Flame,* 160, pp.861-869.

Mannan S. (2004) *Lee's Loss Prevention in the Process Industries, Hazard Identification, Assessment and Control*, Volume 1, 3rd Ed., Butterworth-Heinemann.

Mirza, N. R. Degenkolbe, S. and Witt, W. (2011) Analysis of hydrogen incidents to support risk assessment, *International Journal of Hydrogen Energy*,36, pp.12068 – 12077.

Mkrtchyan, L. Podofillini, L. Dang, V. N. (2016) Bayesian belief networks for human reliability analysis: A review of applications and gaps, *Reliability Engineering and System Safety* 139, pp.1-16.

Mkrtchyan, L. Podofillini, L. Dang, V. N. (2016) Methods of building Conditional Probability Tables of Bayesian Belief Networks from limited judgement: An evaluation of Human Reliability Application, *Reliability Engineering and System Safety,* 151, pp.93-112.

Moura, M. C. Azevedo, R. V. Droguett, E. L. Chaves, L. R. Lins, I. D. Vilela, R. F. and Filho, R. S. (2016) Estimation of expected number of accidents and workforce unavailability through Bayesian variability analysis and Markov-based model, *Reliability Engineering and System Safety,* 150, pp.136-146.

Norsys Software Corporation. (2010) Netica Version 4.16, Available from: https://www.norsys.com. [Accessed 28 March 2021].

Norsys Software Corporation. (2021) Validation of Netica software, Email to F Ahmed, 16 January, 2021.

Nettleton, M. A. (1987) *Gaseous Detonations: their nature, effects and control*, Chapman and Hall.

Nonelectronic Parts Reliability Data NPRD11. (2011) ISBN 978-1-933904-22-1, Available from: https://www.quanterion.com/product/publications/nonelectronic-parts-reliability-data-nprd-2011/ [Accessed 28 March 2021].

Nuclear Decommissioning Authority (NDA). (2016) *Strategy, Effective from April 2016*, ISBN 9781474130431. Available from: https://www.gov.uk/government/publications [Accessed 28 March 2021].

Nuclear Power, Plutonium 239, Available at https://www.nuclear-power.net/nuclear-power-plant/nuclear-fuel/plutonium/plutonium-239/ [Accessed 28 March 2021].

Office for Nuclear Regulation (ONR). (2006) Numerical targets and legal limits in Safety Assessment Principles for Nuclear Facilities - an explanatory note, First

Edition. Available from: http://www.onr.org.uk/saps/numerical-targets-limits-explanatory-note.pdf [Accessed 28 March 2021].

Office for Nuclear Regulation (ONR). (2015) Hazard and risk reduction from highly active liquor, Project Assessment Report, ONR-SEL-PAR-15-009, Revision 0. Available at: http://www.onr.org.uk/pars/2015/sellafield-15-009.pdf. [Accessed 28 March 2021].

Office for Nuclear Regulation (ONR). (2017) ONR's strategy for regulating Sellafield, Available from: www.onr.org.uk/sellafield-strategy.htm. [Accessed 28 March 2021].

Office for Nuclear Regulation (ONR). (2020) *Safety Assessment Principles for Nuclear Facilities*, Revision 1, 2014 Edition. Available from: www.onr.org.uk/saps/saps2014.pdf. [Accessed 28 March 2021].

Palisade (2019) @ Risk software. Available from: https://www.palisade.com/msoffice/risk.asp. [Accessed 28 March 2021].

Pasman, H. J. (2011) Challenges to improve confidence level of risk assessment of hydrogen technologies, *International Journal of Hydrogen Energy,* 36, pp.2407-2413.

Pasman, H. J. and Rogers, W. J. (2012) Risk assessment by means of Bayesian networks: A comparative study of compressed and liquefied H_2 transportation and tank station risks', *International Journal of Hydrogen Energy*, 37, pp. 17415-17425.

Pasman, H. and Rogers, W. (2013) Bayesian networks make LOPA more effective, QRA more transparent and flexible, and thus safety more definable! *Journal of Loss Prevention in the Process Industries,* 26, pp.434-442.

Pasman, H. J. Knegtering, B. and Rogers, W. J. (2013) A holistic approach to process safety risks: Possible ways forward, *Reliability Engineering and System Safety* 117, pp.21-29.

Pitchforth, J. and Mengersen, K. (2013) A proposed validation framework for expert elicited Bayesian Networks, *Expert Systems with Applications*, 40, pp.162-167.

Podofillini, L. and Dang, V. N. (2013) A Bayesian approach to treat expert-elicited probabilities in human reliability analysis model construction, *Reliability Engineering and System Safety*, 117, pp.52-64.

Portinale, L. and Bobbio, A. (2013) Bayesian networks for dependability analysis: An application to digital control reliability, Report No. UAI-P-1999-PG-551-558, *Proceedings of the Fifteenth Conference on Uncertainty in Artificial Intelligence (UAI1999)*. January 2013.

Putley, D. and Prescott, A. (2007) Monk calculations to support criticality safety assessment of irradiated natural uranium and separated plutonium waste packages*, United Kingdom Nirex Limited*. Available from: https://rwm.nda.gov.uk/publication. [Accessed 28 March 2021].

Puttick, S. (2008) Avoidance of ignition sources as a basis of safety- limitations and challenges, *Institution of Chemical Engineers Hazards XXI Conference*, Manchester, 15-17 April, 2008.

Ridley, L.M. (2000) Doctoral Thesis, Dependency modelling using fault tree and cause-consequence modelling, Loughborough University.

Rogers, R. L. Hawksworth, S. Beyer, M. Proust, C. Lakie, D., Gummer, J. and Raveau, D. (2006) Ignition of Dust Clouds and Dust Deposits by Friction, Sparks and Hotspots, *Institution of Chemical Engineers Hazards XIX Conference*, March, 2006.

Røed, W. Mosleh, A. Vinnem, J. E. and Henneman, L. (2014) On the use of the hybrid causal logic method in offshore risk analysis, *Reliability Engineering and System Safety*, 130, pp.1-11.

Sargent, R. (2011) Verification and Validation of Simulation Models". *Proceedings of the 2011 Winter Simulation Conference*. Doi: 10.1109/WSC.2010.5679166. Available from:
https://www.researchgate.net/publication/224209154_Verification_and_validation_of_simulation_models. [Accessed: 13 January 2021].

Shachter, R. and Peat. M. (1992) Decision making using probabilistic inference methods, *Proceedings of the Eighth Conference on Uncertainty in Artificial Intelligence*, pp. 276-283, 1992.

Schiavetti, M. and Carcassi, M. (2017) Maximum overpressure vs. H2 concentration non-monotonic behaviour in vented deflagration. Experimental results, *International Journal of Hydrogen Energy*, 42, pp.7494-7503.

Schietekat S. De Waal, A. and Gopaul, K.G. (2016) Validation & verification of a Bayesian network model for aircraft vulnerability, *12th INCOSE SA Systems*

Engineering Conference, ISBN 978-0-620-72719-8. Available from: https://www.researchgate.net/publication/308266033_Validation_Verification_of_a_Bayesian_Network_Model_for_Aircraft_Vulnerability. [Accessed: 13 January 2021].

Shepherd, J. E. (2009) Structural response of piping to internal gas detonation, *Journal of Pressure Vessel Technology*, 131(3), pp. 031204-1- 031204-13.

Siemens AG. (2019) Services and Support, Mean Time Between Failures, Entry ID 16818490. Available from: https://support.industry.siemens.com/cs/document/16818490/mean-time-between-failures-(mtbf). [Accessed 28 March 2021].

Stamatelatos, M. and Vesely, W. (2002) *Fault Tree Handbook with Aerospace Applications, Version 1.1*, Available from: http://www.semanticscholar.org [Accessed 28 March 2021].

Stamps, D. W. and Tiezen, S. R. (1991) The influence of initial temperature and pressure on hydrogen-air diluent detonations, *Combustion and Flame*, 83(3) pp.353-364.

Structured Data LLC. (2007) RiskAmp, Version 2.5, Available from: https://www.riskamp.com. [Accessed 28 March 2021].

Summers, A. E. Ford, K. A. and Glenn, R. (1999) Estimation and evaluation of common cause failures in SIS, *Loss Prevention Symposium*, Houston, Texas. Available from: www.iceweb.com.au/sis/e_and_e.htm. [Accessed 27 June 2020].

Taylor, C. (2019) Probability of the union of 3 or more sets, ThoughtCo. Available from: https://www.thoughtco.com/probability-union-of-three-sets-more-3126263. [Accessed 16 January 2021].

Tsitsimpelis, I. Taylor C. J. Lennox B. and Joyce M. J. (2019) A review of ground-based robotic systems for the characterization of nuclear environments, *Progress in nuclear energy*, 111, pp. 109-124.

van Kessel, T. and van Kesteren, W. G. M. (2002) Gas production and transport in artificial sludge depots, *Waste Management*, 22, pp.19–28.

Vesley, W. E. Goldberg, F.F. Roberts, N.H. and Haasal, D. F. (1981) Fault Tree Handbook, Systems and Reliability Research Office of Nuclear Regulation Research,

US Nuclear Regulatory Commission, NUREG-0492, Available from: https://www.nrc.gov/docs/ML1007/ML100780465.pdf. [Accessed 31 December 2020].

Vilchez, J. A. Espejo, V. and Casal, J. (2011) Generic event trees and probabilities for the release of different types of hazardous materials', *Journal of Loss Prevention in the Process Industries*, 24, pp.281-287.

Vose, D. (2008) *Risk Analysis – A Quantitative Guide*, 3rd Ed., New York: John Wiley and Sons.

Vose Software. (2020) ModelRisk. Available from: https://www.vosesoftware.com/products/modelrisk/ [Accessed 13 July 2020].

Wisse, B.W. van Gosliga, S.P. van Elst, N.P. and Barros, A.L. (2008) Relieving the elicitation burden of Bayesian Belief Networks, *Proceedings of the sixth Bayesian modelling application workshops on UAI*. Helsinki, Finland.

Yang, X. Rogers, W.J. and Mannan, M.S. (2010) Uncertainty reduction for improved mishap probability prediction: Application to level control of distillation unit, *Journal of Loss Prevention in the Process Industries,* 23, pp.149-156.

Yun, G.W. Rogers, W.J. and Mannan, M.S. (2009) Risk assessment of LNG importation terminals using the Bayesian – LOPA methodology, *Journal of Loss Prevention in the Process Industries* 22, pp. 91-96.

Zalosh, R.G. Short, T.P. Marlin, P.G. and Coughlin, D.A. (1978) Comparative analysis of hydrogen and fire and explosion incidents, United States Department of Energy, Division of Operational and Environmental Safety*,* Progress Report No.3 for Period March 1, 1978 – June 30, 1978. Available from: https://www.osti.gov/servlets/purl/6868081 [Accessed 28 March 2021].

APPENDIX A1: HYDROGEN GENERATION MECHANISMS IN NUCLEAR CHEMICAL PLANTS

Plant (Note 1)	Hydrogen generation mechanism	Key hydrogen safety challenges
P1	Metallic magnesium (Magnox) waste arising from fuel decanning operations, submerged in water, is imported into the plant in approximately 500L flasks, for immobilisation in cement grout formulations. The corrosion of magnesium within the flasks can potentially lead to a build-up of hydrogen gas within the flask ullage space, with a volume of 50L.	Enhanced corrosion of Magnox waste within the flask can lead to an increased hydrogen generation rate. Other possible contributors increasing the risk of hydrogen explosions within the flask are believed to be uranium hydride associated with the waste, which could be a potential ignition source. Diffusion through the vent in the flasks is another area of uncertainty.
P2	Plant P2 requires the raw Magnox swarf and sludge waste retrieved from Plant P5 to be stored under water in skips which are housed within $3m^3$ boxes. Hydrogen gas is continuously generated due to the corrosion reaction of the metallic waste with the water. In sludge waste forms some hydrogen gas may also be held up within the waste matrix, thus giving the potential for a sudden or discontinuous release of a large volume of the gas in the skip ullage space.	The hydrogen gas is continuously generated and will accumulate within the skip ullage space after placement of the skip lid. Filtered vents are connected to the skip lid and the outer box lid to enable the gas to be extracted, such that the hydrogen in air concentration in the skip ullage space is maintained at 1%vol. However, the skip and box filtered vents are not designed to cope with the discontinuous gas release of hydrogen. The hazard management strategy against the discontinuous release scenarios is to employ preventative measures against adverse waste disturbance.
P3	Plant P3 carries out reprocessing of nuclear fuels and active liquors. Hydrogen gas in vessels within the plant is produced either by radiolysis or by chemical reaction of the decanned metal fuel cladding with the acid in the liquor bulk storage tanks.	Similar to plant P4 the key hazard management strategy is to dilute the hydrogen accumulated in the vessel ullage space with air. Therefore, a loss of air supply to the vessel ullage space could result in a hydrogen concentration exceeding the LFL. Back-up air supplies are provided to protect against this fault.
P4	Plant P4 carries out the evaporation and storage of high active liquors. The vessels are cooled using cooling coils. There is the potential for ingress of radioactivity into the cooling coils. Ultimately this could lead to radiolysis of the stagnant water within the cooling coils. Radiolysis of the bulk liquor in the vessels also occurs leading to accumulation of hydrogen in the vessel ullage space.	The key hazard management strategy is to dilute the hydrogen accumulated in the vessel ullage space with air. Therefore, a loss of air supply to the vessel ullage space could result in a hydrogen concentration exceeding the LFL. Back-up air supplies are provided to protect against this fault. To minimise the risk from radiolytic hydrogen generation due to radioactive liquor leaking into the cooling coils, all failed coils are required to be sealed and isolated.

Plant (Note 1)	Hydrogen generation mechanism	Key hydrogen safety challenges
P5	Plant P5 stores large quantities of metallic magnesium (Magnox swarf) under water. The waste is generated from decanning of nuclear fuel rods. Storage of Magnox waste under water results in the corrosion of the metal and chronic liberation of the hydrogen gas into the ullage space of the storage enclosure. Magnesium hydroxide sludge is also generated as a secondary product of the corrosion process, leading to the formation of a swarf and sludge matrix. This can lead to the hold-up of hydrogen within the sludge and swarf matrix and subsequently a transient release of a large volume of the gas into the ullage space can occur. The decommissioning strategy for the plant is to retrieve the swarf and sludge waste and store in $3m^3$ boxes in plant P2 until a geological waste repository becomes available.	A potential unavailability of the plant ventilation extract system could cause accumulation of hydrogen gas in the ullage space of the storage enclosure. A nitrogen inerting system has been incorporated to manage against the sudden gas release scenarios.
P6	Plant P6 primarily provides an ion exchange treatment process for sludge wastes arising from the corrosion of metallic magnesium. Stored hydrogen gas in the magnesium hydroxide sludge and sand, within the bulk storage tanks in the plant, can be released during mobilisation and pumping of the material. The hydrogen gas could accumulate in the tank ullage space.	Continuous and batch releases of the hydrogen gas result in the potential for gas accumulation in the tank ullage space. The key hazard management strategy against such release mechanisms is to limit the disturbance of the tank sludge upon detection of the hydrogen concentration in the tank ullage which exceeds the 1% concentration limit.
P7	The process carried out in Plant P7 is the removal of radioactivity from sheet metal pieces generated during cutting of redundant gloveboxes. Hydrogen is generated during the process of immersing the metal pieces in hot mineral acid.	The main control against the generation of hydrogen in Plant P7 is the acid supply valve trip system, to control the amount of acid added. The reliability and the testing of the valve functionality is identified as an area of uncertainty.
P8	Plant P8 provides the process for treatment and encapsulation of Intermediate Level Wastes (ILWs) retrieved from Plant P5. Hydrogen is generated due to the reaction of the metallic waste with the grout matrix during the encapsulation process.	The hydrogen generation within the plant P8 storage containers presents similar challenges to those for plant P2 packages. However, for plant P8 packages there is an uncertainty associated with effective mixing of the magnesium hydroxide sludge with grout formulations to ensure a good quality product, suitable for encapsulation. Plant

Plant (Note 1)	Hydrogen generation mechanism	Key hydrogen safety challenges
		throughput is a further constraint that needs to be managed by ensuring that the sludge and grouted product is effectively removed from the mixing vessel without adherence.
F1	Fuel flasks are used for transportation of radioactive material between sites. The main mechanisms of hydrogen generation are radiolysis, release of stored hydrogen within the material being transported due to disturbance or due to chemical effects such as corrosion or electrochemical reactions.	A key hydrogen safety challenge for the design of the fuel flasks is the need to meet transport regulations such as the need to seal the flasks which would rule out the passive vent option. There is an uncertainty on whether air flow through the flask filters affects diffusion of hydrogen gas.

Note 1: For the purpose of confidentiality and plant security, direct reference to plant names and location is not given. For cross referencing purposes in this thesis, each plant is given a ‘P1 to P8' and ‘F1’ identification number.

APPENDIX A2: BBN DATA FOR CASE STUDY 1

Node 8: Radiolytic Hydrogen Rate		Node 4: G Value	Node 7: Total radiation field	Radiolysis prevented?
High	Low			
0.05	0.95	High	High	Yes
0.95	0.05	High	High	No
0.05	0.95	High	Low	Yes
0.5	0.5	High	Low	No
0.05	0.95	Low	High	Yes
0.5	0.5	Low	High	No
0.05	0.95	Low	Low	Yes
0.05	0.95	Low	Low	No

Table A-1: CPT for radiolytic hydrogen generation rate

Note on Table A-1: A hydrogen generation rate of 0.1L/hr and 0.01L/hr represent the Low and High states respectively.

Node 14: Hydrogen Flammability			Node 8: Hydrogen Generation Rate	Node 11: Oxygen present?	Node 13: Seal time duration	Node 9: Ullage fraction
High	Low	None				
0	0.5	0.5	High	No	Less than 10 years	Large
0	0.5	0.5	High	No	Less than 10 years	Small
0	0.5	0.5	High	No	Greater than 10 years	Large
0	0.5	0.5	High	No	Greater than 10 years	Small
0.8	0.1	0.1	High	Yes	Less than 10 years	Large
0.85	0.05	0.1	High	Yes	Less than 10 years	Small
0.9	0.05	0.05	High	Yes	Greater than 10 years	Large
0.95	0.05	0	High	Yes	Greater than 10 years	Small
0	0.4	0.6	Low	No	Less than 10 years	Large
0	0.4	0.6	Low	No	Less than 10 years	Small
0	0.4	0.6	Low	No	Greater than 10 years	Large
0	0.4	0.6	Low	No	Greater than 10 years	Small
0.7	0.2	0.1	Low	Yes	Less than 10years	Large
0.75	0.15	0.1	Low	Yes	Less than 10 years	Small
0.8	0.15	0.05	Low	Yes	Greater than 10 years	Large
0.85	0.15	0	Low	Yes	Greater than 10 years	Small

Table A-2: CPT for hydrogen flammability

Node 17: Hydrogen Explosion			Hydrogen Flammability	Ignition source present?	Pipe diameter
Detonation	Deflagration	None			
0.4	0.6	0	High	Yes	Above critical diameter
0	1	0	High	Yes	Below critical diameter
0	0	1	High	No	Above critical diameter
0	0	1	High	No	Below critical diameter
0.15	0.85	0	Low	Yes	Above critical diameter
0	1	0	Low	Yes	Below critical diameter
0	0	1	Low	No	Above critical diameter
0	0	1	Low	No	Below critical diameter
0	0	1	None	Yes	Above critical diameter
0	0	1	None	No	Below critical diameter
0	0	1	None	No	Above critical diameter
0	0	1	None	No	Below critical diameter

Table A-3: CPT for hydrogen explosion in sealed pipe

Notes on Tables A-2 and A-3: A High and Low Hydrogen Flammability represents a hydrogen in air concentration >=18% vol and <18% vol respectively.

Node 22: Radiological Impact			Radiological composition	Explosion	Release Potential
High	Low	No Consequence			
0.9	0.09	0.01	High	Detonation	High
0.8	0.15	0.05	High	Detonation	Low
0.8	0.15	0.05	High	Deflagration	High
0.8	0.1	0.1	High	Deflagration	Low
0	0	1	High	None	High
0	0	1	High	None	Low
0.8	0.15	0.05	Medium	Detonation	High
0.7	0.2	0.1	Medium	Detonation	Low
0.65	0.25	0.1	Medium	Deflagration	High
0.6	0.3	0.1	Medium	Deflagration	Low
0	0	1	Medium	None	High
0	0	1	Medium	None	Low
0.5	0.4	0.1	Low	Detonation	High
0.45	0.45	0.1	Low	Detonation	Low
0.45	0.45	0.1	Low	Deflagration	High
0.35	0.5	0.15	Low	Deflagration	Low
0	0	1	Low	None	High
0	0	1	Low	None	Low

Table A-4: CPT for radiological consequence

Notes on Tables A-4:
A High and Low Radiological Impact represents the High and Low workforce consequence range values, as specified by *ONR, 2020*, respectively.

A High, Medium and Low Radiological Composition represents the radioactivity content range values for High Level, Intermediate Level and Low Level Wastes, respectively as specified by *IAEA, 2009*.

A High, Medium and Low potential for release represents items that could lead to a workforce consequence in the High, Intermediate or Low range, respectively, as specified by *ONR, 2020*.
.

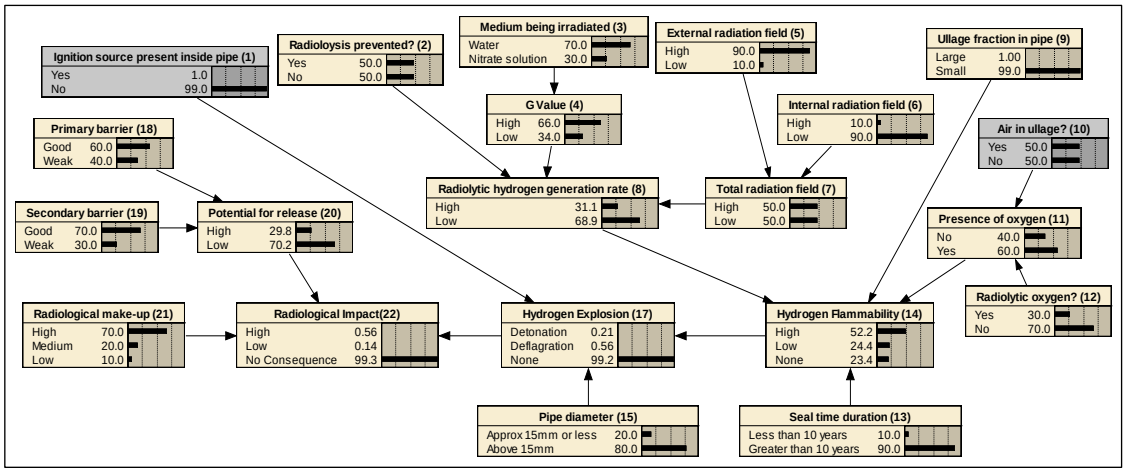

Figure A2-1: Effect of reduced probabilities of ignition and presence of air in pipe ullage

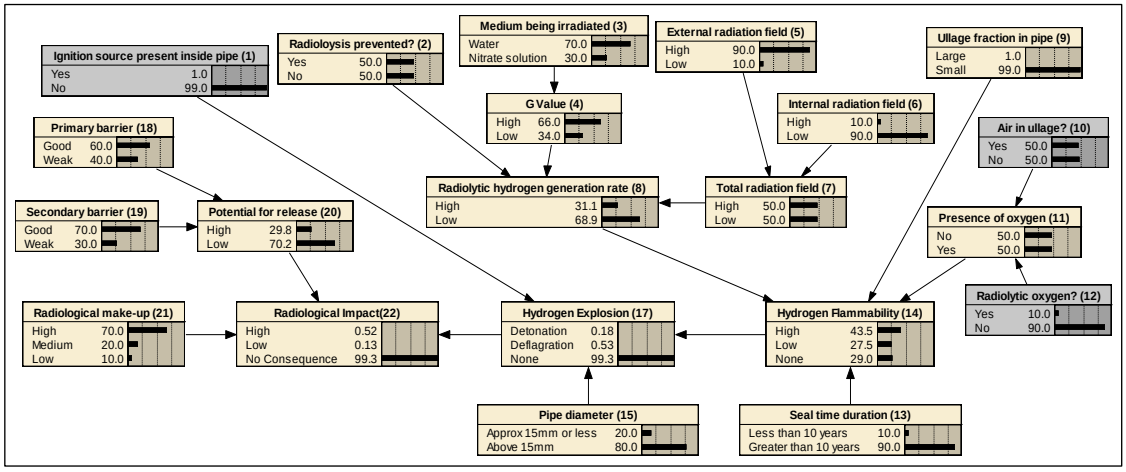

Figure A2-2: Effect of reduced probabilities of ignition, presence of air and radiolytic oxygen in pipe ullage

APPENDIX B: BBN DATA FOR CASE STUDY 2

Node VW: Active Water Volume Fraction					AW, Active Water Mass Fraction % (w/w)
0.5 to 0.6	0.6 to 0.7	0.7 to 0.8	0.8 to 0.9	0.9 to 1	
0.87	0.13	0	0	0	30 to 40
0	0.97	0.03	0	0	40 to 50
0	0	1	0	0	50 to 60
0	0	0.33	0.67	0	60 to 70
0	0	0	0.92	0.08	70 to 80
0	0	0	0	1	80 to 90

Table B-1: CPT for active water volume fraction

DS: Density of Sludge (kg/m^3)					VW : Active Water Volume Fraction
1000 to 1140	1140 to 1280	1280 to 1420	1420 to 1560	1560 to 1700	
0	0	0	0.14	0.86	0.5 to 0.6
0	0	0.11	0.89	0	0.6 to 0.7
0	0.07	0.93	0	0	0.7 to 0.8
0.07	0.93	0	0	0	0.8 to 0.9
1	0	0	0	0	0.9 to 1

Table B-2:CPT for density of sludge

Node IW: Inactive Water Mass (kg)					Vskip Skip Fill Volume %	DPG Dry Powder Grout Mass (kg)
0 to 400	400 to 800	800 to 1200	1200 to 1600	1600 to 2000		
0	0	0	0.04	0.96	0 to 20	700 to 800
0	0	0	0.15	0.85	0 to 20	800 to 900
0	0	0	0.35	0.65	0 to 20	900 to 1000
0	0	0	0.39	0.61	0 to 20	1000 to 1100
0	0	0	0.6	0.4	0 to 20	1100 to 1200
0	0	0	1	0	20 to 40	700 to 800
0	0	0	1	0	20 to 40	800 to 900
0	0	0	1	0	20 to 40	900 to 1000
0	0	0	1	0	20 to 40	1000 to 1100
0	0	0.02	0.98	0	20 to 40	1100 to 1200
0	0	0.45	0.55	0	40 to 60	700 to 800
0	0	0.59	0.41	0	40 to 60	800 to 900
0	0	0.75	0.25	0	40 to 60	900 to 1000
0	0	0.88	0.12	0	40 to 60	1000 to 1100
0	0	0.98	0.02	0	40 to 60	1100 to 1200
0	0	1	0	0	60 to 80	700 to 800
0	0.03	0.97	0	0	60 to 80	800 to 900
0	0.14	0.86	0	0	60 to 80	900 to 1000
0	0.3	0.7	0	0	60 to 80	1000 to 1100
0	0.34	0.66	0	0	60 to 80	1100 to 1200
0	0.9	0.1	0	0	80 to 100	700 to 800
0	0.99	0.01	0	0	80 to 100	800 to 900
0	1	0	0	0	80 to 100	900 to 1000
0	1	0	0	0	80 to 100	1000 to 1100
0	1	0	0	0	80 to 100	1100 to 1200

Table B-3: CPT for inactive water mass

Node SD: Dry Sludge to DPG Mass Ratio		DPG: Dry Powder Grout Mass (kg)	DSM: Dry Sludge Mass (kg)
0 to 1	>= 1		
1	0	700 to 800	0 to 300
1	0	700 to 800	300 to 600
0.51	0.49	700 to 800	600 to 900
0	1	700 to 800	900 to 1200
0	1	700 to 800	1200 to 1500
1	0	800 to 900	0 to 300
1	0	800 to 900	300 to 600
0.81	0.19	800 to 900	600 to 900
0	1	800 to 900	900 to 1200
0	1	800 to 900	1200 to 1500
1	0	900 to 1000	0 to 300
1	0	900 to 1000	300 to 600
1	0	900 to 1000	600 to 900
0.18	0.82	900 to 1000	900 to 1200
0	1	900 to 1000	1200 to 1500
1	0	1000 to 1100	0 to 300
1	0	1000 to 1100	300 to 600
1	0	1000 to 1100	600 to 900
0.42	0.58	1000 to 1100	900 to 1200
0	1	1000 to 1100	1200 to 1500
1	0	1100 to 1200	0 to 300
1	0	1100 to 1200	300 to 600
1	0	1100 to 1200	600 to 900
0.83	0.17	1100 to 1200	900 to 1200
0	1	1100 to 1200	1200 to 1500

Table B-4: CPT for dry sludge to dry powder grout mass

Node FL: Fluidity			SK: Sludge Stickiness	WS: Water/Solids Ratio	SD: Dry Sludge to DPG Mass Ratio
Low	Medium	High			
1	0	0	Low	0 to 0.7	0 to 1
1	0	0	Low	0 to 0.7	>= 1
0	0.6	0.4	Low	0.7 to 1.3	0 to 1
0.7	0.2	0.1	Low	0.7 to 1.3	>= 1
0	0	1	Low	>= 1.3	0 to 1
0	0	1	Low	>= 1.3	>= 1
1	0	0	High	0 to 0.7	0 to 1
1	0	0	High	0 to 0.7	>= 1
0.2	0.5	0.3	High	0.7 to 1.3	0 to 1
0.9	0.1	0	High	0.7 to 1.3	>= 1
0	0	1	High	>= 1.3	0 to 1
0	0	1	High	>= 1.3	>= 1

Table B-5: CPT for fluidity

Node PQ: Product Quality			MT: Mixing Time	MS: Mixing Speed	FL: Fluidity
Hard	**Good**	**Runny**			
1	0	0	Short	Slow	Low
0.5	0.5	0	Short	Slow	Medium
0	0	1	Short	Slow	High
1	0	0	Short	Medium	Low
0	0.5	0.5	Short	Medium	Medium
0	0	1	Short	Medium	High
1	0	0	Short	Fast	Low
0	0.5	0.5	Short	Fast	Medium
0	0	1	Short	Fast	High
1	0	0	Medium	Slow	Low
0.5	0.5	0	Medium	Slow	Medium
0	0	1	Medium	Slow	High
1	0	0	Medium	Medium	Low
0	1	0	Medium	Medium	Medium
0	0	1	Medium	Medium	High
1	0	0	Medium	Fast	Low
0	1	0	Medium	Fast	Medium
0	0	1	Medium	Fast	High
1	0	0	Long	Slow	Low
1	0	0	Long	Slow	Medium
0	0	1	Long	Slow	High
1	0	0	Long	Medium	Low
0.5	0.5	0	Long	Medium	Medium
0	0	1	Long	Medium	High
1	0	0	Long	Fast	Low
0.5	0.5	0	Long	Fast	Medium
0	0	1	Long	Fast	High

Table B-6: CPT for product quality

Node PQ: Product Quality	Will the product come out?	
	No	Yes
Hard	100	0
Good	0	100
Runny	0	100

Table B-7: CPT for will product come out?

APPENDIX C: MONTE CARLO UNCERTAINTY ANALYSIS DATA FOR CASE STUDY 3

Event Group	Description of Events and Fault Tree Logic
Top Event	Under normal operations the hydrogen in air concentration in the vessel ullage space is managed by the purge air system and continuous extraction of the ullage atmosphere by means of an extract fan. A failure to dilute the vessel hydrogen atmosphere could occur due to a loss of the purge air flow. A loss of the extract driving force due to a failure of the fan system would also lead to an inability to dilute the hydrogen. This is because the purge air supply without an extract will cause pressurisation of the ullage space. Against this eventuality the system is designed to automatically trip the purge for the purpose of maintaining radiological containment of the vessel. Hence the fault tree in Figure 6-2 models the occurrence of the Top Event due either a failure of the purge (Event PURGE) OR extract failure (Event EXTRACT).
Events leading to purge air system failure	The purge air system comprises a normal factory compressed air supply, two backup compressors A and B and an additional diesel compressor. In the event of a failure of the factory air supply, revealed by a loss of pressure alarm, the operator is required to start either of the two back-up compressors. Following a loss of site power supply leading to a loss of factor air supply and the back-up compressors A and B, a second operator is required to start the diesel compressor. Therefore, for a complete failure of the purge air system to occur, the factory air (Event MAINSAIR) AND backup compressed air system (Event BACKUP) AND the emergency diesel compressor system (Event EMERGF) would have to fail. The backup compressor system could fail either due to an operator failing to start compressor A or B (Event OPFAIL1) or if the compressors fail mechanically (event BCOMP). For the diesel compressor system to fail, a loss of the site power supply has to occur, and the diesel compressor fails to start on demand. A failure to start the diesel compressor (Event OPFAIL2) could occur either due to an operator error, OR if there is a mechanical failure of the compressor, or if the vent duct pressure alarm fails to indicate a loss of flow.
Events leading to vent extract failure	The vent extract system comprises an extract fan, duct damper, and a power supply for the fan. A failure of any one these plant items has the potential to cause a loss of the extract system. Therefore, the fault tree logic in Figure 6-2 applies an OR gate to these three events. In the event of a loss of the site power supply to the extract fan (Event POWER), a third operator is required to start the diesel generator to supply back-up power to the fan. Therefore, both the normal power supply and the back-up power (Event BPOWER) would need to fail for a total failure of the power supply system to occur (Event FPOWER). As such, an AND gate is applied between the events BPOWER and POWER. For a failure of the backup system to occur (Event BPOWER), either a mechanical failure of the diesel generator would need to take place or if the operator fails to start the diesel generator. Hence an OR gate is applied between these three events. A blockage of the vent extract route (Event BLOCKAGE) could occur either if a mechanical failure of a duct damper occurs or if an operator inadvertently closes a damper. Hence an OR gate is applied to these events.

Table C-1: Description of fault tree analysis events for forced ventilation system failure

Primary Event ID	Description	Failure rate/yr
FAN	This is the frequency of fan failure due to immediate fan stoppage. For ventilation system fans a mean failure rate of 1.5E-6 failures/hr has been specified by *IAEA, 1997.* This equates to an annual failure rate of 0.013/yr.	0.013
DUCT	For automatic ventilation dampers, a mean failure rate of 4.7E-6/hr has been suggested by *IAEA, 1997.* This equates to an annual failure rate of 0.041/y.	0.041
POWER	A mean failure rate of 1.66E-5/hr, i.e.,0.145/yr, has been specified for loss of high voltage power supply, by *IAEA, 1997*.	0.145
MECHFAIL, DIESEL A, DIESEL B	MECHFAIL represents the failure of a single diesel generator. The *IAEA, 1997* database specifies a mean failure rate of 1.1E-5/hr. This is equivalent to a failure rate of 1.1E-5 x 24 x 365/yr i.e., 0.96/y. Events DIESEL A and DIESEL B represent failure of two identical diesel generators, associated with the additional mitigation system (see Table C-7 for further explanation). The failure rate of each of these items is identical to event MECHFAIL.	0.96
FACTAIR	This base event represents a failure of the normal factory compressed air supply to the process vessel. *IAEA, 1997* specifies a compressor instrument air failure rate of 4.57E-4/hr, i.e., 4/yr. In accordance with the revealed failure equation 2-10, using a repair time of 2 days i.e., 2/365 yr, this equates to a revealed failure probability of 1-EXP(-4*2/365], i.e., 0.02.	4
PRINST, EPRINST	Event PRINST represents the pressure detection instrument for the factory compressed air failing to alarm. *IAEA, 1997* specifies a mean failure rate of 1.7E-6/hr for a pressure sensor. This is equivalent to a failure rate of 1.7E-6 x 24 x 365/yr, i.e., 0.015/yr. Event EPRINST represents failure of the second identical pressure instrument associated with the additional mitigation system see Table C-7 for further explanation). The failure rate for this instrument is considered to be the same as for PRINST.	0.015
COMPA	This base event represents the mechanical failure of back-up air compressor A. *IAEA, 1997* specifies a mean failure rate of 6.72E-5/hr, i.e., 0.589/yr for an air compressor failing to function. Since the compressor is standby equipment, its failure would be unrevealed. In accordance with the unrevealed failure equation the failure probability based on a proof test interval of 1 year can be calculated as P =1-((1-EXP(-0.589*1))/(0.589*1))= 0.245	0.589
COMPB	As for COMP A, the failure probability for COPM B is 0.245 and the failure rate is 0.589/yr.	0.589
DCOMP	This is the mechanical failure of a diesel compressor. It is considered that the failure of this system could arise as a result of a failure of the diesel generator. *IAEA, 1997* specifies a mean failure rate of 1.1E-5/hr for an emergency diesel generator. This is equivalent to 1.1E-5 x 24 x 365/yr, i.e., 0.963/y.	0.963

Table C-2: Equipment reliability data for use in the MC simulation for vent system failure

Primary Event ID	Description	Failure Probability
CCF-COMP	This is the common cause failure probability of compressors A and B. Using the failure probability of 0.245 from Table C-2 and equation $\lambda_{dp} = \beta\lambda_t$, for full, partial and zero diversity between the two compressors, the respective CCF probabilities are 0.02x0.245, 0.06x 0.245 and 0.2x0.245, i.e., 4.88E-3, 1.47E-2 and 4.88E-2 (Notes 1,2).The MC simulation takes into consideration the uncertainty associated with the diversity of the compressors and it is considered that the associated CCF probability value is best represented by a Triangular distribution for the reasoning that the range of CCF values can be predicted as follows: Given that the two compressors are identical, but they are physically segregated, it is considered that there is partial diversity. Therefore, the CCF probability of 1.47E-2 is treated as the most likely value. It is extremely unlikely that there is full diversity, therefore the CCF value of 4.88E-3 is the least likely value. The maximum CCF value, 4.88E-2, arises if there is zero diversity between the two compressors.	Maximum 4.88E-2, Most Likely 1.47E-2, Least Likely 4.88E-3
CCF-DIESEL	Given that the additional mitigation consists of multiple diesel generators (DIESELA and DIESELB), a new common cause failure, represented by event CCFDIESEL, is determined. The probability of CCFDIESEL was calculated using the same methodology as for CCFCOMP. The failure probability of each of the two diesel generators is 0.357 (event MECHFAIL), as determined in Table C-4. For the same reasoning as for the common cause failure of compressors (event CCFCOMP), the Triangular probability distribution is used for CCFDIESEL. The most likely, least likely and maximum probabilities of CCFDIESEL are derived as 2.14E-02, 7.14E-03, and 7.14E-02 using beta values of 0.02, 0.06 and 0.2, respectively. For the purpose of the standalone FTA (Figure 6-4) for the additional mitigation system, the most likely value 2.14E-02 is used.	Maximum 7.14E-02 Most Likely 2.14E-02, Least Likely 7.14E-03
CCF-PRINST	This is the common cause failure of the two pressure instruments for the additional mitigation system. The failure probability of each of the two pressure instruments is 7.46E-03. For the same reasoning as for the common cause failure of compressors, event CCFCOMP), a Triangular probability distribution is used for CCFPRINST. The least likely, most likely and maximum probabilities, 1.49E-04, 4.48E-04, 1.49E-03 using beta values of 0.02, 0.06 and 0.2, respectively are used to determine the CCF (Note 2).	Maximum 1.49E-03 Most Likely 4.48E-04 Least Likely 1.49E-04
HE3	This is the probability of an operator failing to start the diesel generator on demand following a loss of the main power supply or following a loss of the back-up air compressors. Based on plant operational experience from existing nuclear chemical plant facilities, in order to ensure an appropriate bias towards designing engineered systems and to account for dependencies, a maximum conservative probability of 0.1 for operator error is used. If there are no operational or environmental constraints on the operator, and the fault is revealed by an audible alarm then typically, the human error probability is likely to be at least an order of magnitude lower, i.e., 0.01. It is considered that the operator would understand the significance of the power failure fault and take immediate remedial action. To allow for any uncertainties in terms of environmental factors that may affect	Maximum 0.1, Most Likely 0.05, Minimum 0.01

Primary Event ID	Description	Failure Probability
	operator performance, a human error probability mid-range between 0.1 and 0.01, i.e. 0.05 is selected as the most likely value in the Triangular distribution.	
HE1	This is the human error probability of an operator failing to start back-up compressors A or B, following the event being revealed by the detection of low pressure in the factory compressed air supply. With similar environmental and operational constraints to those for event HE3 discussed above, it is considered that the human error probability for event HE1 is the same.	As for HE3
HE2	This is the human error probability of a second operator failing to start the back-up emergency diesel compressor, in the event that the back-up air compressors fail to start. Again, due to similar operational and environmental constraints to those for event HE3 discussed above, it is considered that the human error probability for event HE2 is the same.	As for HE3
HE4	This is human error probability of an operator inadvertently closing the vent extract damper hence isolating the duct.	As for HE3
HE5	After revealing an inadvertent duct isolation by the duct pressure instruments, the operators are required to take corrective action by opening the duct. HE5 is the human error probability for failing to take this corrective action. In this case the most likely failure probability of 1E-3 is justified on the grounds that a ventilation extract failure would be a major event which would be immediately revealed to all building operators. Thus, the likelihood of operators failing to take corrective action, is lower in comparison with other human errors such as HE4, which could occur regardless of extract failure. It is considered extremely unlikely that the probability HE5 would be the same as HE4, i.e., 0.01. Hence this is treated as the least likely probability for the Triangular Distribution.	Maximum 0.1, Most Likely 1E-3, Minimum 0.01
HPLV	The operational tasks in relation to events HE1, HE2 and HE3 are performed by different teams of operators on plant. The HPLV differs for single and multiple teams of operators due to the variation in team interaction and hence operator performance. For multiple operating teams, a HPLV of 1E-4 has been suggested by *Kirwan et al, 2008* as a worst case value for use in human reliability assessments. A single value of 1E-4 for the HPLV is used for the reasoning that this is the suggested limit for multiple teams which cannot change unlike other variables in the MC simulation where there is an uncertainty.	1E-4

Table C-3: Human error and CCF data for use in the MC simulation for vent system failure

Notes for Table C-3

1. The calculation of the CCF values is based on the β Factor methodology as detailed by *Summers et al, 1999*. This method considers that if the tendency for the system to a dependent failure is represented by a constant β, then the relationship between the dependent failure probability, λ_{dp}, and the total failure probability, λ_t, can be expressed as $\lambda_{dp} = \beta\lambda_t$.
2. Subject to the diversity, i.e., independence, of the components susceptible to a common cause failure, various values for the β factor are recommended in reliability engineering [*Lees, 1992*]. For unrevealed failures of components with full, partial or zero diversity, a typical β factor of 0.02, 0.06 and 0.2, respectively is applied [Lees, 1992]. The β Factor methodology also requires that the β factor is applied to the most reliable component, i.e., with the lowest failure rate, from a system consisting of multiple components.

Fault tree primary event ID	(A) Failure rate (/yr)	(B) Event failure mode (Notes 1 and 2)	(C) Failure probability (P_n) at repair time distribution, T_R	(D) Standard Deviation (S_n)	(E) Probability Distribution = (NormalValue P_n, S_n) (Note 3)
FAN	0.013	Revealed (Equation 2-4)	P_{1A}	S_{1A}	(P_1)
DUCT	0.041	Revealed (Equation 2-4)	P_{2A}	S_{2A}	(P_2)
POWER	0.145	Revealed (Equation 2-4)	P_{3A}	S_{3A}	(P_3)
FACTAIR	4.0	Revealed (Equation 2-4)	P_{4A}	S_{4A}	(P_4)
COMPA	0.589	Unrevealed (Equation 2-3)	2.44E-01	1.22E-02	(P_5)
COMPB	0.589	Unrevealed (Equation 2-3)	2.44E-01	1.22E-02	(P_6)
DCOMP	0.589	Unrevealed (Equation 2-3)	2.44E-01	1.22E-02	(P_7)
MECHFAIL	0.960	Unrevealed (Equation 2-3)	3.57E-01	1.79E-02	(P_8)
DIESEL A	0.960	Unrevealed (Equation 2-3)	3.57E-01	1.79E-02	(P_{19})
DIESEL B	0.960	Unrevealed (Equation 2-3)	3.57E-01	1.79E-02	(P_{20})
PRINST	0.015	Unrevealed (Equation 2-3)	7.46E-03	3.73E-04	(P_9)
EPRINST	0.015	Unrevealed (Equation 2-3)	7.46E-03	3.73E-04	(P_{22})

Table C-4: Probability distributions primary events for ventilation system equipment failures

Notes for Table C-4

1. Column A uses the mean failure rates derived in Table C-2 and equations 2-10 and 2-11 to calculate the revealed and unrevealed failure probabilities, respectively.
2. Derivation of the revealed failure probabilities in Column C is also based on the repair time distribution, which is dependent on the level of mitigation provided by the ventilation systems. For the system without the enhanced mitigation, Chapter 6 Section 6.9.3 demonstrates that the repair time is equivalent to a Triangular Distribution with the minimum, most likely and maximum values of 24, 36 and 60 hours, respectively. Hence Table C-4 calculates the failure probability of repairable items as a distribution, referenced as P_{1A} , P_{2A} , P_{3A} and $P_{4A.}$
3. Based on the discussion given in Section 6.4.3, column E uses the normal distribution for equipment failures with the mean probability value (P_n) from column A and a low standard deviation taken as 5% of the mean value (S_n), to calculate the failure probability distribution. Hence column B uses the function (NormalValue P_n, S_n) within the RiskAmp software to determine the probability distributions for equipment failure.

Fault tree primary event ID	(A) Minimum Probability (P_{10})	(B) Most likely Probability (P_{11})	(C) Maximum Probability (P_{12})	(D) Failure Probability Distribution = TriangularValue(P_{10} P_{11}, P_{12}) (Note 1)
HE5	1E-3	0.01	0.1	(P_{21})
HE4	0.01	0.05	0.1	(P_{13})
HE1	0.01	0.05	0.1	(P_{14})
HE2	0.01	0.05	0.1	(P_{15})
HE3	0.01	0.05	0.1	(P_{16})
HPLV	1.00E-04	1.00E-04	1.00E-04	(P_{17})
CCFCOMP	4.88E-03	1.47E-02	4.88E-02	(P_{18})
CCFDIESEL	7.14E-03	2.14E-02	7.14E-02	(P_{22})
CCFPRINST	1.49E-04	4.48E-04	1.49E-03	(P_{23})

Table C-5: Probability distributions for human error and common cause failures

Notes for Table C-5

1. Column D applies the Triangular distribution to calculate the failure probabilities for human error, using the least likely (P_1), most likely (P_2) and maximum (P_3) probabilities derived in Table C-4.

Fault tree secondary event ID	Probability distribution of secondary events (Notes 1, 2 and 3)
MAINSAIR	p(MAINSAIR)= P_4
OPFAIL1	p(OPFAIL1) = P_{14}+P_9+ P_{17}
BCOMP	p(BCOMP) = P_5 x P_6
OPFAIL2	p(OPFAIL2)= P_3+ P_{15}+ P_7+ P_9+ P_{17}+ P_{18}
BPOWER	p(BPOWER)= P_8+ P_{16}+ P_{17}
BACKUP	p(BACKUP)= p(OPFAIL1)+p(BCOMP)
EMERGF	P(EMERGF)= P_3 x p(OPFAIL2)
FPOWER	p(FPOWER) = p(BPOWER) x p(POWER)
BLOCKAGE	p(BLOCKAGE)= P_2+ P_{13}+ P_{17}
PURGE	p(Purge)= p(MAINSAIR) x p(BACKUP) x p(EMERGF)
EXTRACT	p(EXTRACT)= P_1+ p(FPOWER) +p(BLOCKAGE)
TOP EVENT	p(TOP EVENT) = p(PURGE)+ p(EXTRACT)

Table C-6: Failure probabilities of secondary events in MC simulation without additional mitigation

Notes for Table C-6

1. The probability distributions here are based on replication of the Boolean algebra for modelling AND and OR logic gates.
2. For replication of the OR logic gate, it is considered that if two events (i) and (ii) are not mutually exclusive events their probability space will overlap so that they cannot be simply added together. In this case, (P(i) OR P (ii) = P(i) + P(ii) – (P((i) and (ii)). However, if the probabilities are small then the probability P((i) and (ii)) becomes relatively insignificant and can be ignored. Similar concepts apply if three or more mutually exclusive events are considered so that small probabilities after an OR gate can be added.
3. For the AND gate logic applied to events (i) and (ii) the probability of the output node is obtained by multiplying the probabilities of these two events together.

Fault tree secondary event ID	Failure probability
MAINSAIR	p(MAINSAIR)= P_4
OPFAIL1	p(OPFAIL1) = P_{14}+P_9+ P_{17}
BCOMP	p(BCOMP) = P_5 x P_6
OPFAIL2	p(OPFAIL2)= P_3+ P_{15}+ P_7+ P_9+ P_{17}+ P_{18}+ P_{23}
BPOWER	p(BPOWER)= p(FANDIESEL)+P_8+ P_{16}+ P_{17}
FANDIESEL	P_{19} x P_{20}
OPFAIL	P_{21}+ P_{22}+ P_{23}+ P_{17}
DISOLATED	P_2+ P_{13}+ P_{17}
BACKUP	p(BACKUP)= p(OPFAIL1)+p(BCOMP)
EMERGF	P(EMERGF)= P_3 x p(OPFAIL2)
FPOWER	p(FPOWER) = p(BPOWER) x p(POWER)
BLOCKAGE	p(BLOCKAGE)= p(DISOLATED) x p(OPFAIL)
PURGE	p(Purge)= p(MAINSAIR) x p(BACKUP) x p(EMERGF)
EXTRACT	p(EXTRACT)= P_1+ p(FPOWER) +p(BLOCKAGE)
TOP EVENT	p(TOP EVENT) = p(PURGE)+ p(EXTRACT)

Table C-7: Failure probability distributions of secondary events in MC simulation with additional mitigation

***Note for* Table C-7**

1. As for Table C-6, the probability distributions here are also based on replication of the Boolean algebra for modelling AND and OR logic gates.

2. The logic for the additional mitigation assumes that for the vent duct blockage to occur, either the duct has to be isolated, represented by new secondary event (DISOLATED) or an operator to fails to open the closed damper (event OPFAIL), revealed by the new vent duct pressure detection instrument EPRINST. Hence an OR logic gate is applied between the two new secondary events to derive the probability for the event BLOCKAGE.

3. For the secondary event OPFAIL to occur either the new pressure instrument has to fail (Event P_{22}) or the operator has to fail to take corrective action (Event HE5, i.e. P_{21}). Given that the additional mitigation system models failure of two pressure instruments (PRINST and EPRINST), both of the same design and manufacturer, a common cause failure is modelled, which is represented by CCFPRINST (Event P_{23}), through an OR gate.

4. For the purpose of improving the availability of the power supply to the fan, the additional mitigation for the extract system also comprises a second diesel generator. Both diesel generators (DIESEL A and B) would need to fail for a mechanical failure of the system to occur (event FANDISEL). Therefore, an AND gate logic is applied between the two items.

5. The FANDIESEL secondary event probability is based on a failure probability distribution of each of the two diesel generators (DIESEAL A and DIESELB) denoted by the probabilities P_{19} and P_{20}. Using the mean failure probability of 0.357 and a standard deviation 1.79E-02 for P_{19} and $P_{20,}$ the MC simulation uses the 'Normal Value' function to calculate the probabilities as for event MECHFAIL in Table C-4.

	Time taken to reach 4% hydrogen concentration (hours)	Time taken to reach 8% hydrogen concentration (hours)	Equipment repair time without additional mitigation (hours)	Equipment repair time with additional mitigation (hours)
Minimum value	21	44	24	12
Value at 5% level	22.3	46.5	26	16.6
Peak value	29	64	38	26
Value at 95% level	49.2	102.7	58	41.5
Maximum value	55	116	60	48

Table C-8: Comparison of MC simulation results for times to hydrogen concentration limits with equipment repair time

APPENDIX D: CPTs AND VERIFICATION DATA FOR CASE STUDY 4

Table D-1: BBN node description and justification CPT data

Node	Derivation of Node Data	Equation Used in BBN	Justification of CPT Data
A- Radiolytic Hydrogen Generation	The CISWG advised that the hydrogen generation due to corrosion is the main source of hydrogen in the skip. However, the meeting members suggested that the radiolytic hydrogen release should also be modelled to determine if there are any sensitivities that could affect the overall results.		
A1 and A6 - Skip alpha and Beta/Gamma activity concentration		Rectangular distribution	The application of an appropriate distribution for skip liquor activity concentration was discussed with CISWG who advised that a Normal Distribution would be difficult to justify, given the significant variation of constituents across Plant P5. The expert opinion of CISWG was that given the uncertainty, it would be more appropriate to assume that there is an equal chance of the skip constituents being within any of the 10 discretised bands identified in this node. Hence a rectangular (uniform) distribution was assumed to represent skip liquor activity concentration. The maximum values of activity concentration as listed in the network are based on the known values from liquor sample analysis.
A3-Skip liquor volume (ml)	The advice from the CISWG is that a full skip contains 270L water	N/A - Constant	For the purpose of this BBN analysis, it is assumed that the skip is full.

Node	Derivation of Node Data	Equation Used in BBN	Justification of CPT Data
A7-K Value	The Hydrogen Technical Guide provides a dimensionless K value of 1.44E-15 for aqueous solutions (if E is expressed in MeV/s)	N/A - Constant	N/A - Constant
A6-Beta/Gamma G Value (molecules of H2/100eV	The Hydrogen Technical Guide (HTG) provides a G(H2 value of 0.45molecules/100eV for beta/gamma activity in aqueous solutions.	N/A - Constant	N/A - Constant
A8-Gamma Decay Energy (MeV)	It is assumed that the gamma radiation is completely absorbed by the skip liquor which contributes to radiolysis. The gamma decay energy for worst case gamma nuclide is given as 0.662MeVin the HTG.	N/A - Constant	N/A - Constant
A9-Beta Decay Energy (MeV)	The worst case beta decay energy is given as 0.186MeVin the HTG.	N/A - Constant	
A10-Gamma Radiolytic H2 Gen Rate (L/hr)	Radiolytic hydrogen generation rate is a product of total gamma activity in the skip, Gamma Decay Energy, Gamma G Value, and the K value.	A10 (A5, A6, A8, A7, A9) = A5*A6*A7*(A8+A9)	Using the equation for Node A10, Netica automatically calculates the CPT data.
A11-Alpha G Value (molecules of H2/100eV	The HTG provides a G(H2) value of 1.66molecules/100eV for alpha activity in aqueous solutions.	N/A - Constant	N/A - Constant
A12-Alpha Decay Energy (MeV)	The HTG provides a Decay Energy of 5.5MeV for alpha nuclides.	N/A - Constant	N/A - Constant

<table>
<tr><th>Node</th><th>Derivation of Node Data</th><th>Equation Used in BBN</th><th>Justification of CPT Data</th></tr>
<tr><td>A13- Alpha Radiolytic H2 Generation Rate (L/Hr)</td><td>Radiolytic hydrogen generation rate is a product of total alpha activity in the skip, Alpha Decay Energy, Alpha G Value, and the K value</td><td>A13 (A4, A12, A11, A7) = A4*A12*A11*A7</td><td>Using the equation for Node A13 (Alpha Radiolytic H2 Generation Rate (L/Hr)), Netica automatically calculates the CPT data.</td></tr>
<tr><td>A14-Total Radiolytic H2 Gen Rate (L/hr)</td><td>Total Radiolytic Hydrogen Generation Rate is a sum of Gamma Radiolytic Hydrogen Generation Rate and Alpha Radiolytic Hydrogen Generation Rate</td><td>A14 (A10, A13) = A10+A13</td><td>Using the equation for Node A14 (Total Radiolytic H2 Gen Rate (L/hr)), Netica automatically calculates the CPT data.</td></tr>
<tr><td>B- Chronic Hydrogen Generation Rate</td><td></td><td></td><td></td></tr>
<tr><td>B1-Corrosion Hydrogen Gen Rate (L/hr)</td><td>The CISWG advised that the maximum rate of chronic hydrogen generation from the donor plant P5 waste is 4.5L/hr. The CPT data are based on the hydrogen generation rate percentile data given by the CISWG, which is converted to probabilities.</td><td>N/A- Corrosion Hydrogen generation rate provided by the CISWG</td><td>Based on the worst case skip baseline hydrogen source percentile data provided by the CISWG, the probability distribution for the CPT is determined as follows:
<table>
<tr><th>Percentile</th><th>Hydrogen generation rate (L/hr)</th><th>%Probability distribution</th></tr>
<tr><td>99.99</td><td>>4.5</td><td>0.01</td></tr>
<tr><td>99.9</td><td>4 to 4.5</td><td>0.09</td></tr>
<tr><td>99</td><td>3.2 to 4</td><td>9.9</td></tr>
<tr><td>90</td><td>1.8 to 3.2</td><td>40</td></tr>
<tr><td>50</td><td>0 to 1.8</td><td>50</td></tr>
</table></td></tr>
</table>

Node	Derivation of Node Data	Equation Used in BBN	Justification of CPT Data
C-Total Hydrogen Generation Rate			
C1- Total Hydrogen Generation Rate (L/hr)	Total hydrogen generation rate is the sum of Total Radiolytic Hydrogen Generation Rate plus Corrosion Hydrogen Gen Rate (L/hr)	C1 (A14, B1) = A14+B1	Using the equation for Node C1(Total Hydrogen Generation Rate (L/hr)), Netica automatically calculates the CPT data.
D- Filter Performance			
D1-Filter metal corrosion	The CISWG opinion is that long-term box storage operations will lead to corrosion of the metallic filter. During initial box handling operations, the filter will be relatively new, therefore the degree of corrosion will be minimal.	N/A- Discrete Node	It is considered that the skip and box filters will only experience corrosion due to long-term storage effects. As the degree of corrosion of the metal filter during box handling operations is minimal, a very low chance (1% probability) of corrosion of the filter metal is assumed.
D2-Condensation	The CISWG considered that condensation in the skip ullage space can also lead to degradation of the filter. Condensation is considered to increase over time. For box handling operations, the likelihood of condensation build-up is considered to be low.	N/A- Discrete Node	Condensation is also considered to worsen over long-term storage. As the likelihood of condensation build-up is considered to be low during box handling operations, a very low chance (1% probability) of condensation build up is assumed.
D3- Blockage by solids	The potential for blockage of the filter by the solids is considered to increase over time due to an increase in airborne particulate in the ullage space during long-term storage. For box handling operations, the likelihood of filter blockage is considered to be low.	N/A- Discrete Node	As the likelihood of blockage by the solids is also considered to be low during box handling operations , a very low chance (1% probability) is assumed for this event.

Node	Derivation of Node Data	Equation Used in BBN	Justification of CPT Data
D4-Filter Fouling Factor	It is believed that filter fouling could occur due to airborne particulate arising within the skip ullage space over periods of long-term storage. The current design basis compensates for a fouling factor of 10%, however there is the possibility that the fouling factor may be higher than the currently perceived value.	N/A- Discrete Node	The risk of fouling will increase over the years during storage. During box handling operations, the filter is still new therefore a very low probability of 1% is assumed in this analysis
D5-Filter Coefficient changes	A key design parameter for the skip and box filters is the selection of an appropriate filter coefficient to enable venting of the hydrogen gas from the skip while preventing any releases of airborne radioactive particulate to the outside atmosphere. The CISWG considered that there is the potential that the selected filter coefficient may not be sufficient to enable adequate venting of the hydrogen gas. As such, there is the possibility that commissioning tests may reveal that the filter coefficient has changed.	N/A- Discrete Node	It is considered that the filter coefficient could change due to variations in manufacturing. A 10% chance of this variation is currently assumed.

Node	Derivation of Node Data	Equation Used in BBN	Justification of CPT Data
D6- Filter performance reduces?	It is considered that the standing hydrogen concentration in the ullage space is dependent on the filter performance. Filter performance in turn is affected by the nodes, 'Filter Coefficient changes' and 'Filter Fouling Factor'.	N/A- Discrete Node	It is considered that the choice of filter coefficient is based on extensive R&D work for filter performance. Hence the CISWG opinion is that there is a high (nominal 90%) chance that the filter coefficient does not change. Also, It is believed that the risk of fouling will increase over the years during storage. During box handling operations, the filter is still new therefore a very low probability of 1% for the likelihood of increase in fouling factor is assumed in this analysis. At 90% chance that filter coefficient does not change and 1% chance that the fouling factor increases, the BBN calculates that there is a 91.7% likelihood that filter performance does not reduce.
E-Standing Hydrogen Concentration			
E1- Normal Standing H2 Conc. (%v/v)	This is the hydrogen concentration in the ullage when the hydrogen released from the waste reaches an equilibrium with the output hydrogen from the skip ullage via the filters. The CISWG filter performance modelling work developed a series of curves of hydrogen concentration in the ullage vs hydrogen generation rate for a series of filter sizes ranging from 200cm^2 to 700cm^2. For effective baseline filter performance, the filter design team recommended a filter size of 400cm^2. The hydrogen concentration data are taken from the hydrogen concentration vs hydrogen generation rate curve for 40,000mm^2 area.	N/A	The CPT data were derived as follows: For each interval of hydrogen generation rate the hydrogen concentration was read from the 400cm^2 and 300cm^2 as tabulated below and a percentage probability applied. E.g., for hydrogen generation rates of up to 1.2L/hr and when the filter performance is normal (not reduced), then the 400cm^2 curve shows that the hydrogen concentration in the ullage is 1.7% v/v, which is in the range 0 to 1.8%v/v in the ranges of hydrogen concentration in the CPT. So, with a maximum hydrogen generation rate of 1.2L/hr, there is a 100% chance that the hydrogen concentration is in the range 0 to 1.8% and 0% chance that the

<table>
<tr><th>Node</th><th>Derivation of Node Data</th><th>Equation Used in BBN</th><th>Justification of CPT Data</th></tr>
<tr><td></td><td>The CISWG recommended that consideration must be given to the potential for reduced filter performance due to filter fouling. The view was that the worst case design is when filter area reduces by 10% due to the fouling factor. Therefore, for reduced filter performance, it is assumed that the filtration area reduces from the 400cm^2 to 300cm^2. For the 10% reduction in filter performance the hydrogen concentration data are taken from the curve for the 30,000mm^2 area.</td><td></td><td>concentration falls in other ranges in the CPT. At 1.2L/hr if the filter performance reduces, then the H_2 concentration is 2%v/v, thus a 100% probability is applied in the CPT for the concentration being the range 1.8 to 3.4%.
<table>
<tr><th>Hydrogen generation rate (L/hr)</th><th>Hydrogen concentration in skip ullage (%/v/v), filter area = 400cm^2</th><th>Hydrogen concn. in skip ullage (%/v/v) for reduced filter area of 300cm^2</th></tr>
<tr><td>0 to 1.2</td><td>1.7</td><td>2.0</td></tr>
<tr><td>Up to 2.4</td><td>3.2</td><td>3.9</td></tr>
<tr><td>Up to 3.6</td><td>4.2</td><td>5.1</td></tr>
<tr><td>Up to 4.8</td><td>5.5</td><td>6.8</td></tr>
<tr><td>Up to 6.0</td><td>6.8</td><td>8.0</td></tr>
</table></td></tr>
<tr><td>E2- Standing Hydrogen Volume (L)</td><td>Standing Hydrogen Volume is calculated knowing the standing hydrogen concentration in the skip ullage (see the node 'Normal Standing H2 Conc. (%v/v)' above), which is divided by the skip ullage volume (See Node F3 below).</td><td>E2 (E1, F3) = (E1/100)*F3</td><td>Using the equation for Node E2- Standing Hydrogen Volume (L), Netica automatically calculates the CPT data</td></tr>
<tr><td>F-Skip Ullage Volume</td><td></td><td></td><td></td></tr>
<tr><td>F1-Skip Internal Volume (L)</td><td>The skip design is such that the free internal volume is 1561L</td><td>N/A - Constant</td><td>N/A - Constant</td></tr>
</table>

Node	Derivation of Node Data	Equation Used in BBN	Justification of CPT Data
F2 - Total Skip Content (L)	It is known that for a full skip the volume of the total contents, including waste and water, is always fixed to 1270L. This operational control ensures that the waste and cover water volume never exceeds the minimal desired ullage volume.	N/A - Constant	N/A - Constant
F3- Skip Ullage Volume (L)	Skip ullage volume is the Skip internal volume (F1) minus the volume of total skip consents (F2) minus the increase in volume due to waste swelling (G4) - see descriptions below for each of these Parent nodes.	E2 (E1, F3) = (E1/100)*F3	Using the equation for Node F3- Skip Ullage Volume (L)Netica automatically calculates the CPT data
G - Hydrogen Retention			
G1-Waste Volume (L)	The process control for skip filling requires that the maximum fill levels for skips from all parts of Plant P5 are: Full skips: 1000L of waste and 270L of cover water Part filled skips: 600L of waste and 670L of cover water. This model assumes that the skip is full.	N/A - Constant	
G2- Waste Type	This model assumes that the likelihood of a particular waste type being received in the skip is dependent on the proportions of the waste types present in the donor plants. It is believed that in the donor plant P5, 30% of the material is sludge, 35% is swarf, 20% is shale and 15% Miscellaneous Beta Gamma Waste (MBGW).	N/A- Discrete Node	

Node	Derivation of Node Data	Equation Used in BBN	Justification of CPT Data
G3- Bed expansion fraction	The CISWG Process Engineering SME advice is that for sludgy material (normal condition) the extent of bed expansion due to hydrogen retention is limited to 15%v/v and for the abnormal condition it is limited to 20%v/v in the short term (up to 6 months). For swarf, the expansion fraction in the short term is limited to 5%v/v both for the normal and abnormal conditions. For Shale, the expansion fraction is 10%v/v for the normal condition and 15%v/v for abnormal condition. For Miscellaneous Beta Gamma Wastes (MBGW), under normal conditions there is no expansion, and in abnormal conditions it is up to 10%v/v.	N/A- Discrete Node	For all normal condition cases, the likelihood probability is considered to be 90% and for all abnormal condition cases, the likelihood is considered to be 10%. For example, for sludgy material in a normal condition, the bed expansion fraction is 15%v/v and 20%v/v for the abnormal case. So, in the CPT for sludge material a probability of 90% is applied for the expansion fraction of up to 15%v/v and a probability of 10% is applied to the 20%v/v expansion fraction.
H- Discontinuous Release			
H1- Hydrogen Retention Volume (L)	In accordance with the study undertaken by *van Kessel and van Kesteren, 2002,* it is that the bulk waste within the skip is capable of retaining, within the pores of the Magnox swarf matrix a proportion of the hydrogen gas released due to corrosion and radiolysis. Any retained gas will lead to expansion of the total waste plus cover water volume, thus leading to a reduction in the ullage volume. Additionally, acute (or discontinuous release) of the held-up hydrogen is possible if the waste is disturbed. The increase in waste volume due to swelling is a product of the original	H1 (G3, G1) = G3*G1	Using the equation for Node H1- Hydrogen Retention Volume (L) , Netica automatically calculates the CPT data.

Node	Derivation of Node Data	Equation Used in BBN	Justification of CPT Data
	volume of the waste within the skip and the fraction of the waste which expands. The volume of hydrogen retained in the waste matrix is the product of the original volume of the waste (Node G1) and the bed expansion fraction (Node G3)		
H2 - Fraction of retained hydrogen released	This node is based on a knowledge of the hydrogen release from different types of waste under various operational constraints. The CISWG considered that for bulk waste during normal box handling operations, the worst case disturbance level is considered to be mild disturbance for which the following release fractions and probabilities are considered appropriate: Normal (0.9 probability), release fraction= 2.5% i.e., 0.025. Abnormal (0.099 probability) release fraction= 5% i.e., 0.05. Outlier (0.001 probability), release fraction= 20%, i.e., 0.2.	N/A- Discrete Node	See 'Derivation of Node Data' column for derivation of the CPT.
H3- Discontinuous H2 release volume	The discontinuous H2 release volume is the product of the H2 Retention Volume (Node H1) and the Fraction of retained hydrogen released (Node H2).	H3 (H1, H2) = H1*H2	Using the equation for Node H3- Discontinuous H2 release volume, Netica automatically calculates the CPT data.

Node	Derivation of Node Data	Equation Used in BBN	Justification of CPT Data
I2- Hydrogen concentration in skip ullage space			
I1- Total hydrogen volume in ullage (L)	The total hydrogen volume in the ullage (L) is the sum of Discontinuous H2 release volume (Node H3) and Standing Hydrogen Volume (Node E2)	I1 (H3, E2) = H3+E2	Using the equation for Node I1- Total hydrogen volume in the ullage (L), Netica automatically calculates the CPT data.
I2- Hydrogen concentration in ullage (%v/v)	The hydrogen concentration in the ullage is the Total hydrogen volume in the ullage (Node I1) divided by the sum of the ullage volume (Node F3) and discontinuous release volume (Node H3)	I2 (I1, F3, H3) = I1*100/(F3+H3)	Using the equation for ullage H_2 concentration (NodeI2), Netica automatically calculates the CPT data.

Node A14: Total Radiolytic H_2 generation rate (L/hr)					A13: Alpha Radiolytic H_2 gen. rate (L/hr)	A10: Beta Gamma radiolytic H_2 gen. rate (L/hr)
0 to 0.00304	0.00304 to 0.006	0.00608 to 0.009	0.00912 to 0.012	0.01216 to 0.015		
1	0	0	0	0	0 to 0.00164	0 to 0.0014
0.573434	0.426566	0	0	0	0 to 0.00164	0.0014 to 0.0028
0.012411	0.987589	0	0	0	0 to 0.00164	0.0028 to 0.0042
0	0.707424	0.292576	0	0	0 to 0.00164	0.0042 to 0.0056
0	0.0499	0.9501	0	0	0 to 0.00164	0.0056 to 0.007
0.42697	0.57303	0	0	0	0.00164 to 0.003	0 to 0.0014
0	1	0	0	0	0.00164 to 0.003	0.0014 to 0.0028
0	0.573577	0.426423	0	0	0.00164 to 0.003	0.0028 to 0.0042
0	0.012427	0.987573	0	0	0.00164 to 0.003	0.0042 to 0.0056
0	0	0.707457	0.292543	0	0.00164 to 0.003	0.0056 to 0.007
0	0.987774	0.012226	0	0	0.00328 to 0.004	0 to 0.0014
0	0.426907	0.573093	0	0	0.00328 to 0.004	0.0014 to 0.0028
0	0	1	0	0	0.00328 to 0.004	0.0028 to 0.0042
0	0	0.573632	0.426368	0	0.00328 to 0.004	0.0042 to 0.0056
0	0	0.012336	0.987664	0	0.00328 to 0.004	0.0056 to 0.007
0	0.292848	0.707152	0	0	0.00492 to 0.006	0 to 0.0014
0	0	0.987767	0.012233	0	0.00492 to 0.006	0.0014 to 0.0028
0	0	0.427048	0.572952	0	0.00492 to 0.006	0.0028 to 0.0042
0	0	0	1	0	0.00492 to 0.006	0.0042 to 0.0056
0	0	0	0.573466	0.426534	0.00492 to 0.006	0.0056 to 0.007
0	0	0.950336	0.049664	0	0.00656 to 0.008	0 to 0.0014
0	0	0.292868	0.707132	0	0.00656 to 0.008	0.0014 to 0.0028
0	0	0	0.987694	0.012306	0.00656 to 0.008	0.0028 to 0.0042
0	0	0	0.426917	0.573083	0.00656 to 0.008	0.0042 to 0.0056
0	0	0	0	1	0.00656 to 0.008	0.0056 to 0.007

Table D-2: CPT for total radiolytic hydrogen generation rate (L/hr)

Node B1: Corrosion H_2 generation rate (L/hr)	Probability distribution
0 to 1.8	0.5
1.8 to 3.2	0.4
3.2 to 4	0.099
4 to 4.5	9E-04
4.5 to 6	1.00E-04

Table D-3: CPT for Node B1, Corrosion hydrogen generation rate (L/hr)

Node C1: Total Hydrogen Generation Rate (L/hr)					Node B1: Corrosion H_2 gen. rate(L/hr)	Node A14: Total Radiolytic H_2 gen rate (L/hr)
0 to 1.204	1.204 to 2.408	2.408 to 3.612	3.612 to 4.816	4.816 to 6.02		
0.668051	0.331949	0	0	0	0 to 1.8	0 to 0.00304
0.666064	0.333936	0	0	0	0 to 1.8	0.00304 to 0.006
0.664597	0.335403	0	0	0	0 to 1.8	0.00608 to 0.009
0.662864	0.337136	0	0	0	0 to 1.8	0.00912 to 0.012
0.661205	0.338795	0	0	0	0 to 1.8	0.01216 to 0.015
0	0.432851	0.567149	0	0	1.8 to 3.2	0 to 0.00304
0	0.430972	0.569028	0	0	1.8 to 3.2	0.00304 to 0.006
0	0.428852	0.571148	0	0	1.8 to 3.2	0.00608 to 0.009
0	0.426658	0.573342	0	0	1.8 to 3.2	0.00912 to 0.012
0	0.424364	0.575636	0	0	1.8 to 3.2	0.01216 to 0.015
0	0	0.513255	0.486745	0	3.2 to 4	0 to 0.00304
0	0	0.509034	0.490966	0	3.2 to 4	0.00304 to 0.006
0	0	0.505564	0.494436	0	3.2 to 4	0.00608 to 0.009
0	0	0.501534	0.498466	0	3.2 to 4	0.00912 to 0.012
0	0	0.498015	0.501985	0	3.2 to 4	0.01216 to 0.015
0	0	0	1	0	4 to 4.5	0 to 0.00304
0	0	0	1	0	4 to 4.5	0.00304 to 0.006
0	0	0	1	0	4 to 4.5	0.00608 to 0.009
0	0	0	1	0	4 to 4.5	0.00912 to 0.012
0	0	0	1	0	4 to 4.5	0.01216 to 0.015
0	0	0	0.209554	0.790446	4.5 to 6	0 to 0.00304
0	0	0	0.207712	0.792288	4.5 to 6	0.00304 to 0.006
0	0	0	0.205562	0.794438	4.5 to 6	0.00608 to 0.009
0	0	0	0.203651	0.796349	4.5 to 6	0.00912 to 0.012
0	0	0	0.201433	0.798567	4.5 to 6	0.01216 to 0.015

Table D-4: CPT for total hydrogen generation rate

Node E1: Normal Standing H_2 Conc. (%v/v)					Node C1: Total Hydrogen Generation Rate (L/hr)	Node D6: Filter performance reduces?
0 to 1.8	1.8 to 3.4	3.4 to 5.1	5.1 to 6.8	6.8 to 8.5		
0	1	0	0	0	0 to 1.204	Yes
1	0	0	0	0	0 to 1.204	No
0	0	1	0	0	1.204 to 2.408	Yes
0	1	0	0	0	1.204 to 2.408	No
0	0	0	1	0	2.408 to 3.612	Yes
0	0	1	0	0	2.408 to 3.612	No
0	0	0	0	1	3.612 to 4.816	Yes
0	0	0	1	0	3.612 to 4.816	No
0	0	0	0	1	4.816 to 6.02	Yes
0	0	0	0	1	4.816 to 6.02	No

Table D-5: CPT for Node E1 normal standing hydrogen concentration

Node F3: Skip ullage volume (L)	Node F1: Skip internal volume (L)	F2: Total skip content (L)	Node H1: Hydrogen retention volume (L)
251 to 291	1561	1270	0 to 40
211 to 251	1561	1270	40 to 80
171 to 211	1561	1270	80 to 120
131 to 171	1561	1270	120 to 160
91 to 131	1561	1270	160 to 200

Table D-6: CPT for skip ullage volume

Node H1: Hydrogen retention volume (L)	Node G3: Bed expansion fraction	Node G1: Skip waste volume(L)
80 to 120	Up to 10 percent	1000
120 to 160	Up to 15 percent	1000
160 to 200	Up to 20 percent	1000
40 to 80	Up to 5 percent	1000
0 to 40	No expansion	1000

Table D-7: CPT for Node H1, hydrogen retention volume

Node H3: Discontinuous H_2 release volume (L)	Node H1: Hydrogen retention volume (L)	Node H2: Fraction of retained hydrogen released
0 to 8	0 to 40	Normal
0 to 8	0 to 40	Abnormal
0 to 8	0 to 40	Outlier
0 to 8	40 to 80	Normal
0 to 8	40 to 80	Abnormal
8 to 16	40 to 80	Outlier
0 to 8	80 to 120	Normal
0 to 8	80 to 120	Abnormal
16 to 24	80 to 120	Outlier
0 to 8	120 to 160	Normal
0 to 8	120 to 160	Abnormal
24 to 32	120 to 160	Outlier
0 to 8	160 to 200	Normal
8 to 16	160 to 200	Abnormal
32 to 40	160 to 200	Outlier

Table D-8: CPT for Node H3, discontinuous hydrogen release volume

Node E2: Standing hydrogen volume (L)					Node E1 Normal Standing H_2 Conc. (%v/v)	Node F3: Skip ullage volume (L)
0 to 5	5 to 10	10 to 15	15 to 20	20 to 25		
1	0	0	0	0	0 to 1.8	91 to 131
1	0	0	0	0	0 to 1.8	131 to 171
1	0	0	0	0	0 to 1.8	171 to 211
1	0	0	0	0	0 to 1.8	211 to 251
0.9921	0.0079	0	0	0	0 to 1.8	251 to 291
1	0	0	0	0	1.8 to 3.4	91 to 131
0.9064	0.0936	0	0	0	1.8 to 3.4	131 to 171
0.5202	0.4798	0	0	0	1.8 to 3.4	171 to 211
0.2336	0.7664	0	0	0	1.8 to 3.4	211 to 251
0.0393	0.9607	0	0	0	1.8 to 3.4	251 to 291
0.6626	0.3374	0	0	0	3.4 to 5.1	91 to 131
0.048	0.952	0	0	0	3.4 to 5.1	131 to 171
0	0.9609	0.0391	0	0	3.4 to 5.1	171 to 211
0	0.558	0.442	0	0	3.4 to 5.1	211 to 251
0	0.1722	0.8278	0	0	3.4 to 5.1	251 to 291
0.019	0.981	0	0	0	5.1 to 6.8	91 to 131
0	0.8296	0.1704	0	0	5.1 to 6.8	131 to 171
0	0.1314	0.8686	0	0	5.1 to 6.8	171 to 211
0	0	0.8052	0.1948	0	5.1 to 6.8	211 to 251
0	0	0.258	0.742	0	5.1 to 6.8	251 to 291
0	0.9171	0.0829	0	0	6.8 to 8.5	91 to 131
0	0.089	0.911	0	0	6.8 to 8.5	131 to 171
0	0	0.6235	0.3765	0	6.8 to 8.5	171 to 211
0	0	0.0197	0.9184	0.0619	6.8 to 8.5	211 to 251
0	0	0	0.3521	0.6479	6.8 to 8.5	251 to 291

Table D-9: CPT for Standing hydrogen volume (L)

Node I1: Total hydrogen volume in the ullage (L)					Node E2: Standing Hydrogen Volume (L)	Node H3: Discontinuous H_2 release vol. (L)
0 to 13	**13 to 26**	**26 to 39**	**39 to 52**	**52 to 65**	**E2**	**H3**
1	0	0	0	0	0 to 5	0 to 8
0.3097	0.6903	0	0	0	0 to 5	8 to 16
0	0.8853	0.1147	0	0	0 to 5	16 to 24
0	0.0492	0.9508	0	0	0 to 5	24 to 32
0	0	0.5609	0.4391	0	0 to 5	32 to 40
0.6847	0.3153	0	0	0	5 to 10	0 to 8
0	1	0	0	0	5 to 10	8 to 16
0	0.3115	0.6885	0	0	5 to 10	16 to 24
0	0	0.8866	0.1134	0	5 to 10	24 to 32
0	0	0.0527	0.9473	0	5 to 10	32 to 40
0.1103	0.8897	0	0	0	10 to 15	0 to 8
0	0.6916	0.3084	0	0	10 to 15	8 to 16
0	0	1	0	0	10 to 15	16 to 24
0	0	0.3089	0.6911	0	10 to 15	24 to 32
0	0	0	0.8863	0.1137	10 to 15	32 to 40
0	0.9484	0.0516	0	0	15 to 20	0 to 8
0	0.1117	0.8883	0	0	15 to 20	8 to 16
0	0	0.6952	0.3048	0	15 to 20	16 to 24
0	0	0	1	0	15 to 20	24 to 32
0	0	0	0.3129	0.6871	15 to 20	32 to 40
0	0.4389	0.5611	0	0	20 to 25	0 to 8
0	0	0.9525	0.0475	0	20 to 25	8 to 16
0	0	0.1132	0.8868	0	20 to 25	16 to 24
0	0	0	0.6857	0.3143	20 to 25	24 to 32
0	0	0	0	1	20 to 25	32 to 40

Table D-10: CPT for total hydrogen volume in the ullage space

Table D-11: Verification matrix for Case Study 4 BBN continuous nodes

Test value for equation variable 1	Test value for equation variable 2	Test value for equation variable 3	Test value for equation variable 4	Result of BBN calculation	Comparison with hand calculation	BBN equation verified?
Node A1-Skip alpha activity concentration: p (A1 |) = UniformDist(A1,0,2.31e6) Minimum value of Node A1 for Discretisation = 0, Maximum value of Node A1 for Discretisation = 3.31E6						
Node A2-Skip Gamma activity concentration : P (A2 |) = UniformDist(A2,0,4.7E7) Minimum value of Node A2 for Discretisation = 0, Maximum value of Node A1 for Discretisation = 3.31E6						
Node A10-Beta Gamma Radiolytic H_2 Gen Rate (L/hr)-A10 (A5, A6, A8, A7, A9) = A5*A6*A7*(A8+A9) Minimum value of A10 for discretisation = 0, Maximum value of A10 for discretisation = 0.0069L/hr						
A5 = Total beta-gamma activity= 1.25E+13	A6 = Beta-gamma G Value= 0.45	Node A7 = K Value = 1.44E-15	A8+A9 = Total alpha and beta gamma decay energy= 0.662+0.186 MeV	0.0069L/hr	0.0069L/hr	Yes
Node A13-Alpha Radiolytic H_2 Gen Rate (L/hr) A13 (A4, A12, A11, A7) = A4*A12*A11*A7 Minimum value of A13 for discretisation = 0, Maximum value of A13 for discretisation = 8.20E-03L/hr						
A4= Total alpha activity = 6.00E+11	A11=Alpha G Value =1.66	A7 = K Value = 1.44E-15	A12=Alpha decay energy =5.5MeV	7.9E-03L/hr	7.89E-03L/hr	Yes
Total Radiolytic H2 Gen Rate (L/hr) A14 (A10, A13) = A10+A13 Minimum value of A14 for discretisation = 0, Maximum value of A14 for discretisation = 0.0152 L/hr						
A10-Beta-gamma radiolytic hydrogen generation rate = 0.006L/hr	A13-Alpha radiolytic hydrogen generation rate = 0.0082 L/hr	N/A	N/A	0.0142 (Figure D-1)	0.0142	
Total H_2 Generation Rate,(L/hr) C1(A14, B1) = A14+B1 Minimum value of C1 for discretisation = 0, Maximum value of C1 for discretisation = 6.02L/hr						
A14-Total hydrogen generation rate =0.008L/hr	Node B1- Hydrogen generation rate from corrosion = 3.5L/hr	N/A	N/A	3.508L/hr (Figure D-2)	3.508L/hr	Yes

Test value for equation variable 1	Test value for equation variable 2	Test value for equation variable 3	Test value for equation variable 4	Result of BBN calculation	Comparison with hand calculation	BBN equation verified?
Skip ullage volume (L) F3 (H1, F1, F2) = F1-F2-H1 Minimum value of F3 for discretisation = 0, Maximum value of F3 for discretisation = 291L						
F1,Skip internal vol(L)= 1561	F2, Total skip content (L) = 1270	H1,Hydrogen retention volume = 100	N/A	191L (Figure D-3)	191L	Yes
Standing hydrogen volume (L) E2(E1, F3) = (E1/100)*F3 Minimum value of E2 for discretisation = 0, Maximum value of E2 for discretisation = 24.735L						
E1,Normal Standing H2 Conc = 4%v/v	F3,Skip Ullage Volume =190L	N/A	N/A	7.6L	7.6L	Yes
Hydrogen retention volume (L) H1(G3, G1) = G3*G1 Minimum value of C1 for discretisation = 0, Maximum value of C1 for discretisation = 200L						
G1,Skip waste volume = 1000L	G3,Bed expansion fraction = 0.2	N/A	N/A	200L	200L	Yes
Hydrogen discontinuous release volume (L) H3(H1, H2) = H1*H2 Minimum value of H3 for discretisation = 0, Maximum value of H3 for discretisation = 40L						
H1,Hydrogen retention volume =39L	H2, Fraction of retained hydrogen released =0.025	N/A	N/A	0.975L (Figure D-4)	0.975L	Yes
Total hydrogen volume in ullage space (L) I1(E2, H3) = H3+E2 Minimum value of I1 for discretisation = 0, Maximum value of I1 for discretisation = 65L						
E2,Standing hydrogen volume = 12L	H3,Discontinuous H_2 release volume =20L	N/A	N/A	32L	32L	Yes
Hydrogen concentration in ullage space (%v/v) I2 (F3, I1, H3)=I1*100/(F3+H3) Minimum value of I2 for discretisation = 0, Maximum value of I2 for discretisation = 71.43L						
F3,Skip ullage volume =91L	H3,Discontinuous H_2 release volume = 5L	I1,Total hydrogen volume in the ullage = 7L	N/A	7.292 (Figure D-5)	7.292	Yes

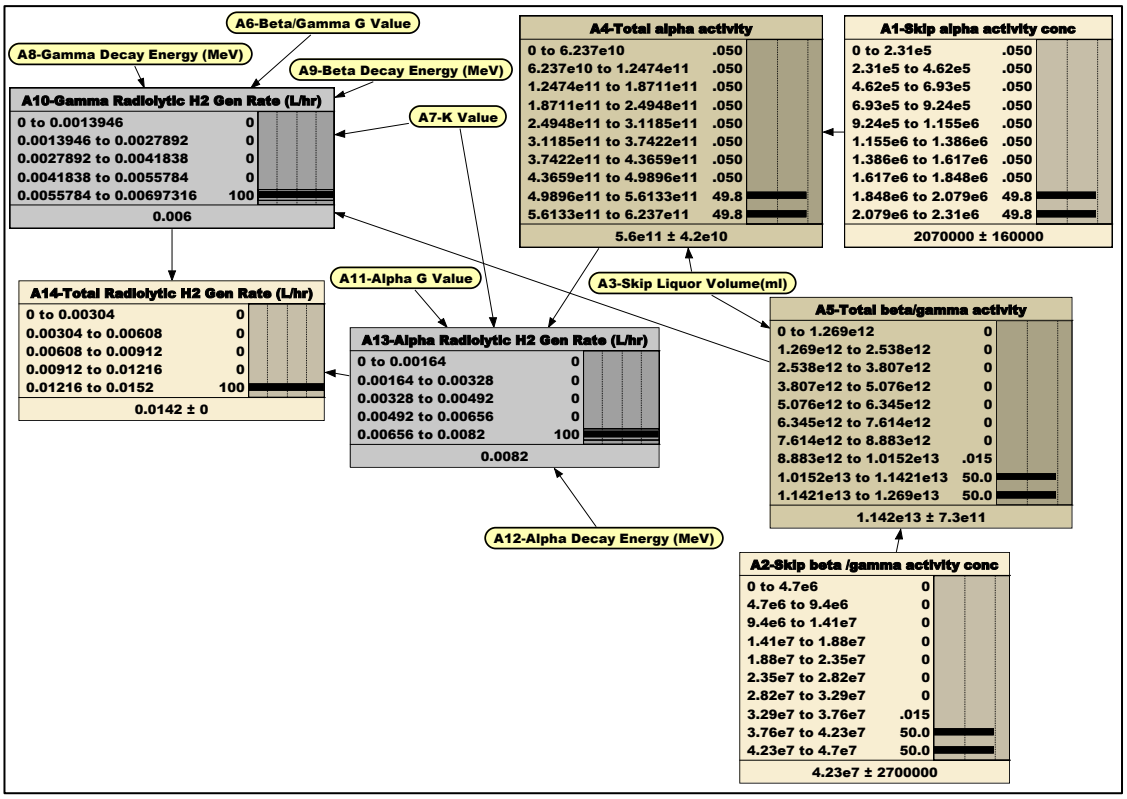

Figure D-1: Verification of BBN for total radiolytic hydrogen generation rate

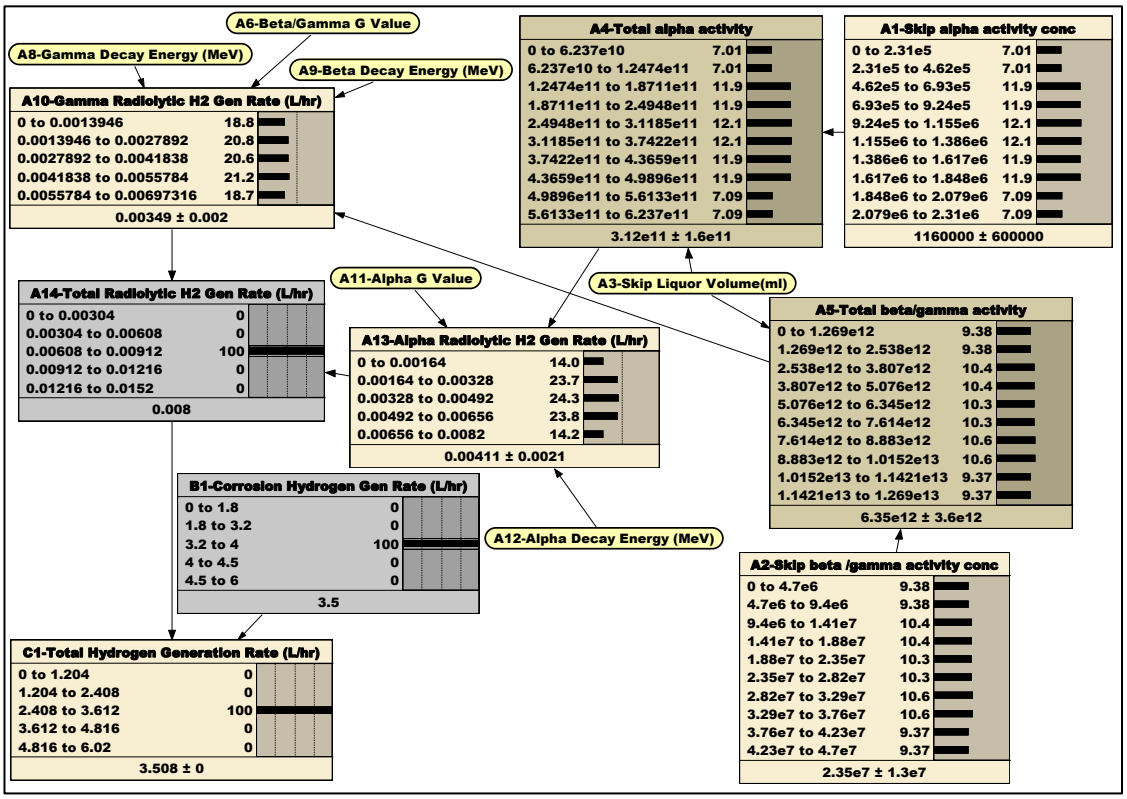

Figure D-2: Verification of BBN for total hydrogen generation rate

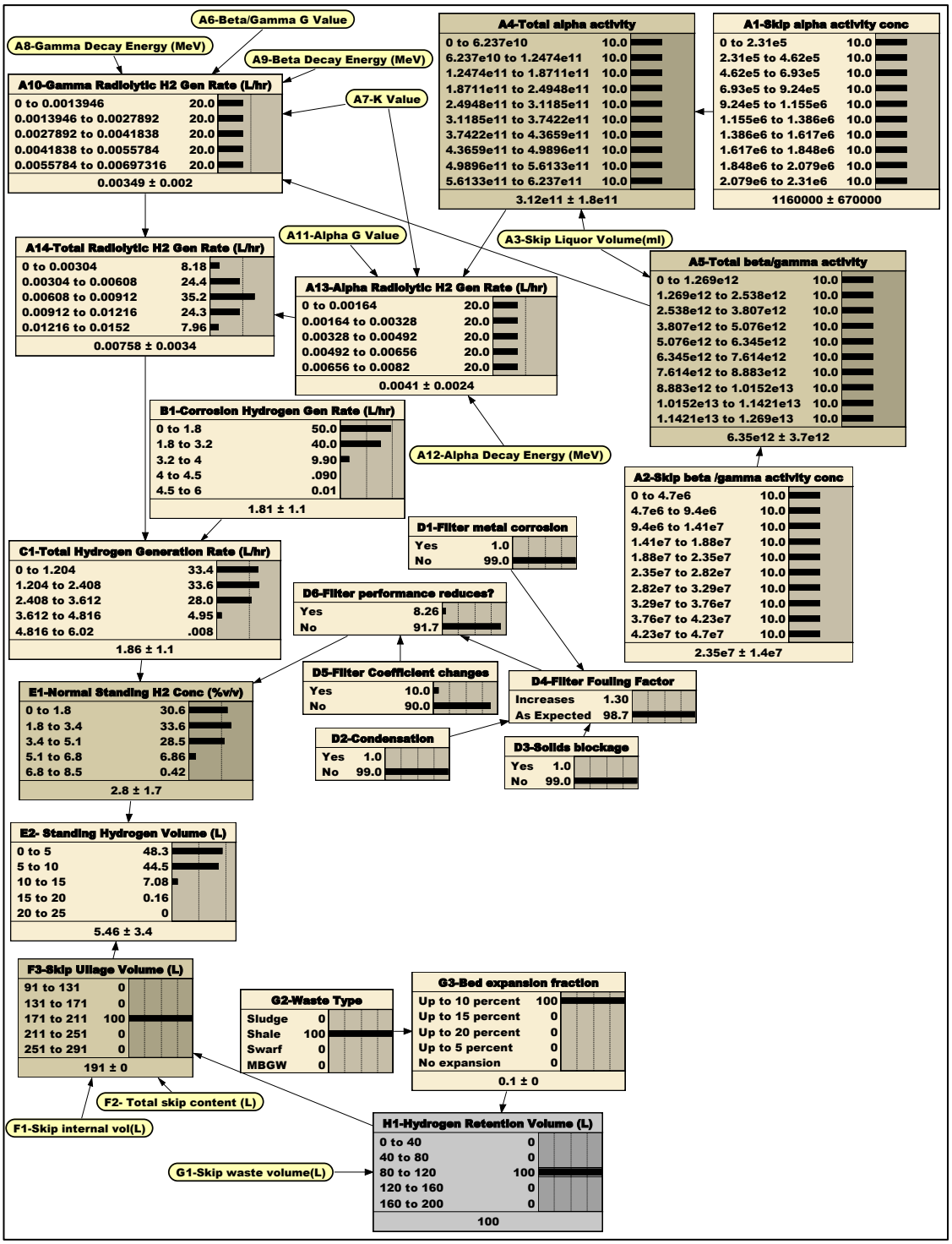

Figure D-3: Verification of BBN for Skip Ullage Volume; Hydrogen Retention Volume = 100L

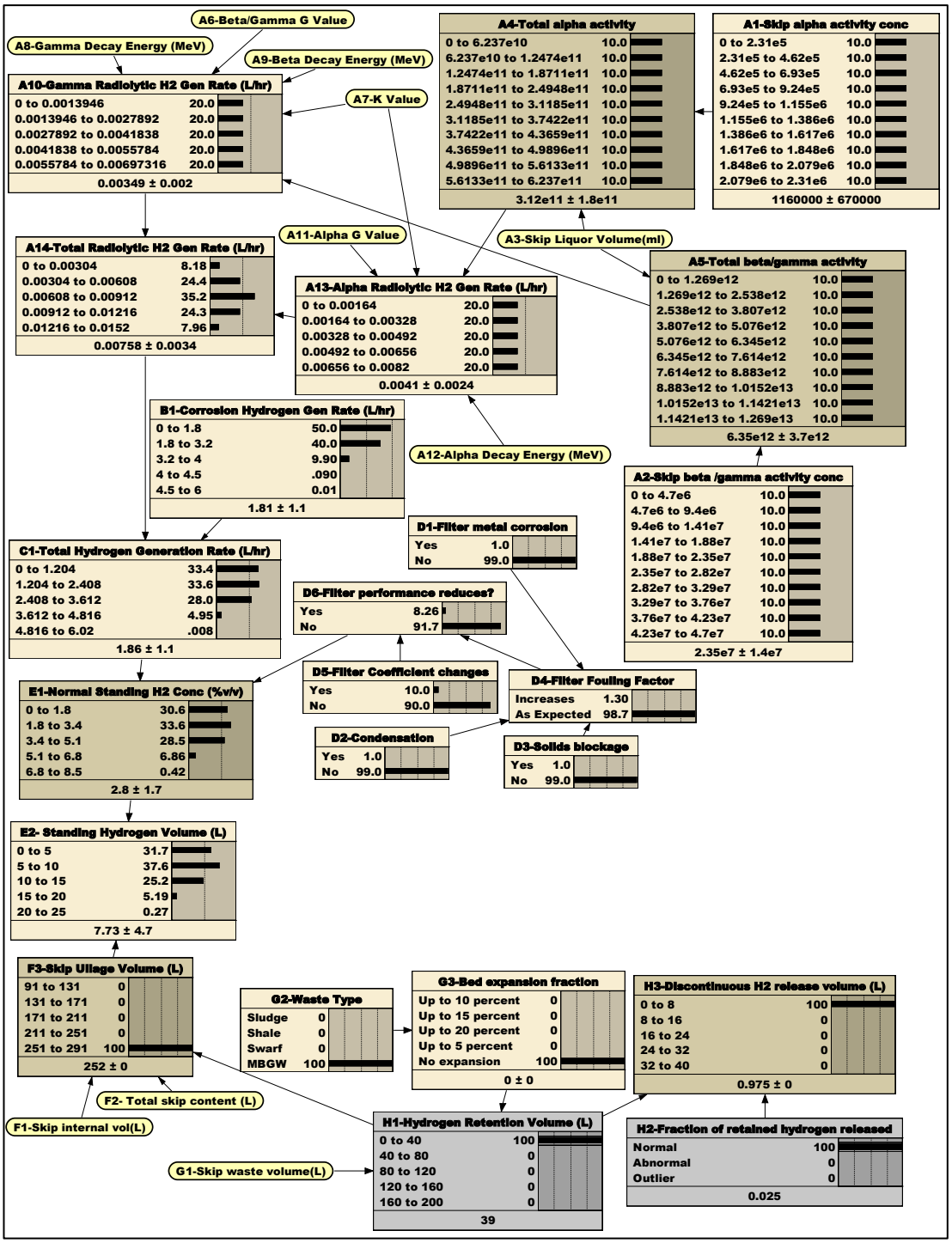

Figure D-4: Verification of BBN for discontinuous hydrogen release volume, H_2 retention volume=39L

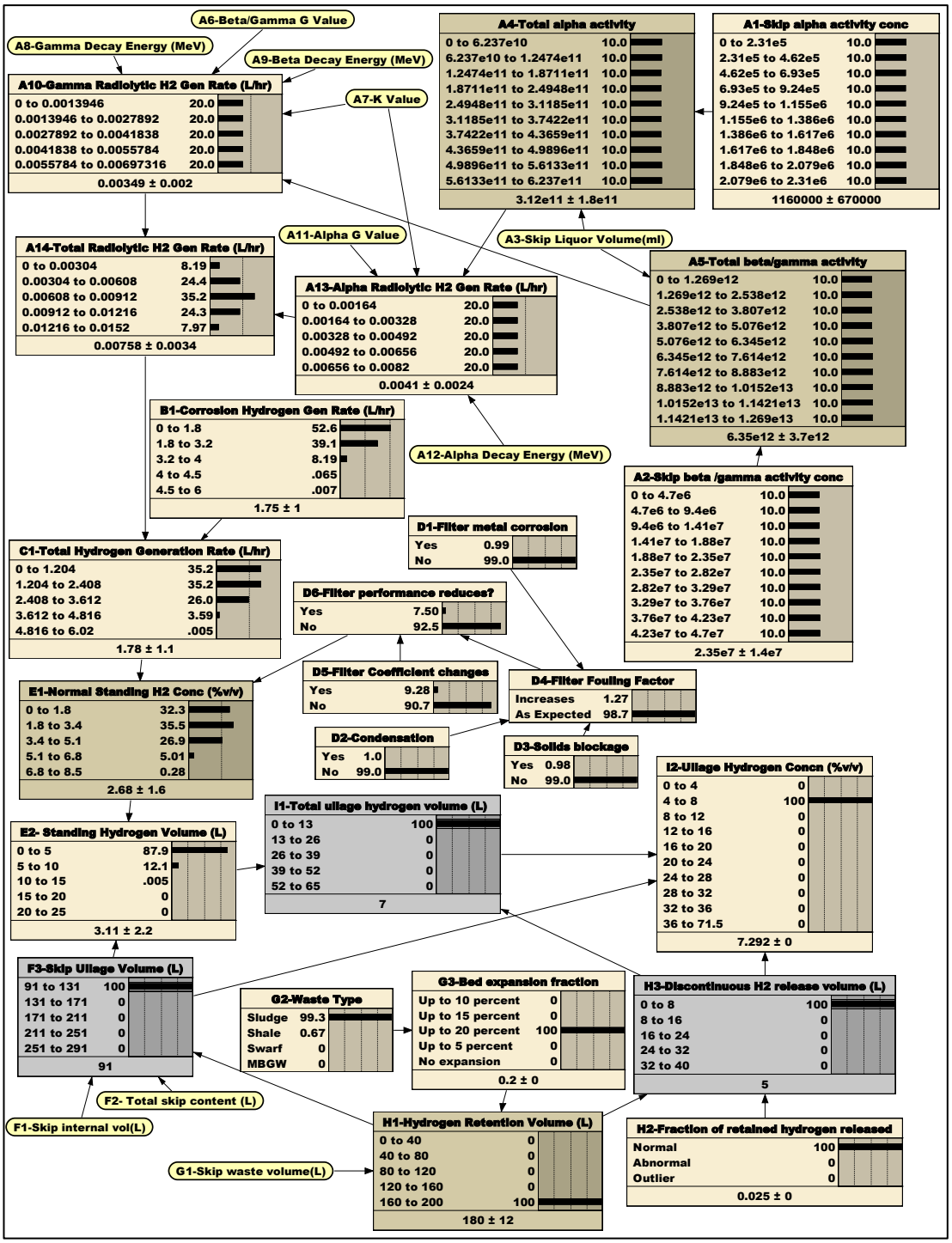

Figure D-5: Verification of BBN for Node I2, hydrogen concentration in ullage space

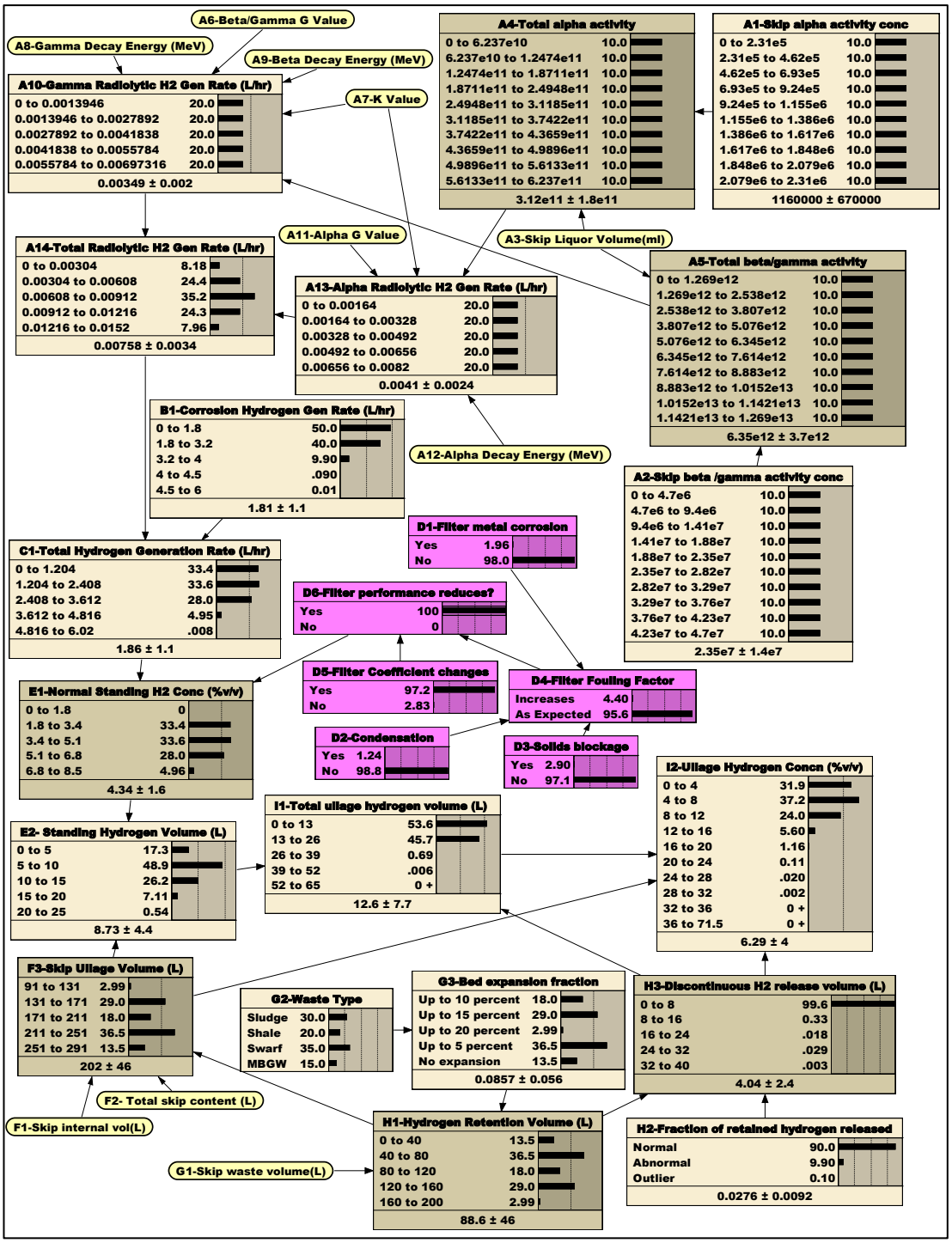

Figure D-6: BBN for sensitivity to filter performance

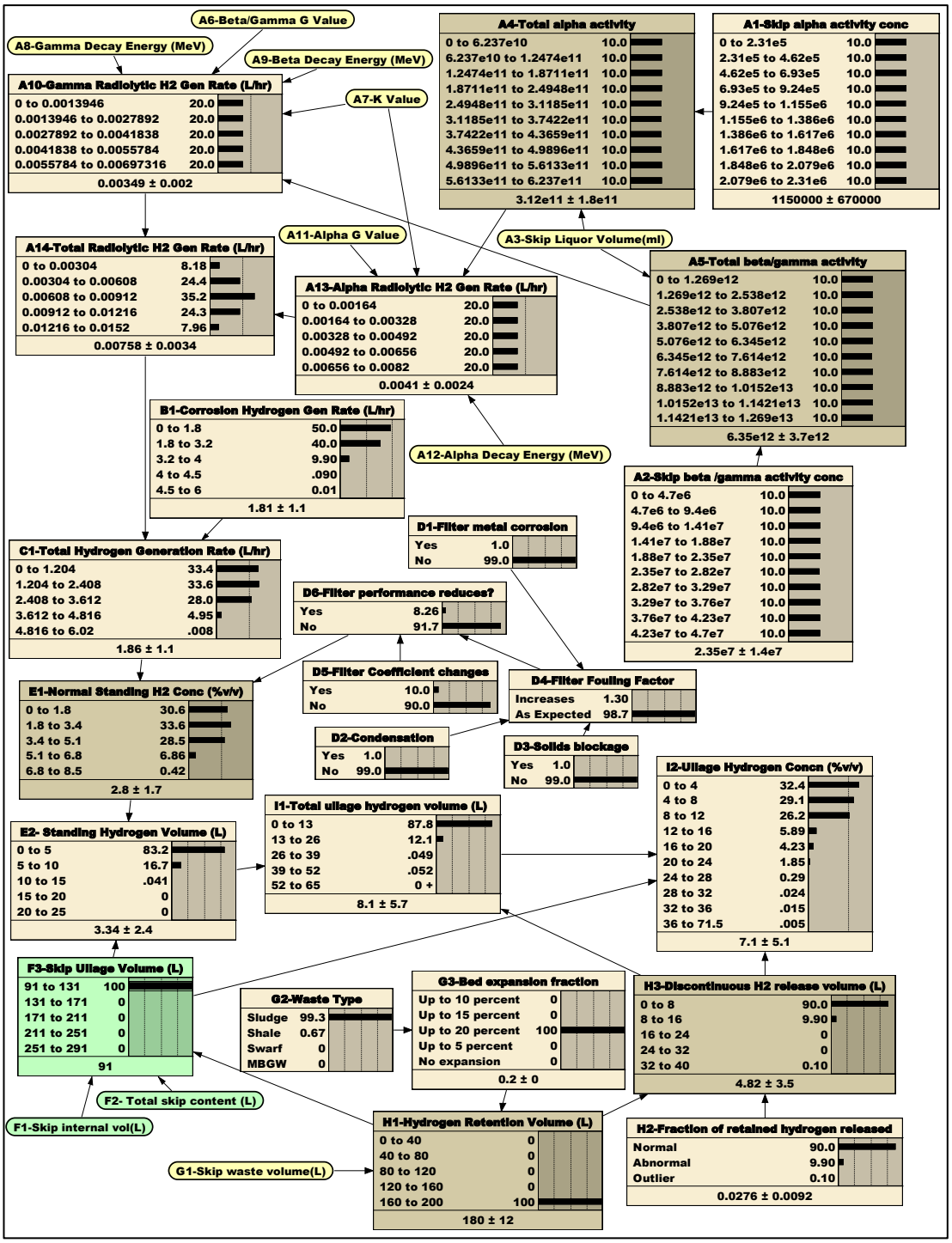

Figure D-7: BBN for sensitivity to lowest ullage volume

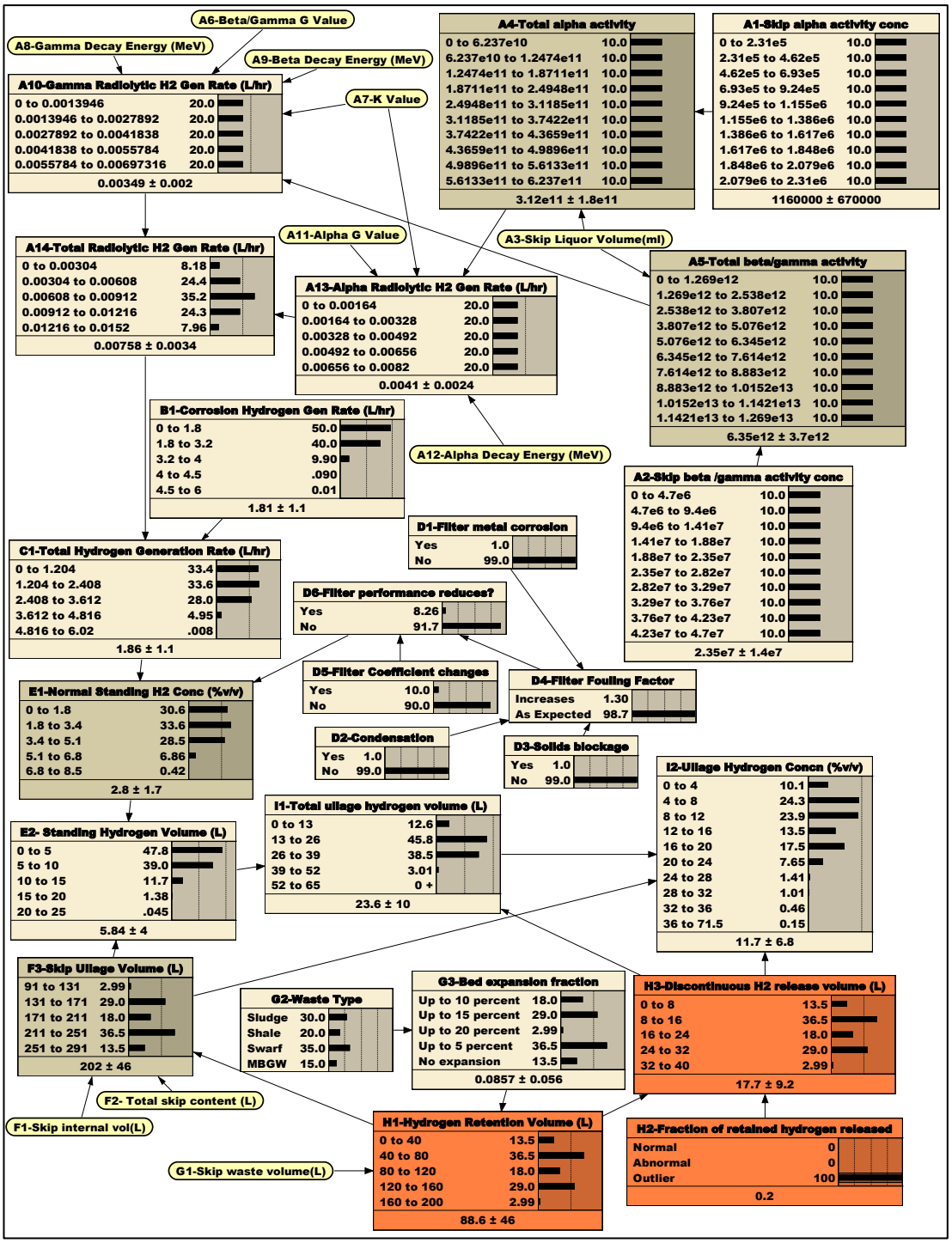

Figure D-8: BBN for sensitivity to high release fraction of hydrogen

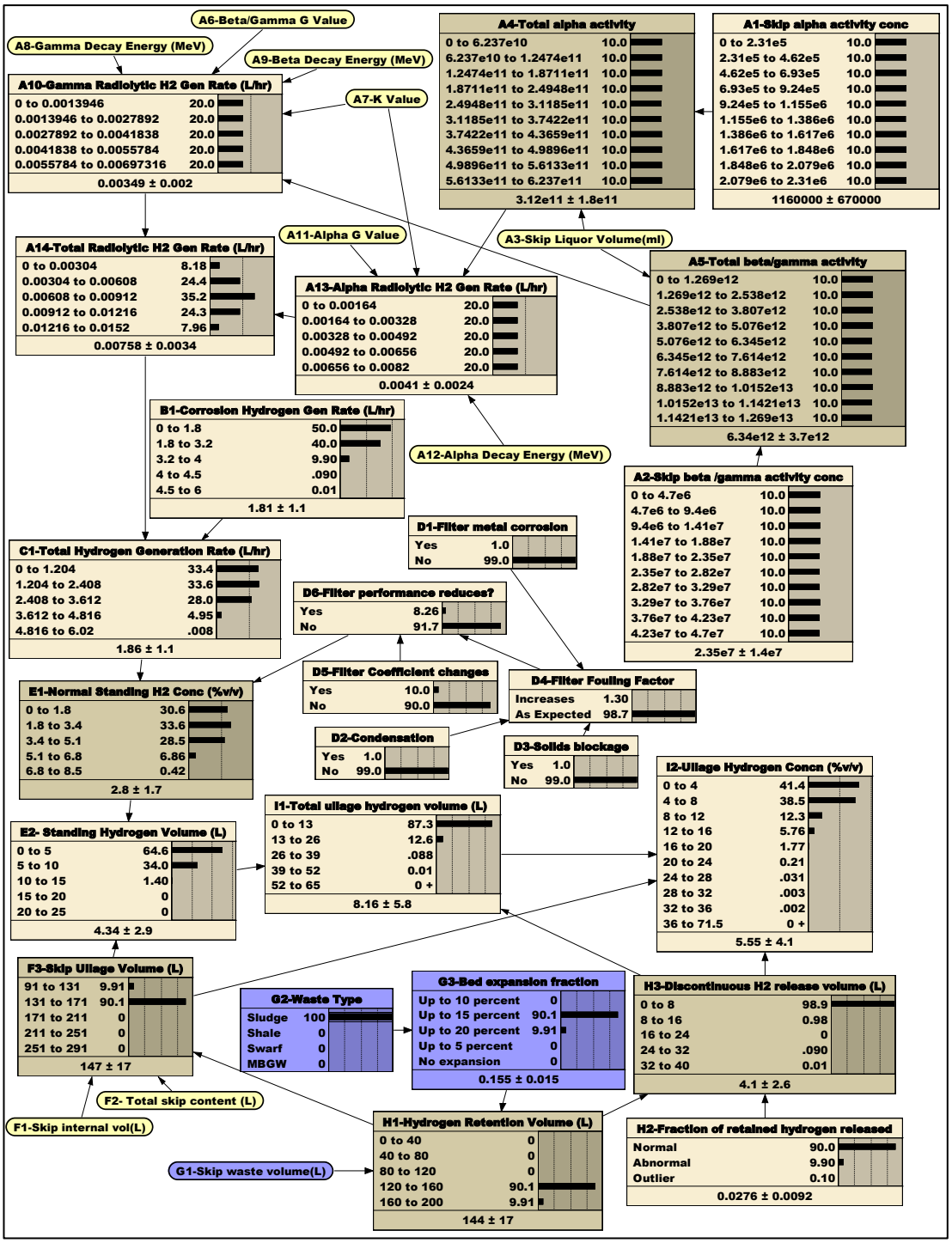

Figure D-9: BBN for sensitivity waste type

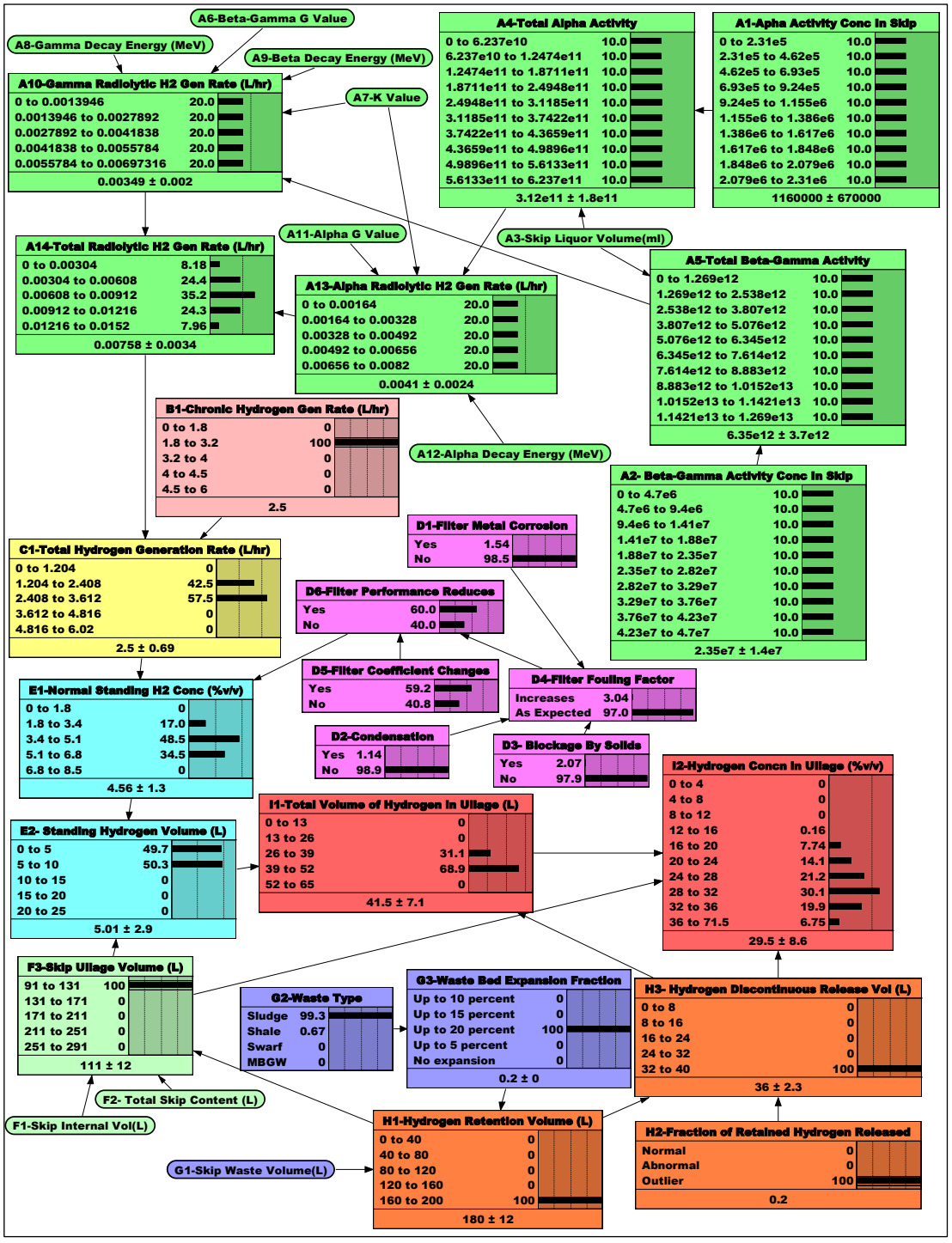

Figure D-10: **Updated BBN for conditions leading to a stoichiometric hydrogen concentration of 29.5%v/v**

APPENDIX E: BBN DATA FOR CASE STUDY 5

Table E-1: Criticality Handbook Data for 0% Pu-240 and 15% Pu240 compositions

Mass PuO_2 for 0% Pu-240 (100% Pu 239 make-up (kg)	Moderator mass for 0% Pu-240 make-up (kg)	Mass of Moderator/ Mass of PuO_2		Mass PuO2 for 15% Pu-240 make-up (kg)	Moderator mass for 15% Pu-240 (kg)	Mass of Moderator/ Mass of PuO_2
19.49062	0	0		22.69375	0	0
20.30547	0.073948	0.003642		23.50938	0.085615	0.003641738
20.8875	0.166308	0.007962		24.325	0.193678	0.007962097
21.81875	0.277414	0.012714		25.4125	0.323107	0.012714491
22.28438	0.400386	0.017967		26.5	0.476129	0.017967132
22.6918	0.540141	0.023803		27.5875	0.656676	0.023803389
23.21562	0.704043	0.030326		27.85938	0.844871	0.030326267
23.44844	0.883173	0.037664		28.40312	1.069789	0.037664489
23.68125	1.088891	0.045981		28.675	1.31851	0.045981168
23.68125	1.313976	0.055486		29.21875	1.621229	0.055485912
23.44844	1.558218	0.066453		29.7625	1.977806	0.066452953
22.75	1.802888	0.079248		30.57812	2.423249	0.079247809
22.51719	2.124925	0.094369		30.98594	2.924113	0.094369027
21.81875	2.454925	0.112514		30.85	3.471072	0.112514489
21.0039	2.829063	0.134692		31.9375	4.301734	0.134692258
20.42188	3.316809	0.162414		31.9375	5.187113	0.162414497
19.025	3.768041	0.198057		31.9375	6.325456	0.198057331
17.62812	4.329134	0.245581		32.48125	7.976783	0.245581158
16.23125	5.066008	0.312114		31.9375	9.968156	0.312114474
13.90312	5.726897	0.411915		31.39375	12.93154	0.411914473
12.97188	6.268015	0.4832		30.03438	14.512618	0.483200186
11.60411	6.710051	0.578248		28.675	16.581256	0.578247812
10.29453	7.322648	0.711314		26.5	18.849834	0.711314491
8.548438	7.786896	0.910914		22.42188	20.424415	0.910914473
8.199219	7.899462	0.963441		21.60625	20.816343	0.96344081
7.966407	8.140102	1.021803		21.0625	21.521734	1.021803395
7.617188	8.280128	1.087032		19.975	21.713467	1.08703214
7.267968	8.433855	1.160414		18.8875	21.917329	1.160414507
6.860547	8.531647	1.243581		17.8	22.135745	1.24358118
6.453125	8.638339	1.338629		16.7125	22.371833	1.338628751
6.103906	8.840282	1.448299		15.89688	23.023437	1.4482991
5.667383	8.9332	1.576248		14.5375	22.914703	1.576247842
5.230859	9.036099	1.72746		13.45	23.234336	1.727459926
4.823438	9.207531	1.908915		12.09062	23.07996	1.908914514
4.357812	9.285156	2.130692		10.73125	22.864991	2.130692231
4.008594	9.652352	2.407915		9.371875	22.566674	2.407914532

Mass PuO_2 for 0% Pu-240 (100% Pu 239 make-up (kg)	Moderator mass for 0% Pu-240 make-up (kg)	Mass of Moderator/ Mass of PuO_2		Mass PuO2 for 15% Pu-240 make-up (kg)	Moderator mass for 15% Pu-240 (kg)	Mass of Moderator/ Mass of PuO_2
3.542969	9.793982	2.764343		8.0125	22.149299	2.764343089
3.048242	9.875027	3.239581		6.789062	21.993717	3.239581109
2.597168	10.14172	3.904915		5.429688	21.202467	3.904914426
2.116992	10.37943	4.902915		4.274219	20.95613	4.902914427
1.680469	11.03438	6.566248		3.11875	20.478485	6.566247695
1.418554	11.2022	7.896915		2.642969	20.8713	7.896914417
1.214844	12.01835	9.892915		2.099219	20.767394	9.89291446
1.112989	12.24489	11.0018		1.946289	21.412689	11.00180343
1.040235	12.88634	12.38791		1.793359	22.215978	12.38791452
0.95293	13.50307	14.17006		1.623438	23.00421	14.17005762
0.865625	14.32285	16.54625		1.453516	24.050236	16.54624786
0.843799	15.23763	18.05836		1.419531	25.634415	18.05836928
0.807422	16.04583	19.87291		1.351562	26.859476	19.87291445
0.792871	16.58959	20.92345		1.351562	28.279327	20.92344043
0.774683	17.11328	22.09068		1.283594	28.35548	22.09069223
0.76377	17.86859	23.39526		1.283594	30.030025	23.39526751
0.749219	18.62776	24.86291		1.283594	31.913888	24.8629146
0.749219	19.87396	26.52624		1.283594	34.048933	26.52624818
0.749219	21.29819	28.42719		1.283594	36.488984	28.4272005
0.734668	22.49598	30.62061		1.283594	39.304427	30.62060667
0.734668	24.37598	33.17958		1.283594	42.589111	33.17958093
0.749219	27.12459	36.20381		1.351562	48.931712	36.20382343
0.77832	31.00277	39.83294		1.419531	56.544057	39.83291453
0.807422	35.74333	44.26846		1.521484	67.353769	44.26847013
0.865625	43.1193	49.81291		1.759375	87.639596	49.81291425
0.894727	46.91877	52.43921		1.827344	95.824513	52.43923038
0.95293	52.75168	55.35735		2.099219	116.20722	55.35735909
1.069337	66.60677	62.28791		2.659961	165.683423	62.28791437
1.214844	80.72183	66.44625		3.11875	207.229235	66.4462477
1.367626	97.3731	71.19863		4.20625	299.479232	71.19862871
1.622266	124.3988	76.68215		5.8375	447.632023	76.68214527
2.05879	171.0434	83.07958		11.275	936.722277	83.07958111
2.786328	252.5533	90.64019		30.85	2796.24978	90.64018723
4.590625	457.7446	99.71291				
13.67031	1514.695	110.8018				

Table E-1 (Continued): Criticality Handbook Data for 0% Pu-240 and 15% Pu240 compositions

Range for Ratio of Mass of Moderator: Mass of PuO_2	Trendline Equation for Nodes D and D1
	0% Pu-240 (100% P-u-239) – Node D
0 to 0.04	$y = 20.042e^{4.8139x}$ $R^2 = 0.9205$
0.04 to 14	$y = 22.147e^{-0.882x}$ $R^2 = 0.9636$
14 to 80	$y = 0.0004x^2 – 0.0292x + 1.2278$ $R^2 = 0.9771$
>80	$y = 0.0212x^2 – 3.711x + 164.12$ $R^2 = 0.9908$
	15%w/o Pu-240 – Node D1
0 to 0.055	$y = 117.92x + 23.641$ $R^2 = 0.9002$
0.055 to 1	$y = 33.809e^{-0.402x}$ $R^2 = 0.8243$
1 to 25.8	$y = 25.783e^{-0.279x}$ $R^2 = 0.9$
25.8 to 55	$y = 0.0013x^2 – 0.0797x + 2.4654$ $R^2 = 0.9638$
>55	$y = 0.0461x^2 – 6.0964x + 203.01$ $R^2 = 0.9625$

Table E-2: Trendline equations for critical mass curves

Node E- ratio of mass to critical mass (0% Pu-240)	Probability of criticality	E1 Node E- ratio of mass to critical mass (> 15% Pu-240)	Probability of criticality
0 to 1	0	0	0
1 to 1.05	0.0002	1	0.0008
1.05 to 1.1	0.0335	1.05	0.134
1.1 to 1.15	0.0668	1.1	0.2672
1.15 to 1.2	0.1001	1.15	0.4004
1.2 to 1.25	0.1334	1.2	0.5336
1.25 to 1.3	0.1667	1.25	0.6668
>1.3	0.2	1.3	0.8

Table E-3: Probability of criticality as a function of Node E and E1

Table E-4: CPT for the probability of criticality (Node F)

Criticality occurs-True	Criticality occurs-False	E- Ratio of mass of PuO_2 to Critical mass (0% Pu-240)	E1- Ratio of mass of PuO_2 to Critical mass (15%w/o Pu-240)
0	1	0 to 1	0 to 1
0.0008	0.9992	0 to 1	1 to 1.05
0.134	0.866	0 to 1	1.05 to 1.1
0.2672	0.7328	0 to 1	1.1 to 1.15
0.4004	0.5996	0 to 1	1.15 to 1.2
0.5336	0.4664	0 to 1	1.2 to 1.25
0.6668	0.3332	0 to 1	1.25 to 1.3
0.8	0.2	0 to 1	1.3 to 3.01e7
0.0002	0.9998	1 to 1.05	0 to 1
0.001	0.999	1 to 1.05	1 to 1.05
0.1342	0.8658	1 to 1.05	1.05 to 1.1
0.2674	0.7326	1 to 1.05	1.1 to 1.15
0.4006	0.5994	1 to 1.05	1.15 to 1.2
0.5338	0.4662	1 to 1.05	1.2 to 1.25
0.667	0.333	1 to 1.05	1.25 to 1.3
0.8002	0.1998	1 to 1.05	1.3 to 3.01e7
0.0335	0.9665	1.05 to 1.1	0 to 1
0.0343	0.9657	1.05 to 1.1	1 to 1.05
0.1675	0.8325	1.05 to 1.1	1.05 to 1.1
0.3007	0.6993	1.05 to 1.1	1.1 to 1.15
0.4339	0.5661	1.05 to 1.1	1.15 to 1.2
0.5671	0.4329	1.05 to 1.1	1.2 to 1.25
0.7003	0.2997	1.05 to 1.1	1.25 to 1.3
0.8335	0.1665	1.05 to 1.1	1.3 to 3.1e7
0.0668	0.9332	1.1 to 1.15	0 to 1
0.0676	0.9324	1.1 to 1.15	1 to 1.05
0.2008	0.7992	1.1 to 1.15	1.05 to 1.1
0.334	0.666	1.1 to 1.15	1.1 to 1.15
0.4672	0.5328	1.1 to 1.15	1.15 to 1.2
0.6004	0.3996	1.1 to 1.15	1.2 to 1.25
0.7336	0.2664	1.1 to 1.15	1.25 to 1.3
0.8668	0.1332	1.1 to 1.15	1.3 to 3.1e7
0.1001	0.8999	1.15 to 1.2	0 to 1
0.1009	0.8991	1.15 to 1.2	1 to 1.05
0.2341	0.7659	1.15 to 1.2	1.05 to 1.1
0.3673	0.6327	1.15 to 1.2	1.1 to 1.15
0.5005	0.4995	1.15 to 1.2	1.15 to 1.2
0.6337	0.3663	1.15 to 1.2	1.2 to 1.25

Criticality occurs-True	Criticality occurs-False	E- Ratio of mass of PuO_2 to Critical mass (0% Pu-240)	E1- Ratio of mass of PuO_2 to Critical mass (15%w/o Pu-240)
0.7669	0.2331	1.15 to 1.2	1.25 to 1.3
0.9001	0.0999	1.15 to 1.2	1.3 to 3.01e7
0.1334	0.8666	1.2 to 1.25	0 to 1
0.1342	0.8658	1.2 to 1.25	1 to 1.05
0.2674	0.7326	1.2 to 1.25	1.05 to 1.1
0.4006	0.5994	1.2 to 1.25	1.1 to 1.15
0.5338	0.4662	1.2 to 1.25	1.15 to 1.2
0.667	0.333	1.2 to 1.25	1.2 to 1.25
0.8002	0.1998	1.2 to 1.25	1.25 to 1.3
0.9334	0.0666	1.2 to 1.25	1.3 to 3.01e7
0.1667	0.8333	1.25 to 1.3	0 to 1
0.1675	0.8325	1.25 to 1.3	1 to 1.05
0.3007	0.6993	1.25 to 1.3	1.05 to 1.1
0.4339	0.5661	1.25 to 1.3	1.1 to 1.15
0.5671	0.4329	1.25 to 1.3	1.15 to 1.2
0.7003	0.2997	1.25 to 1.3	1.2 to 1.25
0.8335	0.1665	1.25 to 1.3	1.25 to 1.3
0.9667	0.0333	1.25 to 1.3	1.3 to 3.01e7
0.2	0.8	1.3 to 7.79182e5	0 to 1
0.2008	0.7992	1.3 to 7.79182e5	1 to 1.05
0.334	0.666	1.3 to 7.79182e5	1.05 to 1.1
0.4672	0.5328	1.3 to 7.79182e5	1.1 to 1.15
0.6004	0.3996	1.3 to 7.79182e5	1.15 to 1.2
0.7336	0.2664	1.3 to 7.79182e5	1.2 to 1.25
0.8668	0.1332	1.3 to 7.79182e5	1.25 to 1.3
1	0	1.3 to 7.79182e5	1.3 to 3.01e7

Table E-4 (Continued): CPT for probability of criticality (Node F)

APPENDIX F: BBN DATA FOR CASE STUDY 6

Table F-1: Derivation of BBN child node failure probabilities and frequencies

Node ID	Parent Node Boolean Logic	Derivation of frequency or failure probability
Frequency of Pneumercator blockage (Child Node 7)	Node 1: Salt crystallisation OR Node 2: Pneumercator valve fails	It is considered that a blockage of the pneumercator pipe (Node 7) could occur due to the dissolved salts in the vessel liquor crystallising (Node 1) or if there is a failure in the pneumercator control valve (Node 2). Blockage of pneumercator dip legs is a known occurrence in chemical plants, particularly where the pneumercator dips into the liquor with soluble salts. Plant operational experience shows that a blockage of the pneumercator due to crystallisation of salts occurs around once every five years. This would equate to a frequency of 0.19/yr. Node 2 models the likelihood of a loss of air supply due to the Pneumercator Control Valve (PCV) failure. Failure rates for control valves have been reported as 0.25-0.3/yr by the *IAEA, 1997*. To ensure a reasonable level of conservatism, the failure rates of 0.19/yr and 0.3/yr are taken as the mean values, such that the maximum failure rates for nodes 1 and 2 are 0.38/yr and 0.6/yr respectively. Node 7 models the likelihood of the pneumercator blockage which can occur either due to parent node 1 or node 2. If the relationship between nodes 1, 2 and 7 is modelled in a Fault Tree, nodes 1 and 2 would be represented by an OR gate to estimate the likelihood of Node 3. Based on the methodology for modelling OR gates discussed in Section 9.4, the application of an OR gate to nodes 1 and 2, which are both frequencies, results in a maximum frequency of 0.38+0.6 for node 7, i.e., 0.98/year. Hence with node 7 discretised over the interval 0 to 0.98/year, Netica generates the CPT for node 7 as presented in Table F-2.
Failure probability of Pneumercator protective measures (Child node 6)	Node 4: Liquor density instruments fail OR Node 3: Supervisory check failure OR	During periods when the liquor is left undisturbed in the vessels and no liquor movements are taking place, normal operations require that the operators periodically monitor the output from the level, density and specific gravity instruments. Any blockage in the pneumercator lines will be revealed by the density instrument. Parent node 4 models the likelihood of a failure of the density instrument. Given that the density instrument performs an important function in revealing pneumercator blockage, it is expected that its performance will be equivalent to at least a Safety Integrity Level (SIL) of SIL 1, i.e., a probability of failure on demand of 0.1-0.01, in accordance with the standard *IEC 61508,2010* for functional safety. A failure probability mid-range between 0.1 and 0.01 is used as the mean in this case. Hence a mean value of 5% chance is applied

Node ID	Parent Node Boolean Logic	Derivation of frequency or failure probability
	Node 5: Operators fail to monitor density	throughout the assessment, to avoid over-conservatism. This probability is expressed as a continuous node, discretised over the range 0 to 0.1. Parent node 5 models the probability of failure to take density measurements. Operational experience and human performance in different working conditions shows that if the task conditions are difficult, then the chances of human error are high. For such conditions, a conservative human error probability (HEP) of 0.1 is commonly applied in nuclear safety cases [*HSE, 2017*]. In this case study the operator is required to take density readings in the control room, so the task can be performed without any environmental constraints. Hence a mean HEP value half the maximum, i.e., 0.05 is considered appropriate in node 5. This probability is expressed as a continuous node, discretised over the range 0 to 0.1 so that the mean is 0.05. Supervisory checks are also undertaken to ensure that the operator has correctly monitored the density and confirm whether a blockage has occurred (node 3). Thus, a failure in the supervisory check would potentially lead to a blockage not being revealed. Similar to node 5, a mean value of 5% chance for a failure to carry out supervisor checks is considered appropriate in node 3. This probability is expressed as a continuous node, discretised over the range 0 to 0.1, so that the mean is 0.05. Operational procedures also require that upon detection of a blockage and a loss of flow in the pneumercator, air supplies to the ancillary vessels is reinstated before the hydrogen in air concentration in the ullage reaches 4%v/v (Node 6). This would be achieved by directing the input air to the vessel via the back-up pneumercator dip leg which is not blocked. Taking into consideration this protective measure (Node 6), this case study assesses whether the risk is still significant enough to warrant the installation of a new pneumercator supply system. The likelihood of occurrence of Node 6, i.e., a failure to reinstate the pneumercator air supply, is either due to Node 4 or due to Node 5, or Node 3. Using the probabilities for nodes 3, 4 and 5 as discussed above, the CPT for node 6 is automatically calculated by Netica using equation 9-5.
Frequency of failure of hydrogen dilution system (Child node 8)	Node 7: Frequency of Pneumercator blockage AND Node 6:	As shown in Figure 9-2, the potential for a flammable atmosphere forming (Node 18) in the vessel ullage space is dependent on the failure frequency of the hydrogen dilution system, i.e., the pneumercator air supply system (Node 8). This frequency is dependent on the frequency of pneumercator blockage (Node 7) AND the failure probability of the pneumercator protective measures (Node 6).

Node ID	Parent Node Boolean Logic	Derivation of frequency or failure probability
	Failure probability of Pneumercator protective measures	In accordance with the Boolean rule number (ii), as listed in Section 9.4, a frequency AND a probability yield the result as a frequency. Thus equation 9-6 was applied to nodes 6 and 7 to calculate the failure frequency of the hydrogen dilution system (Node 8). Since the maximum value for Node 8 equates to the maximum value for Node 6 (0.45/yr) x the maximum for Node 7 (0.15), i.e., 0.075, the discretisation for Node 8 was based on the range 0 to 0.075/yr. Hence using this discretisation and equation 9-6, the CPT for Node 8 was calculated by Netica. This CPT is presented in Table F-3.
Frequency of failure of failure of hydrogen removal system (Child Node 17)	Node 16: Failure to restore extract system AND Node 15: Failure of vent extract system	In addition to the failure of the hydrogen dilution system, the frequency of a flammable atmosphere forming is also affected by the frequency of the hydrogen removal system, i.e., the vent extract system (Node 17). Figure 9-2 shows that the vent extract system could fail either due to a mechanical failure of the vent extract fan (Node 9), a loss of power supply to the fan (Node 12), the vent duct damper failure (Node 13) or due to an inadvertent isolation of the duct (Node 14). Each of these four events is denoted by a frequency, hence an OR gate was applied to these events to determine the overall failure frequency of the vent extract system. In accordance with the IAEA database for generic failure rates of plant components in nuclear power stations *(IAEA, 1997*), the failure rates for vent fans, high voltage power supply and dampers are 0.013/yr, 0.145/yr and 0.041/yr respectively. These values are taken as the mean, so that the maximum values for nodes 9,11 and 13 are 0.026, 0.29 and 0.082, respectively. In the event of a loss of the mains power, the operators are required to start the back-up diesel generators for the fan (Node 10). Using a mean failure rate of 0.96/yr for diesel generators *(IAEA, 1997*) and a standard proof test interval of 1 year for standby equipment, the failure probability of the diesel generator was calculated as 0.357 for Node 10, using the following unrevealed failure equation 2-10 from Chapter 2: $$P = 1 - \left(\frac{1-e^{-\lambda sTs}}{\lambda sTs}\right)$$ Where λs = Failure rate of standby equipment (per yr) and Ts is Proof test interval for standby equipment (years). To ensure a reasonable level of conservatism, the value of 0.357 for Node 10 was taken as the median, with a maximum of twice this value i.e., 0.72. To calculate the overall frequency of power supply failure (Node 12), an AND gate logic was applied between the failure probability of the back-up power supply system (Node 10) and the frequency of mains power supply failure (Node 11). Since the maximum value for Node 12 is 0.72 x 0.29, i.e., 0.208/yr, the discretisation intervals were set in the range 0 and 0.208/yr for this variable.

Node ID	Parent Node Boolean Logic	Derivation of frequency or failure probability
		In accordance with Figure 9-2, the failure frequency of the ventilation extract system (Node 15) was calculated by applying an OR gate between the frequencies for loss of power supply to the fan (Node 12), the vent duct damper failure (Node 13), inadvertent isolation of the duct (Node 14) and mechanical failure of vent fan (Node 9). The frequency for inadvertent duct isolation (Node 14) was based on the understanding that this fault occurs each time a maintenance activity is carried out on the duct. Using a realistic duct maintenance frequency of once per year as the mean value and a worst case operator error probability of 0.05, the mean frequency of accidental duct isolation is 0.05 x 1, i.e., 0.05/yr. For reasonable level of conservatism, the maximum value for Node 14 is taken as twice the mean, i.e., 0.1/yr. Thus, applying the OR gate to nodes 12, 13, 14 and Node 9, an overall failure frequency of the vent extract system (Node 15) was calculated. This frequency was based on the discretisation range of 0 to 0.408/yr using the maximum values for each node. For a failure of the hydrogen removal system to occur (Node 17), the vent extract system (Node 15) needs to fail, and the operators would need to fail to restore the system (Node 16). Assuming that spare parts are readily available, and the plant maintenance team is well trained to restore the system, a realistic human error probability of 0.01 for a failure to restore the system is considered reasonable for Node 16. However, to allow a reasonable level of conservatism, this value is taken as the median such that a maximum human error probability for Node 16 is 0.02. By applying an AND gate between nodes 15 and 16, using equation 9-6, the frequency of failure of the hydrogen removal system (Node 17) was calculated by Netica. This frequency was based on the discretisation range of 0 to 0.005/yr using the maximum values for nodes 15 and 16.
Total frequency of flammable atmosphere arising in vessel ullage (Child node 18)	Node 8: Hydrogen dilution system failure frequency OR Node 17: Failure frequency of hydrogen removal system	The potential for a flammable hydrogen concentration in the ullage (Node 18) arises if the hydrogen dilution system fails (Node 8) or if there is failure of the hydrogen removal system (Node 17). Therefore, the overall frequency for Node 18 was calculated by applying an OR gate between Nodes 8 and 17. Hence equation 9-3 was applied to these two nodes to calculate the CPT for Node 18. This frequency was based on the discretisation range of 0 to 0.24/yr using the maximum values for nodes 8 and 17.

Node ID	Parent Node Boolean Logic	Derivation of frequency or failure probability
Frequency of hydrogen explosion in vessel ullage (Child node 21)	Node 1: Ignition probability AND Node 18: Total frequency of flammable atmosphere arising in vessel ullage	The likelihood of ignition of hydrogen depends on the ignition probability (Node 20) and the frequency of a flammable atmosphere developing in the vessel ullage space (Node 18). The vessel internals are not exposed to any mechanical impacts or any moving parts and the vessel is held in a quiescent state. However, liquor transfers still take place such that the potential for ignition e.g., due to static discharge generated from this activity is considered credible. Predominantly a relatively high ignition probability of up to 0.1 during liquor transfers is therefore considered realistic (Node 20). However, to allow a reasonable level of conservatism in the assessment, the maximum value for the ignition probability is set to 1. Given the regularity of liquor transfers, a 90% probability for this condition is considered plausible (Node 19). For the condition when no liquor transfers take place, only low energy ignition sources are deemed possible. Hence predominantly a low ignition probability in the range 0 to 0.002 is applied for this this condition. Accordingly, the ignition probability in Node 20 was based on the discretisation range of 0 to 1 using the minimum and maximum values for nodes 19 and 20. The CPT for the ignition probability is given in Table F-5. To calculate the frequency of a hydrogen explosion (Node 21), an AND gate was applied to Node 18 (frequency) and Node 20 (probability) using equation 9-6. The frequency for Node 21 was based on the discretisation range of 0 to 0.008/yr using the maximum values for nodes 18 and 20.
Mitigating Systems failure (Child Node 24)	Node 22: Activity in air monitors fail OR Node 23: Operators fail to evacuate	In the event of an ignition of the flammable hydrogen in air mixture in the ancillary vessel, any consequences to the workforce in the adjacent operating areas will be mitigated by the activity in air alarms, which will provide a warning to the operators to evacuate. Hence for a complete loss of the mitigating systems (Node 24) a failure of either the activity in air alarms would need to occur (Node 22) or the operator would need to fail to evacuate (Node 23) even if the alarms are functional. In accordance with the generic component reliability data (*IAEA,1997),* activity in air alarms fail at a rate of 0.63/y. Given that a failure of the alarms would not be revealed to the operators until a routine proof test is carried out, their probability of failure can be calculated using the unrevealed failure equation 2-10 i.e. $= 1-[(1-EXP(-0.63x1))/(0.63x1)] = 0.258$ To allow a reasonable level of conservatism, the value of 0.258/yr for Node 22 is taken as the mean, such that the maximum is twice this value, i.e., 0.52/yr. To calculate the probability of failure of the mitigating system (Node 24), an OR gate is applied, using equation 9-3, to Node 22 (probability) and Node 23 (probability). This probability is based on the discretisation range of 0 to 1 using the maximum values for nodes 22 and 23. .

Node ID	Parent Node Boolean Logic	Derivation of frequency or failure probability
Radiological risk of hydrogen explosion in the vessel (Node 25)	Node 21: Frequency of hydrogen explosion in vessel ullage AND Node 24: Mitigating systems failure probability	For the hydrogen explosion model, it is considered that an overpressure in the vessel would occur and the resultant turbulence in the vessel would lead to a significant amount of radioactivity from the liquor surface becoming airborne. The vessel pressurisation will lead to the airborne radioactivity being released into the operating areas via the vessel penetrations. The activity in air alarms will provide an audible warning. However, it is considered that by the time the increased airborne activity levels are detected in the operating areas, given the high dose rates, it is highly likely that significant dose uptake will have already taken place before the operators evacuate the area. Therefore, a maximum probability of 90% for a failure to evacuate before receiving a high dose, is considered possible. To calculate the radiological risk, i.e., the Top Event frequency, a hydrogen explosion would need to occur, and the mitigation systems would also need to fail. Hence equation 9-6 for AND gate is applied to derive the CPT for Node 25.

Node 7: Pneumercator blockage (per yr)			Node 1: Salt crystallisation (per yr)	Node 2: Pneumercator valve fails (per yr)
CPT for 0 to 0.15 per yr range	CPT for 0.15 to 0.3 per yr range	CPT for 0.3 to 0.97 per yr		
0.438	0.549	0.0135	0 to 0.127	0 to 0.2
0	0.199	0.8011	0 to 0.127	0.2 to 0.4
0	0	1	0 to 0.127	0.4 to 0.6
0.01	0.535	0.4545	0.127 to 0.25	0 to 0.2
0	0	1	0.127 to 0.25	0.2 to 0.4
0	0	1	0.127 to 0.25	0.4 to 0.6
0	0.041	0.9586	0.253 to 0.38	0 to 0.2
0	0	1	0.253 to 0.38	0.2 to 0.4
0	0	1	0.253 to 0.38	0.4 to 0.6

Table F-2: CPT for frequency of Pneumercator blockage

Node 8: Hydrogen dilution system fails (per yr)					Node 7: Pneumercator Blockage (per yr)	Node 6: Pneumercator protective measures fail
0 to 0.0406	0.0406 to 0.0812	0.0812 to 0.1218	0.1218 to 0.1624	0.1624 to 0.2339		
1	0	0	0	0	0 to 0.15	0 to 0.05
1	0	0	0	0	0 to 0.15	0.05 to 0.1
1	0	0	0	0	0 to 0.15	0.1 to 0.24
1	0	0	0	0	0.15 to 0.3	0 to 0.05
1	0	0	0	0	0.15 to 0.3	0.05 to 0.1
0.52	0.48	0	0	0	0.15 to 0.3	0.1 to 0.24
0.98	0.02	0	0	0	0.3 to 0.97	0 to 0.05
0.38	0.57	0.04	0	0	0.3 to 0.97	0.05 to 0.1
0.015	0.24	0.33	0.22	0.20	0.3 to 0.97	0.1 to 0.24

Table F-3: CPT for failure frequency of the hydrogen dilution system

CPT for Node 17: Hydrogen removal system fails (per yr)			Node 16: Probability of Failure to restore extract system	Node 15: Failure of vent extract system frequency (per yr)
0 to 0.00273	0.00273 to 0.005	0.0055 to 0.0082		
1	0	0	0 to 0.0067	0 to 0.027
1	0	0	0 to 0.0067	0.027 to 0.054
1	0	0	0 to 0.0067	0.054 to 0.081
1	0	0	0 to 0.0067	0.081 to 0.108
1	0	0	0 to 0.0067	0.108 to 0.4085
1	0	0	0.00667 to 0.013	0 to 0.027
1	0	0	0.00667 to 0.013	0.027 to 0.054
1	0	0	0.00667 to 0.013	0.054 to 0.081
0.5884	0.4116	0	0.00667 to 0.013	0.081 to 0.108
1	0	0	0.00667 to 0.013	0.108 to 0.4085
1	0	0	0.013 to 0.02	0 to 0.027
1	0	0	0.013 to 0.02	0.027 to 0.054
1	0	0	0.013 to 0.02	0.054 to 0.081
1	0	0	0.013 to 0.02	0.081 to 0.108
0.1869	0.5582	0.2549	0.013 to 0.02	0.108 to 0.4085

Table F-4: CPT for Node 17: Hydrogen removal system failure

Ignition probability range	CPT for Liquor transfer taking place	CPT for no liquor transfer
0 to 0.002	0.3	1
0.002 to 0.004	0.2	0
0.004 to 0.006	0.2	0
0.006 to 0.008	0.1	0
0.008 to 0.01	0.1	0
0.01 to 0.1	0.05	0
0.1 to 0.4	0.02	0
0.4 to 0.8	0.02	0
0.8 to 1	0.01	0

Table F-5: CPT for ignition probability

Risk of hydrogen explosion (per year)	Decision	Utility for summed detriment = £2.384E6	Decision	Utility for summed detriment = £2.384E6
1.00E-04	Install	-2.95E+05	Don't Install	-4.77E+03
2.00E-04	Install	-2.90E+05	Don't Install	-9.53E+03
3.00E-04	Install	-2.86E+05	Don't Install	-1.43E+04
4.00E-04	Install	-2.81E+05	Don't Install	-1.91E+04
5.00E-04	Install	-2.76E+05	Don't Install	-2.38E+04
6.00E-04	Install	-2.71E+05	Don't Install	-2.86E+04
7.00E-04	Install	-2.67E+05	Don't Install	-3.34E+04
8.00E-04	Install	-2.62E+05	Don't Install	-3.81E+04
9.00E-04	Install	-2.57E+05	Don't Install	-4.29E+04
1.00E-03	Install	-2.52E+05	Don't Install	-4.77E+04
0.0012	Install	-2.43E+05	Don't Install	-5.72E+04
0.0014	Install	-2.33E+05	Don't Install	-6.67E+04
0.0016	Install	-2.24E+05	Don't Install	-7.63E+04
0.002	Install	-2.05E+05	Don't Install	-9.53E+04
0.003	Install	-1.57E+05	Don't Install	-1.43E+05
0.004	Install	-1.09E+05	Don't Install	-1.91E+05
0.005	Install	-6.17E+04	Don't Install	-2.38E+05
0.006	Install	-1.40E+04	Don't Install	-2.86E+05
0.007	Install	3.36E+04	Don't Install	-3.34E+05
0.008	Install	8.13E+04	Don't Install	-3.81E+05
0.02	Install	6.53E+05	Don't Install	-9.53E+05
0.04	Install	1.61E+06	Don't Install	-1.91E+06
0.06	Install	2.56E+06	Don't Install	-2.86E+06
0.08	Install	3.51E+06	Don't Install	-3.81E+06
0.27	Install	1.26E+07	Don't Install	-1.29E+07

Table F-6: Decision utility values with changing risk of hydrogen explosion

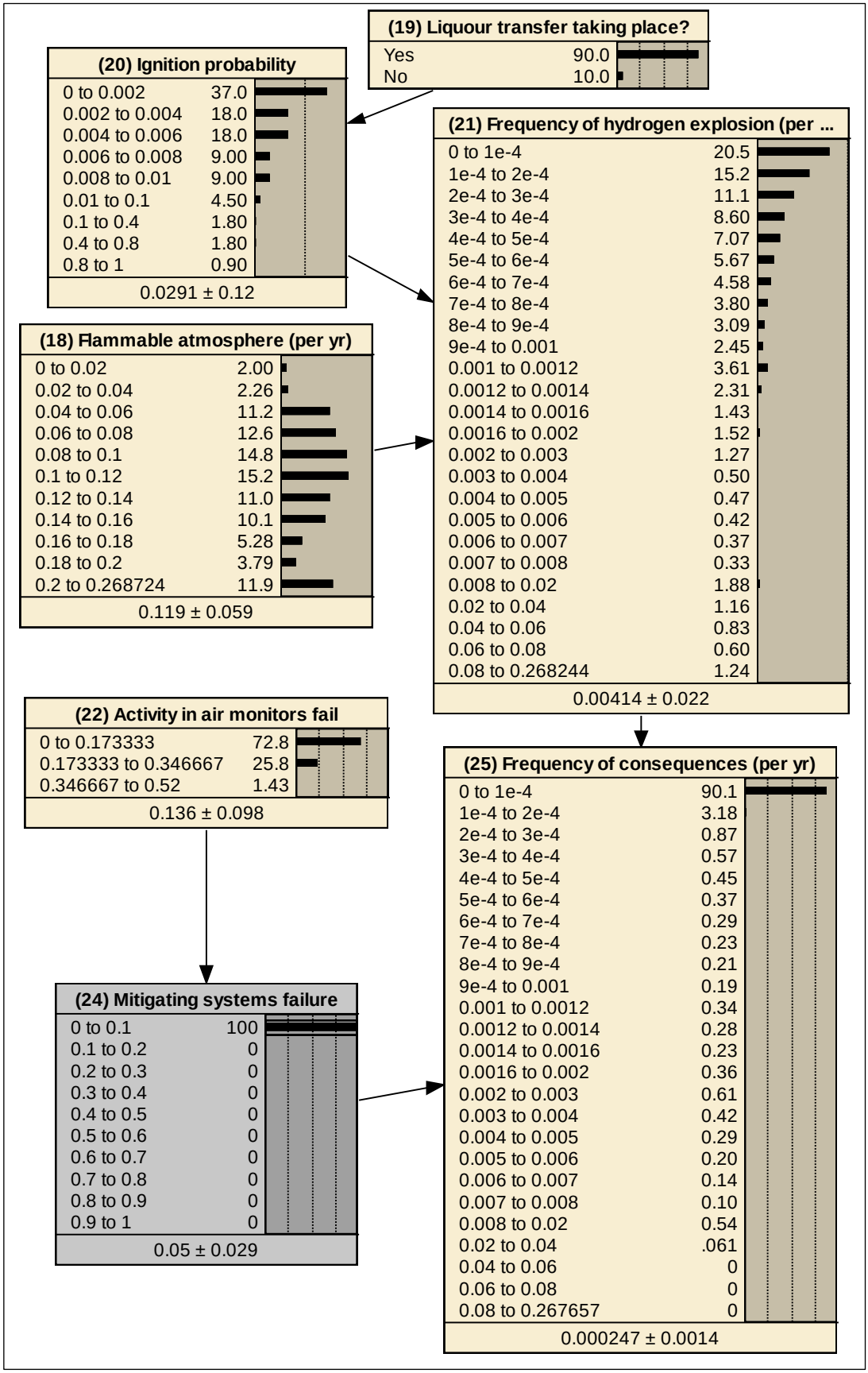

Figure F-1: Updated BBN results for radiological risk, with mitigating system failure probability range of 0 to 0.1

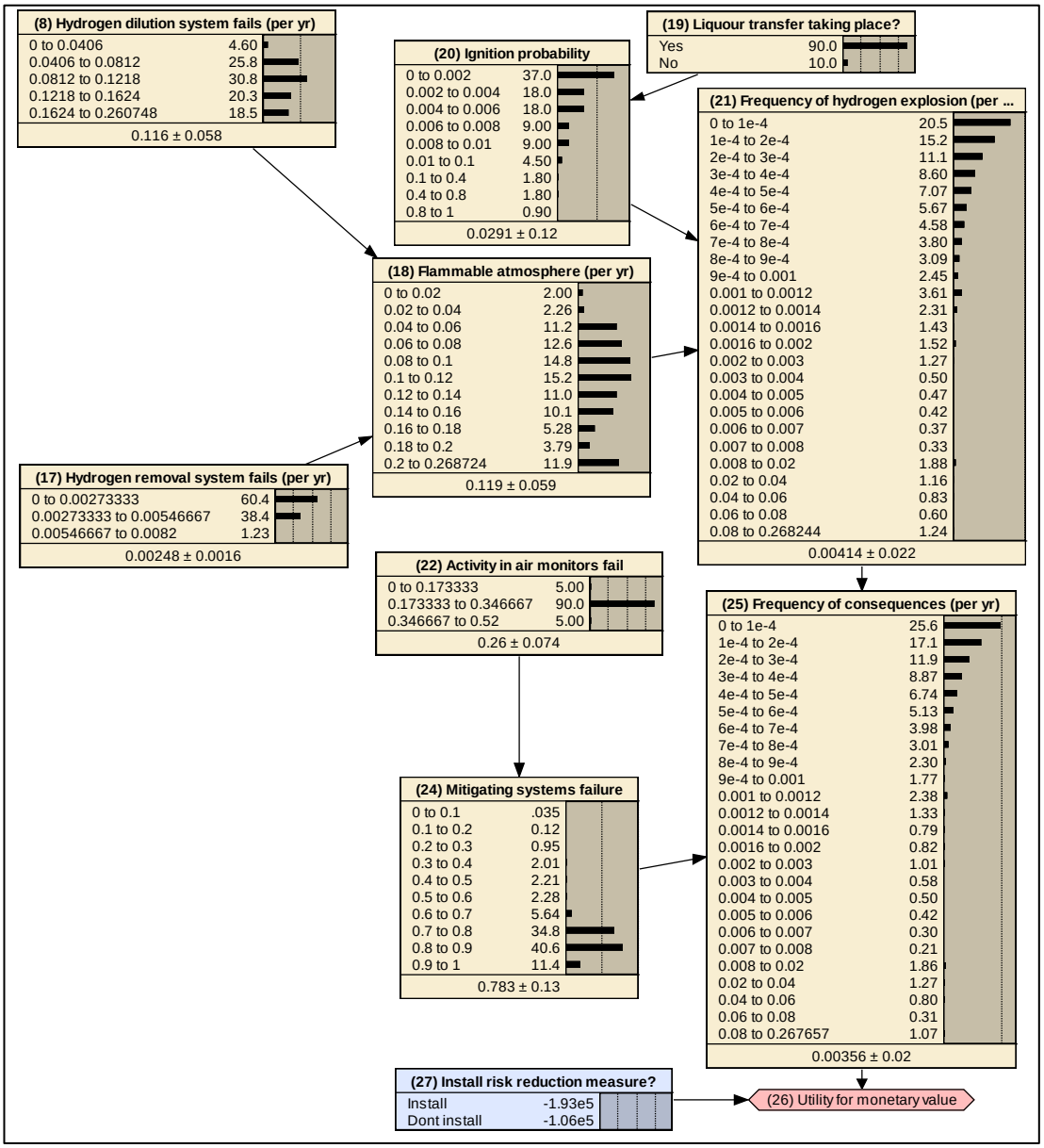

Figure F-2: Decision Network for installation of alternative compressed air system (Cost detriment = £1.192E6)

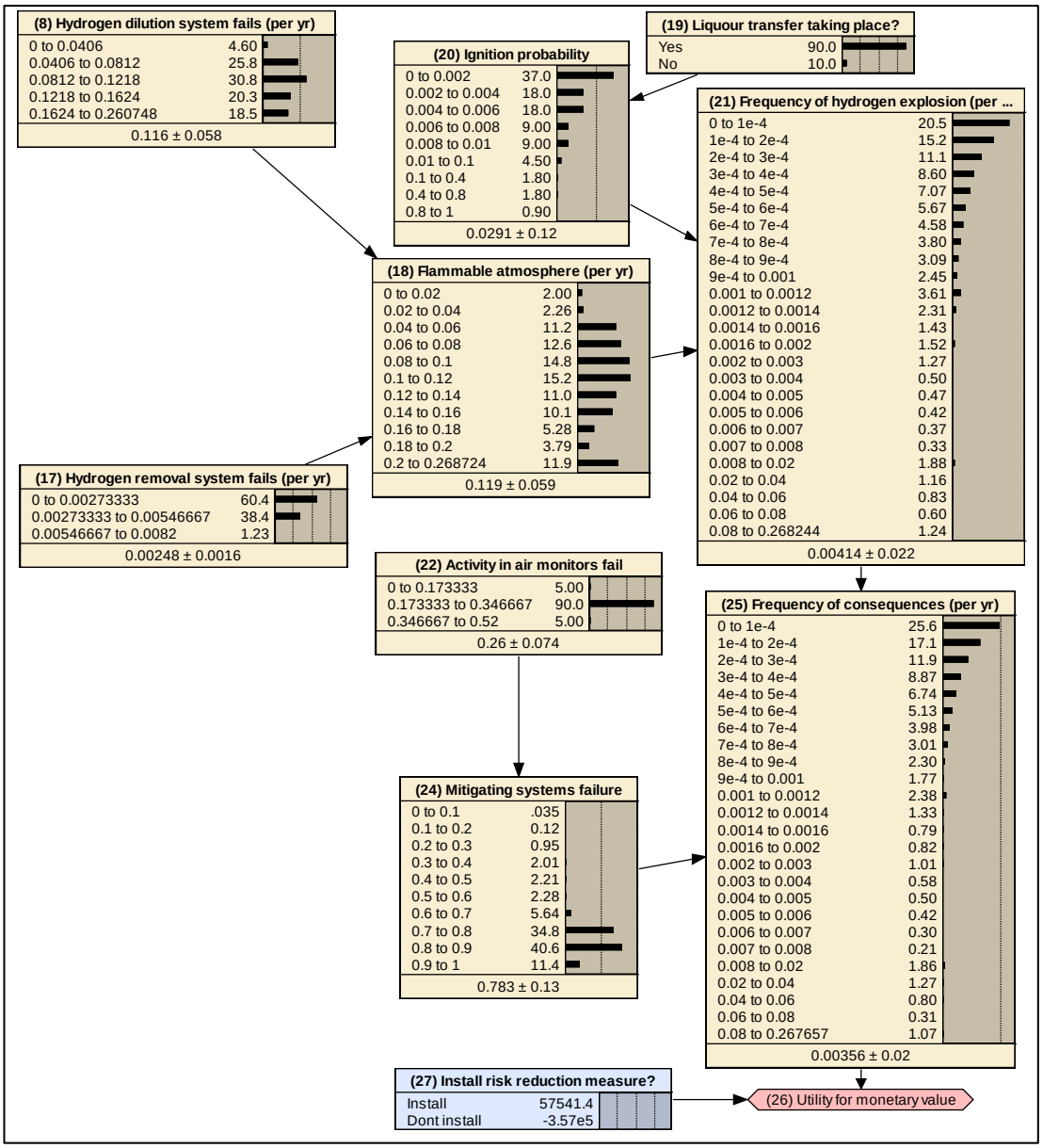

Figure F-3: Decision Network for installation of alternative compressed air system (Cost detriment = £3.576E6)

APPENDIX G: BBN DATA FOR CASE STUDY 7

Table G-1: Derivation of CPTs for robot failure modes

Child Node	Affecting Parent node nodes	Boolean equation for CPT	Equation No.
Derivation of the CPTs for failure modes leading robot equipment failure			
Child Node PW5 – Unable to tighten/untighten bolts from the skip	PW2 - Failure of air supply OR PW4 - Mechanical failure/damage to bolt removal tool OR PW11-Pneumatic leak or rupture	$p(PW5 \mid PW2, PW4, PW11) = or(PW2, PW4, PW11)$	(G-1)
Child Node PW13- Drill tool fails	PW2 - Failure of air supply OR PW11 – Pneumatic leak or rupture OR PW12 – Mechanical failure of drill tool	$p(PW13 \mid PW12, PW2, PW11) = or(PW12, PW2, PW11)$	(G-2)
Child Node PW7 – Failure to connect/ disconnect tools to gripper	PW2 - Failure of air supply OR PW11 – Pneumatic leak or rupture OR PW6- Mechanical failure of primary and secondary tools	$p(PW7 \mid PW6, PW2, PW11) = or(PW6, PW2, PW11)$	(G-3)
Child Node PW10- End effectors fail to open	PW9- Mechanical Failure of end effectors OR PW8- Hydraulic leak or rupture	$p(PW10 \mid PW9, PW8) = or(PW9, PW8)$	(G-4)
Child Node PW17 – Cutting tool fails	PW8 – Hydraulic leak or rupture OR PW16- Mechanical failure of cutting tool	$p(PW17 \mid PW16, PW8) = or(PW16, PW8)$	(G-5)
Child Node PW14- Failure to release waste on to WTT	A failure to release the waste on the Waste Treatment Table is one of the main causes that could lead to the hypothesis, i.e., a failure to process waste in the WPC. It is considered that if the cutting and drilling operations fail part way through the size reduction process, the waste items could potentially become jammed with the tools such that it may not be	$p(PW14 \mid PW10, PW13, PW17) = or(PW10, PW13, PW17)$	(G-6)

Child Node	Affecting Parent node nodes	Boolean equation for CPT	Equation No.
	possible to release the items on the WTT. This event could occur due to the following three parent nodes: PW10- End Effectors fail to open OR PW13- Drill tool fails to drill waste OR PW17 – Cutting tool fails		
Child Node PW15- Robot equipment failure	Node PW15 represents the inability to process waste in the WPC due to robot equipment failures, which is caused by the following Parents: PW14 – failure to release waste on to WTT OR PW5- Unable to tighten/untighten bolts OR PW7 – Failure to Connect/ disconnect tools to gripper OR PW3 – Gripper fails to open or close	$\mathrm{p}(\mathrm{PW15} \mid \mathrm{PW14}, \mathrm{PW5}, \mathrm{PW7}, \mathrm{PW3}) = \mathrm{or}(\mathrm{PW14}, \mathrm{PW5}, \mathrm{PW7}, \mathrm{PW3})$	(G-7)
Derivation of Conditional Probability Tables for failure Modes leading to loss of robot functionality			
RB22- Complete loss of robot functionality	The review meeting with SL Reliability Engineering team considered that a failure of either of the following components and services could lead to a complete loss of robot functionality, Node RB22, thus leading to a failure to process waste in the WPC: RB21- Loss of electrical power supply to robot OR RB5- Failure to start the motors for axes 1 to 6 OR RB4- Failure of axis 1-6 motor gearboxes OR RB11- Failure of resolvers for axes 1-6 OR RB8- Failure of arm brakes	$\mathrm{p}(\mathrm{RB22} \mid \mathrm{RB8}, \mathrm{RB11}, \mathrm{RB21}, \mathrm{RB5}, \mathrm{RB4}) = \mathrm{or}(\mathrm{RB8}, \mathrm{RB11}, \mathrm{RB21}, \mathrm{RB5}, \mathrm{RB4})$	(G-8)
Child Node RB8- Brake fails closed	RB6 - Control or Electrical failure of brake OR	$\mathrm{p}\,(\mathrm{RB8} \mid \mathrm{RB6}, \mathrm{RB7}) = \mathrm{or}(\mathrm{RB6}, \mathrm{RB7})$	(G-9)

Child Node	Affecting Parent node nodes	Boolean equation for CPT	Equation No.
	RB7- Mechanical failure of brake		
Child Node RB11, failure of resolver for Axis 1,2,3,4,5 or 6	RB 10 - Loss of signal to resolver for Axis 1,2,3,4,5 or 6 OR RB9 -Mechanical failure of resolver/shaft for Axis 1,2,3,4,5 or 6	$\mathrm{p}(\mathrm{RB11} \mid \mathrm{RB9}, \mathrm{RB10}) = \mathrm{or}(\mathrm{RB9}, \mathrm{RB10})$	(G-10)
Child Node RB4 – Motor gearbox fails	RB1- Mechanical failure of gearbox OR RB2- Failure of oil supply to the gearbox OR RB3 - Manufacturing defect associated with the gearbox	$\mathrm{p}(\mathrm{RB4} \mid \mathrm{RB1}, \mathrm{RB2}, \mathrm{RB3}) = \mathrm{or}(\mathrm{RB1}, \mathrm{RB2}, \mathrm{RB3})$	(G-11)
Child Node RB21 – Failure of Power Supply to Robot	*Common Cause Failure of Robot Equipment and Robotics Functionality* It is considered that the robot equipment, i.e., PW group of nodes, as well as the robotics functionality, RB group of nodes, all rely on the site electricity supply. Thus, a loss of site power supply from the source would also lead to the Top Event. Therefore, the BBN also models node PO1 for a loss of site power, as a parent to the Top Event.		
Top Event TE1 – Failure to Process Waste	Node TE1 represents the hypothesis being modelled, i.e., the likelihood of a failure to process waste within the Waste Processing Cell. As discussed above, this is caused by three parent nodes, i.e., either failures leading to a loss of site power (node PO1), or a loss of robot functionality (Node RB22) or robot equipment failure (Node PW15).	$\mathrm{p}\ (\mathrm{TE1} \mid \mathrm{PO1}, \mathrm{RB22}, \mathrm{PW15}) = \mathrm{or}(\ \mathrm{PO1}, \mathrm{RB22}, \mathrm{PW15})$	(G-12)

Table G-2: Derivation of robot primary node failure probabilities

Cause (primary node)	Effect	Failure rate of primary node (number per million hours) - A	Failure rate of primary node (per year) – B =A/114.1553	Repair time (yr) - C	Failure probability D = B x C	Justification	Reference
Primary/Secondary Equipment Failures							
PW12- Mechanical failure of Drill Tool	Drill Tool fails to drill waste	17	0.149	0.001	1.49E-04	Expert judgement based on failure rate knowledge of similar industry equipment.	Expert judgement of the SL Reliability Engineering SMEs
PW11- Pneumatic leak or rupture	Drill Tool fails to drill waste	4	0.035	0.001	3.50E-05	Nuclear specific, Hose, lightly stressed	*Dexter and Perkins, 1982*
PW9- Mechanical failure of End Effectors	Large and Small Grab End Effectors fail to open	2	0.018	0.001	1.80E-05	Rigid coupling	*NPRD11, 2011*
PW8- Hydraulic leak or rupture	Large and Small Grab End Effectors fail to open	4	0.035	0.001	3.50E-05	Nuclear specific, Hose, lightly stressed	*Dexter and Perkins, 1982*
PW1- Mechanical failure or damage to Gripper Tool	Gripper tool fails to open or close	2	0.018	0.001	1.80E-05	Expert judgement based on failure rate knowledge of similar industry equipment.	Expert judgement
PW2- Failure of air supply	Gripper tool fails to open or close	5.5	0.048	0.001	4.8E-05	Nuclear specific, Generic air supply system	*Dexter and Perkins, 1982*

Cause (primary node)	Effect	Failure rate of primary node (number per million hours) - A	Failure rate of primary node (per year) – B =A/114.1553	Repair time (yr) - C	Failure probability D = B x C	Justification	Reference
PW4- Mechanical failure or damage of Bolt Removal Tool	Unable to tighten/untighten bolts in fill port covers	2	0.018	0.001	1.80E-05	Expert judgement based on failure rate knowledge of similar industry equipment.	Expert judgement of the SL Reliability Engineering SMEs
PW6- Mechanical failure of primary and secondary tools	Failure to connect/disconnect tools to gripper/tool change interface	2	0.018	0.001	1.60E-05	Expert judgement based on failure rate knowledge of similar industry equipment.	Expert judgement of the SL Reliability Engineering SMEs
PW16- Mechanical failure of Cutting Tools	Cutting tool fails	17	0.149	0.001	1.49E-04	Expert judgement based on failure rate knowledge of similar industry equipment.	Expert judgement of the SL Reliability Engineering SMEs
Failures Leading to Loss of Site Power Supply							
PO1-Loss of site power supply	Loss of power from source to robot equipment and to robot unit for a duration of 24 hours.				1E-03	Expert judgement based on failure rate knowledge of power supplies unavailability of power supply	Expert judgement of the SL Reliability Engineering SMEs

Cause (primary node)	Effect	Failure rate of primary node (number per million hours) - A	Failure rate of primary node (per year) – B =A/114.1553	Repair time (yr) - C	Failure probability D = B x C	Justification	Reference
						for a duration of 24 hours.	
Failures Leading to Loss of Functionality							
RB1- Mechanical failure of Gearbox	Gearbox fails to transmit rotational force from motor to axis 1,2,3,4,5, or 6	14.8	0.779	0.001	7.79E-04	Aggressive environment for generic Gearbox	*NPRD11, 2011*
RB2- Failure of oil supply to Gearbox	Gearbox fails to transmit rotational force from motor to axis 1,2,3,4,5, or 6	4.0	0.210	0.001	2.10E-04	Nuclear specific, Hose, lightly stressed	*Dexter and Perkins, 1982*
RB3- Manufacturing defect in Gearbox	Gearbox fails to transmit rotational force from motor to axis 1,2,3,4,5, or 6	0.8	4.10E-2	0.001	4.10E-05	Generic gearbox	*NPRD11, 2011*
RB5- Failure to start Axis 1,2,3,4,5 or 6 Motor	Direct Loss of Robot Functionality	9.1	0.48	0.001	7.30E-04	Aggressive environment for generic motor	*NPRD11, 2011*
RB6-Control/Electrical failure of brake	Brake fails closed	7.6	0.399	0.001	3.99E-04	Aggressive environment for generic brake system	*NPRD11, 2011*
RB7-Mechanical failure of brake	Brake fails closed	4.3	0.225	0.001	2.25E-04	Generic braking system	*NPRD11, 2011*
RB10- Loss of signal to resolver for Axis 1,2,3,4,5 or 6	Failure of resolver for Axis 1,2,3,4,5 or 6	1.4	7.5E-2	0.001	7.5E-04	Nuclear specific electrical cable faults	*Dexter and Perkins, 1982*

Cause (primary node)	Effect	Failure rate of primary node (number per million hours) - A	Failure rate of primary node (per year) – B =A/114.1553	Repair time (yr) - C	Failure probability D = B x C	Justification	Reference
RB9-Mechanical Failure of resolver or shaft for Axis 1,2,3,4,5 or 6	Failure of resolver for Axis 1,2,3,4,5 or 6	0.02	1E-3	0.001	1E-06	Lightly stressed shaft	*Dexter and Perkins, 1982*
RB12-Electrical Failure of cables to resolvers	Loss of Cables-Resolvers	4.8	0.254	0.001	2.54E-04	Nuclear specific electrical power cable faults	*IEEE Standard 500,1984*
RB13- Mechanical damage to cables to Resolvers during routine operations	Loss of Cables-Resolvers	2.0	0.105	0.001	1.05E-04	Nuclear specific electrical power cable faults (low)	*IEEE Standard 500,1984*
RB15-Mechanical damage to In-Cell cables during routine operations	Loss of In-Cell Electrical Cables, Axis 1-3 or Axis 4-6	15.0	0.788	0.001	7.88E-04	Nuclear specific electrical power cable faults, (high)	*Dexter et al, 1982*
RB16-Electrical Failure of In-Cell Cables	Loss of In-Cell Electrical Cables, Axis 1-3 or Axis 4-6	4.8	0.254	0.001	2.54E-04	Nuclear specific electrical power cable faults	*IEEE Standard 500,1984*
RB19-Mechanical damage to Out-Cell cables during routine operations	Loss of Out-Cell Electrical Cables, Axis 1-3 or Axis 4-6	0.03	2E-3	0.001	2E-06	Nuclear specific electrical cable faults, (low)	*Dexter et al, 1982*
RB18-Electrical Failure of Out-Cell cables	Loss of Out-Cell Electrical Cables, Axis 1-3 or Axis 4-6	1.4	7.50E-2	0.001	7.5E-05	Nuclear specific electrical cable faults	*Dexter et al, 1982*

Table G-2 (continued): Derivation of robot primary node failure probabilities

Table G-3: Comparison of BBN Results with Fault Tree Analysis

Node ID	Cause (primary node)	Fault Tree Results (Percent Probability)	BBN Prior Percent Probability	BBN Updated Posterior Percent Probability
Failures leading to loss of functionality of robot end effector and secondary tool equipment				
PW1	Mechanical failure or damage to Gripper Tool	1.8E-03	0.002	0.35
PW2	Failure of air supply	4.8E-03	0.005	0.93
PW3	Gripper tool fails to open or close	0.11	0.11	21.3
PW4	Mechanical failure or damage of Bolt Removal Tool	2E-03	0.002	0.35
PW5	Unable to tighten/ untighten bolts	0.11	0.11	21.3
PW6	Mechanical failure of primary and secondary tools	1.8E-03	0.002	0.35
PW7	Failure to connect/ disconnect tools	0.11	0.11	21.3
PW8	Hydraulic leak or rupture	3.5E-03	0.003	0.68
PW9	Mechanical failure of End Effectors	1.8E-03	0.002	0.35
PW10	End effectors fail to open	0.11	0.11	20.4
PW11	Pneumatic leak or rupture	3.5E-03	0.004	0.68
PW12	Mechanical failure of Drill Tool	1.49E-02	0.015	2.89
PW13	Drill tool fails to drill waste	0.12	0.12	23.9
PW14	Failure to release waste on to WTT	4.3E-02	0.043	8.41
PW15	Robot Equipment Failure	4.9E-02	0.049	9.45
PW16	Mechanical failure of Cutting Tools	1.49E-02	0.015	2.89
PW17	Cutting tool fails	0.12	0.12	22.9
Failures leading to site power supply				
PO1	Loss of site power supply	0.10	0.10	19.4
Failures leading to loss of robot functionality				
RB1	Mechanical failure of Gearbox	7.8E-02	0.078	15.1
RB2	Failure of oil supply to Gearbox	2.1E-02	0.021	4.07
RB3	Manufacturing defect in Gearbox	4.1E-03	0.004	0.79
RB4	Motor Gearbox fails	0.1	0.1	19.9
RB5	Failure to start Axis 1,2,3,4,5 or 6 Motor	4.8E-02	0.048	9.30
RB6	Control/Electrical failure of brake	4.0E-02	0.04	7.73
RB7	Mechanical failure of brake	2.3E-02	0.023	4.36
RB8	Brake fails closed	6.2E-02	0.062	12.1
RB9	Mechanical Failure of resolver or shaft for Axis 1,2,3,4,5 or 6	1.0E-04	0	0.019
RB10	Loss of signal to resolver for Axis 1,2,3,4,5 or 6	7.5E-03	0.008	1.45

Node ID	Cause (primary node)	Fault Tree Results (Percent Probability)	BBN Prior Percent Probability	BBN Updated Posterior Percent Probability
RB11	Failure of resolver for Axis 1,2,3,4,5 or 6	7.6E-03	0.008	1.47
RB12	Electrical Failure of cables to resolvers	2.5E-02	0.025	4.92
RB13	Mechanical damage to cables to Resolvers during routine operations	1.1E-02	0.011	2.03
RB14	Loss of cables to resolvers	3.6E-02	0.036	6.95
RB15	Mechanical damage to In-Cell cables during routine operations	7.9E-02	0.079	15.2
RB16	Electrical Failure of In-Cell Cables	2.5E-02	0.025	4.92
RB17	Loss of In-Cell cables to axes 1-3 or 4-6	1.0E-01	0.1	20.2
RB18	Electrical Failure of Out-Cell cables	7.5E-03	0.008	1.45
RB19	Mechanical damage to Out-Cell cables during routine operations	2.0E-04	0+	0.039
RB20	Loss of Out-Cell Cables to Axes 1-3 or 4-6	7.7E-03	0.008	1.49
RB21	Failure of power supply to robot	0.25	0.25	47.9
RB22	Loss of Robot Functionality	0.37	0.37	90.6
TOP EVENT		**0.52**	**0.52**	**100**

Table G-3 (Continued): Comparison of BBN Results with Fault Tree Analysis

Primary Event ID	Description	FTA Sensitivity Analysis (probability)	BBN MPE Sensitivity Analysis (percent probability)
PO1	Loss of site power supply	1.93E-01	100
RB15	Mechanical damage to in-cell cables	1.52E-01	78.7
RB1	Mechanical failure of gearbox	1.50E-01	77.8
RB5	Failure to start axis 1,2,3,4,5 or 6 motor	9.27E-02	48.0
RB6	Control electrical failure of brake	7.71E-02	39.9
RB12	Electrical failure of resolver cables	4.91E-02	25.4
RB16	Electrical failure of in-cell cables	4.91E-02	25.4
RB7	Mechanical failure of brake	4.35E-02	22.5
RB2	Failure of oil supply	4.06E-02	21.0
PW16	Mechanical failure of cutting tool	2.88E-02	14.9
PW12	Mechanical failure of drill tool	2.88E-02	14.9
RB13	Mechanical damage to resolver cables	2.03E-02	10.5
RB18	Electrical failure of out-cell cables	1.45E-02	7.49
RB10	Loss of signal to resolver for axis 1,2,3,4,5 or 6	1.45E-02	7.49
PW2	Failure of air supply	9.28E-03	4.80
RB3	Manufacturing defect	7.92E-03	4.10
PW11	Pneumatic leak or rupture	6.76E-03	3.50
PW8	Hydraulic leak or rupture	6.76E-03	3.50
PW4	Mechanical failure of bolt removal tool	3.48E-03	1.80
PW9	Mechanical failure of end effectors	3.48E-03	1.80
PW6	Mechanical failure of primary/secondary tools	3.48E-03	1.80
PW1	Mechanical failure of gripper tool	3.48E-03	1.80
RB19	Mechanical damage to out-cell cables	3.87E-04	0.20
RB9	Mechanical failure of resolver/shaft	1.93E-04	0.10

Table G-4: Comparison of sensitivity analysis output from FTA and BBN

APPENDIX H: SUMMARY OF RESEARCH PAPERS PUBLISHED BY THE AUTHOR

Based on this research project, the author has published technical papers in the IChemE Chemical Engineer magazine, the Nuclear Future journal and in the Proceedings of the IChemE Hazards 29 Conference, including an oral presentation. Tables H-1 to H-3 provide a summary of these papers and the oral presentation.

Publication reference: Ahmed, F. (2017b) Bayesian Belief Networks - A robust approach to quantified risk and uncertainty analysis', *Institution of Chemical Engineers*, *The Chemical Engineer,* Issue 911, pp. 28-32.
Area of research project discussed: The article begins with a discussion about the legal requirement for demonstrating ALARP and why understanding and managing uncertainties is crucial. The benefits of applying BBNs to address key uncertainties in process plant applications are then considered. To introduce the BBN technique to a wide range of audience, the paper provides an explanation of Bayes theorem. A BBN to determine the likelihood of a hydrogen detonation occurring in a pipe containing a mixture hydrogen in air is given as an introductory example. The article focusses on how the BBN technique was applied to assess the uncertainty associated with mixing of sludge wastes and the likelihood of sludge coming out of the mixing vessel. The BBN results illustrated in the paper were based on the concept model (Chapter 5, Figure 5-2) developed in Chapter 5 of this thesis. Based on similar probability distributions, for the input parent nodes, as those in Chapter 5 Figure 5-3 of Chapter 5, the BBN results in the article demonstrated that the probability of sludge coming out of the mixing vessel is 78%.
Main discussion points and conclusions: Having discussed the sludge mixing case study, the article presents an argument on why the BBN methodology is considered advantageous over other approaches such as Fault Tree Analysis (FTA). The following main advantages of BBNs are discussed: • The ability of BBNs to model distributions of the key input variables, as opposed to single values used in FTAs, enables an uncertainty analysis to be performed. • The BBN updating feature enables a sensitivity analysis to be performed. The article concludes by highlighting that the BBN approach is being widely used in other sectors including the medical profession. This provides further confidence that the technique could be applied to uncertainty analysis for hazards in nuclear chemical plants.

Table H-1: Summary of author's publication in the IChemE Chemical Engineer professional magazine

Publication reference: Ahmed, F. (2019a) Managing hydrogen gas hazards, *Nuclear Future, The Professional Journal of the Nuclear Institute*, 15(2), pp.46-50.
Area of research project discussed: This paper presents a Bayesian Network based on the results of the case study in Chapter 7 of this thesis on the uncertainty analysis of hydrogen generation in transportable skips containing Intermediate Level nuclear wastes. Key hydrogen generation mechanisms i.e. corrosion of Magnox due to underwater storage of the metallic waste and radiolysis of the radioactive liquor within the skip are discussed, recognising that corrosion is the dominant source of hydrogen. Other key factors contributing to the accumulation of hydrogen in the skip ullage space were identified as the degree of hydrogen gas hold-up and the potential for a sudden discontinuous release of the gas in the vessel ullage space. The skip filter performance was also identified as a factor affecting the hydrogen concentration in the ullage space. Taking into consideration the prior probability distributions of these key variables, the illustrated BBN in the paper demonstrated that there is less than a 50% chance of the hydrogen concentration in the skip ullage space being below the 4% LFL.
Main discussion points and conclusions: The paper concludes that the key sensitivities affecting the hydrogen concentration in the skip ullage space are hydrogen hold-up and a discontinuous release of the gas from the waste. Provided that a discontinuous release is prevented, there is a high probability that hydrogen concentration in the skip ullage will remain below the 4% LFL.

Table H-2: Summary of author's publication in the Nuclear Future journal

Publication reference: Ahmed, F. (2019b) Application of Bayesian Belief Networks to assess hydrogen gas retention hazards and equipment reliability in nuclear chemical plants, *Proceedings of the Institution of Chemical Engineers Hazards 29 Conference, Symposium Series No.166*, Birmingham, 22-24 May 2019.
Area of research project discussed: Two specific case studies based on this research project are discussed in this paper. In relation to Chapter 7 of this thesis, the first examines in detail the factors that lead to hydrogen hold-up and a discontinuous release within the ILW skip. The previous paper published in the Nuclear Future journal (Table H-2) was based on hydrogen generation from different types of ILW waste forms that are likely to be stored in the skips. This paper focusses on the behaviour of sludge waste forms and the factors that lead to a discontinuous release which were not previously considered. The second case study in this paper applies the BBN method to examine factors that affect the reliability of a hydrogen purge system in process vessels containing radioactive liquors. Such liquors can lead to generation of hydrogen gas through the process of radiolysis. The methodology used in this paper in terms of the assessment of the time taken to reach the hydrogen concentration limits following vent failure and reliability of the hydrogen purge system is based on Chapter 6 of the thesis.
Main discussion points and conclusions: The paper was presented by the author at the IChemE Hazards 29 conference in Birmingham in May 2019 to a wide range of audience. The audience consisted of professional chemical engineers from a variety of sectors including nuclear power, pharmaceuticals and regulators from the petrochemical industry. The main points discussed within the paper as well as during the oral presentation at the conference are that the best means of managing the hazard from hydrogen hold up and discontinuous release scenarios is to minimise the risk of adverse skip disturbance. This could be achieved by providing high reliability vessel transfer zoning systems designed to prevent accidental skip collision with adjacent structures during the handling operations. For the second case study on the reliability of the process vessel purge air system, it was shown that a loss of compressed air and site power supply are the key sensitivities that affect the performance of the system.

Table H-3: Summary of author's publication in Proceedings of the IChemE Hazards 29 Conference